# Molecular regulation of intussusceptive angiogenesis by ephrinB2/EphB4 signaling and its therapeutic potential

## Inauguraldissertation

zur

Erlangung der Würde eines Doktors der Philosophie

vorgelegt der

Philosophisch-Naturwissenschaftlichen Fakultät

der Universität Basel

von

**Šime Brkić**

von Kroatien

Basel, 2017

Genehmigt von der Philosophisch-Naturwissenschaftlichen Fakultät

auf Antrag von:

Prof. Dr. Markus Affolter

PD. Dr. Andrea Banfi

Prof. Dr. Valentin Djonov

Basel, den 17. Oktober 2017

Prof. Dr. Martin Spiess

(Dekan der Philosophisch-Naturwissenschaftlichen Fakultät)

# Table of contents

# I. Introduction

# 1. Vascular development

The circulatory system is the first functional organ system to appear during embryonal development in vertebrates, which is clearly depicting its importance. Developing blood vessels bring nutrients and oxygen to fast growing cells of the embryo, overcoming the limits of simple diffusion of the oxygen to the cells (1). In 1628, William Harvey discovered that the heart pumps blood through arteries which is then returned back to the heart by veins. Later, in 1661, Marcello Malpighi identified capillaries as the smallest blood vessels connecting arteries and veins in developing chick embryo (2).

There are three main processes of vascular formation; i) vasculogenesis, ii) angiogenesis and iii) arteriogenesis. Vasculogenesis is *de novo* formation of new blood vessels from the progenitor cells. Angiogenesis is a process of a growth of vessels from pre-existing ones, while arteriogenesis is a process of arterial vessel diameter expansion upon increase in blood flow or shear stress (Figure 1). Through coordination of all three processes, a complete circulatory system, responsible for tissue oxygenation, nutrient delivery, waste removal, immune response, thermoregulation and maintenance of blood pressure, is built (1).

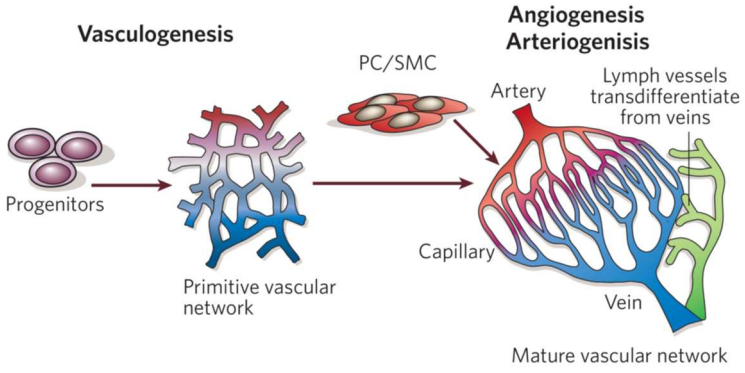


**Figure 1. Vascular development**. Vasculogenesis is a process that implies formation of blood vessels from progenitors, while angiogenesis and arteriogenesis are processes of blood vessel growth from pre-existing vessels and require recruitment of pericytes (P) and smooth muscle cells (SMC). Lymphatic vessels originate from veins [Reprinted from Carmeliet P. et al, 2005 (2)].

## 1.1. Vasculogenesis

Vasculogenesis is the process of *de novo* formation of new blood vessels from endothelial progenitor cells, and it occurs both intra- and extra-embryonically (1). Embryonic mesoderm, extra-embryonic yolk sac, allantois and placenta are the sources of vascular endothelial and hematopoietic progenitor cells (1, 3). The first step in the process is the appearance of the hemangioblast, a common progenitor of endothelial and hematopoietic cell lineages. In the murine yolk sac, hemangioblasts will form clusters, so called blood islands, at embryonic day (E) 6.5-7 and further differentiate into two cell types - angioblasts and hematopoietic progenitors. Angioblasts are endothelial progenitors, which will be located at the periphery of the blood island while hematopoietic progenitors will be located centrally. Angioblasts proliferate, migrate and differentiate into endothelial cells at E8.5 and ultimately form a lumenized primitive vascular plexus and deposit basal lamina (1). This process of coordination of angioblast assembly with concomitant communication with the cells of other embryonic lineages is called vascular patterning and needs to be reproducible both in time and space (4). By the 2-somite stage, intra- and extra-embryonic vasculatures have anastomosed, but the embryo can still retrieve oxygen by diffusion. The vascular plexus then fuses with the developing heart, before the first heartbeat. Blood vessels of some endodermal organs like liver, spleen, lung, stomach/intestine and pancreas are also formed by vasculogenesis (5). It was demonstrated that vasculogenesis also occurs in adults, as a mechanism of capillary formation after ischemic injury (6). The molecular mechanisms of vasculogenesis are not completely clear, but signaling pathways like VEGF (7-9), FGF (10), Hedgehog (11), Neuropilin (12) and TGF-β (13, 14), are implicated in this complex process.

## 1.2. Angiogenesis

Angiogenesis, in contrast to vasculogenesis, is the process of formation of blood vessels from pre-existing ones. During embryonic development, angiogenesis starts around E9.5 and most of the embryonic vessels are formed by this mechanism (1). In the adult organism, most of the vessels are quiescent and angiogenesis occurs only during cyclic changes of the female ovary and uterus, as well as in placenta during pregnancy, or during healing. Endothelial cells retain their ability to be activated and rapidly divide upon a physiological stimulus like hypoxia in case of blood vessels and inflammation in case of lymphatic vessel. Angiogenesis and lymphangiogenesis are therefore especially important during wound healing and injury. Extent of blood vessel growth needs to be tightly controlled since excessive or insufficient angiogenesis is leading to different pathologies. Overgrowth of blood vessel is associated with malignant, ocular and inflammatory disorders, as well as conditions like diabetes, endometriosis, AIDS, bacterial infections, asthma and multiple sclerosis. On the other side, ischemic diseases and preeclampsia are characterized with insufficient angiogenesis causing endothelial cell dysfunction, vessel malformation and lack of tissue vascularization and regeneration (2) . In 1971, Judah Folkman presented a theory that targeting angiogenesis is a strategy for anti-tumor treatment (15). Most of the research about angiogenesis has primarily been driven with the aim to develop anti-angiogenic drugs to fight cancer. The details about angiogenic process will be described in the following chapters.

## 1.3. Arteriogenesis

Arteriogenesis is the process of arterial enlargement under the conditions of increased blood flow and shear stress (16-18). The growth of pre-existing collateral arteries by arteriogenesis is a powerful mechanism by which a blood supply can be delivered to distal ischemic tissues in a situation of chronic occlusion of main feeding artery. During the process,

arteries enlarge in diameter (up to five-fold) and length as they become more tortuous (18). In some cases, patients with a chronic coronary artery occlusion can be asymptomatic due to the collateral artery growth which compensate the lack of blood flow. Collateral artery growth seems not to be regulated by hypoxia, nor by increase in VEGF expression (19). Main driver of arteriogenesis are biomechanical forces and there are evidences that change in fluid shear stress is the main stimulus for arterial enlargement (20). Fluid shear stress acts tangential to the vascular wall and in the arteries ranges between 10-70 dyn $cm^{-2}$ (17). Endothelial cells are the one directly sensing the change in fluid shear stress induced by an increase of blood flow velocity which is the consequence of pressure difference created by the occlusion in the artery (18). Smooth muscle cells in tunica media are not in direct physical contact with endothelial cells since they are separated by internal elastic lamina and basement membranes, so their communication is mediated by secreted factors. The mediation of molecular signal probably goes through expression of nitric oxide (NO) by endothelial nitric oxide synthase (e-NOS) through stress-activated $Ca^{2+}$ channel TRPV4. In turn, NO can activate smooth muscle cells to initiate vasodilatation (18). Monocytes have a central role in arteriogenic process and they are recruited by monocyte chemoattractant protein-1 (MCP-1, or CCL2) expressed by activated endothelial cells. Mice lacking CCR2, receptor for MCP-1 chemokine, have impaired arteriogenesis (21). Expression of intercellular adhesion molecule-1 (ICAM-1) and vascular adhesion molecule-1 (VCAM-1) facilitates monocyte recruitment. Subsequently, monocytes become macrophages and start to secret several factors like tumor necrosis factor-α (TNF-α) (22), granulocyte-monocyte colony stimulating factor (GM-CSF) (23), matrix metalloprotease-2, -9 (MMP-2, MMP-9) (24) that synergistically induce cell proliferation and matrix degradation, ultimately leading to enlarged arteries. Given that arteriogenesis has a clear beneficial therapeutic effect, other stimuli that induce collateral growth have been investigated. One of the simplest way is physical exercise, as it is the most natural way to stimulate

collateralization (25, 26). Other therapeutic avenue could be treatment with statins (3-Hydroxy-3-methylglutaryl-coenzyme A reductase inhibitors) in patients with hypercholesterolemia (27), due to negative effect of hypercholesteremia on monocyte function and arteriogenesis (28).

## 1.4. Vascular heterogeneity

The circulatory system is made of two types of vessel networks; the blood and the lymphatic vasculatures. The blood vascular system is a closed circulatory complex consisting of arteries and veins which are connected by the capillaries. The lymphatic system is blind-ended and unidirectional, and it is comprised of lymphatic vessels (lymphatic capillaries, pre-collecting and collecting lymphatic vessels), lymph nodes and associated lymphoid organs. Main function of lymphatic system is recycling of extravasated fluid and macromolecules through collecting lymphatic vessel and thoracic and right lymphatic ducts, back to the venous blood circulation. Lymphatic vessels also participate in fat absorption, tissue cholesterol clearance and immune cell trafficking. Morphologically, in blood vasculature, larger arteries and veins contain three distinct layers; tunica intima which is composed of endothelial cells, tunica media which contains smooth muscle cells (SMCs) and elastic fibers (thicker in arteries), and tunica adventitia which is made of connective tissue. Smallest blood capillaries can be continuous, fenestrated or discontinuous, depending on the extent of basement membrane (BM) and pericyte coverage, which is determining capillary permeability. Both collecting lymphatic vessels and veins have valves which prevent backflow of blood/lymph. Mural cells (pericytes, SMCs and hepatic stellate cells) coverage also differs among different vessel types. The walls of larger caliber blood vessels contain SMCs, which are essential for vascular stability and tone, and blood pressure regulation. Small vessel like blood capillaries and venules are covered by pericytes. Pericytes make contacts with the endothelium to regulate

vessel stability, transendothelial transport and blood–brain barrier (BBB) formation (29) (Figure 2).

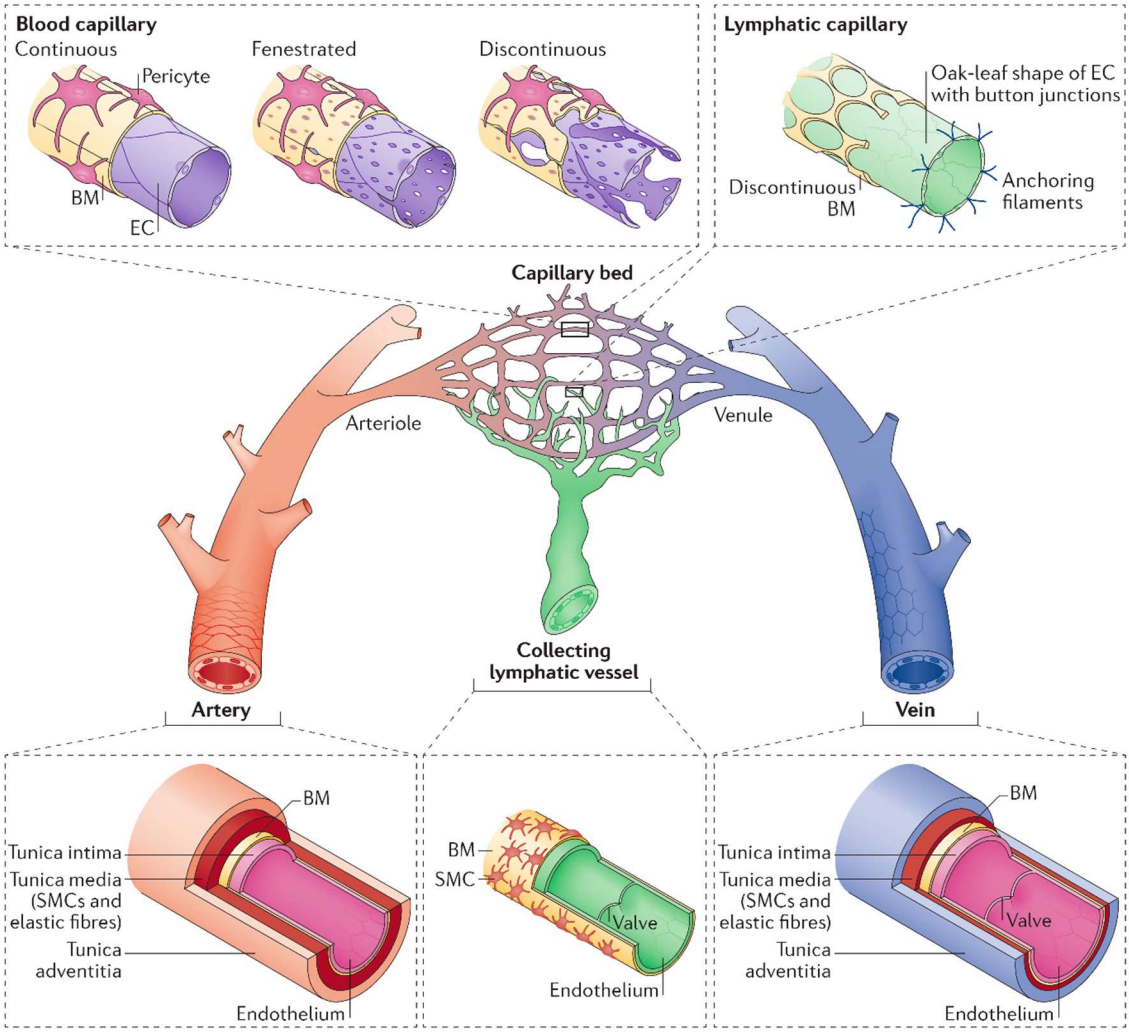


**Figure 2. Vascular organization.** The circulatory system is divided into blood and lymphatic vascular networks. Blood vascular system is hierarchically divided into larger arteries and veins, smaller arterioles and venules and blood capillaries. Arteries and veins are made out of three functional layers; tunica intima (endothelium), tunica media (smooth muscle cells; SMCs) and tunica adventitia (connective tissue). Blood capillaries can be continuous, fenestrated or discontinuous, depending on the extent of basement membrane (BM) and pericyte coverage. Collecting lymphatic vessel contain sparse SMC coverage and luminal valves that help with pumping and prevent backflow of the lymph. Lymphatic capillaries have discontinuous BM and are made out of oak-leaf-shaped ECs with specialized button-like junctions and anchoring filaments that pull the ECs apart and allow the entry of fluid under conditions of high interstitial pressure [Reprinted from Potente, M. et al. 2017 (29)]

### 1.4.1. Tissue-specific vasculature

Different organs have different functions and therefore vasculature of individual tissues and organs needs to adapt according to the specific environment. Endothelial cells in the brain establish the highly selective blood-brain barrier (BBB), which protects neurons from toxic molecules, immune cells and pathogens. Capillaries in the brain have continuous endothelium that is linked by specialized tight junctions and adherens junctions, a low rate of transcytosis, and the suppression of leukocyte adhesion. Since neurons rely on glucose as the major source of energy, ECs in the BBB preferentially express the glucose transporter GLUT1, which facilitates the transfer of glucose from the blood to the brain (29, 30). Organs that are involved in secretion, absorption and filtering, like kidney, small intestine, exocrine and endocrine glands, contain permeable ECs, enabling rapid exchange, uptake and secretion of fluids, solutes and molecules (31). Liver sinusoidal endothelial cells have even higher permeability. These ECs are discontinuous, lack an organized BM and have large non-diaphragmed fenestrae that are organized in sieve plates, allowing the passage of small particles from the blood to hepatocytes (31). Lung ECs are specialized for efficient gas exchange at the extremely thin blood–air barrier. Pulmonary capillaries make dense network through which blood flows as a sheet (32). ECs in bone tissue are divided in two types; type H and type L. Type H ECs have higher expression of CD31 (PECAM1) as compared to type L cells. Type H ECs are located at metaphysis and endosteum of long bones and are responsible for bone angiogenesis, giving rise to type L ECs, found in diaphysis of long bones (33). Contrary to most blood vessels, lymphatic capillaries are highly permeable given that their main function is fluid uptake. Lymphatic capillaries have button-like junctions and anchoring filaments, which together facilitate fluid uptake when interstitial pressure is high (34).

Endothelial specialization can be instructed either by cell-intrinsic mechanisms or by external tissue-derived signals given by the local tissue microenvironment. Some of these

mechanisms involve biochemical signals, transcriptional regulation, biomechanical forces (flow-driven shear stress, luminal pressure, cyclic circumferential stretch, and cellular transmigration) and metabolic environment (29).

# 2. Cellular and molecular mechanisms of angiogenesis

Angiogenesis is a process of formation of new blood vessels from pre-existing ones, and as such is the predominant way of growth of new blood vessels in adult organism. There are two main cellular mechanisms or types of angiogenesis; sprouting and intussusceptive (splitting) angiogenesis (Figure 3).

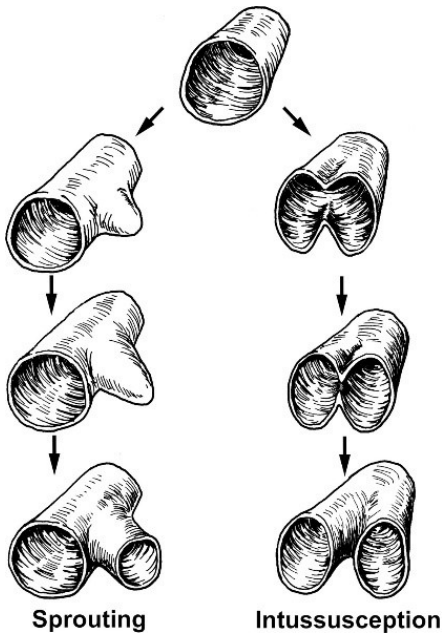


**Figure 3. Types of angiogenesis**. There are two main modes of vessel growth by mechanism of angiogenesis; sprouting and intussusceptive (splitting) angiogenesis. Sprouting angiogenesis implies formation of a vessel sprout that will extend and form a lumen, while intussusception is a process of longitudinal splitting of the mother vessel into two new daughter vessels [Reprinted from Prior, B.M. et al. 2004 (35)]

## 2.1. Sprouting angiogenesis

Sprouting angiogenesis is predominant cellular mechanism of adult angiogenesis and it is most studied and best described (36). The process has several phases. First, endothelial cells are activated by angiogenic stimulus like vascular endothelial growth factor (VEGF). Since ECs and pericytes are joined together with a basement membrane, ECs need to be liberated in order to grow. Pericytes will detach from the vessel and basement membrane will be degraded by matrix metalloproteases. Next, one endothelial cell will be selected to become a tip cell, a migratory and invasive cell that is extending its filopodia, following gradient of VEGF in the surrounding extracellular matrix, and guiding the sprout. The neighboring ECs,

called stalk cells, are proliferating, creating new cells necessary to build growing vessel. Two tip cells will eventually come in contact, bridge the gap and fuse together. Ultimately, lumen of the new vessel will be formed. Process will restart with new tip cell appearing (Figure 4).

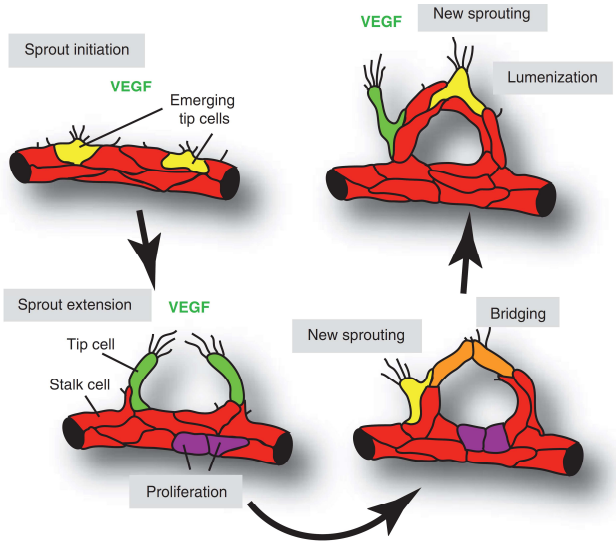


**Figure 4. Sprouting angiogenesis.** The process of sprouting angiogenesis initiates with appearance of a tip cell, a specialized ECs that can sense the gradient of VEGF and guide the sprout by extending its filopodial protrusions. Adjacent ECs, called stalk cells, proliferate and build up a new vessel. When two tip cells meet they fuse together and lumen of new vessel is formed [Reprinted from Adams, R.H. et al. 2010 (37)]

ECs express guidance molecules including ROBO4 (Roundabout 4), UNC5B, Plexin-D1, Neuropilins, and Eph family members, that help guide the nascent sprout (36). ROBO4 maintains vessel integrity and its deficiency induces leakages and hyper-vascularization (38). Molecularly, it decreases the permeability by impeding VEGF-R2-mediated activation of the SRC kinase. ROBO4 does not contain domains for binding of SLITs (ROBO-ligands), but it was shown that ROBO4 can bind UNC5B, another guidance receptor, which suggests that ROBO4/UNC5B complex preserves vessel integrity by UNC5B activation (36, 39). Expression of UNC5B, which is also a Netrin receptor, is enriched in tip cells. Both UNCB5 and Netrin1 are associated with suppression of vessel growth, since inactivation of UNC5B results in enhanced sprouting while Netrin1 is causing filopodia retraction in ECs. Since this

function of Netrin1 has not been described by others, there is a possibility that Netrin1 might have other unidentified receptors (37). It was also shown that UNC5B can induce apoptosis of ECs, even without the ligand (40). Other class of guidance molecules involved in tip cell guidance are semaphorins. They are secreted or membrane-bound proteins that interact with receptor complexes, made solely by Neuropilins (NRPs) or by NRPs and Plexin family proteins (41). Semaphorin 3E (Sema3E) induces vessel repulsion through interaction with Plexin-D1, which is expressed by EC. This interaction fine-tunes balance between tip and stalk cells, especially important for control of even-growing vascular beds (42). Eph receptors and their ephrin ligands are another class of cell guidance molecules involved in angiogenesis. They are regulators of cell-contact-dependent signaling and mostly generate repulsive signals (43). It was demonstrated that disrupted ephrinB2 signaling impairs sprouting because ECs cannot internalize VEGF-R2 and VEGF-R3 and properly transmit VEGF signals (44, 45).

Stalk cells have also very important role in angiogenic process. Compared to tip cells, stalk cells produce fewer filopodia, proliferate more, and form a vascular lumen. They produce components of basement membrane in order to insure integrity of the sprout. Stalk cells establish junctions with neighboring cells and make tubes and branches of nascent vessel (46). Both tip and stalk cells are transient ECs phenotypes and not stable cell fates. In order to expand vascular network, ECs undergo iterative cycles of sprouting, branching, and tubulogenesis, and dynamic transitions between tip and stalk cell phenotypes, are part of this process (46, 47).

In the last phase of sprouting angiogenesis, nascent sprouts need to form a lumen. This happens by different mechanisms, including vacuolar fusion, cord hollowing and inverse membrane blebbing (29). Vacuolar fusion is the process observed in intersomitic vessels and includes lumen formation by coalescence of intracellular (pinocytic) vacuoles, which interconnect with vacuoles from neighboring ECs (36). Cord hollowing is alternative mechanism described in large axial vessels. It suggests that ECs adjust their shape and

rearrange their junctions to open up a lumen (cord hollowing). In this model, apical-basal polarity of endothelial cell is established. Then, apical (luminal) membrane becomes covered by negatively charged glycoproteins that confer a repulsive signal, opening up the lumen. Subsequent changes in endothelial cell shape, driven by VEGF and RHO-associated protein kinase (ROCK), expand the lumen (36, 48, 49). Inverse membrane blebbing is the third described mechanism which involves spherical deformations of the apical membrane of endothelial cells induced by blood flow. Endothelial cells react to these membrane intrusions by local and transient recruitment and contraction of actomyosin. This mechanism is required for single, unidirectional lumen expansion in angiogenic sprouts. This process does not require specific EC polarity (50). Finally, neighboring luminized sprouts anastomose (fuse together), either through sprout hollowing (generating a multicellular tube) or through membrane invagination (resulting in a unicellular tube) (51). After that, newly established blood flow stabilizes the vessel and non-perfused segments regress in the process of vascular pruning (52).

## 2.2. Intussusceptive angiogenesis

Intussusceptive ("growth within itself") or splitting angiogenesis is first described in developing lungs of rabbits (53) and rats (54), but best studied in chicken chorioallantoic membrane (CAM) (55). It is an alternative mechanism of blood vessel growth that does not include specification of tip and stalk cells. The process of intussusceptive angiogenesis (IA) or intussusception is divided in four phases:

I) In the first phase, contact between endothelial cells located directly opposite to each other in capillary wall, is established. This happens by intraluminal endothelial cell protrusion until the contact is made. The contact zone marks the area of interendothelial transluminal pillar bridge which is approximately 1 μm in diameter. This is the initiation step that sets the stage for pillar formation.

II) In the second phase, endothelial bilayer is perforated. Under electron microscope, this can be seen as appearance of tiny holes in the enlarged capillaries.

III) After perforation, a cylindrical tissue bridge is formed and extends across the lumen. Pericytes and fibroblasts insert their cytoplasmic processes inside the newly formed pillar and extend it. At this stage, pillar size is <2.5 μm in diameter.

IV) In the last phase, the pillars increase in girth and can potentially reshape and fuse with the neighboring pillars which results in splitting of the primary vessel into two new daughter vessels. In this phase, morphological structure of the pillar is not changing (56, 57) (Figure 5).

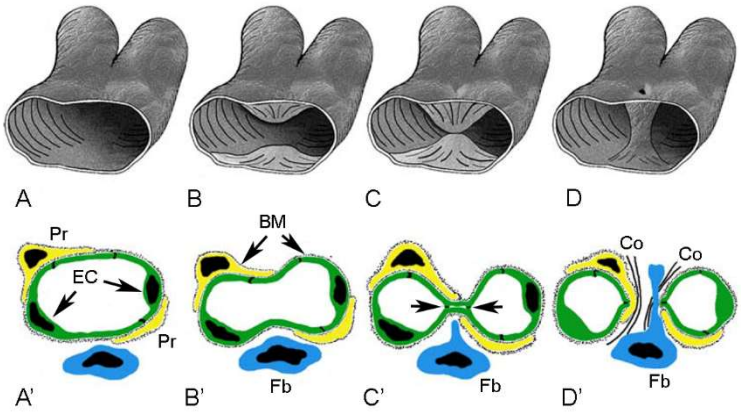


**Figure 5. Intussusceptive or splitting angiogenesis.** The process of intussusception is depicted by three-dimensional scheme of morphological changes (A-D), and two-dimensional representation of cellular events (A'-D'). The process starts when endothelial cells (EC), covered by pericytes (Pr) and basement membrane (BM) start protruding in the capillary lumen (A-B, A'-B'). ECs from opposite capillary walls come into contact (C, C'; arrows pointing to the place of contact). Endothelial bilayer is centrally perforated and the transluminal pillar is formed (D). The pericytes and fibroblasts (Fb) invade the pillar, deposit collagen fibrils (Co) and expand the pillar in girth. ECs retract, creating two daughter vessels (D') [Adapted from Makanya, A.N. et al. 2009 (58)]

Based on the final outcome, the process of intussusceptive angiogenesis can be divided into three major phases. All three phases are characterized by tissue pillar formation, but the difference is inherent in direction and arrangement of the pillars. The three phases include *intussusceptive microvascular growth* (IMG), *intussusceptive arborization* (IAR), and *intussusceptive branching remodeling* (IBR) (58, 59). Intussusceptive microvascular growth

encompasses the process of pillars formation, their growth and subsequent vessel splitting. The process of IMG leads to the amplification of the vascular exchange surface and vascular volume and formation of organ-specific angioarchitecture (59). This process was observed in many animal models (55, 60-63), different organs (64-66) and even in tumors (67). Intussusceptive arborization is the process that results in formation of a supplying vascular tree. The original pattern of blood vessels formed either through vasculogenesis or through sprouting angiogenesis has disorganized structure and does not resemble the tree-like arrangement of the mature vasculature. The fine adaptation of the organ vascular tree is achieved through IAR (58). The process of IAR was observed in two developing vascular systems: in the chorioallantoic membrane of the chicken and the choroid vasculature of the eye (62, 68). The process of intussusceptive branching remodeling results in adaptation of the architecture and number of vascular branches according to local tissue demands and it is influenced by flow properties. The IBR occurs via transluminal pillars that are formed close to arterial or venous bifurcation sites (58). By the means of IBR, hemodynamic conditions can be optimized, leading to optimal branching pattern that resembles the one predicted by Murray's Law of minimal power consumption and constant shear stress (59, 62, 69). Additionally, during the remodeling of mature vessels by IBR, a process known as *intussusceptive vascular pruning* (IPR) also takes place. The IPR is achieved through eccentric repetitive pillar formation at bifurcation sites. Pillars are oriented in rows across the breadth of the target vessel. Expansion and subsequent fusion of pillars results in reduced blood flow, consequently leading to regression, retraction, and atrophy of the affected vessel (58).

Blood flow and shear stress are important factors in angiogenic process. Blood flow within vessels results in stress, referred to as shear stress. Shear stress can be laminar (acting tangentially or parallelly to the endothelial surface), or oscillatory (turbulent) (58). The role of hemodynamics in the control of IA was demonstrated in developing CAM microvasculature.

One of the dichotomous branches of an artery upstream of the investigated area was clamped and increase in blood flow and pressure resulted in almost immediate effect on branching morphology. Transluminal pillars, as a hallmark of IA, began to appear 15–30 min after start of the clamping (62). This indicates that alterations in hemodynamics result in an immediate vascular adaptation without changes in gene expression. Based on the hemodynamic parameters obtained from *in vivo* experiments, computational models calculated that transluminal pillars are appearing in regions of low shear stress (<1 dyn/cm$^2$). Flow simulations indicated that the pillars were spatially constrained by neighboring regions of higher shear stress (70). Generally, pillar development is caused by increased flow and it occurs in areas characterized by low shear and turbulent flow conditions (57, 62, 70).

It was reported that capillary growth in muscles with increased blood flow occurs through intraluminal splitting, without sprouting. It was demonstrated that this happens without endothelial cell proliferation or breakdown of the basement membrane (71). Additionally, VEGF signaling is necessary for shear stress-dependent splitting of capillaries in skeletal muscle (72). Furthermore, we found that overexpression of different VEGF doses in skeletal muscle induces new vascular networks by process of intussusceptive remodeling through endothelial cell proliferation. In skeletal muscle, this process starts with initial vascular enlargements, followed by longitudinal vessel splitting (73). It was also demonstrated that in chicken CAM model, VEGF induces growth of new blood vessel by intussusception (74, 75).

In conclusion, both sprouting angiogenesis and intussusception are processes that are crucial for development of functional organ-specific vasculature, both during development and in adult period. They can complement each other, as it was shown that blood vessels in chick CAM grow initially by sprouting and then mainly by intussusception (76). Intussusception is much faster process in comparison to sprouting. It appears to be more economical from energetic and metabolic point of view, as extensive cell proliferation, basal membrane

degradation and invasion of the surrounding tissue are not required to that extent as for the sprouting angiogenesis. Also, during the IA, blood flow is continuous, in contrast to capillary sprouting (59).

## 2.3. VEGF signaling

Vascular endothelial growth factor (VEGF) is the master regulator of angiogenesis and it starts complex signaling cascade, leading to different morphological and biochemical changes that happen during angiogenesis. In the following text, VEGF receptors and ligands along with downstream signaling, will be described, as well as the role of VEGF in angiogenesis, especially focusing on crosstalk between VEGF and Notch signaling.

### 2.3.1. VEGF ligands and receptors

VEGF was first isolated from a conditioned medium from guinea pig tumor cell line and it was named "vascular permeability factor" (VPF) as it was able to induce vascular leakage in the skin (77). The VEGF family members are secreted, dimeric glycoproteins of molecular weight of around 40 kDa. The family consists of vertebrate VEGF-A, VEGF-B, VEGF-C, VEGF-D, placenta growth factor (PlGF), parapoxvirus VEGF-E and snake venom VEGF-F. Vertebrate VEGFs are structurally similar molecules and have a crucial role in regulation of vascular development and function. VEGF molecules can bind three distinct receptors in mammals; VEGF-R1 (Fms-like tyrosine kinase 1 or Flt-1 in mouse), VEGF-R2 (kinase insert domain receptor or KDR in human; fetal liver kinase-1 or Flk-1 in mouse) and VEGF-R3 (Flt-4 in mouse) (Figure 6). In zebrafish, there are four distinct genes coding for the VEGF receptors. Based on the chromosomal location of *flt-1*, *kdrb*, and *flt-4* genes, which correspond to homologous genes in mammals, we can conclude that they are indeed the zebrafish orthologues of human VEGF-R1, -R2, and -R3. Fourth gene, *flk-1*, is partially similar to both VEGF-R1 and -R2 and its homologue was found in chicken and opossum. It was apparently

eliminated during, or after the divergence of marsupial and placental mammals. Additionally, there are two coreceptors, Neuropilin-1 and -2 (NRP1, NRP2) (78-80).

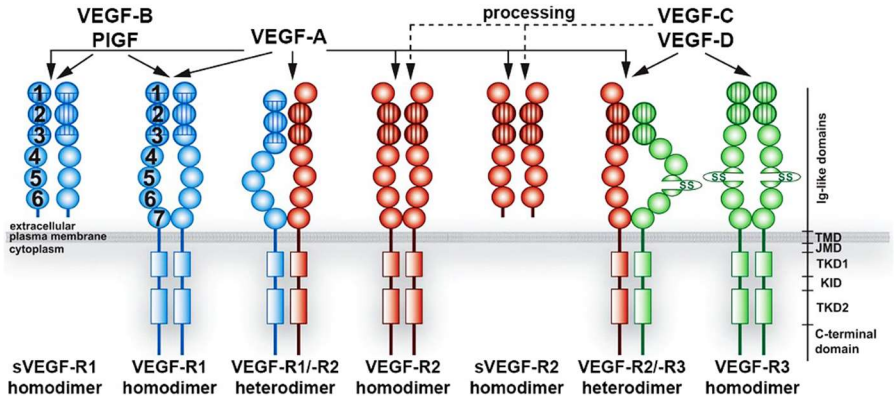


**Figure 6. VEGF receptors and ligands.** In vertebrates, there are five VEGF (vascular endothelial growth factor) ligands (VEGF-A, -B, -C, -D and Placental Growth Factor-PlGF) that bind receptors as homodimers. Transmembrane VEGF receptors contain seven IgG-like domains in extracellular portion, transmembrane domain (TMD), juxtamembrane domain (JMD), two tyrosine kinase domains (TKD), kinase insert domain (KID) and a C-terminal domain. There are three VEGF receptors (VEGF-R1, -R2, and -R3) which assemble as homodimers, but also VEGF-R1/VEGF-R2 and VEGF-R2/VEGF-R3 heterodimers are possible. There are also truncated, soluble forms of VEGF-R1 (sVEGF-R1) and VEGF-R2 (sVEGF-R2) [Adapted from Koch, S. et al. 2011 (81)]

VEGFs have a prominent role in central nervous system (CNS) (82), as well as in kidney, lung and liver (78). VEGF-A is the most important family member controlling blood vessels angiogenesis, while VEGF-C and -D are regulating lymphangiogenesis. Genetic experiments demonstrated crucial role of VEGF-A (referred to as VEGF), as deletion of only one allele of *Vegfa* gene in mice leads to death *in utero* by E11-12 due to lack of functional vasculature and the absence of blood islands (8). The human *Vegfa* gene contains 8 exons and 7 introns. Alternative exon splicing leads to generations of several protein isoforms, some of them being pro-angiogenic and some anti-angiogenic (80, 83) (Figure 7). Generally, VEGF-A isoforms have different heparin-binding affinity, depending on how many heparin-binding domains (HPD) they contain. One very important feature of VEGF is that it can form gradient

of concentration in extracellular matrix, as it diffuses from the source of its production, providing guideline for migration and invasion of tip cells during sprouting angiogenesis. Ability to form gradient is directly correlated with ability of the protein to bind heparin. For example, VEGF-$A_{121}$ does not bind neither extracellular matrix (ECM), nor NRP1, whereas VEGF-$A_{165}$ contains basic amino acid motifs in exon 8 and therefore binds to the ECM and forms gradients. Affinity for heparin is even stronger in VEGF-$A_{189}$ and VEGF-$A_{205}$, as they contain additional HPDs. Importance of VEGF gradient *in vivo* was demonstrated in mouse retina model, where mice expressing only VEGF-$A_{120}$ (corresponds to human VEGF-$A_{121}$, note: mouse isoforms have one amino acid less then human counterparts) had fewer branches, while mice expressing only VEGF-$A_{188}$ had more branches (41, 84).

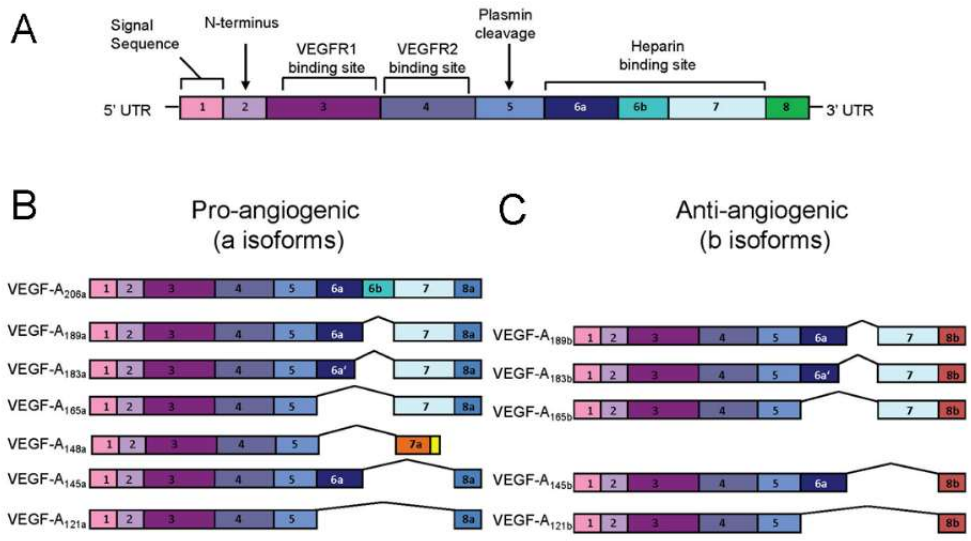


**Figure 7. VEGF-A splice isoforms.** *Vegfa* mRNA and it exons (**A**). By the process of alternative splicing, different pro-angiogenic (**B**) and anti-angiogenic (**C**) VEGF-A isoforms can be produced [Adapted from Fearnley, G.W. et al 2013 (83)]

VEGFRs contain extracellular domain with seven IgG-like subdomains, juxtamembrane domain (JMD), transmembrane domain (TMD), two tyrosine kinase domains (TKD), kinase insert domain (KID) and a C-terminal domain (Figure 6). VEGF binds to VEGFR and induces receptor homodimerization or heterodimerization, leading to

autophosphorylation of tyrosine residues in the receptor intracellular domains, receptor internalization and signaling activation, similarly to activation of other tyrosine kinase receptors (78).

VEGF-R1 is widely expressed, but it seems not to be critical in endothelial cell physiology. It is expressed by monocytes and it is involved in the processes of immune cell recruitment and fatty acid uptake. It binds VEGF-A, PlGF and VEGF-B (85). Mice lacking VEGF-R1 do not have impairment of endothelial cell differentiation, but nevertheless have a disorganized vasculature and die at E8.5-9 (86-88). On the other side, deletion of the VEGF-R1 tyrosine kinase domain is compatible with vascular development (89). Even though there is a tenfold excess of VEGF-R2 molecules on the surface of cultured endothelial cells, in comparison to VEGF-R1 (90), VEGF-R1 has higher affinity for VEGF-A (10 pM) as compared to VEGF-R2 (100 pM) (78, 91). Nevertheless, VEGF-R1 poorly transduces downstream VEGF signaling, and it is generally considered as a negative regulator of VEGF signaling in vascular physiology (78). VEGF-R1 exists as a full-length protein and alternatively spliced soluble form, sVEGF-R1 (sFlt-1) (92). Soluble Flt1 is expressed in a controlled manner during gestation, but its excessive expression was associated with development of preeclampsia (93). Other pathological conditions related with inflammation and recruitment of bone marrow-derived myeloid cells, as well as tumor and metastasis progression, were associated with VEGF-R1 (85).

VEGF-R2 is the main receptor on endothelial cells and it has a key role in angiogenesis. In mice, deletion of *flk-1* leads to death *in utero* between E8.5-9.5 (7, 94). VEGF-R2 binds VEGF-A and processed VEGF-C and -D. VEGF-R2 can also be alternatively spliced to soluble VEGF-R2 (sVEGF-R2), found in different tissues such as ovary, spleen, skin, kidney, heart, and in plasma (85). Soluble VEGF-R2 can bind VEGF-C and prevent it from binding to VEGF-R3, consequently inhibiting lymphatic endothelial cell proliferation (95). VEGF-R2 has also

been associated with pathological conditions, especially with tumor angiogenesis, and several small molecular weight VEGF-R2 inhibitors are being used in clinics in order to block pathological angiogenesis in cancer (85).

VEGF-R3 can bind VEGF-C and -D and it is crucial for lymphangiogenesis. Generally, it mainly functions in lymphatic vessels, but its expression was also confirmed in capillaries and venous endothelium, as well as in neuronal progenitors, macrophages and osteoblasts (78). It was shown that its expression is re-introduced during angiogenic sprouting in retina (96). It was demonstrated that VEGF-C-mediated activation of AKT pathway is required for both embryonic and adult lymphangiogenesis (97). During embryogenesis, activation of VEGF-R3 by VEGF-C induces migration of Prospero homeobox protein 1 (PROX1)-positive lymphatic progenitors from the cardinal vein, giving rise to lymphatic vessels (98). In zebrafish, SoxF transcription factors and transcriptional modulator MafBa, had been identified as downstream effectors regulating lymphatic endothelial cell migration (99).

### 2.3.2. VEGF-R2 signaling complexes

VEGF-R2 can be activated by canonical ligands (VEGFs) and non-canonical mediators (non-VEGF ligands and other stimuli). It is the main transducer of VEGF-A effects and it regulates vascular permeability, endothelial cell differentiation, proliferation, migration, and formation of the vascular tube (78, 85). VEGF-R2 signaling can involve multiprotein complexes composed of ligands, receptors, co-receptors and several other non-VEGF binding auxiliary proteins (78) (Figure 8).

Binding of VEGF dimer to receptor induces its dimerization and stabilization. It was shown that IgG-like subdomain 7 is involved in homotypic receptor interactions (79, 100). Besides VEGF-R2 homodimers, dimerization can also occur through VEGF-R2/VEGF-R3 (101) and VEGF-R1/VEGF-R2 heterodimers. Ligand binding induces change of configuration

of the transmembrane domains, which is accompanied by rotation of the dimers. This rotation is critical for full activation of kinase activity (78).

VEGF co-receptors, Neuropilin-1, Neuropilin-2 (NRP-1 and -2) and heparan sulfate proteoglycans (HSPGs), have important role in modulation of VEGF-R2 signaling. They act as stabilizers of ligand-receptor interactions and in that way, make signaling stronger (78), especially in case of HSPGs (102). NRP-1 and NRP-2 are transmembrane glycoproteins that bind both to VEGFs as well as to class 3 semaphorins, which are axonal guidance molecules that can bind Plexin receptors (103, 104). We recently demonstrated that Sema3A, a member of class 3 semaphorin family, is a mediator of vessel stabilization modulated by VEGF dose (105). VEGF-A binds NRP-1 and NRP-2 through specific motifs in exon 7 and 8, and it has 50-fold higher affinity for NRP-1 as compared to NRP-2 (106). Mice lacking NRP-1 die *in utero* due to severe cardiovascular and CNS defects (107, 108). Interestingly, when *Nrp1* has a mutation in VEGF-A-binding site (Tyr297 or Ser320), vascular development is not affected, suggesting it functions independently of VEGF binding (109, 110). Even though it was demonstrated that VEGF binds to NRPs and VEGFRs and induces formation of NRP-VEGFR complexes (110, 111), configuration of such NRP-1-VEGF-A-VEGF-R2 complex is not known. Potentially, this interaction can be directly or indirectly mediated by HSPGs like syndecan and glypican. NRP-1 can also bind PDZ-domain-containing protein synectin (also known as GIPC1) with its C-terminal PDZ-binding domain, and regulate VEGF-R2 intracellular trafficking by a VEGF-R2-NRP-1-synectin-myoVI complex (78) (Figure 8). Besides *in cis* binding, NRP-1 can also bind *in trans*, between adjacent cells. In that case, NRP-1-VEGF-A–VEGF-R2 complex keeps the receptor on the cell surface and inhibits angiogenesis (112) (Figure 8).

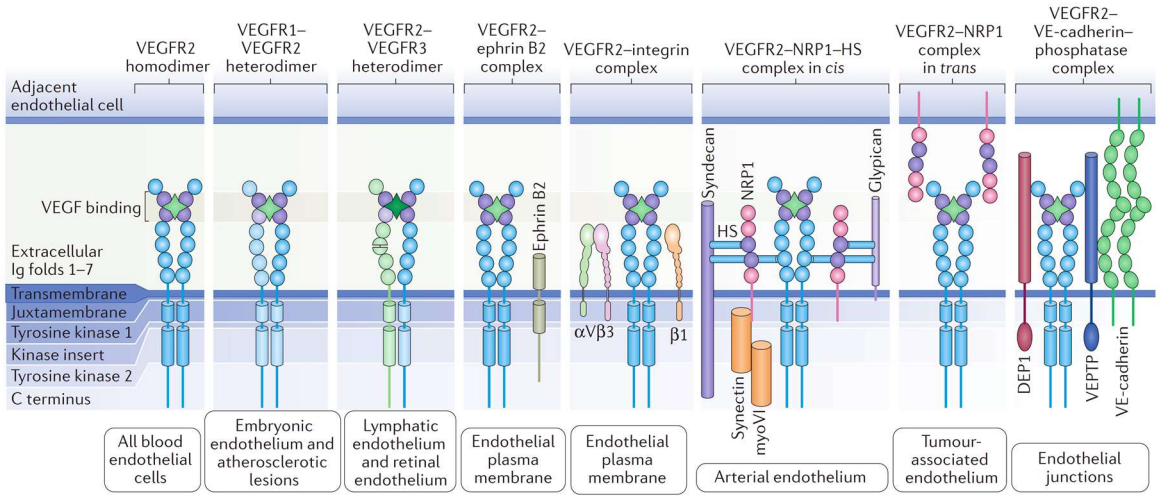


**Figure 8. VEGF-R2 signaling complexes.** Upon VEGF binding, VEGF-R2 dimerizes, either as a homodimer or a heterodimer with VEGF-R1 or VEGF-R3. VEGF-R2 can bind ephrinB2 *in cis*, enhancing the receptor internalization. Complex of VEGF-R2 with integrins (integrin-β1 and integrin-αVβ3) can also enhance downstream signaling. In arterial endothelium, VEGF-R2 can make a complex with Neuropilin (NRP) co-receptors and heparan sulfate (HS) proteoglycans like syndecan and glypican. This complex involves synectin and myosin VI (myoVI). In tumors, VEGF-R2 can bind Neuropilins *in trans.* In endothelial junctions, VEGF-R2 can make a complex with vascular endothelial cadherin (VE-cadherin) and phosphatases DEP1 (density-enhanced phosphatase 1) and VEPTP (vascular endothelial protein tyrosine phosphatase) [Adapted from Simons, M. et al. 2016 (78)]

Other important partners in VEGF-R2 signaling complexes are integrins, particularly integrin-β1 and integrin-β3. The sequence motif involved in this interaction still needs to be clarified. VEGF-A induces VEGF-R2–integrin-β3 association, resulting in integrin-β3 tyrosine phosphorylation (113). This interaction is required for complete VEGF-R2 activation (114), and can involve other partners such as syndecan 1 and SRC. ECM-binding VEGF-A isoforms promote VEGF-R2–integrin-β1 complex formation. This directs VEGF-R2 localization to focal adhesions, which is accompanied by prolonged receptor activation (115) (Figure 8). Tetraspanin CD63 is another member of the VEGF-R2–integrin-β1 complex, and loss of CD63 expression impairs VEGF-R2 signaling (116).

EphrinB2, a member of a family of axon guidance molecules, is involved in VEGFR trafficking. Deletion of ephrinB2, which interacts with both VEGF-R2 and VEGF-R3, leads to

a complete lack of VEGF-R2 endocytosis in blood vascular endothelial cells after stimulation with VEGF-A (44). Same effect is observed for VEGF-R3 uptake after stimulation with VEGF-C in lymphatic endothelial cells (45). EphrinB2 deletion is consequently leading to disruption of both postnatal angiogenesis and lymphangiogenesis. Molecularly, ephrinB2 regulates VEGF-R2 endocytosis through interaction with disabled homologue 2 (DAB2) and the cell polarity regulator partitioning defective 3 homologue (PAR3) (117). This complex favors internalization of the VEGF-R2 in $RAB5^{+}EEA1^{+}$ endosomes, enhancing VEGF signaling (Figure 9). The details about ephrin/Eph signaling will be discussed in next chapters.

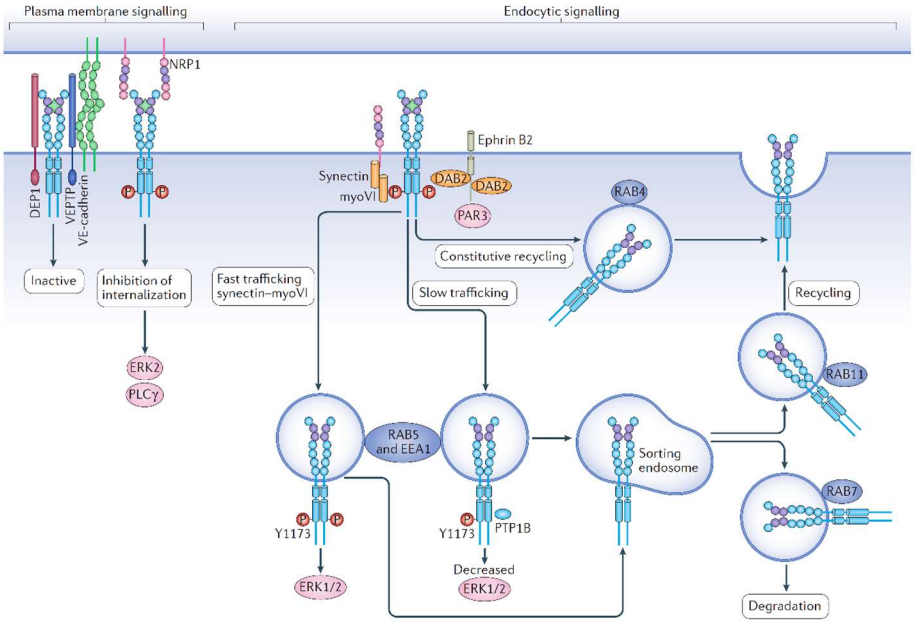


**Figure 9. VEGF-R2 receptor endocytosis.** VEGF-R2 internalization is modulating downstream signaling activation. When VEGF-R2 is associated with VE-cadherin-VEPTP (vascular endothelial protein tyrosine phosphatase) -DEP1 (density-enhanced phosphatase 1) complex at endothelial cell junctions, the receptor is dephosphorylated and inactive. Neuropilin-1 (NRP-1) can bind VEGF-R2 *in trans* and prevent its internalization, favoring activation of ERK2 and PLCγ over other signaling molecules. When NRP-1 binds VEGF-R2 *in cis*, receptor is internalized and trafficked to $RAB5^{+}$ $EEA1^{+}$ (early endosome antigen 1) endosomes by a NRP-1–synectin–myoVI complex. VEGF-R2 may also be constitutively recycled via RAB4 endosomes independently of ligand binding. EphrinB2 can form a complex with VEGF-R2 together with DAB2 (disabled homologue 2) and PAR3 (partitioning defective 3 homologue), which enhance receptor internalization and downstream signaling. Signaling continues within endosomes until p-Tyr1173 (pY1173) in VEGF-R2 is dephosphorylated by PTP1B (protein tyrosine phosphatase 1B). After that, VEGF-R2 can be degraded by shuttling to RAB7 endosome or it can be recycled to the cell surface by RAB11 endosomes [Adapted from Simons, M. et al. 2016 (78)]

VE-cadherin is another VEGF-R2-interacting protein that controls its endocytosis. Interactions between these two molecules occur at cell-cell junctions (118). VE-cadherin keeps VEGF-R2 inactive by recruitment of VEPTP and DEP1 phosphatases (Figure 8, Figure 9). Deletion of *Cdh5* gene, coding for VE-cadherin, leads to enhanced VEGF-R2 endocytosis and activation of ERK signaling (78, 119).

Epsins, membrane proteins involved in regulation of membrane curvature, have also been reported to affect VEGF-R2 and VEGF-R3 endocytosis. Specific deletion of both epsins in endothelium, leads to enhanced VEGF-R2 signaling and excessive non-productive angiogenesis (78, 120).

Besides VEGFs, non-canonical ligands and stimuli can also activate VEGF-R2. Some non-VEGF ligands include β-galactoside-binding proteins, called galectins (121), lactate, low-density lipoproteins (122-124), bone morphogenetic protein (BMP) antagonist gremlin (GREM1) (125) and mechanical forces, such as shear stress (126, 127). Fluid shear stress can induce phosphorylation of VEGF-R2 through formation of mechanosensory complex that includes, in addition to VEGF-R2, platelet endothelial cell adhesion molecule 1 (PECAM1, also called CD31) and VE-cadherin (81, 127). Alternatively, purinergic receptor P2Y2 and G proteins Gq and G11 ($G_q$/$G_{11}$) have also been implicated in fluid shear stress-induced endothelial responses by activation of SRC, AKT, endothelial nitric oxide synthase (eNOS) and phosphorylation of PECAM1 and VEGF-R2 (128).

### 2.3.3. Downstream VEGF-R2 signaling

After stimulation of VEGF-R2 either by canonical or non-canonical activators, VEGF-R2 is auto-phosphorylated, internalized and further downstream signaling leads to expression of specific genes which regulate angiogenesis (Figure 10). There are three main intracellular signaling pathways downstream of VEGF-R2. First one involves phospholipase Cγ (PLCγ)–ERK1/2 pathway. This signaling branch controls cell proliferation and has a central role during

vascular development and in adult arteriogenesis. Second one is the PI3K–AKT–mTOR pathway, controlling cell survival, vasomotion and barrier function. The third pathway involves SRC and small GTPases and it regulates cell migration, polarization, cell shape, endothelial junctions and barrier function. Other pathways involving stress kinases like p38 MAPK, STATs and G protein-coupled receptor (GPCR)-dependent signaling, are poorly understood (78).

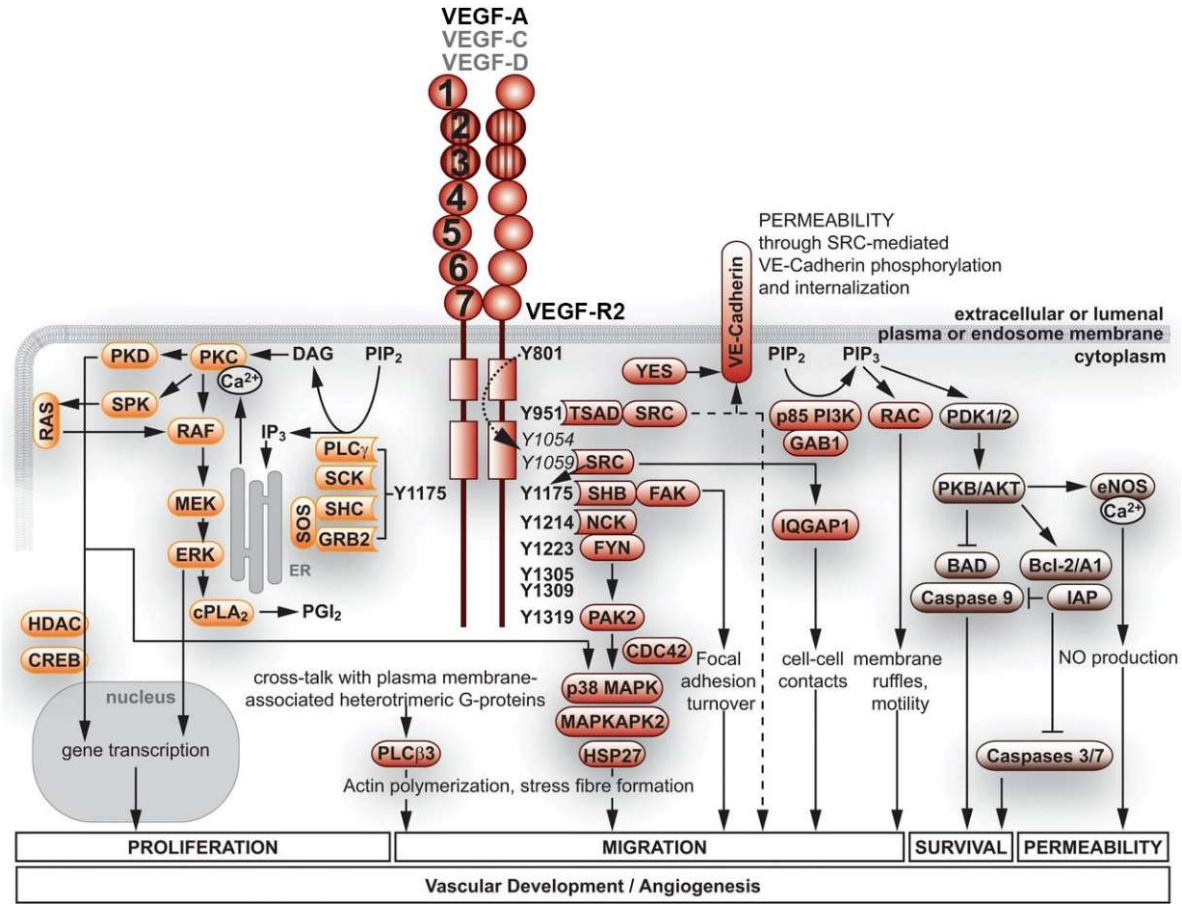


**Figure 10. VEGF-R2 downstream signaling.** Binding of VEGF to VEGF-R2 induces phosphorylation of several tyrosines (marked with numbers) in the receptor. Phosphorylated Y1175 (Y1173 in mouse) is a docking site for PLCγ and adapter proteins SHB (SH2-domain-containing adaptor protein B), SCK [SHC (SRC homology and collagen homology)-transforming protein] and GRB2 (Growth factor receptor-bound protein 2) which then recruits nucleotide-exchange factor SOS (Son of sevenless). MAPK pathway (RAF-MEK-ERK), regulating proliferation, is activated through $Ca^{2+}$-dependent protein kinase C (PKC), protein kinase D (PKD) and sphingosine kinase (SPK). PKD activation promotes nuclear translocation of HDAC (histone deacetylase) followed by phosphorylation of CREB (cAMP-response-element-binding protein) as well as HSP27 (heat-shock protein 27). VEGF-induced RAS activation leads to production of prostaglandins like PGI2 (prostaglandin I2) via cPLA2 (cytoplasmic phospholipase A2). Phosphorylated Y951 is a binding site for SH2-domain-containing TSAd

(T-cell-specific adapter molecule) which forms a complex with SRC and regulates cell permeability together with VE-cadherin. Phosphorylated Y1214 is a docking site for NCK–FYN complex which mediates phosphorylation of PAK2 (p21-activated protein kinase 2) and activation of CDC42 (cell division cycle 42) and p38MAPK, ultimately regulating cell migration. The docking protein GAB1 (GRB2-binding protein 1) contains a binding site for the p85 subunit of PI3K which activates AKT, also known as PKB (protein kinase B) through PDK1 (phosphoinositide-dependent kinase 1) and PDK2. AKT phosphorylates BAD [Bcl (B-cell lymphoma)-2-associated death promoter] and caspase 9 and inhibits apoptosis together with anti-apoptotic proteins Bcl-2, A1 and IAP (inhibitor of apoptosis) [Adapted from Koch, S. et al. 2011 (81)]

*PLCγ–ERK1/2 pathway*

ERK1/2 signaling induced by VEGF is crucial in endothelial cell biology since it controls endothelial cell proliferation, migration, arterial fate specification and homeostasis. The pathway activation cascade initiates by phosphorylation of Y1173 in VEGF-R2 in mice (Y1175 in the human protein). Phosphorylated Y1173 is the docking site for PLCγ. Mutation of tyrosine 1173 to phenylalanine is lethal and phenocopies *Vegfr2* gene inactivation (129, 130). Upon binding, PLCγ is activated and through its enzymatic activity generates inositol 1,4,5- trisphosphate (IP3) and diacylglycerol (DAG). IP3 induces release of $Ca^{2+}$ from the endoplasmic reticulum, which together with DAG activates $Ca^{2+}$-dependent protein kinase Cβ2 (PKCβ2), which then regulates the RAF1–MEK–ERK1/2 cascade. Phosphorylation of the activating Ser338 and de-phosphorylation of the inhibitory Ser259 site are required for RAF1 activation. Many kinases are controlling this process so this is the point of interaction with other signaling like PI3K–AKT and LATS–Hippo (78). VEGF-R2 signaling bypasses the more common RTK-induced RAS activation of the RAF1–MEK–ERK1/2 cascade (78, 131). Still, it was reported that VEGF can induce activation of RAS in cultured cells (132). Knockdown of PLCγ in zebrafish leads to a complete loss of VEGF-induced ERK1/2 activation (133), but deletion of *Prkcb* in mice, encoding both PKCβ1 and PKCβ2 isoforms, did not induce any vascular malformations (134). This suggests that PKCβ-RAF1–MEK–ERK1/2 pathway can be either compensated by other PKCs or there is alternative non-PKCβ- dependent pathways for activation of VEGF-induced ERK1/2 activation (78). The pY1173 is also a docking site for

adapters SH2 domain-containing adapter protein B (SHB) and SHC-transforming protein 2 (SHC2; also known as SCK). The PLCγ–PKC pathway activates E26 transformation-specific (ETS) family of transcription factors (135) and mediates phosphorylation of histone deacetylase 7 (HDAC7) (136), both of which are regulating many genes involved in endothelial cell physiology. Fibroblast growth factor (FGF) and VEGF signaling are probably connected through ERK1/2 pathway. FGF can upregulate *Vegfr2* expression through ERK1/2 dependent pathway. Additionally, VEGF inhibition is blocking FGF-driven angiogenesis, suggesting that FGF controls angiogenesis upstream of VEGF (78).

*PI3K-AKT-mTOR pathway*

Phosphoinositide 3 kinase (PI3K) is not activated directly by VEGF-R2 since VEGF-R2 does not contain a binding site for the SH2-domain-containing p85 subunit of PI3K, but indirectly, either by SRC, VE-cadherin (137) or by AXL (138). Activated PI3K phosphorylates phosphatidylinositol (4,5)-bisphosphate (PIP2) to phosphatidylinositol (3,4,5)-trisphosphate (PIP3), a second messenger that binds to plextrin homology (PH) domain of AKT family of serine/threonine kinases. AKT kinases are regulating cell survival, proliferation and apoptosis (139). The AKT family consists of three members (AKT1-3), with AKT1 being the predominant isoform which regulates both pathological and adult angiogenesis, as well as vascular maturation and metabolism, through activation of the mTOR complex 2 (140). It was demonstrated that p110α catalytic subunit of PI3K is necessary for normal vascular development as embryos with kinase dead p110α subunit develop vascular defects that are caused by the reduction in small GTPases activation and suppression of endothelial migration (141). In endothelial cells, small GTPases RHO, CDC42 and RAC1 are responsible for regulation of cell morphology, adhesion, migration, junctional integrity and cytoskeletal organization (78).

*SRC pathway*

The SRC proteins are a family of cytoplasmic tyrosine kinases and the members found in endothelium are SRC, YES and FYN. Activation of the SRC pathway is controlled by phosphorylation of Y949 (in the mouse protein; Y951 in the human protein) in the receptor kinase insert of VEGF-R2, which is a docking site for SH2 domain of T cell- specific adapter (TSAd), which in turn binds to the SH3 domain of SRC. SRC pathway is controlling cytoskeleton remodeling, such as actin and cell–cell adhesion components, vascular permeability and leakage, as well as the cell-matrix adhesion process (78). SRC signaling can be activated by shear stress (142). SRC can phosphorylate focal adhesion kinase (FAK) and in that way, regulate cell shape and adhesion (143). Furthermore, SRC regulates endothelial adherens junctions by phosphorylating VE-cadherin in response to VEGF, leading to increased vascular permeability (78).

## 2.4. Notch signaling

Besides VEGF, Notch signaling also has a critical role in vascular system. Notch pathway is evolutionary highly conserved and it is controlling many different biological processes. Mutation in genes involved in Notch pathway have been associated with several disorders like T-cell acute lymhoblastic leukemia, Alagille syndrome (developmental abnormalities affecting many tissues), spondylocostal dysostosis (vertebral development disorder), CADASIL (cerebral autosomal dominant arteriopathy with subcortical infarcts and leukoencephalopathy) syndrome and some congenital heart defects like tetralogy of Fallot and aortic valve disease (144). All disorders are characterized by dysregulation of cell proliferation and differentiation, but it is important to note that the outcome of Notch signaling is context dependent so it can promote tissue growth and cancer progression in some cases, while in the other situations it can induce cell death and tumor suppression (145).

### 2.4.1. Notch receptors and ligands

In mammals, Notch receptor family consist of four type I transmembrane receptors (Notch1-4) that regulate cell fate through cell-cell interactions. There are five Notch ligands: Jagged1 (Serrate1), Jagged2 (Serrate2), Delta-like1 (Dll1), Delta-like3 (Dll3), and Delta-like4 (Dll4), collectively referred to as the DSL (Delta/Serrate/Lag-2) family (Figure 11).

Notch receptors are translated as large precursor proteins (~300 kDa) which are cleaved in trans-Golgi network by furin at S1 cleavage site producing extracellular fragment (NotchEC) and an extracellular-transmembrane-intracellular fragment (NotchTM) that is expressed on the cell surface as a noncovalently linked heterodimer stabilized by a $Ca^{2+}$ ions (Figure 13). Extracellular domain (ECD) of mature Notch receptors contains 29–36 multiple epidermal growth factor (EGF)-like repeats and 3 lin-12/Notch (LNR) motifs. EGF-like repeats are involved in ligand binding, while LNR motifs are preventing activation of receptor in the absence of a ligand (146) (Figure 11).

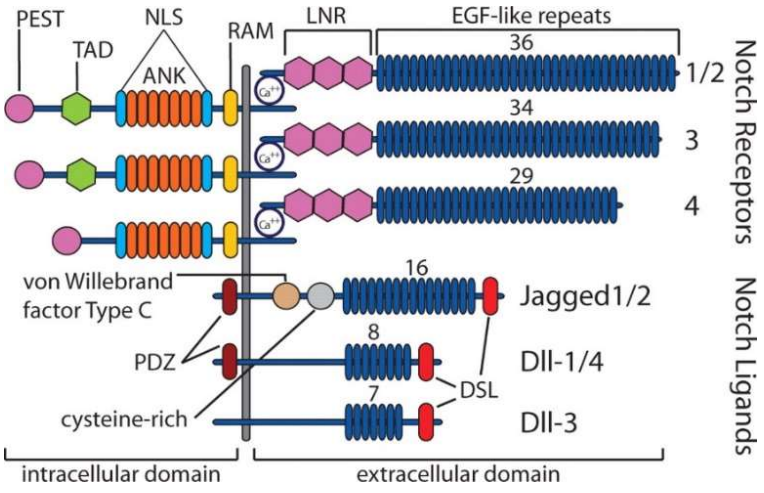


**Figure 11. Notch ligands and receptors.** In mammals, there are four Notch receptors (Notch1-4) and five ligands (Jagged1, Jagged2, Dll1, Dll3 and Dll4). Notch receptors are expressed on the cell surface as heterodimers stabilized by calcium ions. Extracellular domain of human Notch receptors contains 29–36 epidermal growth factor (EGF)-like repeats, 3 Lin- 12/Notch (LNR) repeats, and a heterodimerization domain. The intracellular domain contains an RBP-Jκ-associated molecule (RAM) domain, 7 ankyrin (ANK) repeats, 2 nuclear localization signals (NLS), a transactivation (TAD) domain, and a PEST domain. The extracellular domain of Notch ligands contains unique a Delta/Serrate/Lag2 (DSL) domain and 7-16 EGF repeats. Jagged1 and Jagged2 also contain a cysteine-rich domain and a von Willebrand factor type C domain. PDZ (PSD-95/Dlg/ZO-1) domain is found in Jagged1 and Dll1, and it plays a role in downstream signaling [Reprinted from Niessen, K. et al. 2007 (146)]

Glycosylation in EGF repeats in ECD domain is profoundly affecting receptor activation by the ligands. Modifications include O-fucosylation, O-glucosylation, and O-GlcNAcylation. This process is controlled by several glycosyltransferases like POFUT1 (Protein O-fucosyltransferase 1), POGLUT1 (Protein O-glucosyltransferase 1), and EOGT1 [(Epidermal growth factor (EGF) domain-specific O-linked N-acetylglucosamine (GlcNAc) transferase 1)]. Xylosyltransferases GXYLT1/2 (Glucoside xylosyltransferase 1) and XXYLT1 (Xyloside Xylosyltransferase 1) can further modify O-glucose, while Fringe family of GlcNAc-transferases modifies O-Fucose. Interestingly, modifications at EGF6 and 36 in Notch1 ECD (added by Manic and Lunatic, but not Radical Fringe) specifically inhibited Notch1 activation by Jagged1, clearly depicting importance of glycosylation in modulation of Notch signaling (147).

The intracellular domain (ICD) of Notch receptors contains a RAM [recombination signal binding protein-1 for Jκ (RBP-Jκ)-associated molecule] domain, 7 cdc10/ankyrin repeats (only six C-terminal repeats assume proper ankyrin fold), and a transactivation domain (TAD), which is not present in Notch4 receptor. Additionally, there are two nuclear localization signals, glutamine-rich stretch and a PEST [rich in proline (P), glutamic acid (E), serine (S) and threonine (T) residues] domain (146). The RAM domain and ankyrin repeats are interacting with the transcription factor CSL, also known as RBP-Jκ in mouse or CBF1 in human [CSL: C promoter binding factor-1 (CBF1), suppressor of hairless, Lag-1; RBP-Jκ: Recombination Binding Protein for immunoglobulin kappa J region; CBF-1: C-repeat/DRE Binding Factor 1]. Additionally, the seventh ankyrin repeat together with TAD domain recruit transcriptional activators such as mastermind-like (MAML) and the histone acetyltransferase (HAT) complex. The PEST domain regulates protein half-life of the Notch receptors (146) (Figure 11).

Notch ligands are also type I transmembrane proteins, with an extracellular domain comprised of 7–16 EGF-like repeats and a DSL domain, which is unique to Notch ligands. Jagged1 and Jagged2 have additional cysteine-rich domain and a von Willebrand factor type C domain in the extracellular region. The EGF-like repeats probably stabilize receptor-ligand complex while the DSL domain interacts with EGF-like repeats 11 and 12 of the Notch receptors and is responsible for Notch receptor activation. The cysteine-rich domains of Jagged ligands are thought to control Notch receptor binding specificity, while the von Willebrand factor type C domain regulates ligand dimerization. DSL ligands have short intracellular regions that contain PDZ domain (absent in Dll3), which is believed to activate downstream signaling (146) (Figure 11). Notch receptors and ligands can interact *in cis* (in the same cell) and *in trans* (different cells). *In trans* ligand-receptor binding will activate receptor, while *in cis* interaction will lead to inhibition of signaling (148). Dll3 does not bind Notch receptor *in trans*, and does not activate Notch signaling (149), so the role of Dll3 in Notch signaling still needs to be clarified (148).

Besides canonical ligands, Notch signaling can also be regulated by non-canonical ligands, which can have both inhibitory or activating role. So far, several non-canonical Notch ligands have been identified and the members found in vertebrates will be shortly described. They can be divided into three groups: transmembrane, glycosylphosphatidylinositol (GPI)-linked and secreted (Figure 12). Transmembrane ligands include Dlk-1 (Delta-like 1), Dlk-2 (Delta-like 2)/EGFL9 (Epidermal growth factor-like protein 9), DNER (Delta/Notch-like EGF-related receptor) and Jedi (Jagged and Delta protein). Dlk-1 and Dlk-2 can antagonize Jagged-1-induced Notch activation (150, 151). DNER can bind Notch receptor *in trans* and activate CSL reporter (152). Jedi has very weak inhibitory effect on Notch signaling and its role as a non-canonical Notch ligand has been poorly investigated (148). Other two members are F3/contactin1 and NB3/contactin6, GPI-linked neural cell adhesion molecules that can induce

oligodendrocyte differentiation by activation of Notch signaling (153, 154). However, it has not been demonstrated that they can induce CSL-dependent activation of Notch downstream target genes (148). Secreted non-canonical Notch ligands are CCN3 (connective tissue growth factor/ cysteine-rich 61/nephroblastoma overexpressed gene), MAGP-1 (microfibril-associated glycoprotein-1), MAGP-2, thrombospondin 2 (TSP2), YB1 (Y-box protein-1) and EGFL7 (EGF-like domain-containing protein 7). CCN3, MAGP-1, MAGP-2, TSP-2 and YB1 were described as activators of Notch signaling (148, 155-157), while EGFL7 inhibits Notch signaling and reduces neural stem cell renewal and proliferation (158). EGFL7 is expressed by endothelial cells during active angiogenesis (159).

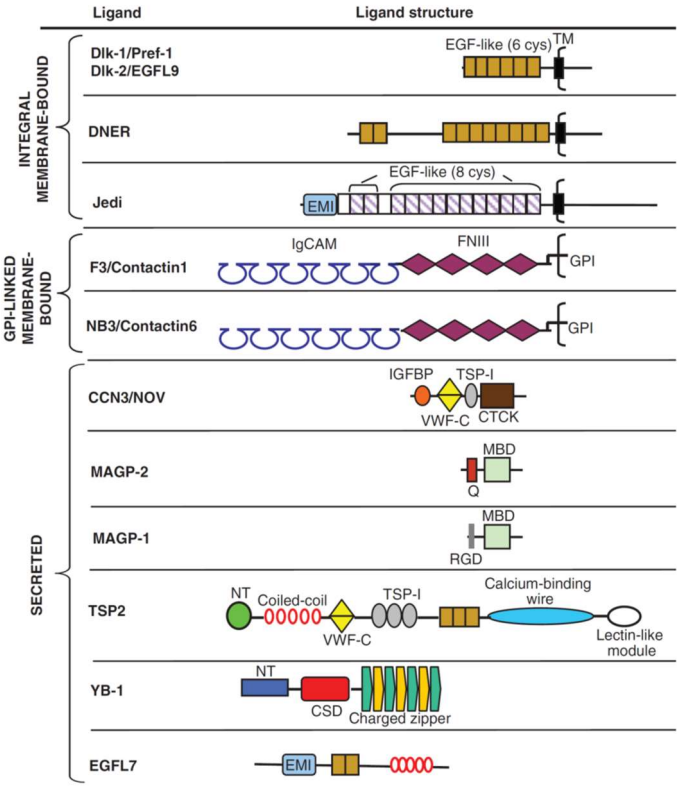


**Figure 12. Non-canonical Notch ligands.** Non-canonical Notch ligands in vertebrates are structurally diverse and lack a DSL (Delta/Serrate/LAG-2) domain. They can be divided into three groups: integral-membrane bound, GPI (glycosylphosphatidylinositol)-linked and secreted. Integral members (Dlk-1, -2, DNER, Jedi) contain EGF-like domains, either the one with 6 cysteines (6-cysteine epidermal growth factor-like repeat), found in canonical ligands or the one with 8 cysteines (EGF-like motif with 8 cysteines that is not laminin-like), transmembrane domain (TM) and emilin-like domain (EMI). GPI -linked members (F3, NB3) contain immunoglobulin-containing cell adhesion molecule domain (IgCAM) and fibronectin type III domain (FNIII). Secreted members are structurally very diverse. CCN3/NOV contains insulin-like growth factor-binding protein-like domain (IGFBP), von Willebrand factor type C-like domain (VWF-C), thrombospondin type 1-like domain (TSP-1) and Notch receptor binding C-terminal cysteine knot domain (CTCK). MAGP-1 and MAGP-2 contain matrix binding domain (MBD) which binds Notch receptor, and either glutamine-rich region (Q) or integrin- binding motif (RGD). TSP-2 additionally contains N-terminal domain (NT), calcium-binding wire and lectin-like domain. YB-1 has specific cold shock domain (CSD), while EGFL7 contains EGF-like repeats and EMI domain, which are both Notch receptor binding regions [Adapted from D'Souza, B. et al. 2010 (148)].

### 2.4.2. Downstream Notch signaling

After binding of the ligand, Notch receptor is enzymatically cleaved at three sites. First, extracellular domain is cleaved by ADAM10 (A disintegrin and metalloprotease 10) or ADAM17/TACE (tumor necrosis factor-α converting enzyme) at the S2 cleavage site. Next two intramembranous cleavage steps, at S4 (between Ala1731-Ala1732 in mouse Notch1) and S3 site (Val1744 in mouse Notch1), are processed by γ-secretase which is a 170 kDa integral membrane protein complex composed of four proteins. Presenilin (Presenilin1 or Presenilin2) provides catalytic domain to the complex, Pen-2 is required for the maturation of the Presenilin, Aph-1 (Aph-1a or Aph-1b) helps in γ-secretase complex assembly, while Nicastrin stabilizes the complex, and is potentially involved in substrate recognition. After two cleavage steps, Notch intracellular domain (NICD) is released, and subsequently translocates in the nucleus mediating gene expression (Figure 13). Endocytosis of ligand-receptor complex into ligand-bearing cell via clathrin-dependent vesicles, seems to play a crucial role in activation of the Notch cleavage, as it generates mechanical forces that trigger enzymatic cleavage (147, 160). It was demonstrated that ubiquitinoylation by E3 ubiquitin ligases Mindbomb and Neuralized, and subsequent endocytosis of the ligand is a prerequisite to render the ligand active (144, 148, 161).

CSL transcription factor is the main effector of Notch signaling pathway. In non-activated state, it binds to one of two repressor complexes; SMRT/NcoR/HDAC-1 (SMRT: silencing mediator of retinoid and thyroid hormone receptors, NcoR: nuclear receptor corepressor, HDAC-1: histone deacetylase-1) or CIR/HDAC2/SAP30 (CIR: CBF1 interacting corepressor, HDAC-2: histone deacetylase-2, SAP30: Sin3A-associated protein, 30 kDa). When NICD translocates to the nucleus it binds to CSL. The mechanism of activation is not completely elucidated, but it was shown that NICD complex includes Ski interacting protein (SKIP), a protein that can interact with CSL, Notch, or SMRT, but promotes NICD-CSL

interactions over CSL-SMRT interaction. Additionally, the coactivator MAML can bind to transcription machinery, help in displacement of co-repressor complex and enhance gene expression. MAML binds only NICD-CSL complex but does not bind either NICD or CSL independently. *Hairy and enhancer of split-related* (*HESR*) genes, which encode basic helix-loop-helix (bHLH) transcriptional repressors, are key genes activated by Notch signaling. Two most important families in this group of genes are *Hes* (*hairy enhancer of split*) and *Hey* (*hairy/enhancer of split-related with YRPW motif),* also called *CHF* or *Hrt*. Other activated gens are *cyclinD1*, *p21*, *glial fibrillary acidic protein* (*GFAP*), *Nodal*, *Myc*, *PTEN*, *ephrinB2*, and *smooth muscle α-actin* (*SMA*) (146, 162).

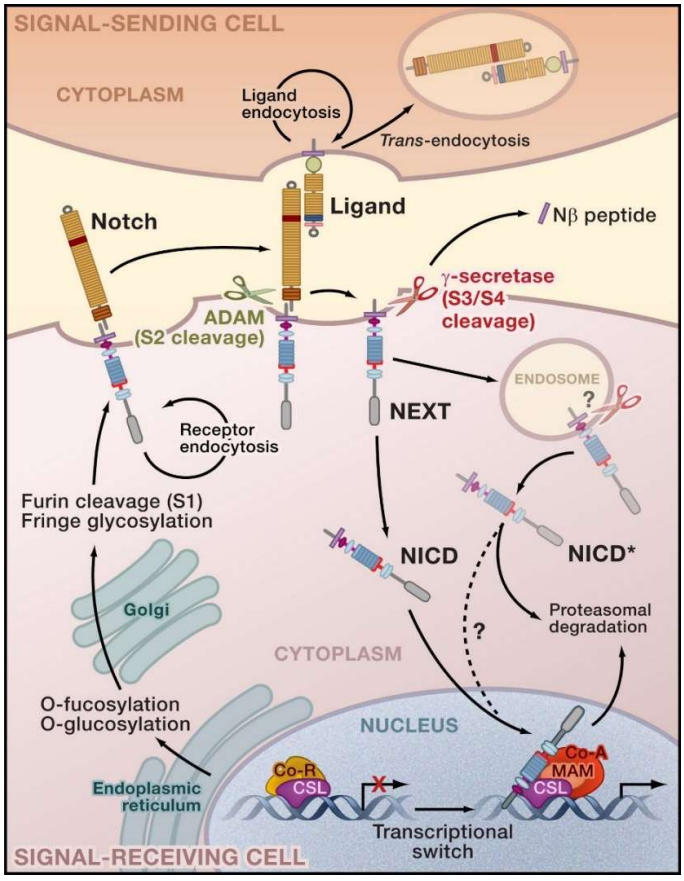


**Figure 13. Notch processing and downstream signaling**. Full length Notch receptor protein is glycosylated and subsequently cleaved in Golgi at S1 site by PC5/furin, further glycosylated by glycosyltransferase Fringe and then translocated to the cell surface as a functional heterodimer receptor stabilized by noncovalent interactions. Upon ligand binding, receptor is cleaved at S2 site by ADAM metalloproteases generating the membrane-anchored Notch extracellular truncation (NEXT) fragment, a substrate for the γ-secretase complex which further cleaves at S4 and S3 sites. This generates Notch intracellular domain (NICD) and Nβ peptide. γ-Secretase cleavage can occur both at the cell surface and in endosomal compartments, but cleavage in the endosome results in a less stable form of NICD (NICD*). NICD then enters the nucleus where it associates with the DNA-binding protein CSL (CBF1/Su(H)/Lag-1). In the absence of NICD, CSL can associate with ubiquitous corepressor (Co-R) proteins and histone deacetylases (HDACs) and repress gene transcription. Upon NICD binding, allosteric changes may occur in CSL facilitating displacement of transcriptional repressors. Subsequently, transcriptional coactivator Mastermind (MAM) binds NICD/CSL complex, further association of coactivators (Co-A) proceeds and transcription is activated [Reprinted from Kopan, R. et al. 2009. (163)]

The NICD is phosphorylated in the PEST domain by the cyclin C/cyclin-dependent kinase-8 (Cyc:CDK8) complex and glycogen synthase kinase 3β (GSK-3β). NICD phosphorylation is followed by ubiquitylation by E3 ubiquitin ligase Fbxw7 (F-box and WD-40 domain protein 7) also known as CDC4 and SEL10, leading to the its rapid proteasomal degradation and termination of downstream signaling (162, 164).

### 2.4.3. Notch signaling in the vascular system

Notch signaling is regulating vasculogenesis, angiogenesis and arterio-venous specification. At embryonic day 9.5 (E9.5) Notch1, Notch4 and Dll4 are expressed in primitive vascular plexus. At E13.5 Notch1, Notch2, Notch4, Dll4, Jagged1 and Jagged2 are mainly expressed by the arteries, while Notch1 and Dll4 can also be found in capillaries (146).

Notch signaling is regulating arterio-venous specification by promoting arterial, while suppressing venous phenotype. The arterio-venous specification begins even before the start of the circulation and differential gens expression is crucial for this process. Both VEGF and Notch signaling were shown to positively regulate expression of arterial marker ephrinB2 (165-169). VEGF initially upregulates Dll4, one of the main arterial markers (170), but later, Notch activity is maintaining Dll4 expression through RBPJ and SoxF transcription factors (171). In venous endothelium, COUP-TFII (chicken ovalbumin upstream promoter transcription factor II), a nuclear orphan receptor transcription factor, suppresses arterial phenotype by suppressing Notch activity, NRP-1 expression and MAPK signaling. Downregulation of Notch signaling leads to reduced expression of ephrinB2 and upregulation of EphB4 (168, 172).

**Table 1. Mutants of Notch pathway components and their phenotype**

| Mouse model | Survival | Vascular defects |
|---|---|---|
| ***Notch1*-null** | Embryonic lethal before E10.5 | - Defective remodeling of vascular plexus<br>- Highly disorganized intersomitic vessels<br>- Dorsal aorta and cardinal vein reduced in size (173) |
| ***Notch2*-null** | Embryonic lethal at E11.5 | - Several cardiovascular and renal defects (174, 175) |
| ***Notch3*-null** | Mice are viable | - Some arteries are covered with thinner smooth muscle cell coating (176, 177) |
| ***Notch4*-null** | Mice are viable | - No vascular defects<br>- Slightly elevated systolic blood pressure after induction of ischemia (178, 179) |
| ***Jagged1*-null** | Embryonic lethal at E11.5 | - Defective remodeling of vascular plexus<br>- Hemorrhage early during embryogenesis (180) |
| ***Jagged2*-null** | Mice die perinatally | - No vascular defects<br>- Defects in craniofacial morphogenesis<br>- Syndactyly (181) |
| ***Dll1*-null** | Embryonic lethal at E12 | - Severe hemorrhages (182) |
| ***Dll3*-null** | Mice are viable | - No vascular defects<br>- Severe vertebral and rib deformities (183) |
| ***Dll4*-haploinsufficiency** | Embryonic lethal | - Defective remodeling of vascular plexus<br>- Severe defects of arterial vasculature (184) |

Some disorders in human, which affect vascular system, are associated with mutations in some of the components of Notch pathway. CADASIL (Cerebral autosomal dominant arteriopathy with subcortical infarcts and leukoencephalopathy) is a disorder characterized by the defect in arterial vascular homeostasis, migraine headaches and mood disturbances (185). Missense point mutations in *Notch3* gene, expressed mostly in smooth muscle cells, that result in an odd number of cysteine residues in the EGF repeat regions, are found in 95% of CADASIL cases. This disorder is characterized by loss of arterial vascular smooth muscle cells and increased vascular fibrosis, leading to narrowing of the lumen of small and medium arteries. Mutations in the *Notch1* locus have been associated with different heart defects like bicuspid aortic valve disease and calcification of the aortic valve (186). Mutations in the *Jagged1* locus are found in 94% of patients with Alagille syndrome (AGS), a disorder

associated with abnormalities of the intrahepatic bile ducts, kidney, heart, eyes and the skeleton. Most common cardiovascular defect in patients with AGS is peripheral pulmonic stenosis. Furthermore, 13% of AGS patients have Tetralogy of Fallot (187, 188). Jagged1-independent AGS can also be caused by mutation in *Notch2* locus (146, 189).

Notch4 or int-3 was first identified for its oncogenic effects in MMTV (mouse mammary tumor virus)-induced mammary gland tumors, as *int-3* locus is a frequent target for insertional activation by MMTV proviral DNA (190). It is interesting that Notch1/Notch4 double deficient mice have more severe vascular phenotype, as compared to Notch1-deficient mice. This suggests that loss of Notch4 can somehow worsen the phenotype of Notch-1 null mice (178), even though Notch4-deficient mice show no apparent vascular phenotype and are viable (178). Notch4 is mostly produced by endothelial cells, but its role in the vasculature is still not completely clear (190). Polymorphisms in *Notch4* gene are associated with development of brain arterio-venous malformations and hemorrhagic presentations (191). Constitutively active Notch4 signaling induces arterio-venous malformations (AVM) (192-196) accompanied with lack of small branched vessels and vessel integrity (197). During the process of AVM development, expression of EphB4 is markedly reduced, but restored during the AVM normalization, as the process of normalization is accompanied by venous phenotype restoration (195). Some groups demonstrated that Notch4 can be activated by canonical Notch ligands (198, 199), but others reported that Notch4, unlike Notch1, cannot be activated by the ligands (200, 201). Additionally, it was shown that Notch4 can even dose-dependently inhibit ligand-induced Notch1 signal activation in cultured cells (201). The role of Notch4 in the angiogenic process remains to be elucidated.

### 2.4.4. Notch signaling in sprouting angiogenesis

VEGF is activating endothelial cell and starting the complex signaling cascade. In sprouting angiogenesis, specification of tip and stalk cell, as an initial step in this process, is

regulated by Notch signaling (36, 46, 47). Notch ligand Dll4 is expressed at high levels in tip cells. VEGF activates VEGF-R2 and upregulates expression of Dll4 in all cells, but some of them will express it faster or at higher levels and get an advantage to become tip cell. Repressor complex TEL/CtBP at the Dll4 promoter can be transiently disassembled upon VEGF stimulation, allowing fast pulse of Dll4 expression, allowing fast specification into tip cell (202). Dll4 will activate Notch1 in neighboring endothelial cells, which then become stalk cells, by downregulating VEGF-R2, VEGF-R3 and NRP-1, while upregulating VEGF-R1 (46, 203). VEGF-R1 is helping in the guidance of the sprout and inhibits tip cell formation (203). Inhibition of Dll4 or Notch signaling in tumor or during development leads to hypersprouting due to increase in tip cell number (204). Jagged1, in contrast to Dll4, is expressed in stalk cells. Jagged1 is a poor Notch1 activator, as modification of Notch by Fringe glycosyltransferases favors activation by Dll4 (47, 205). Some Dll4 can still be detected in the stalk cells, but Jagged1 antagonizes Dll4 signaling back to the tip cells, and in that way maintains differential Notch activity (36) (Figure 14).

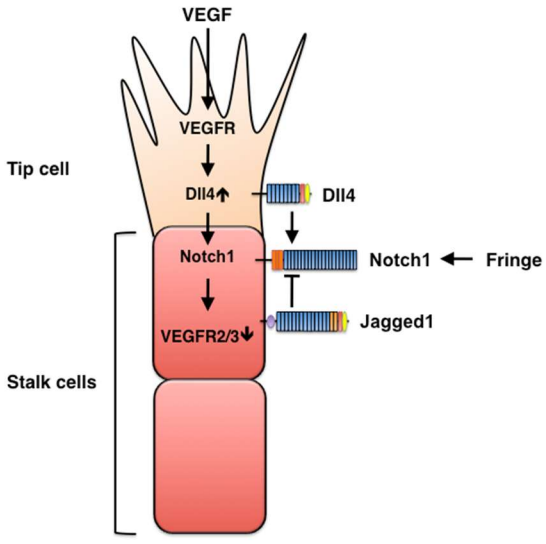


**Figure 14. Notch signaling in tip-stalk specification.** During sprouting angiogenesis, VEGF upregulates Dll4 expression in tip cell, which in turn activates Notch1 on stalk cells, downregulating VEGF-R2 and -R3, and upregulating Jagged1 in stalk cells. Jagged1 antagonizes Notch1-Dll4 signaling back to the tip cell, maintaining tip-stalk phenotype. Differential regulation of Notch1 activity by Dll4 and Jagged1 is controlled by glycosylation of the receptor by Fringe [Reprinted from Kume, T. 2009 (206)]

# 3. Vessel maturation

After vessel network had expanded through either process of sprouting or splitting angiogenesis, it needs to mature. Vessel maturation is the process that involves vessel network remodeling according to the local tissue needs. This process involves recruitment of mural cells; pericytes and vascular smooth muscle cells (vSMCs) and deposition of extracellular matrix (36). Pericytes were first described by Rouget in 1873, and Zimmerman later coined a term 'pericytes' to describe their close proximity to endothelial cells (207). Definition of a pericyte is still not completely clear, but it is generally considered that a pericyte is the cell that is imbedded within the vascular basement membrane (207). Vascular smooth muscle cells on the other side are separated from endothelial cells by matrix (208). Pericytes are defined by their location and morphology, but recent studies tried to understand their unique gene expression profile as well (209). Pericytes are embedded in vascular basement membrane, and over 1000 direct contacts between two cells occur in a *peg-socket* interface, where pericyte cytoplasmic fingers (pegs) are inserted into endothelial invaginations (pockets). Other contact morphologies include *close*/*occluding* contacts, when membrane of a pericyte and endothelial cell come very close together. These types of connections possible play a role in anchoring since they are found at the edge of the pericyte processes. Third type of contacts, referred to as *adhesion plaques*, resemble adherence junctions, but are not completely investigated. Under electron microscope, adhesion plaques are seen as microfilament bundles at pericyte membrane and electron-dense material in the endothelial cytoplasm (207) (Figure 15).

Pericytes can be defined by different makers, like PDGF-Rβ (platelet-derived growth factor receptor-beta), αSMA (α-smooth muscle actin), NG2 (chondroitin sulfate proteoglycan 4), CD13 and desmin, but none of which is entirely unique pericyte marker (207).

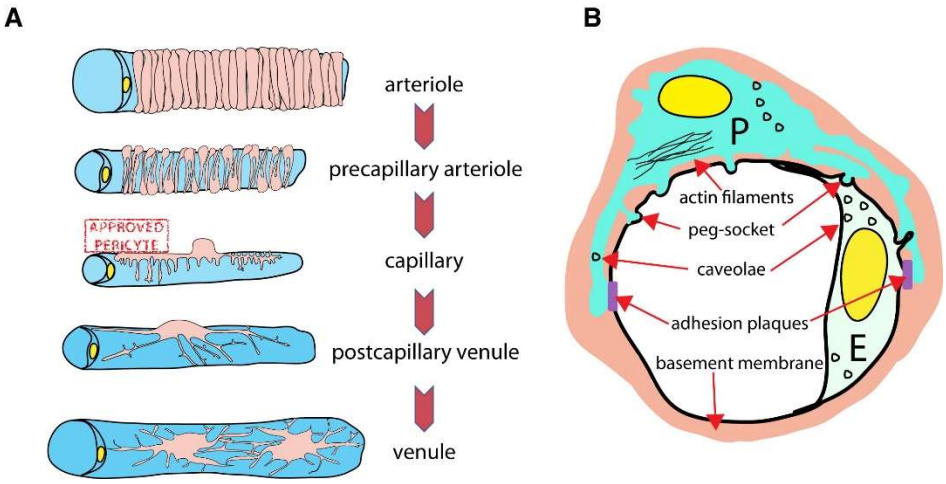


**Figure 15. Vessel mural cell coverage.** (**A**) Arterioles are wrapped by circular layer of smooth muscle cells (SMC) which are flattened, spindle-shaped cells with few cytoplasmic processes. Precapillary arterioles are associated with SMC that extend their processes around the endothelium. Capillaries, on the other hand, are covered by pericytes, which have round cell body, from which primary and then perpendicular, secondary processes extend. Postcapillary venules are associated with flattened mural cells with many slender, branching processes. Venules have big, stellate-shape SMCs that, unlike arteriolar SMCs, do not wrap circularly around endothelium. (**B**) Pericytes (P) and endothelial cells (E) share basement membrane, but they come into direct contact only through adhesion plaques and peg-socket contacts. Many actin filaments stretch in primary and secondary cytoplasmic processes of pericytes and numerous caveolae are found in abluminal pericyte surface [Reprinted from Armulik, A. et al. 2011 (207)]

Pericyte abundance also greatly varies between different tissue and organs. Vasculature in central nervous system has the highest pericyte coverage, with EC: pericyte ratio of 1:1-3:1 (210). In some studies, it was reported that EC: pericyte ratio in human skeletal muscle vasculature is 100:1 (211, 212), while others reported it to be higher (213). The pericyte coverage is correlating with the permeability of endothelial-blood barrier (very low in CNS), endothelial proliferation (higher EC turnover correlates with less coverage) and orthostatic blood pressure (207). Pericyte origin is not completely clarified. Generally, it is believed that pericyte are mesenchymal cells. Probably, all the SMCs and pericytes in CNS (214-217) and thymus (218, 219) are coming from ectoderm-derived neural crest. Pericytes of coelomic organs like gut (220), lung (221), and liver (222) have been mapped to the mesothelium, the single-layer squamous epithelium that lines the coelomic cavities and its organs. Interestingly,

SMCs of the aorta and its proximal branches are derived from at least four different sources, i.e. secondary heart field, neural crest, somites, and splanchnic mesoderm (207).

Vessel maturation is connected with vessel quiescence. Quiescence is a reversible state in which ECs are not dividing or migrating. It is common for both blood and lymphatic vessel, but its regulation is not completely elucidated. Different signaling molecules like RAS, PTEN phosphatase, FOXO1, Alk-1, endoglin, BMP-9, -10 and others have been implicated in vessel quiescence. Understanding of endothelial quiescence is especially important in order to understand different vascular pathologies where this process is dysregulated (29). Endothelial cell-pericyte crosstalk is regulated by different signaling pathways (Figure 16). PDGF/PDGF-Rβ, Ang/Tie-2, TGFβ/TGF-Rβ, ephrinB2/EphB4 are one of the most important so they will be briefly described.

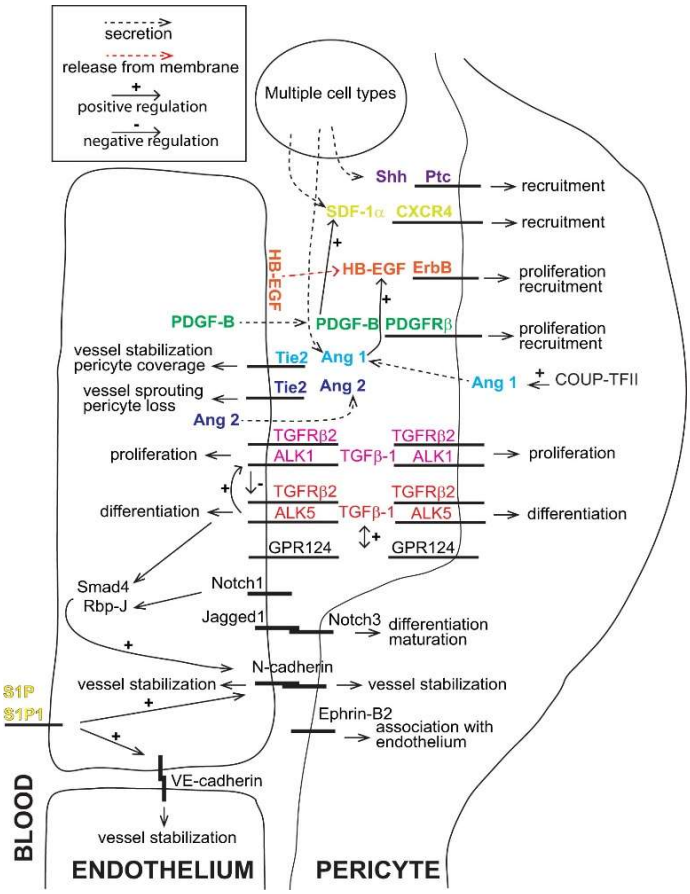


**Figure 16. Pericyte-endothelial crosstalk.** Recruitment of pericytes to the endothelium is controlled by many ligand/receptor complexes (the ligand and receptor are indicated with the same color): PDGF-B /PDGFRβ, SDF-1α (stromal-derived factor 1-alpha)/CXC4R, heparin- binding epidermal growth factor (HB-EGF)/ErbB, sonic hedgehog (Shh)/Patched (Ptc), Ang1/Tie-2 and sphingosine-1 phosphate (S1P)/$S1P_1$. Ang-2 induces vessel destabilization and pericyte loss. TGFβ signaling regulates proliferation and differentiation of both pericytes and endothelial cells. Notch, ephrinB2 and N-cadherin signaling require direct contact between pericyte and endothelial cell [Reprinted from Armulik, A. et al. 2011 (207)]

## 3.1. PDGF signaling in pericyte recruitment

Platelet derived growth factor (PDGF) signaling plays a central role in pericyte recruitment. Two tyrosine kinase receptors, PDGF-Rα and PDGF-Rβ, are evolutionarily and structurally related to VEGF receptors. There are four PDGF isoforms (PDGF-A, -B, -C, -D) that make homo- or heterodimers, giving rise to five different ligands, namely PDGF-AA, -BB, -AB, -CC, and -DD. Endothelial cells, especially tip cells, express PDGF, while mural cells express PDGF receptors (168). Mice that have null-mutation of either *Pdgfb* or *Pdgfrb*, die *in utero* due to capillary dilatations and microaneurism ruptures leading to severe hemorrhaging together with renal, cardiac and placental defects. Mutant mice displayed pericyte/SMC detachment and overall reduction of mural cell coverage (223-225). VEGF can have a negative effect on pericyte recruitment by formation of receptor complex between VEGF-R2 and PDGF-Rβ (226). We have demonstrated that PDGF-BB can normalize aberrant angiogenesis induced by high VEGF doses, demonstrating the importance of pericytes in prevention of pathological angiogenesis (227, 228).

## 3.2. Angiopoietin/Tie2 signaling

Angiopoietins are other signaling molecules important for EC-pericyte crosstalk. There are four ligands- Angiopoietin-1 (Ang-1), Ang-2, Ang-3 and Ang-4 that bind to two Tie (tyrosine kinase with immunoglobulin and EGF homology domains) receptors- Tie-1 (Tie in mouse) and Tie-2 (Tek in mouse) (229) (Figure 17). Ang-1 and Ang-2 are best studied and it was demonstrated that even though both of them bind Tie-2 with similar affinities, they have different effects on angiogenic process (168, 230). Ang-1 has positive effect since it can promote vascular growth, endothelial cell survival and maturation process by preventing apoptosis and inflammation. Ang-2, on the other side, acts like Ang-1 antagonist and enhances vascular regression, pericyte detachment, vessel destabilization and endothelial cell death (231,

232). It also increases vascular permeability, facilitating infiltration of immune cells and cytokine and growth factor secretion (229). Ang-1 is expressed by perivascular mesenchymal cells like pericytes, vascular smooth muscle cells, fibroblast and tumor cells (207, 229), while Ang-2 is mostly produced by endothelial cells and upon stimulation released from vesicles called Weibel–Palade bodies. Tie-2 is predominantly produced by endothelial cells (207). Ang-2 promotes dissociation of pericytes and mice with inactivated *Tek* (Tie-2) die in midgestation due to the abnormalities in capillary plexus remodeling and maturation, hematopoiesis and heart development. Inactivation of *Tie* (Tie-1) is also lethal, causing impairment of vascular integrity, but with normal hematopoiesis (231). Mice with null mutation for *Ang-1* die *in utero* having similar phenotype of *Tek*-deficient mice, while *Ang-2*-null mice are born normally, but die postnatally due to defects in lymphatic system (233, 234).

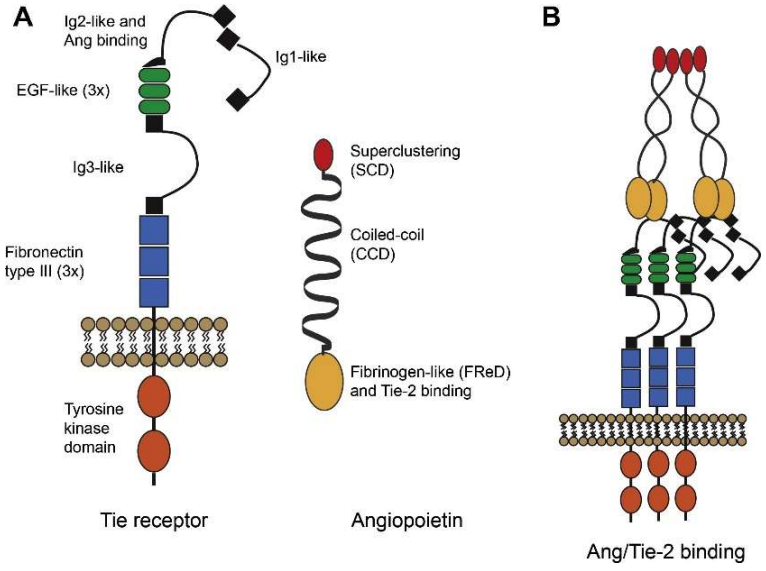


**Figure 17. Angiopoietin/Tie-2 signaling.** (**A**) Extracellular domain of Tie receptors contains 3 IgG-like domains, 3 EGF-like repeats and 3 fibronectin type II domains. Tyrosine kinase domain is located intracellularly. Angiopoietins are soluble proteins that contain superclustering domain (SCD) that allows homodimers to multimerize, coiled-coil domain (CCD) and Tie-receptor-binding fibrinogen-like domain (FReD). (**B**) Upon ligand-receptor binding, the complexes multimerize, bringing receptor tyrosine kinase domains in close proximity, leading to phosphorylation and signal initiation [Reprinted from Fagiani, E. et al. 2013 (229)]

## 3.3. TGF-β signaling

Transforming growth factor β (TGFβ) signaling is important in physiology of both endothelial cells as well as pericytes. It can induce mural cell proliferation and their differentiation from undifferentiated mesenchyme. TGFβ signaling regulates proliferation and differentiation of endothelial cells as well. There are three major types of TGFβ receptors: TGF-β receptor type I (TβRI), type II (TβRII) and type III (TβRIII). Ligand binding assembles a hetero-tetrameric receptor complex consisting of two type I (signal propagating) receptor components and two type II (activator) components (235, 236). Type II receptor components phosphorylate type I components, which in turn propagate the signal through activation of SMAD [*Caenorhabditis elegans* SMA protein; mothers against decapentaplegic (MAD)] proteins. SMAD2 and SMAD3 are inducing cell cycle arrest while SMAD1/5/8 are activating cell proliferation (235) (Figure 18). The TGF-β superfamily is composed of more than 30 chemokines that can be ligands for TGFβ receptors. The superfamily includes TGF-β1-3, activins, anti-Müllerian hormone (AMH), bone morphogenetic proteins (BMPs), growth and differentiation factors (GDFs) and NODAL (235). TGF-β1 is translated as a large precursor pre-proprotein, which undergoes two proteolytic cleavage events. First, signal peptide is cleaved in rough endoplasmic reticulum, Then, furin convertase cleaves the protein in two fragments-mature TGF-β1 and latency-associated protein (LAP). LAP remains in the complex and it serves as a functional inhibitor, and it needs to be displaced from the complex to release mature TGF-β1, and allow signaling (235).

In humans, there are seven TβRIs, also known as activin receptor-like kinases (Alk), and five TβRIIs. Alk-1 and Alk-5, expressed in both endothelial and mural cells, are the most investigated, in the context of angiogenesis. It is interesting that Alk-1 and Alk-5 trigger different and opposing cellular effects, where Alk-5, through SMAD2/3, promotes proliferation arrest and differentiation of mesenchymal cells into smooth muscle cells, while

Alk-1, through SMAD1/5 promotes cell proliferation and migration, inhibiting SMC differentiation (207). TGF-β accessory receptor, endoglin, enhances Alk-1 signaling and inhibits Alk-5 cytostatic action (235).

Knockout of different TGF-β signaling pathway genes in mice like *tgfb1* (237), *alk1* (238), *alk5* (239), *tgfbr2* (14), *smad4* (240), *smad5* (241, 242) and *endoglin* (243), is embryonically lethal due to severe vascular abnormalities like defects in yolk sac vasculature remodeling, arterio-venous anastomoses, defective mural cells differentiation and in some mutants, defective hematopoiesis (207). TGF-β in endothelial cells cooperates with other signaling pathways like Notch by cooperatively regulating expression of N-cadherin (244), a molecule important in pericyte-endothelial crosstalk (207). TGF-β also upregulates the expression of other molecules involved in angiogenic process such as VEGF, PDGF-A, PDGF-B and nitric oxide synthase 3 (NOS3) (235).

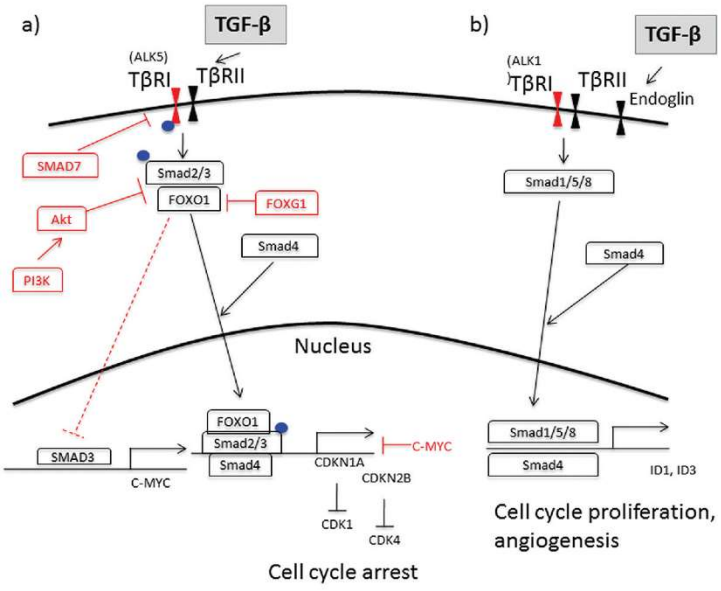


**Figure 18. TGFβ signaling.** TGFβ signaling can have opposing effects on cell proliferation. (**A**) It can induce cell cycle arrest by downstream activation of SMAD2/3 effector proteins, that associate to SMAD4 and FOXO1 (foxhead box O-1) protein, and act as transcription factors. They can upregulate expression of p21Cip1 (CDKN1A) and p15Inkab (CDKN2B), which in turn inhibit cyclin-dependent kinase 1 (CDK1) and CDK4, resulting in cell cycle arrest. FOXG1 (Foxhead box G1), AKT and SMAD7 are antagonizing this pathway. Blue dots represent protein phosphorylation. (**B**) TGFβ can also induce cell proliferation and angiogenesis thorough activation of SMAD1/5/8 effector proteins and subsequent expression of transcription factors ID1 (inhibitor of DNA-binding protein 1) and ID3, which are involved in cell cycle progression [Reprinted from Guerrero, P.A. et al. 2017 (235)]

## 3.4. Ephrin/Eph signaling

Eph (erythropoietin-producing human hepatocellular) receptors are the largest family of tyrosine kinase receptors in human (245-249). They were first identified in human carcinomas, were they were found overexpressed. The Eph receptors with their ligands, called ephrins (Eph receptor-interacting proteins) transmit the signal upon cell-cell contact and regulate cell shape, movement, survival, and proliferation. In human, there are nine type A (EphA1-9) and five type B (EphB1-5) receptors, as well as five glycosylphosphatidylinositol (GPI)-linked type A (ephrinA1-5) and 3 transmembrane type B (ephrinB1-3) ligands (245) (Figure 19A). B-class receptors promiscuously bind B-class ligands while A-class receptors bind A-class ligands, with some exceptions. When interacting *in trans*, ephrin/Eph downstream signaling can be bidirectional, which means it can proceed both in receptor-bearing cell (forward signaling), as well as in ligand-bearing cell (reverse signaling) (Figure 19B). When expressed in the same cell, ephrins and Eph receptors can inhibit the signaling induced by *in trans* interactions (248, 250, 251).

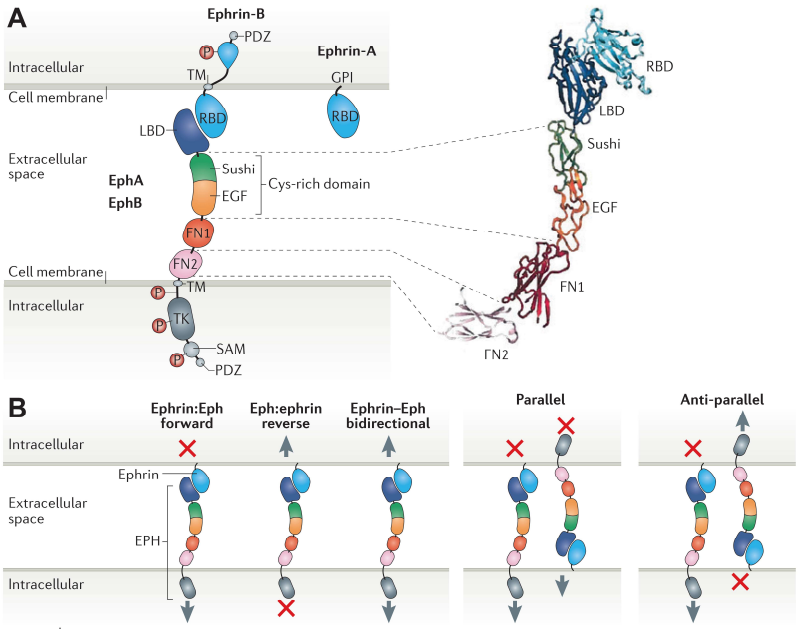


**Figure 19. Ephrin/Eph and signaling possibilities.** Both Eph receptors and ephrin ligands are membrane bound proteins that signal upon cell-cell contact. (**A**) Eph receptors are divided into two classes-class A and class B. Both EphA and EphB receptors are transmembrane tyrosine kinase receptors composed of ligand binding domain

(LBD), Cys-rich domain made of Sushi domain and epidermal growth factor (EGF)-like domain. There are two fibronectin (FN) domains, transmembrane (TM) region, as well as tyrosine kinase (TK) domain, the sterile alpha motif (SAM) and PDZ domain, located intracellularly. Ephrin ligands exist as ephrinA and ephrinB class and both classes contain receptor-binding domain (RBD). EphrinA ligands are linked to the membrane via a glycosylphosphatidylinositol (GPI) anchoring, whereas the ephrinB class has a transmembrane domain and an intracellular PDZ domain. (**B**) Ephrin/Eph signaling can proceed both in receptor-bearing cell (forward signaling) and in ligand-bearing cell (reverse signaling), or in both cells (bidirectional). Parallel signaling is occurring when both ephrins and Ephs are expressed on the same cell, and they signal in response to Ephs and ephrins, respectively, present on a neighboring cell. Anti-parallel signaling is, on the other side, a simultaneously occurring forward signaling. Unlike parallel signaling, in anti-parallel signaling, ephrin–Eph signals are propagated in both cells [Adapted from Kania, A. et al. 2016 (247)]

In developing nervous system, ephrin/Eph signaling controls tissue patterning and serves as axonal guidance cue, inducing collapse or immobilization of axonal growth cones. Besides nervous system, ephrin/Eph signaling controls bone homeostasis, insulin secretion, stem cell renewal, but it also plays an important role in vascular system, as ephrinB2/EphB4 interaction is regulating arterio-venous specification (245, 247, 248). Ephrin/Eph signaling is also implicated in many pathologies like neurodegeneration, neuropathic pain, cancer and androgen-induced alopecia. EphrinB2 and ephrinB3 can even serve as entry molecules for henipaviruses (245). Generally, tyrosine kinase receptor (RTK) signaling induces cell migration, proliferation and survival, while Eph signaling can also mediate inhibition of cell growth and induce cell repulsion.

Ephrin/Eph downstream signaling is complex and involves many interactions. After ephrin/Eph interaction, many such ligand-receptor complexes oligomerize, forming a cluster, which is critical for activation of the downstream signaling (252, 253). Close proximity of the receptors will lead to trans-phosphorylation of two conserved tyrosines in the juxtamembrane domain (248). It seems that phosphorylation of Eph receptors is less critical for receptor activation, as compared to other RTKs, but might be important for its maximal activity (254, 255). Phosphorylation of the receptor will lead to recruitment of SH2-domain containing proteins like members of non- receptor tyrosine kinases SRC and ABL families and adaptors

NCK and CRK, which are crucial for signal transduction. RTKs are usually internalized through endocytosis and can continue to signal intracellularly until they are dephosphorylated and degraded. Eph receptors and ligands are both membrane bound so endocytosis is carried out in a different way (43, 256, 257). Ligand-receptor complex can be internalized in both cells, where endocytic vesicles contain plasma membrane of both cells. This process is called trans-endocytosis, and it can be "forward"-when the complex is internalized in receptor-expressing cell or, "reverse"-when the complex is internalized in ligand-expressing cell (Figure 20). Trans-endocytosis is regulated by RAC1 and ubiquitin ligase Cbl which can ubiquitinylate several Eph receptors and induce their internalization and degradation (258, 259).

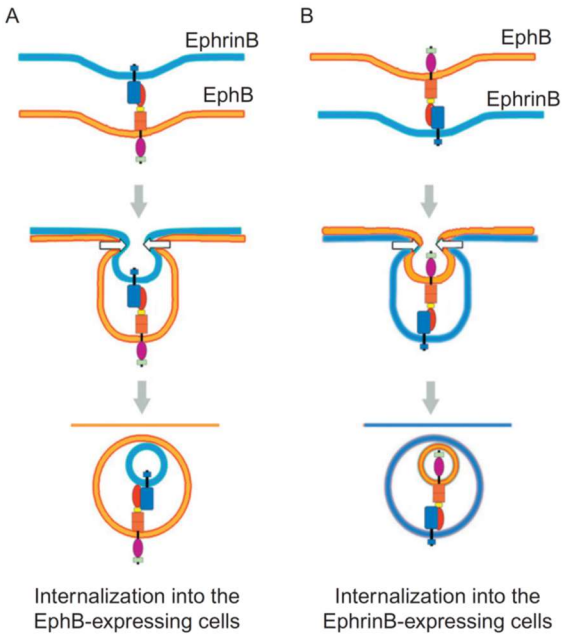


**Figure 20. Trans-endocytosis.** Upon EphrinB/EphB interaction, the trans-endocytosis of the ligand-receptor complex can proceed in the receptor-bearing cell (forward endocytosis) (**A**) or in the ligand-bearing cell (reverse endocytosis) (**B**). Both processes lead to internalization of full-length ligand and receptor [Reprinted from Salvucci, O. et al 2012 (249)]

Eph receptor-ephrin complex can induce cell repulsion by activating metalloproteases, such as ADAM family members (248). Transmembrane ADAM10 protease can bind to ephrinA2 *in cis* and cleave it following EphA receptor binding *in trans* to enable repulsive axon guidance (260) (Figure 21).

PDZ domain-containing proteins are also binding to the carboxy-terminal tails of Eph receptors and they also contribute to forward signaling. RHO and RAS family GTPases as well

as AKT/mTORC1 are particularly important. RHO GTPase family members RHOA, RAC1 and CDC42, which are involved in reorganization of actin cytoskeleton, are activated by Eph forward signaling (261, 262). RHOA is mostly involved in the formation of stress fibers and focal adhesions and contraction of the actomyosin cytoskeleton, whereas RAC1 and CDC42 regulate the formation of protrusive structures such as lamellipodia and filopodia, respectively (248, 263). Most of RTKs phosphorylate ERK1 and ERK2 through activation of H-RAS GTPase, but it was shown that Eph signaling can inhibit ERK activation induced by FGF receptor (264, 265). Common mechanism of Eph-inhibition of ERK is through activation of p120RASGAP, which inactivates H-RAS (266, 267) (Figure 21). Still, it was demonstrated that ephrinB1/EphB signaling can also activate ERK to promote proliferation and regulate immediate early gene transcription (268), suggesting that Eph signaling is far more complex and needs further investigation. Similarly, Eph signaling can inhibit and activate PI3K-AKT pathway, common downstream effector of many RTKs (248).

Reverse signaling, i.e. signaling in ligand-bearing cell is mediated by ephrins, which lack an enzymatic domain, but upon receptor-ligand interaction, are phosphorylated by SRC kinases like FYN, creating binding sites for the SH2 domains of signaling proteins such as the adaptor Grb4 (248). Termination of forward signaling can be mediated by phosphatases like protein tyrosine phosphatase 1B (PTP1B) which dephosphorylate Eph receptor (269).

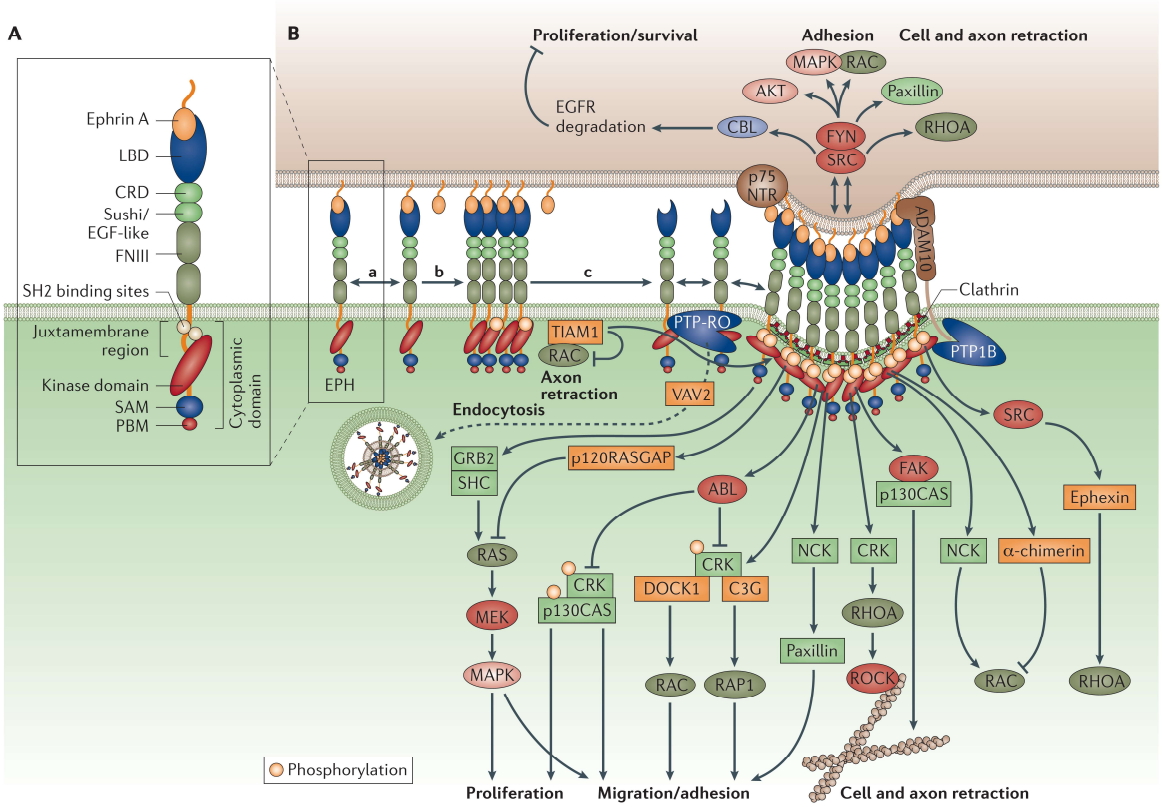


**Figure 21. Ephrin/Eph downstream signaling.** (**A**) Ephrin/Eph complex structure. (**B**) Upon ephrin/Eph interaction, the ligand-receptor complexes multimerize and the clusters comprising four Ephs and four ephrins are a functional signaling unit. Eph receptor activation involves the release of the Eph juxtamembrane domain leading to extension of the cytoplasmic domain allowing Eph kinase domain to be activated. Activated Ephs recruit the metalloprotease ADAM10 (a disintegrin and metalloprotease domain-containing protein 10), which cleaves ephrins from the interacting cell surface to allow endocytosis to proceed, probably via a clathrin-mediated mechanism. Protein tyrosine phosphatases (PTPs), including PTP-RO and PTP1B are controlling Eph phosphorylation. Clustering of ephrinA ligands causes recruitment and activation of SRC kinases as well as RAC, RHOA, ROCK (RHO-associated protein kinase) and paxillin, which all together promote cytoskeletal changes. Additionally, ephrin reverse signaling might be implicated in cell survival regulation through p75 neurotrophin receptor (p75NTR) and inhibition of epidermal growth factor receptor (EGFR) degradation. Mediators of forward signaling are tyrosine kinases (red), serine/threonine kinases (pink), SH2 adaptors (light green), RHO GTPases (green) and their GTPase-activating proteins (GAPs) and guanine nucleotide exchange factors (GEFs) (orange). Regulation of cell cytoskeleton is mediated by RHOA, RAC, and repressor/activator protein 1 (RAP1; also known as TERF2IP), resulting in cell contraction or spreading and adhesion. This process is regulated by a range of kinases and signaling mediators such as SRC kinases and focal adhesion kinases (FAKs). Activation of the Eph downstream signaling leads to recruitment of SH2 adaptors such as p130CAS, CT10 regulator of kinase (CRK), CRK2, non-catalytic region of tyrosine kinase adaptor protein 1 (Nck1) and GAPs and GEFs (including ephexin, α-chimerin and C3G), as well as activation of Vav and Tiam1 (T lymphoma invasion and metastasis-inducing protein 1). Inhibition of cell migration, adhesion and proliferation is achieved through phosphorylation of CRK

by ABL kinase, disrupting CRK–p130CAS and CRK– DOCK1 (dedicator of cytokinesis protein 1) complexes. FAK kinases are positively regulating these processes through phosphorylation of p130CAS that promotes its binding to CRK33. Eph downstream signaling can inhibit cell proliferation via activation of p120RASGAP which inhibits RAS–MAPK/ERK kinase (MEK)–mitogen-activated protein kinase (MAPK) signaling [Reprinted from Boyd, A.W. et al. 2014 (246)]

### 3.4.1. EphrinB2/EphB4 signaling in angiogenesis

EphrinB2/EphB4 signaling has a very important role in vascular system, specifically during arterio-venous specification in embryonal development. While there is promiscuity in binding of different Eph receptor and ephrin ligands members, ephrinB2/EphB4 interaction is specific (270). EphrinB2 is an arterial while EphB4 is a venous marker (249, 271, 272). These two molecules regulate first arterial-venous differentiation event in development i.e. formation of dorsal aorta and cardinal vein. It was demonstrated, both in zebrafish and mouse models, that dorsal aorta assembles first and it contains a mixed of ephrinB2$^+$ and EphB4$^+$ precursor cells. EphrinB2:EphB4 repulsive signaling repels arterial (ephrinB2$^+$) from venous (EphB4$^+$) endothelial cells. EphB4$^+$ endothelial cells then assemble the cardinal vein (247, 273, 274).

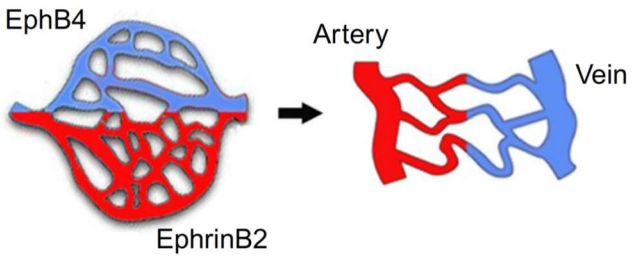


**Figure 22. EphrinB2/EphB4 signaling**. EphrinB2/EphB4 is regulating arterio-venous differentiation in primary vascular plexus, where ephrinB2 is marking arterial and EphB4 venous territory, later leading to formation of ephrinB2$^+$ arteries and EphB4$^+$ veins [Reprinted from Salvucci, O. et al. 2012 (249)]

Mice with deletion of either *ephrinB2* or *EphB4* die *in utero* due to defects in remodeling of primary vascular plexus (271). Since knockout of both proteins has similar phenotype, it is clear that early vascular remodeling requires both forward and reverse ephrinB2/EphB4 signaling. EphrinB2 is expressed in the endothelium and mural cells of adult arteries, arterioles, and capillaries in many tissues, and its expression increases during

angiogenic process (275-277). EphrinB is broadly phosphorylated in angiogenic vessels, but not in the resting endothelium (278). Since EphB4 is expressed mostly in venous endothelial cells, first it was thought that ephrinB2/EphB4 signaling can occur only on arterial/vein boundaries. Later, it was shown that expression of ephrinB2 and EphB4 partially overlaps in retinal vessels, as well as in endothelial cells of umbilical vein, human aorta, and dermal microvasculature, suggesting that ephrinB2/EphB4 interactions can occur in many locations (249).

In development, ephrinB2 is phosphorylated in retinal vessels, and after they have been fully developed, it subsequently dephosphorylates (249, 278). During sprouting, ephrinB2 is specifically expressed by tip cells and their filopodia (44, 45). It was demonstrated that mice carrying an allele of *ephrinb2* with the mutation in PDZ domain, had impaired retinal vascular development, as tip cells displayed significantly reduced ability to form filopodia (44). Cultured endothelial cells with silenced *ephrinB2* fail to assemble in networks. The same outcome has been observed if ephrinB2 is overexpressed in endothelial cells, suggesting that expression of ephrinB2 needs to be tightly controlled (44, 45, 278). EphrinB2 reverse signaling can directly regulate VEGF signaling by controlling the internalization of both VEGF-R2 and VEGF-R3 upon ligand binding. EphrinB2 promotes clathrin-dependent VEGF receptor internalization, and consequently downstream signaling and sprouting through interaction with the clathrin-associated protein disabled 2 (DAB2) and the cell polarity regulator PAR3 (44, 45, 117, 247) (Figure 9). It is interesting that phosphorylation of ephrinB2 is not necessary for modulation of VEGF receptor internalization, but this process depends on its PDZ-binding site, possibly through activation of SRC kinases (44, 45, 247). With that in line, experiments showed that inactivation of ephrinB2 leads to defective VEGF-R2 and VEGF-R3 signaling, i.e. VEGFR phosphorylation is decreased and activation of downstream signaling effectors RAC1,

ERK1/2, and AKT is reduced (44, 45). Furthermore, ephrinB2 can, to a certain extent, modulate VEGF-R2 internalization even in the absence of VEGF (44).

Regulation of VEGF signaling by EphB4 forward signaling is still not clear. Some experiments demonstrate that activation of EphB4 has opposite outcome as compared to ephrinB2 reverse signaling, as EphB4 decreased endothelial cell proliferation, migration and adhesion (279, 280). Other instead showed that EphB4 activation stimulates cell proliferation (281). EphB4 forward signaling seems to play an important role in lymphatic valve development (282).

EphrinB2 signaling plays an important role in pericyte-endothelial crosstalk. Inactivation of ephrinB2 specifically in mural cells by using *Pdgfrb*-cre mice, led to perinatal death due to edema and extensive hemorrhaging in a variety of tissues. Interestingly, even though the ephrinB2-null pericytes were morphologically normal, they associated poorly with the vessels (283). When these pericytes/smooth muscle cells were cultured, they were elongated, did not properly spread, and cell-cell contact was impaired. Even though the cells were migrating more, migration was random, due to defective focal adhesion formation. This phenotype could be reversed by re-expression of ephrinB2 or RHO-like GTPases (283). EphB4, which is expressed by endothelial cells, can activate ephrinB2 on mural cell and enhance association of these two cell types within tumor blood vessels (284).

Mechanistically, ephrinB2 in mural cells interacts with PDGFRβ. Specifically, ephrinB2 controls membrane distribution, endocytosis and signaling output of PDGFRβ and in that way, promotes proliferation of vascular smooth muscle cells and prevents their differentiation (247, 285). *In vitro* experiments with vascular smooth muscle cells suggested that ephrinB2 is required for the balanced activation of multiple signaling cascades in the PDGF pathway (247).

# 4. Therapeutic angiogenesis

Therapeutic angiogenesis is a strategy for induction of growth of new blood vessel for therapeutic purposes. It is especially important in field of tissue engineering, as well for treatment of ischemic diseases and non-healing wounds. Ischemic diseases are group of conditions characterized by low blood tissue perfusion and hypoxia, leading to tissue damage. There are three main types of ischemic diseases: peripheral artery disease (PAD), coronary artery disease (CAD) and cerebrovascular disease (286, 287). The main pathophysiological process causing ischemia is atherosclerosis. Atherosclerosis is a progressive disease that is characterized by accumulation of lipids, immune cells and fibrotic material in the inner arterial wall. This leads to lumen stenosis and ultimately to the occlusion of the artery. Patients with significant stenosis of the arterial lumen will experience pain during exercise, and this condition is associated with stable angina pectoris or intermittent claudication. Further progression of stenosis leads to serious ischemia and pain at rest. This condition is associated with development of unstable angina pectoris or critical chronic limb ischemia (CLI). Ultimately, rupture of atherosclerotic lesion can lead to life-threatening events like myocardial infarction and stroke, caused by atherothrombotic events (286).

## 4.1. Peripheral artery disease

Peripheral artery disease (PAD) is mostly caused by atherosclerosis, but vasculitis, thrombosis and embolic disease can also lead to development of the disease. Major risk factors for PAD are smoking, diabetes, dyslipidemia and hypertension (288-290). PAD can affect arteries of lower and upper extremities, the carotid and mesenteric vessels. We will concentrate on PAD of lower limb extremities, due to its clinical importance (288, 290). PAD was affecting 202 million of people worldwide in 2010, 69.7% of them in low- or middle-income countries (288, 289) with 15% to 20% of patients being over 70 years of age. PAD is slightly more

prevalent in men than in women (291). The annual incidence of critical limb ischemia is 500 to 1000 and of major amputations from 120 to 500 new cases per million population (288). Atherosclerosis, as a systemic disease, can also lead to coronary artery and cerebrovascular diseases, which are the major causes of death in people with PAD (288, 290). Depending on the degree of arterial stenosis and claudication, patients suffering from PAD can be or asymptomatic, have leg pain during exercise or walking (intermittent claudication) or at severe degree of stenosis (critical limb ischemia) have pain of the affected leg even at rest and ulceration and gangrene of the foot. Clinical severity of PAD is classified according to Fontaine and Rutherford classifications (292). PAD is a major cause of decreased mobility, functional capacity, quality of life and it increases the risks of amputation and/or death (290, 293, 294).

## 4.2. Gene therapy in PAD

Therapeutic angiogenesis is a strategy to improve blood flow by induction of new capillary growth. Increase in blood flow and shear stress created by new vessels can subsequently lead to opening of collateral arteries in the process of arteriogenesis, leading to functional improvement and tissue regeneration. Proangiogenic molecule like VEGFs, FGFs, HIF-1α (hypoxia-induced factor 1α) and HGF (hepatocyte growth factor) were used in almost all the clinical trials for PAD and CAD. First-in-human trials using gene transfer of VEGF and FGF-2 for treatment of PAD were performed in late 90-s by intramuscular plasmid delivery (295, 296). Initial trials with intramuscular adenoviral gene delivery were also performed in that period (297). Shortly after that, RAVE trial, first randomized, double-blind, placebo-controlled study of intramuscular adenoviral gene transfer for the treatment of PAD, was performed. The study found no significant differences between groups in the primary or secondary efficacy endpoints (298). The appearance of peripheral edema was associated with use of short isoform VEGF-$A_{121}$. Parallelly, in two separate clinical trials, recombinant VEGF

and FGF-2 proteins were used as an alternative to gene transfer. Both VIVA (VEGF protein) (299) and TRAFFIC (FGF-2 protein) (300) trials failed to show a significant improvement in the treated patient group. The reason for poor outcome was fast protein clearance upon intramuscular injection (301). Since then, other clinical trials were performed using various gene transfer vectors, like plasmids, adenoviruses, adeno-associated viruses, and retroviruses. Most recently, 40 different clinical trials using gene delivery of VEGF, FGF and HGF for PAD treatment, were systematically reviewed and the conclusions are: i) growth factors may improve hemodynamic measures as well as ulceration and rest pain in people with PAD of the lower extremities up to one year, but they have little or no effect on walking ability, ii) rate of major amputation was similar, while rate of minor limb amputations was decreased in patients treated with growth factor. However, effects on major limb amputations and on death are uncertain, iii) there was no relevant difference in effects between growth factors (FGF, HGF and VEGF) (290).

### 4.2.1. Gene therapy limitations

The reasons for not very successful clinical translation of cardiovascular gene therapy can be many, but the main ones are: i) induction of leaky, non-stable vessels insufficient for functional improvement, ii) transduction efficacy is too low or duration of gene expression is too short, iii) insufficient knowledge about underlying pathophysiological mechanism, iv) underpowered clinical trial design and patient selection (302).

Currently, it is difficult to achieve more than 10% - 20% transduction efficiency in human heart or peripheral muscle (302) so selection of vector type, as well as gene transfer route are very important in order to achieve sufficient local concentration of growth factor in the affected tissue. Intra-muscular gene transfer is more efficient than intra-arterial delivery (297) and virus-mediated gene delivery is more efficient then naked plasmid. It is challenging to deliver locally enough growth factor using safe vector doses. High amounts of VEGF

delivered to the limb skeletal muscle can induce aberrant vessel growth and fibrosis (303). Normalization of the aberrant, leaky and non-stable vessels is one important avenue that needs to be further explored. Recently, retroviral delivery of both VEGF-A and pro-stabilizing factor Angiopietin-1 is going in that direction (287). Usage of modified growth factors, like VEGF-$D^{dNdC}$, that can induce both blood and lymphatic vessel growth, can potentially lead to a better outcome in comparison to induction of blood vessel growth alone (302).

The selection of patients is probably responsible for the observed outcome as well, as most of them were "no option" cases and were not eligible for any other type of treatment. As such, they potentially already have serious impairment of endogenous angiogenesis and are not able to respond to angiogenic therapies. This is the reason for recruitment of healthier patients in future trials, or by development of novel biomarkers, select responder patients. Ultimately, clinical trial endpoints should be revised as well, in order to evaluate improvement in severely affected patients more rationally (302).

## 4.3. Total vs microenvironmental VEGF dose: myoblast-mediated gene delivery

Previous work from our group has investigated the dose-dependent effects of VEGF gene delivery to the clinically relevant target tissue of skeletal muscle. We developed a specific cell-based gene delivery system in which primary myoblasts were retrovirally transduced to produce VEGF (304). Once these transduced myoblasts were implanted in skeletal muscle, they induced aberrant angiogenesis, and ultimately led to hemangioma growth. Dilution of cells could not prevent hemangioma growth, even though total dose of produced VEGF was decreased from 60 ng/$10^6$ cells/day to only 5 ng/$10^6$ cells/day (305). Every cell in the population produces different levels of VEGF depending on the number of viral vector copies integrated and site of integration. That is why we next sorted single cells from the parental

polyclonal myoblasts population and expanded them. Now we got a series of monoclonal cell populations, where every single cell within a population produced the same amount of VEGF. A range of different clones expressing increasing amount of VEGF (5-200 ng/$10^6$ cells/day) was implanted in murine muscles, and now we could identify a threshold of concentration below we could induce only normal, pericyte-covered capillaries (5-70 ng/$10^6$ cells/day), and above hemangiomas were observed (100 ng/$10^6$ cells/day and above) (Figure 23) (305). After myoblast transduction, a polyclonal population consists of cells that express heterogenous VEGF levels, and high-producing cell will always be "hotspots" for angioma growth due to high microenvironmental VEGF concentration caused by limited diffusion of VEGF from a producing cell. Dilution of polyclonal cell population, and decrease of total dose of VEGF, still leads to appearance of aberrant vessel, since there will always be some high-producing cells present in the population (306). By using monoclonal myoblast population, we can achieve that all the cells produce VEGF at the concentration below the one at which hemangiomas are induced. In that way, angiogenesis can be induced in an efficient and safe way (306). This clearly demonstrated that in order to prevent aberrant angiogenesis, the dose of VEGF needs to be controlled at the microenvironmental level, rather at the level of total dose. The concept of microenvironmental dose can also explain inefficacy of gene delivery in previous clinical trials for therapeutic angiogenesis, since only total dose of viral vector or plasmid was controlled, but not its microenvironmental distribution in the affected tissue (306).

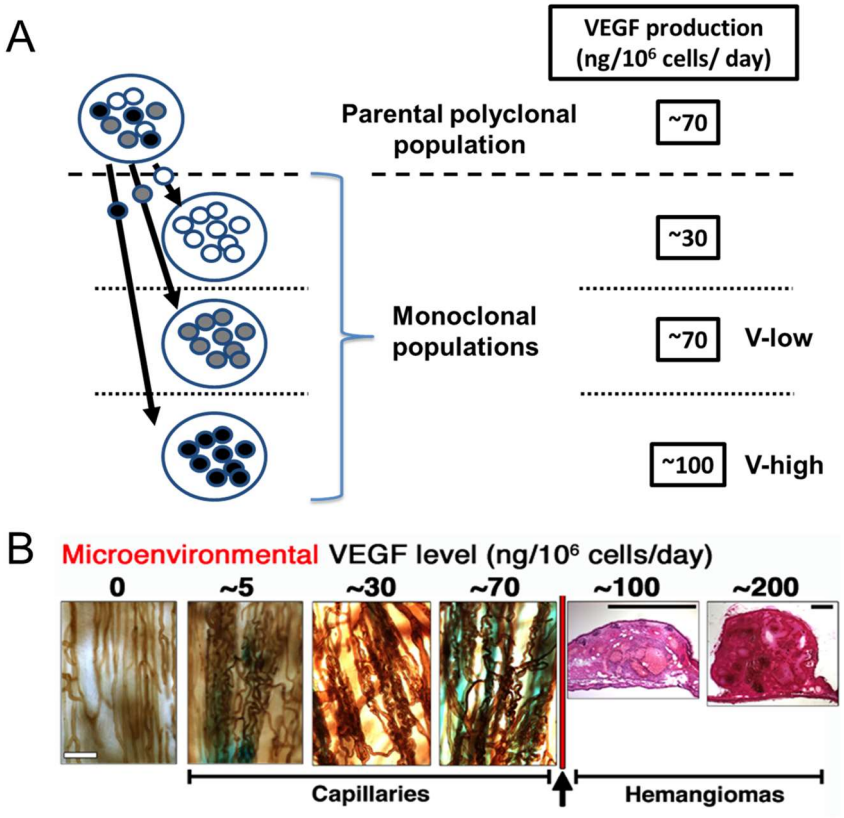


**Figure 23. Myoblast based VEGF-delivery.** (**A**) Myoblast are retrovirally transduced to express VEGF. Parental polyclonal population of transduced myoblast is composed of cells expressing different levels of VEGF. Individual cells can be isolated and expanded in order to produce monoclonal cell populations were every cell within a population expresses same amount of VEGF. (**B**) After intramuscular implantation of different monoclonal populations expressing increasing microenvironmental VEGF concentrations, a dose threshold can be identified, below which only normal capillaries are induced, and above, hemangiomas are formed. The clone expressing low levels of VEGF (V-low) is inducing normal angiogenesis, while V-high clone expresses high levels of VEGF and induces aberrant angiogenesis.

Myoblast based delivery of VEGF is a very useful tool in order to study the effect of VEGF dose on vessel growth. Here, we used two different VEGF clones, namely V-low, producing ~70 ng/$10^6$cells/day that induces normal capillaries and V-high, producing ~100 ng/$10^6$cells/day and induces aberrant angiogenesis (Figure 23). Myoblast-based VEGF delivery, was also complemented with other systems, like fibrin-based VEGF protein delivery system, as well as adenoviral gene transfer.

# References

1. Patel-Hett S, D'Amore PA. Signal transduction in vasculogenesis and developmental angiogenesis. *Int J Dev Biol*. 2011;55(4-5):353-63.

2. Carmeliet P. Angiogenesis in life, disease and medicine. *Nature*. 2005;438(7070):932-6.

3. Caprioli A, Minko K, Drevon C, Eichmann A, Dieterlen-Lievre F, Jaffredo T. Hemangioblast commitment in the avian allantois: cellular and molecular aspects. *Dev Biol*. 2001;238(1):64-78.

4. Hogan KA, Bautch VL. Blood vessel patterning at the embryonic midline. *Curr Top Dev Biol*. 2004;62:55-85.

5. Ribatti D, Nico B, Crivellato E. Morphological and molecular aspects of physiological vascular morphogenesis. *Angiogenesis*. 2009;12(2):101-11.

6. Tongers J, Roncalli JG, Losordo DW. Role of endothelial progenitor cells during ischemia-induced vasculogenesis and collateral formation. *Microvasc Res*. 2010;79(3):200-6.

7. Shalaby F, Rossant J, Yamaguchi TP, Gertsenstein M, Wu XF, Breitman ML, et al. Failure of blood-island formation and vasculogenesis in Flk-1-deficient mice. *Nature*. 1995;376(6535):62-6.

8. Carmeliet P, Ferreira V, Breier G, Pollefeyt S, Kieckens L, Gertsenstein M, et al. Abnormal blood vessel development and lethality in embryos lacking a single VEGF allele. *Nature*. 1996;380(6573):435-9.

9. Ferrara N, Carver-Moore K, Chen H, Dowd M, Lu L, O'Shea KS, et al. Heterozygous embryonic lethality induced by targeted inactivation of the VEGF gene. *Nature*. 1996;380(6573):439-42.

10. Cox CM, Poole TJ. Angioblast differentiation is influenced by the local environment: FGF-2 induces angioblasts and patterns vessel formation in the quail embryo. *Dev Dyn*. 2000;218(2):371-82.

11. Dyer MA, Farrington SM, Mohn D, Munday JR, Baron MH. Indian hedgehog activates hematopoiesis and vasculogenesis and can respecify prospective neurectodermal cell fate in the mouse embryo. *Development*. 2001;128(10):1717-30.

12. Takashima S, Kitakaze M, Asakura M, Asanuma H, Sanada S, Tashiro F, et al. Targeting of both mouse neuropilin-1 and neuropilin-2 genes severely impairs developmental yolk sac and embryonic angiogenesis. *Proc Natl Acad Sci U S A*. 2002;99(6):3657-62.

13. Letterio JJ, Geiser AG, Kulkarni AB, Roche NS, Sporn MB, Roberts AB. Maternal rescue of transforming growth factor-beta 1 null mice. *Science*. 1994;264(5167):1936-8.

14. Oshima M, Oshima H, Taketo MM. TGF-beta receptor type II deficiency results in defects of yolk sac hematopoiesis and vasculogenesis. *Dev Biol*. 1996;179(1):297-302.

15. Folkman J. Tumor angiogenesis: therapeutic implications. *N Engl J Med*. 1971;285(21):1182-6.

16. Arras M, Ito WD, Scholz D, Winkler B, Schaper J, Schaper W. Monocyte activation in angiogenesis and collateral growth in the rabbit hindlimb. *J Clin Invest*. 1998;101(1):40-50.

17. Grundmann S, Piek JJ, Pasterkamp G, Hoefer IE. Arteriogenesis: basic mechanisms and therapeutic stimulation. *Eur J Clin Invest*. 2007;37(10):755-66.

18. Troidl K, Schaper W. Arteriogenesis versus angiogenesis in peripheral artery disease. *Diabetes Metab Res Rev*. 2012;28 Suppl 1:27-9.

19. Deindl E, Buschmann I, Hoefer IE, Podzuweit T, Boengler K, Vogel S, et al. Role of ischemia and of hypoxia-inducible genes in arteriogenesis after femoral artery occlusion in the rabbit. *Circ Res*. 2001;89(9):779-86.

20. Pipp F, Boehm S, Cai WJ, Adili F, Ziegler B, Karanovic G, et al. Elevated fluid shear stress enhances postocclusive collateral artery growth and gene expression in the pig hind limb. *Arterioscler Thromb Vasc Biol*. 2004;24(9):1664-8.

21. Heil M, Ziegelhoeffer T, Wagner S, Fernandez B, Helisch A, Martin S, et al. Collateral artery growth (arteriogenesis) after experimental arterial occlusion is impaired in mice lacking CC-chemokine receptor-2. *Circ Res*. 2004;94(5):671-7.

22. Hoefer IE, van Royen N, Rectenwald JE, Bray EJ, Abouhamze Z, Moldawer LL, et al. Direct evidence for tumor necrosis factor-alpha signaling in arteriogenesis. *Circulation*. 2002;105(14):1639-41.

23. Seiler C, Pohl T, Wustmann K, Hutter D, Nicolet PA, Windecker S, et al. Promotion of collateral growth by granulocyte-macrophage colony-stimulating factor in patients with coronary artery disease: a randomized, double-blind, placebo-controlled study. *Circulation*. 2001;104(17):2012-7.

24. Cai W, Vosschulte R, Afsah-Hedjri A, Koltai S, Kocsis E, Scholz D, et al. Altered balance between extracellular proteolysis and antiproteolysis is associated with adaptive coronary arteriogenesis. *J Mol Cell Cardiol*. 2000;32(6):997-1011.

25. Prior BM, Lloyd PG, Yang HT, Terjung RL. Exercise-induced vascular remodeling. *Exerc Sport Sci Rev*. 2003;31(1):26-33.

26. Niebauer J, Cooke JP. Cardiovascular effects of exercise: role of endothelial shear stress. *J Am Coll Cardiol*. 1996;28(7):1652-60.

27. Sata M, Nishimatsu H, Osuga J, Tanaka K, Ishizaka N, Ishibashi S, et al. Statins augment collateral growth in response to ischemia but they do not promote cancer and atherosclerosis. *Hypertension*. 2004;43(6):1214-20.

28. Czepluch FS, Bergler A, Waltenberger J. Hypercholesterolaemia impairs monocyte function in CAD patients. *J Intern Med*. 2007;261(2):201-4.

29. Potente M, Makinen T. Vascular heterogeneity and specialization in development and disease. *Nat Rev Mol Cell Biol*. 2017;18(8):477-94.

30. Zhao Z, Nelson AR, Betsholtz C, Zlokovic BV. Establishment and Dysfunction of the Blood-Brain Barrier. *Cell*. 2015;163(5):1064-78.

31. Aird WC. Endothelial cell heterogeneity. *Cold Spring Harb Perspect Med*. 2012;2(1):a006429.

32. Aird WC. Phenotypic heterogeneity of the endothelium: II. Representative vascular beds. *Circ Res*. 2007;100(2):174-90.

33. Kusumbe AP, Ramasamy SK, Adams RH. Coupling of angiogenesis and osteogenesis by a specific vessel subtype in bone. *Nature*. 2014;507(7492):323-8.

34. Aspelund A, Robciuc MR, Karaman S, Makinen T, Alitalo K. Lymphatic System in Cardiovascular Medicine. *Circ Res*. 2016;118(3):515-30.

35. Prior BM, Yang HT, Terjung RL. What makes vessels grow with exercise training? *J Appl Physiol (1985)*. 2004;97(3):1119-28.

36. Potente M, Gerhardt H, Carmeliet P. Basic and therapeutic aspects of angiogenesis. *Cell*. 2011;146(6):873-87.

37. Adams RH, Eichmann A. Axon guidance molecules in vascular patterning. *Cold Spring Harb Perspect Biol*. 2010;2(5):a001875.

38. London NR, Smith MC, Li DY. Emerging mechanisms of vascular stabilization. *J Thromb Haemost*. 2009;7 Suppl 1:57-60.

39. Koch AW, Mathivet T, Larrivee B, Tong RK, Kowalski J, Pibouin-Fragner L, et al. Robo4 maintains vessel integrity and inhibits angiogenesis by interacting with UNC5B. *Dev Cell*. 2011;20(1):33-46.

40. Castets M, Mehlen P. Netrin-1 role in angiogenesis: to be or not to be a pro-angiogenic factor? *Cell Cycle*. 2010;9(8):1466-71.

41. Carmeliet P, Tessier-Lavigne M. Common mechanisms of nerve and blood vessel wiring. *Nature*. 2005;436(7048):193-200.

42. Kim J, Oh WJ, Gaiano N, Yoshida Y, Gu C. Semaphorin 3E-Plexin-D1 signaling regulates VEGF function in developmental angiogenesis via a feedback mechanism. *Genes Dev*. 2011;25(13):1399-411.

43. Pitulescu ME, Adams RH. Eph/ephrin molecules--a hub for signaling and endocytosis. *Genes Dev*. 2010;24(22):2480-92.

44. Sawamiphak S, Seidel S, Essmann CL, Wilkinson GA, Pitulescu ME, Acker T, et al. Ephrin-B2 regulates VEGFR2 function in developmental and tumour angiogenesis. *Nature*. 2010;465(7297):487-91.

45. Wang Y, Nakayama M, Pitulescu ME, Schmidt TS, Bochenek ML, Sakakibara A, et al. Ephrin-B2 controls VEGF-induced angiogenesis and lymphangiogenesis. *Nature*. 2010;465(7297):483-6.

46. Phng LK, Gerhardt H. Angiogenesis: a team effort coordinated by notch. *Dev Cell*. 2009;16(2):196-208.

47. Eilken HM, Adams RH. Dynamics of endothelial cell behavior in sprouting angiogenesis. *Curr Opin Cell Biol*. 2010;22(5):617-25.

48. Zeeb M, Strilic B, Lammert E. Resolving cell-cell junctions: lumen formation in blood vessels. *Curr Opin Cell Biol*. 2010;22(5):626-32.

49. Strilic B, Kucera T, Eglinger J, Hughes MR, McNagny KM, Tsukita S, et al. The molecular basis of vascular lumen formation in the developing mouse aorta. *Dev Cell*. 2009;17(4):505-15.

50. Gebala V, Collins R, Geudens I, Phng LK, Gerhardt H. Blood flow drives lumen formation by inverse membrane blebbing during angiogenesis in vivo. *Nat Cell Biol*. 2016;18(4):443-50.

51. Herwig L, Blum Y, Krudewig A, Ellertsdottir E, Lenard A, Belting HG, et al. Distinct cellular mechanisms of blood vessel fusion in the zebrafish embryo. *Curr Biol*. 2011;21(22):1942-8.

52. Korn C, Augustin HG. Mechanisms of Vessel Pruning and Regression. *Dev Cell*. 2015;34(1):5-17.

53. Short RH. Alveolar epithelium in relation to growth of the lung. *Philos Trans R Soc Lond B Biol Sci*. 1950;235(622):35-86.

54. Caduff JH, Fischer LC, Burri PH. Scanning electron microscope study of the developing microvasculature in the postnatal rat lung. *Anat Rec*. 1986;216(2):154-64.

55. Patan S, Haenni B, Burri PH. Implementation of intussusceptive microvascular growth in the chicken chorioallantoic membrane (CAM): 1. pillar formation by folding of the capillary wall. *Microvasc Res*. 1996;51(1):80-98.

56. Burri PH, Hlushchuk R, Djonov V. Intussusceptive angiogenesis: its emergence, its characteristics, and its significance. *Dev Dyn*. 2004;231(3):474-88.

57. Gianni-Barrera R, Bartolomeo M, Vollmar B, Djonov V, Banfi A. Split for the cure: VEGF, PDGF-BB and intussusception in therapeutic angiogenesis. *Biochem Soc Trans*. 2014;42(6):1637-42.

58. Makanya AN, Hlushchuk R, Djonov VG. Intussusceptive angiogenesis and its role in vascular morphogenesis, patterning, and remodeling. *Angiogenesis*. 2009;12(2):113-23.

59. Styp-Rekowska B, Hlushchuk R, Pries AR, Djonov V. Intussusceptive angiogenesis: pillars against the blood flow. *Acta Physiol (Oxf)*. 2011;202(3):213-23.

60. Djonov V, Schmid M, Tschanz SA, Burri PH. Intussusceptive angiogenesis: its role in embryonic vascular network formation. *Circ Res*. 2000;86(3):286-92.

61. Djonov VG, Galli AB, Burri PH. Intussusceptive arborization contributes to vascular tree formation in the chick chorio-allantoic membrane. *Anat Embryol (Berl)*. 2000;202(5):347-57.

62. Djonov VG, Kurz H, Burri PH. Optimality in the developing vascular system: branching remodeling by means of intussusception as an efficient adaptation mechanism. *Dev Dyn*. 2002;224(4):391-402.

63. Patan S, Haenni B, Burri PH. Implementation of intussusceptive microvascular growth in the chicken chorioallantoic membrane (CAM). *Microvasc Res*. 1997;53(1):33-52.

64. Gargett CE, Lederman F, Heryanto B, Gambino LS, Rogers PA. Focal vascular endothelial growth factor correlates with angiogenesis in human endometrium. Role of intravascular neutrophils. *Hum Reprod*. 2001;16(6):1065-75.

65. Gambino LS, Wreford NG, Bertram JF, Dockery P, Lederman F, Rogers PA. Angiogenesis occurs by vessel elongation in proliferative phase human endometrium. *Hum Reprod*. 2002;17(5):1199-206.

66. Zhang ZG, Zhang L, Jiang Q, Chopp M. Bone marrow-derived endothelial progenitor cells participate in cerebral neovascularization after focal cerebral ischemia in the adult mouse. *Circ Res*. 2002;90(3):284-8.

67. Hlushchuk R, Riesterer O, Baum O, Wood J, Gruber G, Pruschy M, et al. Tumor recovery by angiogenic switch from sprouting to intussusceptive angiogenesis after treatment with PTK787/ZK222584 or ionizing radiation. *Am J Pathol*. 2008;173(4):1173-85.

68. Burri PH, Djonov V. Intussusceptive angiogenesis--the alternative to capillary sprouting. *Mol Aspects Med*. 2002;23(6S):S1-27.

69. Kurz H, Burri PH, Djonov VG. Angiogenesis and vascular remodeling by intussusception: from form to function. *News Physiol Sci*. 2003;18:65-70.

70. Filipovic N, Tsuda A, Lee GS, Miele LF, Lin M, Konerding MA, et al. Computational flow dynamics in a geometric model of intussusceptive angiogenesis. *Microvasc Res*. 2009;78(3):286-93.

71. Egginton S, Zhou AL, Brown MD, Hudlicka O. Unorthodox angiogenesis in skeletal muscle. *Cardiovasc Res*. 2001;49(3):634-46.

72. Williams JL, Cartland D, Rudge JS, Egginton S. VEGF trap abolishes shear stress- and overload-dependent angiogenesis in skeletal muscle. *Microcirculation*. 2006;13(6):499-509.

73. Gianni-Barrera R, Trani M, Fontanellaz C, Heberer M, Djonov V, Hlushchuk R, et al. VEGF over-expression in skeletal muscle induces angiogenesis by intussusception rather than sprouting. *Angiogenesis*. 2013;16(1):123-36.

74. Baum O, Suter F, Gerber B, Tschanz SA, Buergy R, Blank F, et al. VEGF-A promotes intussusceptive angiogenesis in the developing chicken chorioallantoic membrane. *Microcirculation*. 2010;17(6):447-57.

75. Gianni-Barrera R, Trani M, Reginato S, Banfi A. To sprout or to split? VEGF, Notch and vascular morphogenesis. *Biochem Soc Trans*. 2011;39(6):1644-8.

76. Schlatter P, Konig MF, Karlsson LM, Burri PH. Quantitative study of intussusceptive capillary growth in the chorioallantoic membrane (CAM) of the chicken embryo. *Microvasc Res*. 1997;54(1):65-73.

77. Senger DR, Galli SJ, Dvorak AM, Perruzzi CA, Harvey VS, Dvorak HF. Tumor cells secrete a vascular permeability factor that promotes accumulation of ascites fluid. *Science*. 1983;219(4587):983-5.

78. Simons M, Gordon E, Claesson-Welsh L. Mechanisms and regulation of endothelial VEGF receptor signalling. *Nat Rev Mol Cell Biol*. 2016;17(10):611-25.

79. Stuttfeld E, Ballmer-Hofer K. Structure and function of VEGF receptors. *IUBMB Life*. 2009;61(9):915-22.

80. Ferrara N. Vascular endothelial growth factor: basic science and clinical progress. *Endocr Rev*. 2004;25(4):581-611.

81. Koch S, Tugues S, Li X, Gualandi L, Claesson-Welsh L. Signal transduction by vascular endothelial growth factor receptors. *Biochem J*. 2011;437(2):169-83.

82. Ruiz de Almodovar C, Lambrechts D, Mazzone M, Carmeliet P. Role and therapeutic potential of VEGF in the nervous system. *Physiol Rev*. 2009;89(2):607-48.

83. Fearnley GW, Smith GA, Harrison MA, Wheatcroft SB, Tomlinson DC, Ponnambalam S. Vascular endothelial growth factor-A regulation of blood vessel sprouting in health and disease. *OA Biochemistry*. 2013;01(1):5.

84. Stalmans I, Ng YS, Rohan R, Fruttiger M, Bouche A, Yuce A, et al. Arteriolar and venular patterning in retinas of mice selectively expressing VEGF isoforms. *J Clin Invest*. 2002;109(3):327-36.

85. Koch S, Claesson-Welsh L. Signal transduction by vascular endothelial growth factor receptors. *Cold Spring Harb Perspect Med*. 2012;2(7):a006502.

86. Fong GH, Rossant J, Gertsenstein M, Breitman ML. Role of the Flt-1 receptor tyrosine kinase in regulating the assembly of vascular endothelium. *Nature*. 1995;376(6535):66-70.

87. Fong GH, Klingensmith J, Wood CR, Rossant J, Breitman ML. Regulation of flt-1 expression during mouse embryogenesis suggests a role in the establishment of vascular endothelium. *Dev Dyn*. 1996;207(1):1-10.

88. Fong GH, Zhang L, Bryce DM, Peng J. Increased hemangioblast commitment, not vascular disorganization, is the primary defect in flt-1 knock-out mice. *Development*. 1999;126(13):3015-25.

89. Hiratsuka S, Minowa O, Kuno J, Noda T, Shibuya M. Flt-1 lacking the tyrosine kinase domain is sufficient for normal development and angiogenesis in mice. *Proc Natl Acad Sci U S A*. 1998;95(16):9349-54.

90. Imoukhuede PI, Popel AS. Quantification and cell-to-cell variation of vascular endothelial growth factor receptors. *Exp Cell Res*. 2011;317(7):955-65.

91. Papadopoulos N, Martin J, Ruan Q, Rafique A, Rosconi MP, Shi E, et al. Binding and neutralization of vascular endothelial growth factor (VEGF) and related ligands by VEGF Trap, ranibizumab and bevacizumab. *Angiogenesis*. 2012;15(2):171-85.

92. Kendall RL, Thomas KA. Inhibition of vascular endothelial cell growth factor activity by an endogenously encoded soluble receptor. *Proc Natl Acad Sci U S A*. 1993;90(22):10705-9.

93. Maynard SE, Min JY, Merchan J, Lim KH, Li J, Mondal S, et al. Excess placental soluble fms-like tyrosine kinase 1 (sFlt1) may contribute to endothelial dysfunction, hypertension, and proteinuria in preeclampsia. *J Clin Invest*. 2003;111(5):649-58.

94. Shalaby F, Ho J, Stanford WL, Fischer KD, Schuh AC, Schwartz L, et al. A requirement for Flk1 in primitive and definitive hematopoiesis and vasculogenesis. *Cell*. 1997;89(6):981-90.

95. Albuquerque RJ, Hayashi T, Cho WG, Kleinman ME, Dridi S, Takeda A, et al. Alternatively spliced vascular endothelial growth factor receptor-2 is an essential endogenous inhibitor of lymphatic vessel growth. *Nat Med*. 2009;15(9):1023-30.

96. Benedito R, Rocha SF, Woeste M, Zamykal M, Radtke F, Casanovas O, et al. Notch-dependent VEGFR3 upregulation allows angiogenesis without VEGF-VEGFR2 signalling. *Nature*. 2012;484(7392):110-4.

97. Zhou F, Chang Z, Zhang L, Hong YK, Shen B, Wang B, et al. Akt/Protein kinase B is required for lymphatic network formation, remodeling, and valve development. *Am J Pathol*. 2010;177(4):2124-33.

98. Karkkainen MJ, Haiko P, Sainio K, Partanen J, Taipale J, Petrova TV, et al. Vascular endothelial growth factor C is required for sprouting of the first lymphatic vessels from embryonic veins. *Nat Immunol*. 2004;5(1):74-80.

99. Koltowska K, Paterson S, Bower NI, Baillie GJ, Lagendijk AK, Astin JW, et al. mafba is a downstream transcriptional effector of Vegfc signaling essential for embryonic lymphangiogenesis in zebrafish. *Genes Dev*. 2015;29(15):1618-30.

100. Ruch C, Skiniotis G, Steinmetz MO, Walz T, Ballmer-Hofer K. Structure of a VEGF-VEGF receptor complex determined by electron microscopy. *Nat Struct Mol Biol*. 2007;14(3):249-50.

101. Dixelius J, Makinen T, Wirzenius M, Karkkainen MJ, Wernstedt C, Alitalo K, et al. Ligand-induced vascular endothelial growth factor receptor-3 (VEGFR-3) heterodimerization with VEGFR-2 in primary lymphatic endothelial cells regulates tyrosine phosphorylation sites. *J Biol Chem*. 2003;278(42):40973-9.

102. Grunewald FS, Prota AE, Giese A, Ballmer-Hofer K. Structure-function analysis of VEGF receptor activation and the role of coreceptors in angiogenic signaling. *Biochim Biophys Acta*. 2010;1804(3):567-80.

103. Ochsenbein AM, Karaman S, Proulx ST, Berchtold M, Jurisic G, Stoeckli ET, et al. Endothelial cell-derived semaphorin 3A inhibits filopodia formation by blood vascular tip cells. *Development*. 2016;143(4):589-94.

104. van der Zwaag B, Hellemons AJ, Leenders WP, Burbach JP, Brunner HG, Padberg GW, et al. PLEXIN-D1, a novel plexin family member, is expressed in vascular endothelium and the central nervous system during mouse embryogenesis. *Dev Dyn*. 2002;225(3):336-43.

105. Groppa E, Brkic S, Bovo E, Reginato S, Sacchi V, Di Maggio N, et al. VEGF dose regulates vascular stabilization through Semaphorin3A and the Neuropilin-1+ monocyte/TGF-beta1 paracrine axis. *EMBO Mol Med*. 2015;7(10):1366-84.

106. Parker MW, Xu P, Li X, Vander Kooi CW. Structural basis for selective vascular endothelial growth factor-A (VEGF-A) binding to neuropilin-1. *J Biol Chem*. 2012;287(14):11082-9.

107. Kawasaki T, Kitsukawa T, Bekku Y, Matsuda Y, Sanbo M, Yagi T, et al. A requirement for neuropilin-1 in embryonic vessel formation. *Development*. 1999;126(21):4895-902.

108. Jones EA, Yuan L, Breant C, Watts RJ, Eichmann A. Separating genetic and hemodynamic defects in neuropilin 1 knockout embryos. *Development*. 2008;135(14):2479-88.

109. Gelfand MV, Hagan N, Tata A, Oh WJ, Lacoste B, Kang KT, et al. Neuropilin-1 functions as a VEGFR2 co-receptor to guide developmental angiogenesis independent of ligand binding. *Elife*. 2014;3:e03720.

110. Fantin A, Herzog B, Mahmoud M, Yamaji M, Plein A, Denti L, et al. Neuropilin 1 (NRP1) hypomorphism combined with defective VEGF-A binding reveals novel roles for NRP1 in developmental and pathological angiogenesis. *Development*. 2014;141(3):556-62.

111. Plein A, Fantin A, Ruhrberg C. Neuropilin regulation of angiogenesis, arteriogenesis, and vascular permeability. *Microcirculation*. 2014;21(4):315-23.

112. Koch S, van Meeteren LA, Morin E, Testini C, Westrom S, Bjorkelund H, et al. NRP1 presented in trans to the endothelium arrests VEGFR2 endocytosis, preventing angiogenic signaling and tumor initiation. *Dev Cell*. 2014;28(6):633-46.

113. West XZ, Meller N, Malinin NL, Deshmukh L, Meller J, Mahabeleshwar GH, et al. Integrin beta3 crosstalk with VEGFR accommodating tyrosine phosphorylation as a regulatory switch. *PLoS One*. 2012;7(2):e31071.

114. Byzova TV, Goldman CK, Pampori N, Thomas KA, Bett A, Shattil SJ, et al. A mechanism for modulation of cellular responses to VEGF: activation of the integrins. *Mol Cell*. 2000;6(4):851-60.

115. Chen TT, Luque A, Lee S, Anderson SM, Segura T, Iruela-Arispe ML. Anchorage of VEGF to the extracellular matrix conveys differential signaling responses to endothelial cells. *J Cell Biol*. 2010;188(4):595-609.

116. Tugues S, Honjo S, Konig C, Padhan N, Kroon J, Gualandi L, et al. Tetraspanin CD63 promotes vascular endothelial growth factor receptor 2-beta1 integrin complex formation, thereby regulating activation and downstream signaling in endothelial cells in vitro and in vivo. *J Biol Chem*. 2013;288(26):19060-71.

117. Nakayama M, Nakayama A, van Lessen M, Yamamoto H, Hoffmann S, Drexler HC, et al. Spatial regulation of VEGF receptor endocytosis in angiogenesis. *Nat Cell Biol*. 2013;15(3):249-60.

118. Grazia Lampugnani M, Zanetti A, Corada M, Takahashi T, Balconi G, Breviario F, et al. Contact inhibition of VEGF-induced proliferation requires vascular endothelial cadherin, beta-catenin, and the phosphatase DEP-1/CD148. *J Cell Biol*. 2003;161(4):793-804.

119. Lampugnani MG, Orsenigo F, Gagliani MC, Tacchetti C, Dejana E. Vascular endothelial cadherin controls VEGFR-2 internalization and signaling from intracellular compartments. *J Cell Biol*. 2006;174(4):593-604.

120. Pasula S, Cai X, Dong Y, Messa M, McManus J, Chang B, et al. Endothelial epsin deficiency decreases tumor growth by enhancing VEGF signaling. *J Clin Invest*. 2012;122(12):4424-38.

121. Dalziel M, Crispin M, Scanlan CN, Zitzmann N, Dwek RA. Emerging principles for the therapeutic exploitation of glycosylation. *Science*. 2014;343(6166):1235681.

122. Jin F, Hagemann N, Brockmeier U, Schafer ST, Zechariah A, Hermann DM. LDL attenuates VEGF-induced angiogenesis via mechanisms involving VEGFR2 internalization and degradation following endosome-trans-Golgi network trafficking. *Angiogenesis*. 2013;16(3):625-37.

123. Kumar VB, Viji RI, Kiran MS, Sudhakaran PR. Endothelial cell response to lactate: implication of PAR modification of VEGF. *J Cell Physiol*. 2007;211(2):477-85.

124. Ruan GX, Kazlauskas A. Lactate engages receptor tyrosine kinases Axl, Tie2, and vascular endothelial growth factor receptor 2 to activate phosphoinositide 3-kinase/Akt and promote angiogenesis. *J Biol Chem*. 2013;288(29):21161-72.

125. Mitola S, Ravelli C, Moroni E, Salvi V, Leali D, Ballmer-Hofer K, et al. Gremlin is a novel agonist of the major proangiogenic receptor VEGFR2. *Blood*. 2010;116(18):3677-80.

126. Jin ZG, Ueba H, Tanimoto T, Lungu AO, Frame MD, Berk BC. Ligand-independent activation of vascular endothelial growth factor receptor 2 by fluid shear stress regulates activation of endothelial nitric oxide synthase. *Circ Res*. 2003;93(4):354-63.

127. Tzima E, Irani-Tehrani M, Kiosses WB, Dejana E, Schultz DA, Engelhardt B, et al. A mechanosensory complex that mediates the endothelial cell response to fluid shear stress. *Nature*. 2005;437(7057):426-31.

128. Wang S, Iring A, Strilic B, Albarran Juarez J, Kaur H, Troidl K, et al. P2Y(2) and Gq/G(1)(1) control blood pressure by mediating endothelial mechanotransduction. *J Clin Invest*. 2015;125(8):3077-86.

129. Sakurai Y, Ohgimoto K, Kataoka Y, Yoshida N, Shibuya M. Essential role of Flk-1 (VEGF receptor 2) tyrosine residue 1173 in vasculogenesis in mice. *Proc Natl Acad Sci U S A*. 2005;102(4):1076-81.

130. Takahashi T, Yamaguchi S, Chida K, Shibuya M. A single autophosphorylation site on KDR/Flk-1 is essential for VEGF-A-dependent activation of PLC-gamma and DNA synthesis in vascular endothelial cells. *EMBO J*. 2001;20(11):2768-78.

131. Takahashi T, Ueno H, Shibuya M. VEGF activates protein kinase C-dependent, but Ras-independent Raf-MEK-MAP kinase pathway for DNA synthesis in primary endothelial cells. *Oncogene*. 1999;18(13):2221-30.

132. Meadows KN, Bryant P, Pumiglia K. Vascular endothelial growth factor induction of the angiogenic phenotype requires Ras activation. *J Biol Chem*. 2001;276(52):49289-98.

133. Lawson ND, Mugford JW, Diamond BA, Weinstein BM. phospholipase C gamma-1 is required downstream of vascular endothelial growth factor during arterial development. *Genes Dev*. 2003;17(11):1346-51.

134. Leitges M, Schmedt C, Guinamard R, Davoust J, Schaal S, Stabel S, et al. Immunodeficiency in protein kinase cbeta-deficient mice. *Science*. 1996;273(5276):788-91.

135. Murakami M, Nguyen LT, Hatanaka K, Schachterle W, Chen PY, Zhuang ZW, et al. FGF-dependent regulation of VEGF receptor 2 expression in mice. *J Clin Invest*. 2011;121(7):2668-78.

136. Wang S, Li X, Parra M, Verdin E, Bassel-Duby R, Olson EN. Control of endothelial cell proliferation and migration by VEGF signaling to histone deacetylase 7. *Proc Natl Acad Sci U S A*. 2008;105(22):7738-43.

137. Carmeliet P, Lampugnani MG, Moons L, Breviario F, Compernolle V, Bono F, et al. Targeted deficiency or cytosolic truncation of the VE-cadherin gene in mice impairs VEGF-mediated endothelial survival and angiogenesis. *Cell*. 1999;98(2):147-57.

138. Ruan GX, Kazlauskas A. Axl is essential for VEGF-A-dependent activation of PI3K/Akt. *EMBO J*. 2012;31(7):1692-703.

139. Shiojima I, Walsh K. Role of Akt signaling in vascular homeostasis and angiogenesis. *Circ Res*. 2002;90(12):1243-50.

140. Zhuang G, Yu K, Jiang Z, Chung A, Yao J, Ha C, et al. Phosphoproteomic analysis implicates the mTORC2-FoxO1 axis in VEGF signaling and feedback activation of receptor tyrosine kinases. *Sci Signal*. 2013;6(271):ra25.

141. Graupera M, Guillermet-Guibert J, Foukas LC, Phng LK, Cain RJ, Salpekar A, et al. Angiogenesis selectively requires the p110alpha isoform of PI3K to control endothelial cell migration. *Nature*. 2008;453(7195):662-6.

142. Jalali S, Li YS, Sotoudeh M, Yuan S, Li S, Chien S, et al. Shear stress activates p60src-Ras-MAPK signaling pathways in vascular endothelial cells. *Arterioscler Thromb Vasc Biol*. 1998;18(2):227-34.

143. Westhoff MA, Serrels B, Fincham VJ, Frame MC, Carragher NO. SRC-mediated phosphorylation of focal adhesion kinase couples actin and adhesion dynamics to survival signaling. *Mol Cell Biol*. 2004;24(18):8113-33.

144. Fortini ME. Notch signaling: the core pathway and its posttranslational regulation. *Dev Cell*. 2009;16(5):633-47.

145. Bray SJ. Notch signalling in context. *Nat Rev Mol Cell Biol*. 2016;17(11):722-35.

146. Niessen K, Karsan A. Notch signaling in the developing cardiovascular system. *Am J Physiol Cell Physiol*. 2007;293(1):C1-11.

147. Kovall RA, Gebelein B, Sprinzak D, Kopan R. The Canonical Notch Signaling Pathway: Structural and Biochemical Insights into Shape, Sugar, and Force. *Dev Cell*. 2017;41(3):228-41.

148. D'Souza B, Meloty-Kapella L, Weinmaster G. Canonical and non-canonical Notch ligands. *Curr Top Dev Biol*. 2010;92:73-129.

149. Ladi E, Nichols JT, Ge W, Miyamoto A, Yao C, Yang LT, et al. The divergent DSL ligand Dll3 does not activate Notch signaling but cell autonomously attenuates signaling induced by other DSL ligands. *J Cell Biol*. 2005;170(6):983-92.

150. Baladron V, Ruiz-Hidalgo MJ, Nueda ML, Diaz-Guerra MJ, Garcia-Ramirez JJ, Bonvini E, et al. dlk acts as a negative regulator of Notch1 activation through interactions with specific EGF-like repeats. *Exp Cell Res*. 2005;303(2):343-59.

151. Sanchez-Solana B, Nueda ML, Ruvira MD, Ruiz-Hidalgo MJ, Monsalve EM, Rivero S, et al. The EGF-like proteins DLK1 and DLK2 function as inhibitory non-canonical ligands of NOTCH1 receptor that modulate each other's activities. *Biochim Biophys Acta*. 2011;1813(6):1153-64.

152. Eiraku M, Tohgo A, Ono K, Kaneko M, Fujishima K, Hirano T, et al. DNER acts as a neuron-specific Notch ligand during Bergmann glial development. *Nat Neurosci*. 2005;8(7):873-80.

153. Cui XY, Hu QD, Tekaya M, Shimoda Y, Ang BT, Nie DY, et al. NB-3/Notch1 pathway via Deltex1 promotes neural progenitor cell differentiation into oligodendrocytes. *J Biol Chem*. 2004;279(24):25858-65.

154. Hu QD, Ang BT, Karsak M, Hu WP, Cui XY, Duka T, et al. F3/contactin acts as a functional ligand for Notch during oligodendrocyte maturation. *Cell*. 2003;115(2):163-75.

155. Albig AR, Becenti DJ, Roy TG, Schiemann WP. Microfibril-associate glycoprotein-2 (MAGP-2) promotes angiogenic cell sprouting by blocking notch signaling in endothelial cells. *Microvasc Res*. 2008;76(1):7-14.

156. Gupta R, Hong D, Iborra F, Sarno S, Enver T. NOV (CCN3) functions as a regulator of human hematopoietic stem or progenitor cells. *Science*. 2007;316(5824):590-3.

157. Meng H, Zhang X, Hankenson KD, Wang MM. Thrombospondin 2 potentiates notch3/jagged1 signaling. *J Biol Chem*. 2009;284(12):7866-74.

158. Schmidt MH, Bicker F, Nikolic I, Meister J, Babuke T, Picuric S, et al. Epidermal growth factor-like domain 7 (EGFL7) modulates Notch signalling and affects neural stem cell renewal. *Nat Cell Biol*. 2009;11(7):873-80.

159. Bambino K, Lacko LA, Hajjar KA, Stuhlmann H. Epidermal growth factor-like domain 7 is a marker of the endothelial lineage and active angiogenesis. *Genesis*. 2014;52(7):657-70.

160. Meloty-Kapella L, Shergill B, Kuon J, Botvinick E, Weinmaster G. Notch ligand endocytosis generates mechanical pulling force dependent on dynamin, epsins, and actin. *Dev Cell*. 2012;22(6):1299-312.

161. Wang W, Struhl G. Distinct roles for Mind bomb, Neuralized and Epsin in mediating DSL endocytosis and signaling in Drosophila. *Development*. 2005;132(12):2883-94.

162. Andersson ER, Sandberg R, Lendahl U. Notch signaling: simplicity in design, versatility in function. *Development*. 2011;138(17):3593-612.

163. Kopan R, Ilagan MX. The canonical Notch signaling pathway: unfolding the activation mechanism. *Cell*. 2009;137(2):216-33.

164. Carrieri FA, Dale JK. Turn It Down a Notch. *Front Cell Dev Biol*. 2016;4:151.

165. Iso T, Maeno T, Oike Y, Yamazaki M, Doi H, Arai M, et al. Dll4-selective Notch signaling induces ephrinB2 gene expression in endothelial cells. *Biochem Biophys Res Commun*. 2006;341(3):708-14.

166. Lamont RE, Childs S. MAPping out arteries and veins. *Sci STKE*. 2006;2006(355):pe39.

167. Lawson ND, Vogel AM, Weinstein BM. sonic hedgehog and vascular endothelial growth factor act upstream of the Notch pathway during arterial endothelial differentiation. *Dev Cell*. 2002;3(1):127-36.

168. Pitulescu ME, Adams RH. Regulation of signaling interactions and receptor endocytosis in growing blood vessels. *Cell Adh Migr*. 2014;8(4):366-77.

169. Torres-Vazquez J, Kamei M, Weinstein BM. Molecular distinction between arteries and veins. *Cell Tissue Res*. 2003;314(1):43-59.

170. Wythe JD, Dang LT, Devine WP, Boudreau E, Artap ST, He D, et al. ETS factors regulate Vegf-dependent arterial specification. *Dev Cell*. 2013;26(1):45-58.

171. Sacilotto N, Monteiro R, Fritzsche M, Becker PW, Sanchez-Del-Campo L, Liu K, et al. Analysis of Dll4 regulation reveals a combinatorial role for Sox and Notch in arterial development. *Proc Natl Acad Sci U S A*. 2013;110(29):11893-8.

172. You LR, Lin FJ, Lee CT, DeMayo FJ, Tsai MJ, Tsai SY. Suppression of Notch signalling by the COUP-TFII transcription factor regulates vein identity. *Nature*. 2005;435(7038):98-104.

173. Swiatek PJ, Lindsell CE, del Amo FF, Weinmaster G, Gridley T. Notch1 is essential for postimplantation development in mice. *Genes Dev*. 1994;8(6):707-19.

174. Hamada Y, Kadokawa Y, Okabe M, Ikawa M, Coleman JR, Tsujimoto Y. Mutation in ankyrin repeats of the mouse Notch2 gene induces early embryonic lethality. *Development*. 1999;126(15):3415-24.

175. McCright B, Lozier J, Gridley T. Generation of new Notch2 mutant alleles. *Genesis*. 2006;44(1):29-33.

176. Domenga V, Fardoux P, Lacombe P, Monet M, Maciazek J, Krebs LT, et al. Notch3 is required for arterial identity and maturation of vascular smooth muscle cells. *Genes Dev*. 2004;18(22):2730-5.

177. Krebs LT, Xue Y, Norton CR, Sundberg JP, Beatus P, Lendahl U, et al. Characterization of Notch3-deficient mice: normal embryonic development and absence of genetic interactions with a Notch1 mutation. *Genesis*. 2003;37(3):139-43.

178. Krebs LT, Xue Y, Norton CR, Shutter JR, Maguire M, Sundberg JP, et al. Notch signaling is essential for vascular morphogenesis in mice. *Genes Dev*. 2000;14(11):1343-52.

179. Takeshita K, Satoh M, Ii M, Silver M, Limbourg FP, Mukai Y, et al. Critical role of endothelial Notch1 signaling in postnatal angiogenesis. *Circ Res*. 2007;100(1):70-8.

180. Xue Y, Gao X, Lindsell CE, Norton CR, Chang B, Hicks C, et al. Embryonic lethality and vascular defects in mice lacking the Notch ligand Jagged1. *Hum Mol Genet*. 1999;8(5):723-30.

181. Jiang R, Lan Y, Chapman HD, Shawber C, Norton CR, Serreze DV, et al. Defects in limb, craniofacial, and thymic development in Jagged2 mutant mice. *Genes Dev*. 1998;12(7):1046-57.

182. Hrabe de Angelis M, McIntyre J, 2nd, Gossler A. Maintenance of somite borders in mice requires the Delta homologue DII1. *Nature*. 1997;386(6626):717-21.

183. Kusumi K, Sun ES, Kerrebrock AW, Bronson RT, Chi DC, Bulotsky MS, et al. The mouse pudgy mutation disrupts Delta homologue Dll3 and initiation of early somite boundaries. *Nat Genet*. 1998;19(3):274-8.

184. Gale NW, Dominguez MG, Noguera I, Pan L, Hughes V, Valenzuela DM, et al. Haploinsufficiency of delta-like 4 ligand results in embryonic lethality due to major defects in arterial and vascular development. *Proc Natl Acad Sci U S A*. 2004;101(45):15949-54.

185. Chabriat H, Vahedi K, Iba-Zizen MT, Joutel A, Nibbio A, Nagy TG, et al. Clinical spectrum of CADASIL: a study of 7 families. Cerebral autosomal dominant arteriopathy with subcortical infarcts and leukoencephalopathy. *Lancet*. 1995;346(8980):934-9.

186. Garg V, Muth AN, Ransom JF, Schluterman MK, Barnes R, King IN, et al. Mutations in NOTCH1 cause aortic valve disease. *Nature*. 2005;437(7056):270-4.

187. Oda T, Elkahloun AG, Pike BL, Okajima K, Krantz ID, Genin A, et al. Mutations in the human Jagged1 gene are responsible for Alagille syndrome. *Nat Genet*. 1997;16(3):235-42.

188. Warthen DM, Moore EC, Kamath BM, Morrissette JJ, Sanchez-Lara PA, Piccoli DA, et al. Jagged1 (JAG1) mutations in Alagille syndrome: increasing the mutation detection rate. *Hum Mutat*. 2006;27(5):436-43.

189. McDaniell R, Warthen DM, Sanchez-Lara PA, Pai A, Krantz ID, Piccoli DA, et al. NOTCH2 mutations cause Alagille syndrome, a heterogeneous disorder of the notch signaling pathway. *Am J Hum Genet*. 2006;79(1):169-73.

190. Uyttendaele H, Marazzi G, Wu G, Yan Q, Sassoon D, Kitajewski J. Notch4/int-3, a mammary proto-oncogene, is an endothelial cell-specific mammalian Notch gene. *Development*. 1996;122(7):2251-9.

191. Delev D, Pavlova A, Grote A, Bostrom A, Hollig A, Schramm J, et al. NOTCH4 gene polymorphisms as potential risk factors for brain arteriovenous malformation development and hemorrhagic presentation. *J Neurosurg*. 2017;126(5):1552-9.

192. Carlson TR, Yan Y, Wu X, Lam MT, Tang GL, Beverly LJ, et al. Endothelial expression of constitutively active Notch4 elicits reversible arteriovenous malformations in adult mice. *Proc Natl Acad Sci U S A*. 2005;102(28):9884-9.

193. Kitajewski J. Arteriovenous malformations in five dimensions. *Sci Transl Med*. 2012;4(117):117fs3.

194. Murphy PA, Kim TN, Huang L, Nielsen CM, Lawton MT, Adams RH, et al. Constitutively active Notch4 receptor elicits brain arteriovenous malformations through enlargement of capillary-like vessels. *Proc Natl Acad Sci U S A*. 2014;111(50):18007-12.

195. Murphy PA, Kim TN, Lu G, Bollen AW, Schaffer CB, Wang RA. Notch4 normalization reduces blood vessel size in arteriovenous malformations. *Sci Transl Med*. 2012;4(117):117ra8.

196. Murphy PA, Lam MT, Wu X, Kim TN, Vartanian SM, Bollen AW, et al. Endothelial Notch4 signaling induces hallmarks of brain arteriovenous malformations in mice. *Proc Natl Acad Sci U S A*. 2008;105(31):10901-6.

197. Uyttendaele H, Ho J, Rossant J, Kitajewski J. Vascular patterning defects associated with expression of activated Notch4 in embryonic endothelium. *Proc Natl Acad Sci U S A*. 2001;98(10):5643-8.

198. Shawber CJ, Das I, Francisco E, Kitajewski J. Notch signaling in primary endothelial cells. *Ann N Y Acad Sci*. 2003;995:162-70.

199. Shawber CJ, Funahashi Y, Francisco E, Vorontchikhina M, Kitamura Y, Stowell SA, et al. Notch alters VEGF responsiveness in human and murine endothelial cells by direct regulation of VEGFR-3 expression. *J Clin Invest*. 2007;117(11):3369-82.

200. Aste-Amezaga M, Zhang N, Lineberger JE, Arnold BA, Toner TJ, Gu M, et al. Characterization of Notch1 antibodies that inhibit signaling of both normal and mutated Notch1 receptors. *PLoS One*. 2010;5(2):e9094.

201. James AC, Szot JO, Iyer K, Major JA, Pursglove SE, Chapman G, et al. Notch4 reveals a novel mechanism regulating Notch signal transduction. *Biochim Biophys Acta*. 2014;1843(7):1272-84.

202. Roukens MG, Alloul-Ramdhani M, Baan B, Kobayashi K, Peterson-Maduro J, van Dam H, et al. Control of endothelial sprouting by a Tel-CtBP complex. *Nat Cell Biol*. 2010;12(10):933-42.

203. Jakobsson L, Franco CA, Bentley K, Collins RT, Ponsioen B, Aspalter IM, et al. Endothelial cells dynamically compete for the tip cell position during angiogenic sprouting. *Nat Cell Biol*. 2010;12(10):943-53.

204. Thurston G, Noguera-Troise I, Yancopoulos GD. The Delta paradox: DLL4 blockade leads to more tumour vessels but less tumour growth. *Nat Rev Cancer*. 2007;7(5):327-31.

205. Benedito R, Roca C, Sorensen I, Adams S, Gossler A, Fruttiger M, et al. The notch ligands Dll4 and Jagged1 have opposing effects on angiogenesis. *Cell*. 2009;137(6):1124-35.

206. Kume T. Novel insights into the differential functions of Notch ligands in vascular formation. *J Angiogenes Res*. 2009;1:8.

207. Armulik A, Genove G, Betsholtz C. Pericytes: developmental, physiological, and pathological perspectives, problems, and promises. *Dev Cell*. 2011;21(2):193-215.

208. Gaengel K, Genove G, Armulik A, Betsholtz C. Endothelial-mural cell signaling in vascular development and angiogenesis. *Arterioscler Thromb Vasc Biol*. 2009;29(5):630-8.

209. He L, Vanlandewijck M, Raschperger E, Andaloussi Mae M, Jung B, Lebouvier T, et al. Analysis of the brain mural cell transcriptome. *Sci Rep*. 2016;6:35108.

210. Sims DE. The pericyte--a review. *Tissue Cell*. 1986;18(2):153-74.

211. Diaz-Flores L, Gutierrez R, Madrid JF, Varela H, Valladares F, Acosta E, et al. Pericytes. Morphofunction, interactions and pathology in a quiescent and activated mesenchymal cell niche. *Histol Histopathol*. 2009;24(7):909-69.

212. Shepro D, Morel NM. Pericyte physiology. *FASEB J*. 1993;7(11):1031-8.

213. Tilton RG, Kilo C, Williamson JR. Pericyte-endothelial relationships in cardiac and skeletal muscle capillaries. *Microvasc Res*. 1979;18(3):325-35.

214. Bergwerff M, Verberne ME, DeRuiter MC, Poelmann RE, Gittenberger-de Groot AC. Neural crest cell contribution to the developing circulatory system: implications for vascular morphology? *Circ Res*. 1998;82(2):221-31.

215. Etchevers HC, Vincent C, Le Douarin NM, Couly GF. The cephalic neural crest provides pericytes and smooth muscle cells to all blood vessels of the face and forebrain. *Development*. 2001;128(7):1059-68.

216. Heglind M, Cederberg A, Aquino J, Lucas G, Ernfors P, Enerback S. Lack of the central nervous system- and neural crest-expressed forkhead gene Foxs1 affects motor function and body weight. *Mol Cell Biol*. 2005;25(13):5616-25.

217. Korn J, Christ B, Kurz H. Neuroectodermal origin of brain pericytes and vascular smooth muscle cells. *J Comp Neurol*. 2002;442(1):78-88.

218. Foster K, Sheridan J, Veiga-Fernandes H, Roderick K, Pachnis V, Adams R, et al. Contribution of neural crest-derived cells in the embryonic and adult thymus. *J Immunol*. 2008;180(5):3183-9.

219. Muller SM, Stolt CC, Terszowski G, Blum C, Amagai T, Kessaris N, et al. Neural crest origin of perivascular mesenchyme in the adult thymus. *J Immunol*. 2008;180(8):5344-51.

220. Wilm B, Ipenberg A, Hastie ND, Burch JB, Bader DM. The serosal mesothelium is a major source of smooth muscle cells of the gut vasculature. *Development*. 2005;132(23):5317-28.

221. Que J, Wilm B, Hasegawa H, Wang F, Bader D, Hogan BL. Mesothelium contributes to vascular smooth muscle and mesenchyme during lung development. *Proc Natl Acad Sci U S A*. 2008;105(43):16626-30.

222. Asahina K, Zhou B, Pu WT, Tsukamoto H. Septum transversum-derived mesothelium gives rise to hepatic stellate cells and perivascular mesenchymal cells in developing mouse liver. *Hepatology*. 2011;53(3):983-95.

223. Leveen P, Pekny M, Gebre-Medhin S, Swolin B, Larsson E, Betsholtz C. Mice deficient for PDGF B show renal, cardiovascular, and hematological abnormalities. *Genes Dev*. 1994;8(16):1875-87.

224. Soriano P. Abnormal kidney development and hematological disorders in PDGF beta-receptor mutant mice. *Genes Dev*. 1994;8(16):1888-96.

225. Tallquist M, Kazlauskas A. PDGF signaling in cells and mice. *Cytokine Growth Factor Rev*. 2004;15(4):205-13.

226. Greenberg JI, Shields DJ, Barillas SG, Acevedo LM, Murphy E, Huang J, et al. A role for VEGF as a negative regulator of pericyte function and vessel maturation. *Nature*. 2008;456(7223):809-13.

227. Banfi A, von Degenfeld G, Gianni-Barrera R, Reginato S, Merchant MJ, McDonald DM, et al. Therapeutic angiogenesis due to balanced single-vector delivery of VEGF and PDGF-BB. *FASEB J*. 2012;26(6):2486-97.

228. Gianni-Barrera R, Burger M, Wolff T, Heberer M, Schaefer DJ, Gurke L, et al. Long-term safety and stability of angiogenesis induced by balanced single-vector co-expression of PDGF-BB and VEGF164 in skeletal muscle. *Sci Rep*. 2016;6:21546.

229. Fagiani E, Christofori G. Angiopoietins in angiogenesis. *Cancer Lett*. 2013;328(1):18-26.

230. Maisonpierre PC, Suri C, Jones PF, Bartunkova S, Wiegand SJ, Radziejewski C, et al. Angiopoietin-2, a natural antagonist for Tie2 that disrupts in vivo angiogenesis. *Science*. 1997;277(5322):55-60.

231. Augustin HG, Koh GY, Thurston G, Alitalo K. Control of vascular morphogenesis and homeostasis through the angiopoietin-Tie system. *Nat Rev Mol Cell Biol*. 2009;10(3):165-77.

232. Koh GY. Orchestral actions of angiopoietin-1 in vascular regeneration. *Trends Mol Med*. 2013;19(1):31-9.

233. Gale NW, Thurston G, Hackett SF, Renard R, Wang Q, McClain J, et al. Angiopoietin-2 is required for postnatal angiogenesis and lymphatic patterning, and only the latter role is rescued by Angiopoietin-1. *Dev Cell*. 2002;3(3):411-23.

234. Suri C, Jones PF, Patan S, Bartunkova S, Maisonpierre PC, Davis S, et al. Requisite role of angiopoietin-1, a ligand for the TIE2 receptor, during embryonic angiogenesis. *Cell*. 1996;87(7):1171-80.

235. Gurrerero PA, McCarthy JH. TGF-β Activation and Signaling in Angiogenesis. In: Simionescu D, Simionescu A, editors. Physiologic and Pathologic Angiogenesis - Signaling Mechanisms and Targeted Therapy: InTech; 2017.

236. Massague J. TGFbeta signalling in context. *Nat Rev Mol Cell Biol*. 2012;13(10):616-30.

237. Dickson MC, Martin JS, Cousins FM, Kulkarni AB, Karlsson S, Akhurst RJ. Defective haematopoiesis and vasculogenesis in transforming growth factor-beta 1 knock out mice. *Development*. 1995;121(6):1845-54.

238. Urness LD, Sorensen LK, Li DY. Arteriovenous malformations in mice lacking activin receptor-like kinase-1. *Nat Genet*. 2000;26(3):328-31.

239. Larsson J, Goumans MJ, Sjostrand LJ, van Rooijen MA, Ward D, Leveen P, et al. Abnormal angiogenesis but intact hematopoietic potential in TGF-beta type I receptor-deficient mice. *EMBO J*. 2001;20(7):1663-73.

240. Lan Y, Liu B, Yao H, Li F, Weng T, Yang G, et al. Essential role of endothelial Smad4 in vascular remodeling and integrity. *Mol Cell Biol*. 2007;27(21):7683-92.

241. Chang H, Huylebroeck D, Verschueren K, Guo Q, Matzuk MM, Zwijsen A. Smad5 knockout mice die at mid-gestation due to multiple embryonic and extraembryonic defects. *Development*. 1999;126(8):1631-42.

242. Yang X, Castilla LH, Xu X, Li C, Gotay J, Weinstein M, et al. Angiogenesis defects and mesenchymal apoptosis in mice lacking SMAD5. *Development*. 1999;126(8):1571-80.

243. Li DY, Sorensen LK, Brooke BS, Urness LD, Davis EC, Taylor DG, et al. Defective angiogenesis in mice lacking endoglin. *Science*. 1999;284(5419):1534-7.

244. Li F, Lan Y, Wang Y, Wang J, Yang G, Meng F, et al. Endothelial Smad4 maintains cerebrovascular integrity by activating N-cadherin through cooperation with Notch. *Dev Cell*. 2011;20(3):291-302.

245. Barquilla A, Pasquale EB. Eph receptors and ephrins: therapeutic opportunities. *Annu Rev Pharmacol Toxicol*. 2015;55:465-87.

246. Boyd AW, Bartlett PF, Lackmann M. Therapeutic targeting of EPH receptors and their ligands. *Nat Rev Drug Discov*. 2014;13(1):39-62.

247. Kania A, Klein R. Mechanisms of ephrin-Eph signalling in development, physiology and disease. *Nat Rev Mol Cell Biol*. 2016;17(4):240-56.

248. Lisabeth EM, Falivelli G, Pasquale EB. Eph receptor signaling and ephrins. *Cold Spring Harb Perspect Biol*. 2013;5(9).

249. Salvucci O, Tosato G. Essential roles of EphB receptors and EphrinB ligands in endothelial cell function and angiogenesis. *Adv Cancer Res*. 2012;114:21-57.

250. Bohme B, VandenBos T, Cerretti DP, Park LS, Holtrich U, Rubsamen-Waigmann H, et al. Cell-cell adhesion mediated by binding of membrane-anchored ligand LERK-2 to the EPH-related receptor human embryonal kinase 2 promotes tyrosine kinase activity. *J Biol Chem*. 1996;271(40):24747-52.

251. Yin Y, Yamashita Y, Noda H, Okafuji T, Go MJ, Tanaka H. EphA receptor tyrosine kinases interact with co-expressed ephrin-A ligands in cis. *Neurosci Res*. 2004;48(3):285-96.

252. Davis S, Gale NW, Aldrich TH, Maisonpierre PC, Lhotak V, Pawson T, et al. Ligands for EPH-related receptor tyrosine kinases that require membrane attachment or clustering for activity. *Science*. 1994;266(5186):816-9.

253. Vearing C, Lee FT, Wimmer-Kleikamp S, Spirkoska V, To C, Stylianou C, et al. Concurrent binding of anti-EphA3 antibody and ephrin-A5 amplifies EphA3 signaling and downstream responses: potential as EphA3-specific tumor-targeting reagents. *Cancer Res*. 2005;65(15):6745-54.

254. Binns KL, Taylor PP, Sicheri F, Pawson T, Holland SJ. Phosphorylation of tyrosine residues in the kinase domain and juxtamembrane region regulates the biological and catalytic activities of Eph receptors. *Mol Cell Biol*. 2000;20(13):4791-805.

255. Singla N, Erdjument-Bromage H, Himanen JP, Muir TW, Nikolov DB. A semisynthetic Eph receptor tyrosine kinase provides insight into ligand-induced kinase activation. *Chem Biol*. 2011;18(3):361-71.

256. Marston DJ, Dickinson S, Nobes CD. Rac-dependent trans-endocytosis of ephrinBs regulates Eph-ephrin contact repulsion. *Nat Cell Biol*. 2003;5(10):879-88.

257. Zimmer M, Palmer A, Kohler J, Klein R. EphB-ephrinB bi-directional endocytosis terminates adhesion allowing contact mediated repulsion. *Nat Cell Biol*. 2003;5(10):869-78.

258. Fasen K, Cerretti DP, Huynh-Do U. Ligand binding induces Cbl-dependent EphB1 receptor degradation through the lysosomal pathway. *Traffic*. 2008;9(2):251-66.

259. Walker-Daniels J, Riese DJ, 2nd, Kinch MS. c-Cbl-dependent EphA2 protein degradation is induced by ligand binding. *Mol Cancer Res*. 2002;1(1):79-87.

260. Hattori M, Osterfield M, Flanagan JG. Regulated cleavage of a contact-mediated axon repellent. *Science*. 2000;289(5483):1360-5.

261. Pasquale EB. Eph-ephrin bidirectional signaling in physiology and disease. *Cell*. 2008;133(1):38-52.

262. Pasquale EB. Eph receptors and ephrins in cancer: bidirectional signalling and beyond. *Nat Rev Cancer*. 2010;10(3):165-80.

263. Heasman SJ, Ridley AJ. Mammalian Rho GTPases: new insights into their functions from in vivo studies. *Nat Rev Mol Cell Biol*. 2008;9(9):690-701.

264. Picco V, Hudson C, Yasuo H. Ephrin-Eph signalling drives the asymmetric division of notochord/neural precursors in Ciona embryos. *Development*. 2007;134(8):1491-7.

265. Shi W, Levine M. Ephrin signaling establishes asymmetric cell fates in an endomesoderm lineage of the Ciona embryo. *Development*. 2008;135(5):931-40.

266. Elowe S, Holland SJ, Kulkarni S, Pawson T. Downregulation of the Ras-mitogen-activated protein kinase pathway by the EphB2 receptor tyrosine kinase is required for ephrin-induced neurite retraction. *Mol Cell Biol*. 2001;21(21):7429-41.

267. Minami M, Koyama T, Wakayama Y, Fukuhara S, Mochizuki N. EphrinA/EphA signal facilitates insulin-like growth factor-I-induced myogenic differentiation through suppression of the Ras/extracellular signal-regulated kinase 1/2 cascade in myoblast cell lines. *Mol Biol Cell*. 2011;22(18):3508-19.

268. Bush JO, Soriano P. Ephrin-B1 forward signaling regulates craniofacial morphogenesis by controlling cell proliferation across Eph-ephrin boundaries. *Genes Dev*. 2010;24(18):2068-80.

269. Nievergall E, Janes PW, Stegmayer C, Vail ME, Haj FG, Teng SW, et al. PTP1B regulates Eph receptor function and trafficking. *J Cell Biol*. 2010;191(6):1189-203.

270. Dai D, Huang Q, Nussinov R, Ma B. Promiscuous and specific recognition among ephrins and Eph receptors. *Biochim Biophys Acta*. 2014;1844(10):1729-40.

271. Gerety SS, Wang HU, Chen ZF, Anderson DJ. Symmetrical mutant phenotypes of the receptor EphB4 and its specific transmembrane ligand ephrin-B2 in cardiovascular development. *Mol Cell*. 1999;4(3):403-14.

272. Wang HU, Chen ZF, Anderson DJ. Molecular distinction and angiogenic interaction between embryonic arteries and veins revealed by ephrin-B2 and its receptor Eph-B4. *Cell*. 1998;93(5):741-53.

273. Herbert SP, Huisken J, Kim TN, Feldman ME, Houseman BT, Wang RA, et al. Arterial-venous segregation by selective cell sprouting: an alternative mode of blood vessel formation. *Science*. 2009;326(5950):294-8.

274. Lindskog H, Kim YH, Jelin EB, Kong Y, Guevara-Gallardo S, Kim TN, et al. Molecular identification of venous progenitors in the dorsal aorta reveals an aortic origin for the cardinal vein in mammals. *Development*. 2014;141(5):1120-8.

275. Gale NW, Baluk P, Pan L, Kwan M, Holash J, DeChiara TM, et al. Ephrin-B2 selectively marks arterial vessels and neovascularization sites in the adult, with expression in both endothelial and smooth-muscle cells. *Dev Biol*. 2001;230(2):151-60.

276. Korff T, Braun J, Pfaff D, Augustin HG, Hecker M. Role of ephrinB2 expression in endothelial cells during arteriogenesis: impact on smooth muscle cell migration and monocyte recruitment. *Blood*. 2008;112(1):73-81.

277. Shin D, Garcia-Cardena G, Hayashi S, Gerety S, Asahara T, Stavrakis G, et al. Expression of ephrinB2 identifies a stable genetic difference between arterial and venous vascular smooth muscle as well as endothelial cells, and marks subsets of microvessels at sites of adult neovascularization. *Dev Biol*. 2001;230(2):139-50.

278. Salvucci O, Maric D, Economopoulou M, Sakakibara S, Merlin S, Follenzi A, et al. EphrinB reverse signaling contributes to endothelial and mural cell assembly into vascular structures. *Blood*. 2009;114(8):1707-16.

279. Fuller T, Korff T, Kilian A, Dandekar G, Augustin HG. Forward EphB4 signaling in endothelial cells controls cellular repulsion and segregation from ephrinB2 positive cells. *J Cell Sci*. 2003;116(Pt 12):2461-70.

280. Kim I, Ryu YS, Kwak HJ, Ahn SY, Oh JL, Yancopoulos GD, et al. EphB ligand, ephrinB2, suppresses the VEGF- and angiopoietin 1-induced Ras/mitogen-activated protein kinase pathway in venous endothelial cells. *FASEB J*. 2002;16(9):1126-8.

281. Steinle JJ, Meininger CJ, Forough R, Wu G, Wu MH, Granger HJ. Eph B4 receptor signaling mediates endothelial cell migration and proliferation via the phosphatidylinositol 3-kinase pathway. *J Biol Chem*. 2002;277(46):43830-5.

282. Zhang G, Brady J, Liang WC, Wu Y, Henkemeyer M, Yan M. EphB4 forward signalling regulates lymphatic valve development. *Nat Commun*. 2015;6:6625.

283. Foo SS, Turner CJ, Adams S, Compagni A, Aubyn D, Kogata N, et al. Ephrin-B2 controls cell motility and adhesion during blood-vessel-wall assembly. *Cell*. 2006;124(1):161-73.

284. Erber R, Eichelsbacher U, Powajbo V, Korn T, Djonov V, Lin J, et al. EphB4 controls blood vascular morphogenesis during postnatal angiogenesis. *EMBO J*. 2006;25(3):628-41.

285. Nakayama A, Nakayama M, Turner CJ, Hoing S, Lepore JJ, Adams RH. Ephrin-B2 controls PDGFRbeta internalization and signaling. *Genes Dev*. 2013;27(23):2576-89.

286. Dragneva G, Korpisalo P, Yla-Herttuala S. Promoting blood vessel growth in ischemic diseases: challenges in translating preclinical potential into clinical success. *Dis Model Mech*. 2013;6(2):312-22.

287. Yla-Herttuala S, Bridges C, Katz MG, Korpisalo P. Angiogenic gene therapy in cardiovascular diseases: dream or vision? *Eur Heart J*. 2017;38(18):1365-71.

288. European Stroke O, Tendera M, Aboyans V, Bartelink ML, Baumgartner I, Clement D, et al. ESC Guidelines on the diagnosis and treatment of peripheral artery diseases: Document covering atherosclerotic disease of extracranial carotid and vertebral, mesenteric, renal, upper and lower extremity arteries: the Task Force on the Diagnosis and Treatment of Peripheral Artery Diseases of the European Society of Cardiology (ESC). *Eur Heart J*. 2011;32(22):2851-906.

289. Fowkes FG, Rudan D, Rudan I, Aboyans V, Denenberg JO, McDermott MM, et al. Comparison of global estimates of prevalence and risk factors for peripheral artery disease in 2000 and 2010: a systematic review and analysis. *Lancet*. 2013;382(9901):1329-40.

290. Gorenoi V, Brehm MU, Koch A, Hagen A. Growth factors for angiogenesis in peripheral arterial disease. *Cochrane Database Syst Rev*. 2017;6:CD011741.

291. Norgren L, Hiatt WR, Dormandy JA, Nehler MR, Harris KA, Fowkes FG, et al. Inter-Society Consensus for the Management of Peripheral Arterial Disease (TASC II). *J Vasc Surg*. 2007;45 Suppl S:S5-67.

292. Gardner AW, Afaq A. Management of lower extremity peripheral arterial disease. *J Cardiopulm Rehabil Prev*. 2008;28(6):349-57.

293. Hirsch AT, Haskal ZJ, Hertzer NR, Bakal CW, Creager MA, Halperin JL, et al. ACC/AHA 2005 Practice Guidelines for the management of patients with peripheral arterial disease (lower extremity, renal, mesenteric, and abdominal aortic): a collaborative report from the American Association for Vascular Surgery/Society for Vascular Surgery, Society for Cardiovascular Angiography and Interventions, Society for Vascular Medicine and Biology, Society of Interventional Radiology, and the ACC/AHA Task Force on Practice Guidelines (Writing Committee to Develop Guidelines for the Management of Patients With Peripheral Arterial Disease): endorsed by the American Association of Cardiovascular and Pulmonary Rehabilitation; National Heart, Lung, and Blood Institute; Society for Vascular Nursing; TransAtlantic Inter-Society Consensus; and Vascular Disease Foundation. *Circulation*. 2006;113(11):e463-654.

294. Ouma GO, Jonas RA, Usman MH, Mohler ER, 3rd. Targets and delivery methods for therapeutic angiogenesis in peripheral artery disease. *Vasc Med*. 2012;17(3):174-92.

295. Baumgartner I, Pieczek A, Manor O, Blair R, Kearney M, Walsh K, et al. Constitutive expression of phVEGF165 after intramuscular gene transfer promotes collateral vessel development in patients with critical limb ischemia. *Circulation*. 1998;97(12):1114-23.

296. Isner JM, Pieczek A, Schainfeld R, Blair R, Haley L, Asahara T, et al. Clinical evidence of angiogenesis after arterial gene transfer of phVEGF165 in patient with ischaemic limb. *Lancet*. 1996;348(9024):370-4.

297. Laitinen M, Makinen K, Manninen H, Matsi P, Kossila M, Agrawal RS, et al. Adenovirus-mediated gene transfer to lower limb artery of patients with chronic critical leg ischemia. *Hum Gene Ther*. 1998;9(10):1481-6.

298. Rajagopalan S, Mohler ER, 3rd, Lederman RJ, Mendelsohn FO, Saucedo JF, Goldman CK, et al. Regional angiogenesis with vascular endothelial growth factor in peripheral arterial disease: a phase II randomized, double-blind, controlled study of adenoviral delivery of vascular endothelial growth factor 121 in patients with disabling intermittent claudication. *Circulation*. 2003;108(16):1933-8.

299. Henry TD, Annex BH, McKendall GR, Azrin MA, Lopez JJ, Giordano FJ, et al. The VIVA trial: Vascular endothelial growth factor in Ischemia for Vascular Angiogenesis. *Circulation*. 2003;107(10):1359-65.

300. Lederman RJ, Mendelsohn FO, Anderson RD, Saucedo JF, Tenaglia AN, Hermiller JB, et al. Therapeutic angiogenesis with recombinant fibroblast growth factor-2 for intermittent claudication (the TRAFFIC study): a randomised trial. *Lancet*. 2002;359(9323):2053-8.

301. Gupta R, Tongers J, Losordo DW. Human studies of angiogenic gene therapy. *Circ Res*. 2009;105(8):724-36.

302. Yla-Herttuala S, Baker AH. Cardiovascular Gene Therapy: Past, Present, and Future. *Mol Ther*. 2017;25(5):1095-106.

303. Karvinen H, Pasanen E, Rissanen TT, Korpisalo P, Vahakangas E, Jazwa A, et al. Long-term VEGF-A expression promotes aberrant angiogenesis and fibrosis in skeletal muscle. *Gene Ther*. 2011;18(12):1166-72.

304. Banfi A, Springer ML, Blau HM. Myoblast-mediated gene transfer for therapeutic angiogenesis. *Methods Enzymol*. 2002;346:145-57.

305. Ozawa CR, Banfi A, Glazer NL, Thurston G, Springer ML, Kraft PE, et al. Microenvironmental VEGF concentration, not total dose, determines a threshold between normal and aberrant angiogenesis. *J Clin Invest*. 2004;113(4):516-27.

306. Banfi A, von Degenfeld G, Blau HM. Critical role of microenvironmental factors in angiogenesis. *Curr Atheroscler Rep*. 2005;7(3):227-34.

# II. Aims

Ischemic diseases are characterized by reduced blood flow leading to poor tissue oxygenation and tissue damage (1, 2), Peripheral artery disease (PAD) is a type of ischemic condition caused by peripheral artery occlusions. PAD is a major cause of decreased mobility, functional capacity and quality of life. It increases the risks of amputation and/or death (3-5). Therapeutic angiogenesis is a promising strategy for PAD treatment, as it aims to induce growth of new blood vessels, restore blood flow and ultimately improve tissue regeneration. Different growth factors, predominantly VEGF, are used for induction of angiogenesis. Gene therapy approach was employed in almost all the clinical trials that aimed to deliver growth factors to the affected tissue, as direct protein delivery did not give satisfying results due to fast protein degradation. Systemic review of results obtained from 40 different clinical trials, that used VEGF, FGF or HGF gene delivery, showed no clear therapeutic benefit of the treatment. Even though treatment improved hemodynamic measures as well as ulceration and rest pain in patients, there was no clear improvement in walking ability and amputation rate (3). A potential reason has been identified in low transduction efficiency, leading to low local growth factor concentrations, at safe vector doses. Increasing the dose of delivered gene therapy vectors can lead to higher VEGF concentrations in the tissue, but it is accompanied by side effects like aberrant vessel growth and tissue damage (6). This creates an apparently very narrow therapeutic window, as low vector doses are inefficient, while higher doses become rapidly toxic. Therefore, there is a need to elucidate the molecular mechanisms of aberrant vessel growth in order to develop druggable targets to normalize vessel morphology, and allow the safe use of higher vector doses, ultimately leading to more robust induction of physiological functional vessels and increased therapeutic efficacy. We have previously demonstrated that stimulation of pericytes recruitment by PDGF-BB co-expression can normalize aberrant vessel growth induced by high and uncontrolled VEGF levels and ensure the induction of exclusively normal and mature microvascular networks (7, 8). Further, our group has also previously found

that VEGF expression in skeletal muscle, at the doses required for therapeutic benefit, induced vascular growth essentially without sprouting and rather by the process of intussusception (9), whose molecular regulation is still poorly understood. Therefore, the aim of the Thesis is to elucidate molecular signals in the pericyte-endothelial cell crosstalk that regulate intussusceptive angiogenesis and are responsible for the switch between normal and aberrant angiogenesis in skeletal muscle, in order to identify druggable targets to enable safe and effective vascular growth by robust therapeutic delivery of VEGF.

In Aim 1 (Chapter III), we focused on the three most important pathways regulating pericyte-endothelial interaction, namely TGFβ/TGFβR, Ang/Tie-2 and ephrinB2/EphB4. By complementary loss- and gain-of-function approaches, we identified a specific role for ephrinB2/EphB4 signaling in determining the outcome of VEGF-induced intussusceptive angiogenesis. We further showed that pharmacologic stimulation of EphB4 signaling can prevent aberrant angiogenesis despite high and uncontrolled VEGF levels, yielding instead robust growth of normal and mature microvascular networks, with functional benefit in a mouse model of hind-limb ischemia.

In Aim 2 (Chapter IV), we investigated the crosstalk between EphB4 and Notch4 signaling, as other findings in our group showed that Notch4 loss-of-function phenocopies EphB4 stimulation in switching aberrant angiogenesis by VEGF to normal.

# References

1. Dragneva G, Korpisalo P, Yla-Herttuala S. Promoting blood vessel growth in ischemic diseases: challenges in translating preclinical potential into clinical success. *Dis Model Mech*. 2013;6(2):312-22.

2. Yla-Herttuala S, Baker AH. Cardiovascular Gene Therapy: Past, Present, and Future. *Mol Ther*. 2017;25(5):1095-106.

3. Gorenoi V, Brehm MU, Koch A, Hagen A. Growth factors for angiogenesis in peripheral arterial disease. *Cochrane Database Syst Rev*. 2017;6:CD011741.

4. Hirsch AT, Haskal ZJ, Hertzer NR, Bakal CW, Creager MA, Halperin JL, et al. ACC/AHA 2005 Practice Guidelines for the management of patients with peripheral arterial disease (lower extremity, renal, mesenteric, and abdominal aortic): a collaborative report from the American Association for Vascular Surgery/Society for Vascular Surgery, Society for Cardiovascular Angiography and Interventions, Society for Vascular Medicine and Biology, Society of Interventional Radiology, and the ACC/AHA Task Force on Practice Guidelines (Writing Committee to Develop Guidelines for the Management of Patients With Peripheral Arterial Disease): endorsed by the American Association of Cardiovascular and Pulmonary Rehabilitation; National Heart, Lung, and Blood Institute; Society for Vascular Nursing; TransAtlantic Inter-Society Consensus; and Vascular Disease Foundation. *Circulation*. 2006;113(11):e463-654.

5. Ouma GO, Jonas RA, Usman MH, Mohler ER, 3rd. Targets and delivery methods for therapeutic angiogenesis in peripheral artery disease. *Vasc Med*. 2012;17(3):174-92.

6. Karvinen H, Pasanen E, Rissanen TT, Korpisalo P, Vahakangas E, Jazwa A, et al. Long-term VEGF-A expression promotes aberrant angiogenesis and fibrosis in skeletal muscle. *Gene Ther*. 2011;18(12):1166-72.

7. Banfi A, von Degenfeld G, Gianni-Barrera R, Reginato S, Merchant MJ, McDonald DM, et al. Therapeutic angiogenesis due to balanced single-vector delivery of VEGF and PDGF-BB. *FASEB J*. 2012;26(6):2486-97.

8. Gianni-Barrera R, Burger M, Wolff T, Heberer M, Schaefer DJ, Gurke L, et al. Long-term safety and stability of angiogenesis induced by balanced single-vector co-expression of PDGF-BB and VEGF164 in skeletal muscle. *Sci Rep*. 2016;6:21546.

9. Gianni-Barrera R, Trani M, Fontanellaz C, Heberer M, Djonov V, Hlushchuk R, et al. VEGF over-expression in skeletal muscle induces angiogenesis by intussusception rather than sprouting. *Angiogenesis*. 2013;16(1):123-36.

# III. EphrinB2/EphB4 signaling regulates intussusceptive angiogenesis by VEGF

# EphrinB2/EphB4 signaling regulates non-sprouting angiogenesis by VEGF

Elena Groppa[1,2,5,*], Sime Brkic[1,2,*], Galina Wirth[3], Petra Korpisalo-Pirinen[3], Veronica Sacchi[1,2,6], Manuele Giuseppe Muraro[1,2], Marianna Trani[1,2], Silvia Reginato[1,2], Roberto Gianni-Barrera[1,2], Seppo Ylä-Herttuala[3,4] and Andrea Banfi[1,2]

[1]Department of Biomedicine, University Hospital, University of Basel, Basel, Switzerland.
[2]Department of Surgery, University Hospital, Basel, Switzerland.
[3]A. I. Virtanen Institute, University of Eastern Finland, Kuopio, Finland.
[4]Heart Center, Kuopio University Hospital, Kuopio, Finland.
[5]Current address: The Biomedical Research Centre, The University of British Columbia, Vancouver, Canada.
[6]Current address: Heart Institute and Biology Department, San Diego State University, San Diego, CA, USA.

[*]These authors contributed equally

# Introduction

Angiogenesis plays a key role in the pathophysiology of a widespread variety of human diseases, both degenerative and neoplastic, as well as in physiological tissue regeneration (1). Vascular Endothelial Growth Factor-A (VEGF) is the master regulator of vascular growth in development and postnatal life, and it is therefore the key molecular target to promote the growth of new blood vessels in ischemic diseases, such as myocardial infarction, stroke or peripheral vascular disease (2, 3). However, simple VEGF gene delivery for therapeutic angiogenesis has failed to prove clinical efficacy to date, despite the clear biological activity of the factor (2, 4), highlighting the need to better understand the mechanisms of physiological vascular growth by VEGF, especially under therapeutically relevant conditions of factor delivery.

The best understood mode of angiogenesis is sprouting, which is mostly studied during development, when specialized endothelial tip cells migrate from pre-existing vessels, followed by proliferating stalk cells, to invade surrounding avascular tissue (5). However, blood vessels can also grow by the alternative mechanism of intussusception, or splitting angiogenesis, whereby rows of intraluminal endothelial pillars split pre-existing vessels longitudinally into new ones (6). Intussusception is increasingly recognized as a therapeutically important mode of angiogenesis, both in tumor resistance to anti-angiogenic treatments and in reparative vascular growth (7-9), but very little is known about its molecular regulation due to a paucity of appropriate models.

Taking advantage of a cell-based platform that we developed for the controlled expression of specific and homogeneous doses of angiogenic factors *in vivo*, we previously found that: 1) VEGF can induce either normal and functional capillary networks or aberrant angioma-like vascular structures depending on its concentration in the microenvironment around each producing cell *in vivo* (10); and 2) VEGF doses required for therapeutic efficacy

(11), induce robust vascular growth in skeletal muscle essentially through intussusception (9). Interestingly, both normal and aberrant vascular structures form through a first stage of circumferential enlargement within the first 4 days, followed by intussusceptive remodeling by 7 days (9), whereas the transition from normal to aberrant angiogenesis is determined by the retention or loss of pericytes during the initial stage of vascular enlargement (12).

Here, we took advantage of this unique and well-characterized model of VEGF dose-dependent intussusceptive angiogenesis to investigate its molecular regulation. We dissected the role of specific pericyte-mediated signaling pathways and we identified a critical function for ephrinB2/EphB4 signaling, but not TGF-β or angiopoietin signaling. Specifically, we show that the endothelial receptor EphB4 controls the outcome of intussusceptive angiogenesis by fine-tuning the degree of endothelial proliferation caused by specific VEGF doses and therefore the size of initial vascular enlargement, without directly affecting VEGF-R2 activation, but rather modulating its downstream signaling through MAPK/ERK. Together, these results identify the ephrinB2/EphB4 pathway as a key regulator of intussusceptive angiogenesis and a druggable target to modulate the therapeutic outcome of VEGF delivery.

# Materials and Methods

## Construction of blocker retroviral vectors

Retroviral vectors were constructed encoding the following soluble blockers of TGF-β1, Ang/Tie2 and ephrinB2/EphB4 signaling, respectively: a) the Latency-Associated Peptide (LAP), which associates with TGF-β1 to form the non-functional latent TGFβ complex, thereby inhibiting the biological activity of endogenous TGF-β1 (13); b) a receptor-body formed by fusing a truncated version of the receptor Tie2 and the Fc portion of IgG immunoglubulin (sTie2Fc), which sequesters angiopoietins and prevents them from signaling (14); and c) a monomeric truncated version of the receptor EphB4 (sEphB4), which binds membrane-bound ephrinB2 without activating it, as it does not form multimers, but prevents it from binding and activating the endogenous endothelial EphB4 receptor (15). The cDNAs of human LAP, murine sTie2Fc and human sEphB4 were cloned into the pAMFG retroviral vector in a bicistronic cassette (16), linked through an internal ribosomal entry sequence (IRES) to a truncated version of rabbit CD4 as a convenient cell surface marker, producing the pAMFG.CD4, pAMFG.CD4.LAP, pAMFG.CD4.sTie2Fc and pAMFG.CD4.sEphB4 retroviral vectors.

## $VEGF_{164}$ ELISA

The production of $VEGF_{164}$ in cell culture supernatants was quantified by a Quantikine mouse VEGF Immunoassay ELISA kit (R&D Systems, Abingdon, UK). One ml of fresh medium was incubated for 4 hours on myoblasts seeded overnight in a 60 mm dish, filtered and analyzed in duplicate. Results were normalized by the number of cells and time of incubation. Four dishes of cells were assayed per cell type (n=4).

## *In vivo* myoblast implantation

To avoid an immunological response to transduced myoblasts expressing xenogenic proteins (LacZ, rabbit CD4, human LAP and sEphB4), immunodeficient SCID CB.17 mice (Charles River Laboratories, Sulzfeld, Germany) were used. Myoblasts were dissociated in trypsin, resuspended at a concentration of $10^8$ cells/ml in sterile PBS with 0.5% BSA (Sigma-Aldrich Chemie GmbH, Steinheim, Germany) and $10^6$ cells were injected into the *Tibialis anterior* (TA) and *Gastrocnemius* (GC) muscles in the lower hindlimb, using a 30-gauge needle syringe, as previously described (10). All experiments were performed with similar number of samples from both muscle locations and the results were pooled together. Mice of 8-12 weeks of age, with equal representation of both genders, were randomly assigned to experimental groups, with a minimum of n=4 mice/group.

## Recombinant VEGF delivery by fibrin hydrogels

The transglutaminase substrate sequence NQEQVSPL (α2-$PI_{1–8}$) was fused to the N terminus of the mouse VEGF-$A_{164}$ cDNA by PCR. The fusion protein was expressed into *Escherichia coli* strain BL21 (De3) pLys (Novagen, Madison, WI) and isolated as described previously (17). Fibrin matrices of optimized composition were prepared as previously described (18), incorporating 56 mg/ml of aprotinin-α2-$PI_{1–8}$, to ensure controlled duration of degradation over 4 weeks, and 50 µg/ml of α2-$PI_{1–8}$-$VEGF_{164}$. For *in vivo* delivery, 6- to 8-wk-old immunodeficient CB.17 SCID mice (Charles River Laboratories) were used to avoid an immunological response to human fibrinogen and cross-linking enzymes. A liquid volume of 50 µl was aspirated rapidly with a 0.3-ml insulin syringe with integrated 30-gauge needle (Becton Dickinson, Basel, Switzerland) and injected into the GC muscle of the mice previously anesthetized with 3% isofluorane inhalation. After injection, *in situ* polymerization was allowed for 20 s before slowly extracting the needle.

## Recombinant adenovirus production and *in vivo* implantation

Recombinant adenoviruses expressing mouse $VEGF_{164}$ or human $VEGF_{165}$, were produced using the Adeno-XTM Expression System (Clontech, Saint- Germain-en-Laye, France) according to the manufacturer's recommendations. Adenoviral vectors were diluted in physiological solution and injected in TA and GC muscles in the lower hind limb of immune-deficient CB.17 SCID mice (Charles River Laboratories) at the titer of $1x10^8$ infectious units/injection, with a 30-gauge needle syringe, as previously described (19). Information on ischemia experiments is provided below.

## EphrinB2-Fc treatment

To stimulate EphB4 signaling *in vivo*, mice received 1 mg/kg of mouse ephrinB2-Fc (R&D Systems) or control Fc (Abcam, Cambridge, UK) by intraperitoneal injections twice weekly, starting 3 days before the myoblast injection, according to published protocols (20).

## RNA extraction and quantitative real-time PCR

For RNA extraction from total muscles, freshly harvested tissue was frozen in liquid nitrogen and disrupted using a Qiagen Tissue Lyser (Qiagen) in 1 ml TRIzol reagent (Invitrogen, Basel, Switzerland) for 100 mg of tissue. Total RNA was isolated from lysed tissues or *in vitro* cultured myoblasts, RAW264.7 and human dermal microvascular endothelial cells (HDMEC) with an RNeasy Mini Kit (Qiagen, Basel, Switzerland) according to manufacturer's instruction. RNA was reverse transcribed into cDNA using the Omniscript Reverse Transcription kit (Qiagen) at 37°C for 60 minutes. Quantitative Real-Time PCR (qRT-PCR) was performed on an ABI 7300 Real-Time PCR system (Applied Biosystems, Basel, Switzerland). Expression of genes of interest was determined using the following TaqMan Gene Expression assays (Applied Biosystems) according to manufacturer's instructions:

mouse *Tnfa* (Mm00443258_m1); mouse *Gapdh* (Mm03302249_g1); mouse *Pdgfb* (Mm00440678_m1); mouse *Pdgfrb* (Mm00435545_m1); human *Igfbp3* (Hs00365742_g1); human *Esm1* (Hs00199831_m1) and human *Gapdh* (Hs02758991_g1). Reactions were performed in triplicate for each template, averaged and normalized to expression of the same-species *Gapdh* housekeeping gene.

## Immunofluorescence tissue staining

Mice were anesthetized with ketamine (100 mg/kg) and xylazine (10 mg/kg) and sacrificed by intravascular perfusion of 1% paraformaldehyde in PBS pH 7.4. TA and GC muscles were harvested, post-fixed in 0.5% paraformaldehyde in PBS for 2 h, cryoprotected in 30% sucrose in PBS overnight at 4°C, embedded in OCT compound (CellPath, Newtown, Powys, UK), frozen in isopentane, and cryosectioned. The areas of engraftment were identified by tracking implanted myoblasts by X-gal staining (20-µm sections) or adenoviral infection sites by the typical mononuclear infiltrate with H&E (10-µm sections) in adjacent serial sections, as described previously (10). For immunofluorescence staining, 10-µm tissue sections were stained with the following primary antibodies and dilutions: rat monoclonal anti-mouse CD31 (clone MEC 13.3, BD Biosciences, Basel, Switzerland) at 1:100; mouse monoclonal anti-mouse α-SMA (clone 1A4, MP Biomedicals, Basel, Switzerland) at 1:400; rabbit polyclonal anti-NG2 (Merck Millipore, Darmstadt, Germany) at 1:200; rat monoclonal anti-VE-Cadherin (clone 11D4.1, BD Biosciences, Basel, Switzerland) at 1:200, rabbit polyclonal anti-Ki67 (Abcam, Cambridge, UK) at 1:100; rabbit polyclonal anti-laminin (Abcam) at 1:200, rabbit polyclonal anti-pHH3-Ser28 (Cell Signaling Technology, Danvers, USA) at 1:100 and goat polyclonal anti-EphB4 at 1:50 (R&D Systems). Fluorescently labeled secondary antibodies (Invitrogen) were used at 1:200.

For pERK1/2 staining, tissue sections were permeabilized with ice-cold methanol for 10 min, and blocked with 5% goat serum and 2% BSA in PBS with 0.3% Triton-X for 1 h at RT. Rabbit monoclonal anti-phospho-ERK1/2 antibody (Thr202/Tyr204, clone D13.14.4E, Cell Signaling Technology) was used at 1:100.

To study vessel perfusion, 100 µg of FITC-labeled *Lycopersicon esculentum* lectin in 50 µl (Vector Laboratories, Burlingame, USA) was injected into the femoral vein and allowed to circulate for 4 minutes before intravascular perfusion with 1% paraformaldehyde and muscle collection as described above.

## Vascular analyses

Qualitative analysis of vascular morphology in immunofluorescence images was performed on all vascular structures visible in at least 3 fields/section with a 40X objective on a Carl Zeiss LSM710 3-laser scanning confocal microscope (Carl Zeiss, Feldbach, Switzerland) in at least 5 sections/muscle, cut at 100-150 µm of distance from each other (n=4 muscles/group).

Vessel diameters were measured in fluorescently immunostained sections as described (10). Briefly, 10 to 20 fields/muscle (n=4 muscles/group) were analyzed, measuring a total of minimum 300 diameters/group. Captured microscopic images were overlaid with a square grid, squares were randomly chosen and the diameter of each vessel (if any) in the center of selected squares was measured. To avoid selection bias, the shortest diameter in the selected vascular segment was systematically measured. All images were taken with a 20X objective on an Olympus BX63 microscope (Olympus, Volketswil, Switzerland) and analyses were performed with Cell Sens software (Olympus).

$Ki67^+$ and $pHH3^+$ endothelial cells were quantified as a percentage of all endothelial cells in analyzed vascular structures. 300–3000 endothelial cells were analyzed/group in 3–5

fields taken from each area of effect. At least five areas with a clear angiogenic effect were analyzed per group (n=4 muscles/group).

## HDMEC *in vitro* assays

Human microvascular endothelial cells (HDMEC) were isolated as previously described (21) and cultured in Endothelial Cell Basal Medium (EBM, Vitaris, Baar, Switzerland) supplemented with 10% FBS, 1% penicillin/streptomycin, 10 µg/ml sodium heparin, and 2.5 ng/ml FGF-2. Before each assay, cells were starved in EBM with 1% FBS for 2 hours.

Flow Cytometry analysis was performed with the following antibodies and dilutions: PE-conjugated mouse anti-VE-Cadherin (clone BV9, Biolegend, San Diego, CA) and PE-Cy7-conjugated rat anti-CD31 (clone 390, Biolegend) at 1:100; goat anti-EphB4 and goat anti-ephrinB2 (R&D Systems) at 1:50.

***Cell cycle analysis***. 100,000 HDMEC were seeded in p60 dishes overnight and then stimulated with different combinations of the following reagents: 50 ng/ml $hVEGF_{165}$ (R&D Systems), 50 ng/ml or 2 µg/ml ephrinB2-Fc (R&D Systems) and 25 ng/ml FGF-2 (BD Biosciences). After 24 hours, cells were collected, fixed and permeabilized with the FOXP3 Fix/Perm kit (Biolegend) according to the manufacturer's instructions, stained with rabbit polyclonal anti-Ki67 (Abcam), detected with an Alexa546-anti-rabbit secondary (Invitrogen), and with Alexa647-anti-pHH3 (clone HTA28, Biolegend). Finally, cells were incubated with Hoechst 33342 (Life Technologies, Zug, Switzerland) for 2 hours in the dark at 4°C and analyzed with a Fortessa FACS analyzer (Becton Dickinson).

***Internalization assay.*** 50,000 HDMEC were seeded in 6-well plate overnight and then stimulated with different combinations of the following reagents: 50 ng/ml $hVEGF_{165}$, 2 µg/ml ephrinB2-Fc, and 30 µM Axitinib (Tocris Bioscience, Bristol, UK) (22). After 30 minutes of

stimulation, cells were collected and stained for surface and total VEGF-R2, as previously described (23). Briefly, non-fixed and non-permeabilized HDMEC were first stained with Alexa647-anti-VEGF-R2 (clone HKDR-1; Biolegend) to label only the surface receptor. Subsequently, cells were fixed and permeabilized with the FOXP3 Fix/Perm buffer (Biolegend) and were split into two tubes, where one half was stained again with PE-anti-VEGF-R2 (clone 7D4-6, Biolegend) in FOXP3 Perm buffer to visualize total cellular VEGF-R2, while the other half was not stained. Analysis was performed with a Fortessa FACS analyzer (Becton Dickinson).

***Phosphorylation assay.*** 10,000-15,000 HDMEC were cultured in 8-well culture slides (Corning) and stimulated with 50 ng/ml $hVEGF_{165}$ and 2 µg/ml ephrinB2-Fc alone or together for 10 min. Cells were immediately washed with PBS, fixed with 4% paraformaldehyde in PBS, blocked with 5% goat serum and 2% BSA in PBS with 0.3 % Triton-X for 1h at RT and stained with a rabbit monoclonal anti-phosphoTyr1175-VEGF-R2 antibody (clone D5B11, Cell Signaling Technology) and a goat anti-VE-Cadherin (C-19, Santa Cruz Biotechnology, Santa Cruz, CA), both at 1:200, followed by secondary antibody detection as described above. All samples were batch-stained together with same master mix of antibodies. In order to quantify the amount of phosphoVEGF-R2, stained cells where analyzed on a LSM710 3-laser scanning confocal microscope (Carl Zeiss), acquiring 8-bit images (Z-Stack, 1024x1024) with a 40X objective and maintaining the same acquisition settings for all samples. The amount of phosphoVEGF-R2 protein was measured by quantifying the staining intensity and normalized by the endothelial volume from the VE-Cadherin staining, using the Imaris 7.6.4 software (Bitplane, Zürich, Switzerland) to measure total pixel intensity of endothelial-specific phosphoVEGF-R2 immunostaining.

## Hind-limb ischemia, gene transfer and analysis

Immune-competent genetically hyperlipidemic female $LDLR^{-/-}ApoB^{100/100}$ mice (age of 14-15 months, n=20), which are deficient for the LDL receptor and express only apolipoprotein B100 in C57Bl/6J genetic background (24), were fed on a standard chow diet. Experimental unilateral hindlimb ischemia was induced by permanent ligation of both common femoral artery and vein proximal to the origin of the profound femoral artery branch. Post-operatively, the posterior calf muscles received intramuscular injections of $2x10^{10}$ pfu/ml adenoviral vectors expressing either human VEGF-$A_{165}$ (Ad-hVEGF) or beta-galactosidase (Ad-LacZ) as control. Mice were treated with i.p. injections of ephrinB2-Fc (R&D Systems) or control Fc (Abcam) as described above 0, 3, 6 and 9 days after the gene transfer. All animals were assigned to the different treatment groups by randomization before surgery.

***Contrast enhanced ultrasound imaging of perfusion and data analysis.*** To follow muscle blood flow recovery after ischemia, contrast enhanced ultrasound imaging (CEU) was performed pre-operatively and 0, 4, 7 and 11 days post-operation with a Siemens Acuson Sequoia 512 system equipped with 15L8 transducer using the Cadence contrast pulse sequencing (CPS) imaging mode with the following parameters: frequency 14 MHz, power 8 dB, mechanical index 0.25, CPS gain 0 and depth 20 mm (25). Transverse plane perfusion video clips of both ischemic and intact hind limbs were recorded upon the administration of an intravenous bolus injection of 50 µl of Sonovue contrast agent (Bracco, Milano, Italy) via the jugular vein. Maximal signal intensity (dB) of the video clips, representing relative perfusion, was quantified with Datapro software v2.13 (Noesis, Courtaboeuf, France) and signal intensity-time curves were created (n=4-6 animals/group).

***Histological analyses.*** Animals were sacrificed on day 11. Posterior calf muscles were collected for histological analysis after perfusion-fixation with 1% paraformaldehyde. Muscle samples were further immersed for 4h in 4% paraformaldehyde-sucrose and then in 15%

sucrose before paraffin embedding. Four-µm thick transversely cut sections were used to analyze muscle tissue damage by H&E staining and vascularity by CD31 immunohistochemistry. For tissue damage assessment, four different histological muscle areas were classified on H&E-stained sections as: 1) normal; 2) necrotic (myofibers with no nuclei); 3) early regeneration (appearance of basophilic satellite cells), or 4) late regeneration (eosinophilic myofibers with angular shape and centrally positioned nuclei). Each corresponding muscle area was quantified using analySIS imaging software (Soft Imaging System GmbH, Münster, Germany) and expressed as a percentage of the whole cross-sectional muscle area (n=4-5 animals/group).

Vascularity was assessed by immunohistochemical staining with a rat monoclonal anti-mouse CD31 primary antibody (clone MEC 13.3, BD Biosciences Pharmingen, dilution 1:25, overnight at +4°C), with blocking in 10% rabbit serum, 2% mouse serum and 1% BSA 1h at RT, followed by a biotinylated rabbit anti-rat secondary antibody (BA-4001, Vector laboratories, dilution 1:200, 30min at RT) and detection with the avidin-biotin-horseradish peroxidase system (Vector Laboratories) with tyramide signal amplification (TBA, Biotin System, PerkinElmer, Shelton, USA) and DAB as a chromogen (Zymed, San Francisco, USA). Micrographs of the stained sections were acquired with 200x magnification using an Olympus AX-70 light microscope (Olympus Optical, Tokyo, Japan) and analySIS imaging software (Soft Imagining System GmbH). Vessel diameters were quantified from 5 fields/sample of CD31-stained sections acquired within regenerating muscle tissue (n=4-5 muscles/group), using Cell Sens software (Olympus) and the smallest diameter was measured. All measurements were performed by a blinded observer.

## Statistical analysis

Data are presented as mean±standard error. The significance of differences was assessed with the GraphPad Prism 6 software (GraphPad Software). The normal distribution of all data sets was tested and, depending on the results, multiple comparisons were performed with the parametric 1-way analysis of variance (ANOVA) followed by the Bonferroni test, or with the non-parametric Kruskal-Wallis test followed by Dunn's post-test, while single comparisons were analyzed with the non-parametric Mann-Whitney test or the parametric one-tailed t-test. Gene expression data representing fold-changes versus control, which are asymmetrically distributed, were first normalized by logarithmic transformation and then analyzed by 1-way ANOVA followed by the Bonferroni test for multiple comparisons, or by t-test with Welch's correction for single comparisons. Vessel diameter values were first normalized by $\log_2$-transformation and then analyzed by 1-way ANOVA followed by Bonferroni test for multiple comparisons or by one-tailed t-test for single comparisons. $p<0.05$ was considered statistically significant.

## Study approval

Animal studies were performed in accordance with the Swiss Federal guidelines for animal welfare and were approved by the Veterinary Office of the Canton of Basel-Stadt (Basel, Switzerland; Permit 2071). All experimental procedures for ischemia studies in $LDLR^{-/-}ApoB^{100/100}$ mice were approved by the National Animal Experiment Board of Finland (license number: ESAVI/5343/04.10.07/2014) and carried out in accordance with the guidelines of the Finnish Act on Animal Experimentation.

# Results

## Generation and validation of blockers of pericyte-endothelium paracrine signaling

To determine whether and which pericyte-derived signals may control normal vascular morphogenesis induced by moderate VEGF doses, we blocked the three main signaling pathways responsible for the crosstalk between pericytes (P) and endothelial cells (EC), i.e. the TGF-β1, Angiopoietin (Ang)/Tie2 and ephrinB2/EphB4 axes. A clonal myoblast population that homogeneously expresses moderate VEGF levels (V-low=61±2.9 ng/$10^6$ cells/day) was selected to induce normal angiogenesis (9, 16), or myoblasts that do not express VEGF as control (Ctrl). Both populations were transduced with retroviral vectors co-expressing soluble blockers of the TGF-β1 (Latency-Associated Peptide, LAP), Ang/Tie2 (sTie2Fc) and ephrinB2/EphB4 (sEphB4) signaling, together with a truncated version of CD4 (trCD4) in a bicistronic cassette (Supplementary Figure 1A) as a FACS-quantifiable surface marker (16) (Supplementary Figure 1B). ELISA measurements confirmed that all blocker-expressing V-low populations maintained a similar VEGF production as the original V-low clone (V-low = 64±3, V-low LAP = 64±6, V-low sTie2Fc = 79±4, V-low sEphB4 = 62±5 ng/$10^6$ cells/day). Specific expression of each blocker was confirmed by RT-PCR on the *in vitro* cultured myoblast populations (Supplementary Figure 1C), while the functional activity of the secreted proteins was verified by appropriate *in vitro* assays on myoblast conditioned media (Supplementary Figure 1D-F).

## Blockade of ephrinB2/EphB4 signaling, but not of TGF-β1/TGF-βR or Angiopoietin/Tie2, switches VEGF-induced angiogenesis from normal to aberrant

Simultaneous blockade of all three pathways of the P-EC crosstalk was achieved by co-implanting the individual blocker-expressing populations into hind-limb muscles of adult mice (Figure 1). After 2 weeks, myoblasts expressing only the blockers in the absence of VEGF (Ctrl 3b) did not perturb the pre-existing vasculature compared to controls (Ctrl CD4). Low levels of VEGF induced the growth of normal mature capillaries, tightly associated with $NG2^{+}/\alpha\text{-}SMA^{-}$ pericytes, but co-expression of the three soluble inhibitors converted these into aberrant vascular structures, characterized by enlarged and irregular diameters and covered by a patchy layer of $SMA^{+}/NG2^{-}$ smooth muscle cells instead of pericytes (V-low 3b), similar to the angioma-like structures induced by another monoclonal myoblast population expressing high VEGF levels alone (10) (V-high = 137.7±1.6 ng/$10^{6}$ cells/day).

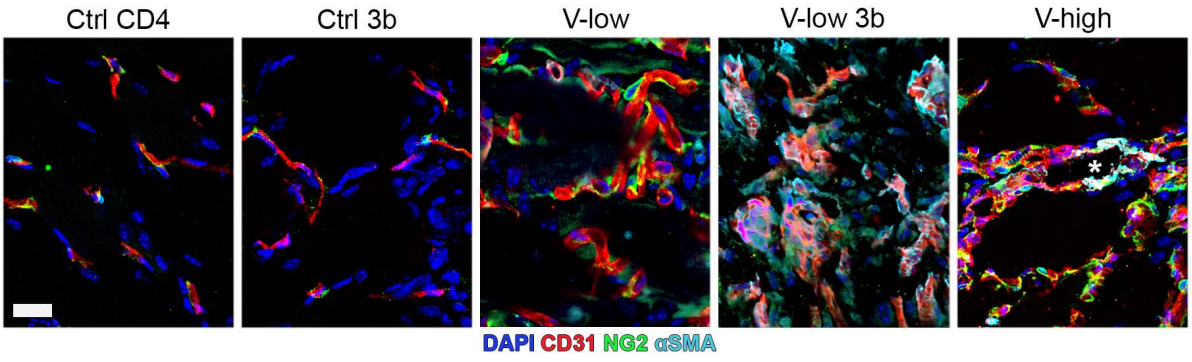


**Figure 1. Triple blockade of TGF-β1, Angiopoietin/Tie2, and ephrinB2/EphB4 paracrine signals causes aberrant angiogenesis with low VEGF levels.** Immunofluorescence staining of endothelium (CD31, red), pericytes (NG2, green), smooth muscle cells (α-SMA, cyan) and nuclei (DAPI, blue) on frozen sections of limb muscles injected with myoblast clones expressing different VEGF levels (V-low and V-high, respectively) or co-expressing low VEGF with blockers of the TGF-β1, Angiopoietin/Tie2 and ephrinB2/EphB4 pathways (V-low 3b). Cells expressing only CD4 surface marker (Ctrl CD4) or blockers (Ctrl 3b) served as controls. After two weeks V-low induced normal pericyte-covered capillary networks compared to controls, but these were switched to aberrant, enlarged and smooth muscle-covered vessels in the presence of the three blockers, similar to those induced by high VEGF alone (V-high). Scale bar = 25 μm.

To determine whether any of the three signaling pathways was individually responsible for the switch, each blocker-secreting V-low population was injected separately (Figure 2A). By 2 weeks ephrinB2/EphB4 blockade caused the appearance of irregularly enlarged aberrant vascular structures, similar to those induced by high VEGF alone, whereas neither TGF-β1/TGF-βR nor Ang/Tie2 blockade affected the normal angiogenesis induced by V-low. Quantification of vessel diameter distributions showed that V-low induced angiogenesis characterized by homogeneous capillary-size vessels with a median of 4.0 μm and 90$^{th}$ percentile of 6.1 μm. However, inhibition of ephrinB2/EphB4 signaling gave rise to a fraction of significantly enlarged structures, with 13% of vessels having diameter >10 μm, compared to 2% and 1% that could be observed in muscles implanted with control cells expressing only sEphB4 and no VEGF, or with V-low cells alone, respectively (Figure 2B). The nature of mural cells associated with vessels induced by V-low alone or with sEphB4 was further investigated by co-staining for the vascular basal lamina. As can be seen in Figure 2C, normal capillaries induced by low VEGF were associated with NG2$^{+}$ pericytes that were completely embedded in the laminin-positive basal lamina, whereas the mural cells associated with the aberrant vascular structures induced in the presence of sEphB4 were both α-SMA$^{+}$ and positioned externally to the basement membrane, and were therefore identified as smooth muscle cells rather than pericytes.

Intravascular staining by FITC-labeled tomato lectin, which binds to the luminal surface of endothelial structures only if they are connected to the systemic circulation, co-localized with endothelium staining (CD31), indicating that the aberrant structures caused by V-low sEphB4 cells were not simply endothelial clusters, but were functionally perfused (Supplementary Figure 2). This is in agreement with previous findings for angioma-like structures induced by high VEGF alone (11). Lastly, to determine the evolution of the morphological changes caused by ephrinB2/EphB4 blockade, tissues were analyzed after 12

weeks, showing that the aberrant structures observed by 2 weeks continued growing in size (Supplementary Figure 3).

Altogether, these results suggest that the ephrinB2/EphB4 pathway, but not TGF-β1/TGF-βR and Ang/Tie2, has a function in the development of normal angiogenesis by low VEGF doses and its blockade causes the switch to an aberrant phenotype resembling the angioma-like vascular structures induced by high VEGF alone.

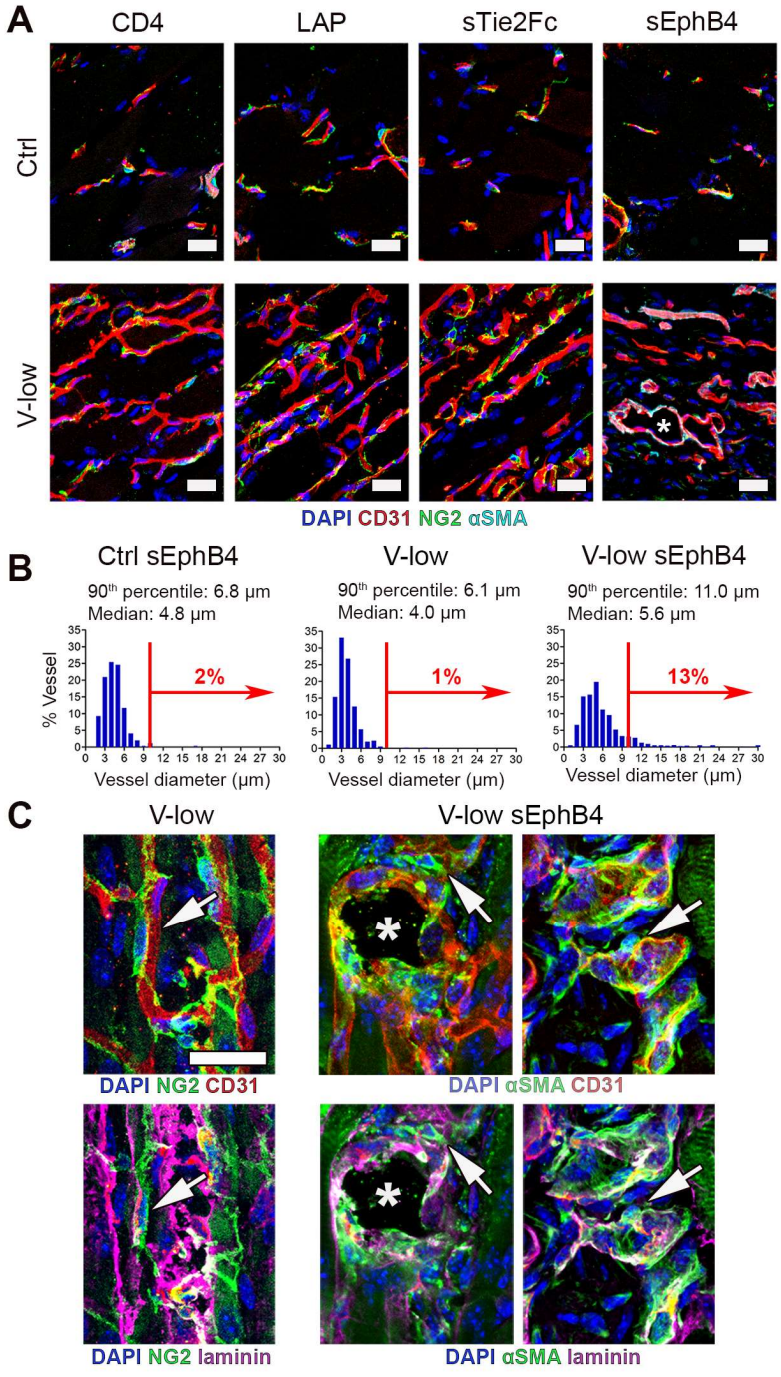

**Figure 2. Blockade of ephrinB2/EphB4 signaling switches VEGF-induced angiogenesis from normal to aberrant.** (**A**) Immunofluorescence staining of endothelium (CD31, red), pericytes (NG2, green), smooth muscle cells (α-SMA, cyan) and nuclei (DAPI, blue) on frozen sections of limb muscles injected with the V-low myoblast clone or control cells (Ctrl) co-expressing either of the 3 soluble blockers (LAP, sTie2Fc or sEphB4) or just the CD4 marker. Two weeks later inhibition of ephrinB2/EphB4 signaling, but not of the other two pathways, switched the normal angiogenesis induced by low VEGF to aberrant vascular structures. (**B**) Distribution of vessel diameters, showing the induction of a population of aberrantly enlarged vessels >10μm by ephrinB2/EphB4 blockade. (**C**) Immunofluorescence staining for mural cell markers (NG2 or α-SMA, both green) and basal lamina (laminin, purple) shows that aberrant vessels induced by ephrinB2/EphB4 blockade are associated with smooth muscle (α-SMA$^+$ outside the basal lamina) rather than pericytes (NG2$^+$ embedded inside the basal lamina). Scale bar = 25 μm.

## Activation of EphB4 signaling prevents aberrant angiogenesis induced by high VEGF doses

To complement the ephrinB2/EphB4 inhibition data above, we asked whether the pharmacological activation of EphB4 might prevent aberrant angiogenesis by high VEGF levels. A recombinant ephrinB2-Fc chimeric protein, whereby fusion with the immunoglobulin Fc portion enables the formation of dimers of ephrinB2 extracellular domains, was used to activate the EphB4 receptor (26). V-high clonal myoblasts were injected in leg muscles of adult mice that were treated systemically with ephrinB2-Fc or Fc control protein by intraperitoneal injection (27). Two weeks later, high VEGF induced heterogenous enlarged vascular structures associated with smooth muscles cells (Figure 3A). As normal muscle capillaries have homogeneous sizes smaller than 10 μm, vessel diameter distribution was quantified and showed that 12% of induced structures were larger than 10 μm (Figure 3C). On the other hand, treatment with ephrinB2-Fc yielded networks of pericyte-covered normal capillaries (Figure 3B), similar to those induced by V-low alone (Figure 2A) and with a homogeneous diameter distribution (Figure 3C; median = 4.0 μm and 2% of vessels larger than 10 μm).

These results were confirmed independently of cell-based VEGF delivery, using an optimized fibrin-based platform that we recently developed for controlled release of VEGF recombinant protein at specific doses and with duration up to 4 weeks in skeletal muscle (18). An engineered version of murine $VEGF_{164}$ was fused to the transglutaminase substrate octapeptide NQEQVSPL ($\alpha_2$-$PI_{1-8}$-VEGF), to allow its covalent cross-linking into fibrin hydrogels by the coagulation factor XIIIa and release only by enzymatic cleavage (28, 29). Fibrin hydrogels containing a high dose of $\alpha_2$-$PI_{1-8}$-VEGF (50 μg/ml), which we previously found to induce aberrant angiogenesis (18), were injected in gastrocnemius muscles and the animals were treated systemically with ephrinB2-Fc. In agreement with the myoblast-based experiments, ephrinB2-Fc treatment prevented the appearance of heterogeneous, enlarged and smooth muscle-covered vascular structures induced by the high VEGF dose, yielding instead homogeneous networks of pericyte-covered capillaries by 7 days (Figure 3D-F).

The observed prevention of aberrant vascular structures could be due to either their switch to a normal phenotype or to their regression. Since regressing vessels leave behind their basal lamina, a staining for laminin was performed to detect so-called “empty sleeves” of vascular basement membrane, which provide a sort of historical record of pre-existing vessels (30). As shown in Supplementary Figure 4, by 7 days after injection of V-high myoblasts we could not identify laminin sleeves in the tissues treated with ephrinB2-Fc compared with the controls treated with Fc only. On the other hand, many empty sleeves were clearly visible in positive control tissues treated with the potent VEGF blocker Aflibercept, which caused the regression of vascular structures induced by high VEGF, suggesting that EphB4 stimulation could prevent the formation of aberrant structures by regulating VEGF-induced vascular morphogenesis.

Altogether, the results of these inhibition and stimulation experiments indicate that the ephrinB2/EphB4 signaling pathway determines whether a specific VEGF dose induces normal or aberrant angiogenesis.

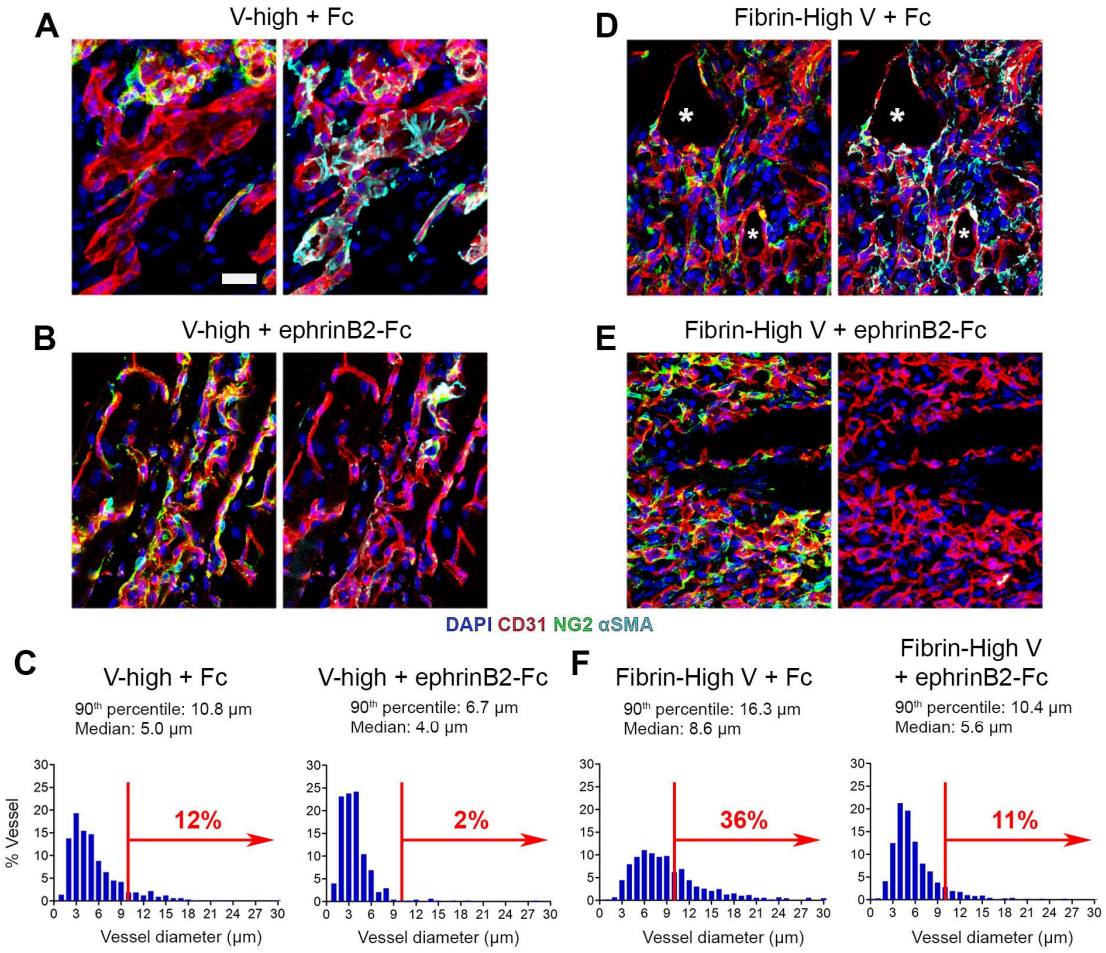


**Figure 3. Activation of EphB4 by ephrinB2-Fc prevents aberrant angiogenesis.** A high VEGF dose was delivered to limb muscles of mice either by genetically modified myoblasts (V-high clone, **A-C**) or as fibrin-bound recombinant protein (Fibrin-High V, **D-F**) and animals were treated intraperitoneally with ephrinB2-Fc or control Fc recombinant protein. (**A-B** and **D-E**) Immunostaining of frozen sections for endothelium (CD31, red), pericytes (NG2, green), smooth muscle cells (α-SMA, cyan) and nuclei (DAPI, blue) showed that, with both delivery platforms, ephrinB2-Fc treatment prevented the induction of aberrant vascular structure by high VEGF and yielded only normal capillary networks. * = lumen of an aberrant structure; scale bar = 25 µm. (**C** and **F**) Quantification of vessel diameter distributions showed a consistent decrease in vessel sizes after treatment with ephrinB2-Fc. Red arrows and numbers indicate the fraction of vessel diameters > 10 µm.

## EphrinB2/EphB4 signaling controls the degree of initial vascular enlargement induced by VEGF

In order to understand how ephrinB2/EphB4 signaling regulates the switch between normal and aberrant angiogenesis, we investigated the effects of EphB4 inhibition or stimulation on the early morphogenic events after delivery of low and high VEGF levels, respectively, which comprise an initial stage of circumferential enlargement of pre-existing vessels by 3-4 days, followed by longitudinal splitting by 7 days (9). As shown in Figure 4A, by 4 days both V-low and V-high myoblasts induced vascular enlargements, whose diameter was proportional to VEGF dose (V-low: median=8.8 μm, average=10.5±0.8 μm; V-high: median=11.9 μm, average=14.5±1.7 μm). However, co-expression of sEphB4 increased the average size of vascular enlargements induced by low VEGF (V-low sEphB4=15.1±1.1 μm, $p<0.01$ vs V-low; Figure 4E) to values similar to those caused by high VEGF alone (Figure 4F). Conversely, EphB4 stimulation by systemic treatment with ephrinB2-Fc significantly reduced the diameter of vascular enlargements induced by high VEGF (Figure 4F; V-high+ephrinB2-Fc=9.5±1.0 μm, $p<0.05$ vs V-high+Fc). By 7 days the smaller enlargements induced by V-low remodeled to normal capillaries, whereas the larger ones induced by V-high failed to split and some segments gave rise to aberrantly enlarged structures (Figure 4C-D). However, upon modulation of EphB4 signaling the fate of initial enlargements was determined by their size rather than the dose of VEGF. In fact, ephrinB2-Fc treatment caused proper remodeling to homogeneous normal capillary networks despite high VEGF, whereas EphB4 inhibition led to failure of splitting despite low VEGF (Figure 4C-D), as shown also by the quantification of vessel diameters (Figure 4G-H).

The transition from normal to aberrant angiogenesis by increasing VEGF doses has been shown to be associated with loss of pericytes at the initial stage of circumferential enlargement 4 days after factor delivery (9). Analysis of mural cell coverage showed that

inhibition of ephrinB2/EphB4 signaling did not interfere with pericyte coverage of initial vascular enlargements induced by low VEGF, both at 3 and 4 days (Figure 5A). In the presence of low VEGF alone pericytes were positive for NG2 and negative for α-SMA, as expected and typical for microvasculature of skeletal muscle. However, upon co-expression of the sEphB4 blocker most mural cells associated with vascular enlargements became double-positive for both NG2 and α-SMA (Figure 5A). Co-staining for laminin revealed that $NG2^{+}$/α-$SMA^{+}$ mural cells were completely embedded into the vascular basement membrane (Figure 5B), thereby confirming their identity as pericytes and excluding a transition to a smooth muscle cell phenotype (31). In line with this, gene expression analysis in muscles 3 days after myoblast implantation, showed that both *Pdgfb* and its receptor *Pdgfrb*, which regulate pericyte recruitment, were similarly upregulated after stimulation with VEGF regardless of EphB4 inhibition (Figure 5C).

Altogether, these results indicate that ephrinB2/EphB4 signaling: 1) modulates the degree of vascular enlargement induced by a given VEGF dose, determining whether splitting into normal capillaries succeeds or fails; and 2) does not interfere with pericyte recruitment.

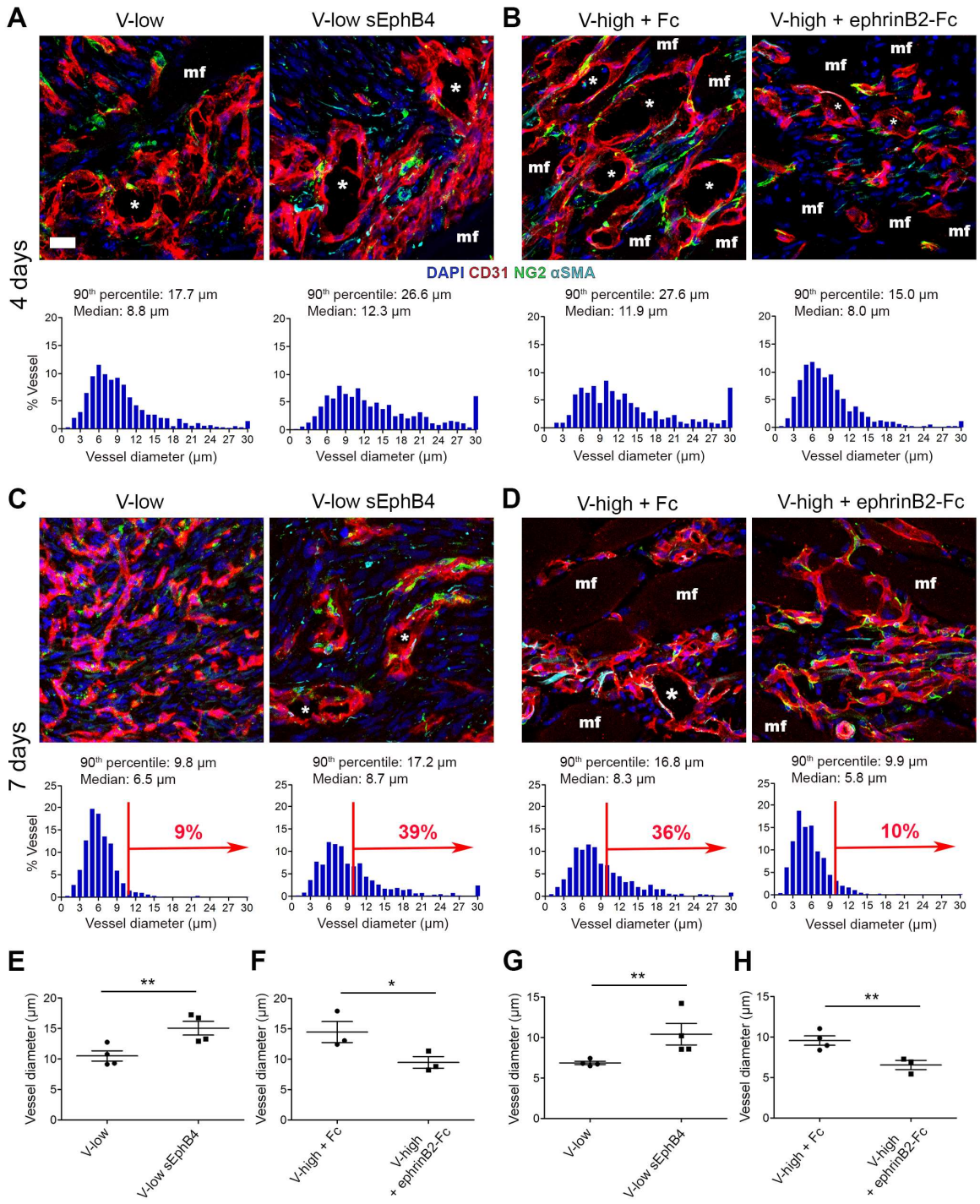


**Figure 4. EphrinB2/EphB4 signaling regulates the degree of vascular enlargement by VEGF dose.** Mouse limb muscles were implanted with myoblast clones expressing low (V-low) or high (V-high) VEGF doses, while the ephrinB2/EphB4 signaling pathway was inhibited by co-expression of the sEphB4 blocker (V-low sEphB4, **A**, **C** and **E-F**) or stimulated by intraperitoneal treatment with ephrinB2-Fc or control Fc protein (**B**, **D** and **G-H**). Immunostaining of frozen sections stained for endothelium (CD31, red), pericytes (NG2, green), smooth muscle cells (α-SMA, cyan) and nuclei (DAPI, blue) and quantification of vessel diameter distribution showed that 4 days after VEGF delivery the size of initial circumferential enlargements was increased by ephrinB2/EphB4 inhibition

and reduced by its stimulation (**A** and **B**). By 7 days, after completion of remodeling, EphB4 inhibition switched normal angiogenesis by V-low to aberrant (**C**) and its stimulation converted aberrant structures by V-high into normal capillary networks (**D**). Red arrows and numbers indicate the fraction of vessel diameters > 10 µm. * = lumen of aberrant structures; mf = muscle fibers; scale bar = 25 µm. (**E**-**H**) Quantification of vessel diameters after 4 days (**E** and **G**) and 7 days (**F** and **H**). Values represent means of individual measurements in each sample ± SEM (n=3-4 independent samples/group). * $p<0.05$ and ** $p<0.01$ by one-tail t-test, after data normalization by logarithmic transformation.

## EphrinB2/EphB4 signaling modulates VEGF-induced endothelial proliferation

The initial vascular enlargement caused by VEGF overexpression is associated with endothelial proliferation (9). Therefore, we investigated whether ephrinB2/EphB4 signaling may regulate the amount of endothelial proliferation induced by specific VEGF doses *in vivo*. The degree of proliferation depends both on the proportion of cycling cells and on the speed with which they cycle. Therefore, we performed co-immunostaining for CD31 and either Ki67, which is expressed throughout all phases of the cell cycle and marks all proliferating cells, but not quiescent ones in G0 (32), or phosphorylated Histone H3 (pHH3), which is only detectable during the G2-M phase (33, 34). Since the duration of the cell cycle depends on how long cells spend in G1, while the G2-M phase has a constant duration, the proportion of $pHH3^+$ cells reflects how often proliferating cells are cycling and provides an indication of the endothelial proliferation rate.

Vascular enlargements induced by V-low alone or with sEphB4 co-expression contained similar proportions of $Ki67^+$ endothelial cells at both 3 and 4 days after myoblast implantation (Figure 6A). However, at 3 days EphB4 inhibition caused a significant increase by about 40% in the frequency of $pHH3^+$ endothelial cells compared to low VEGF alone (Figure 6B), suggesting a faster proliferation rate.

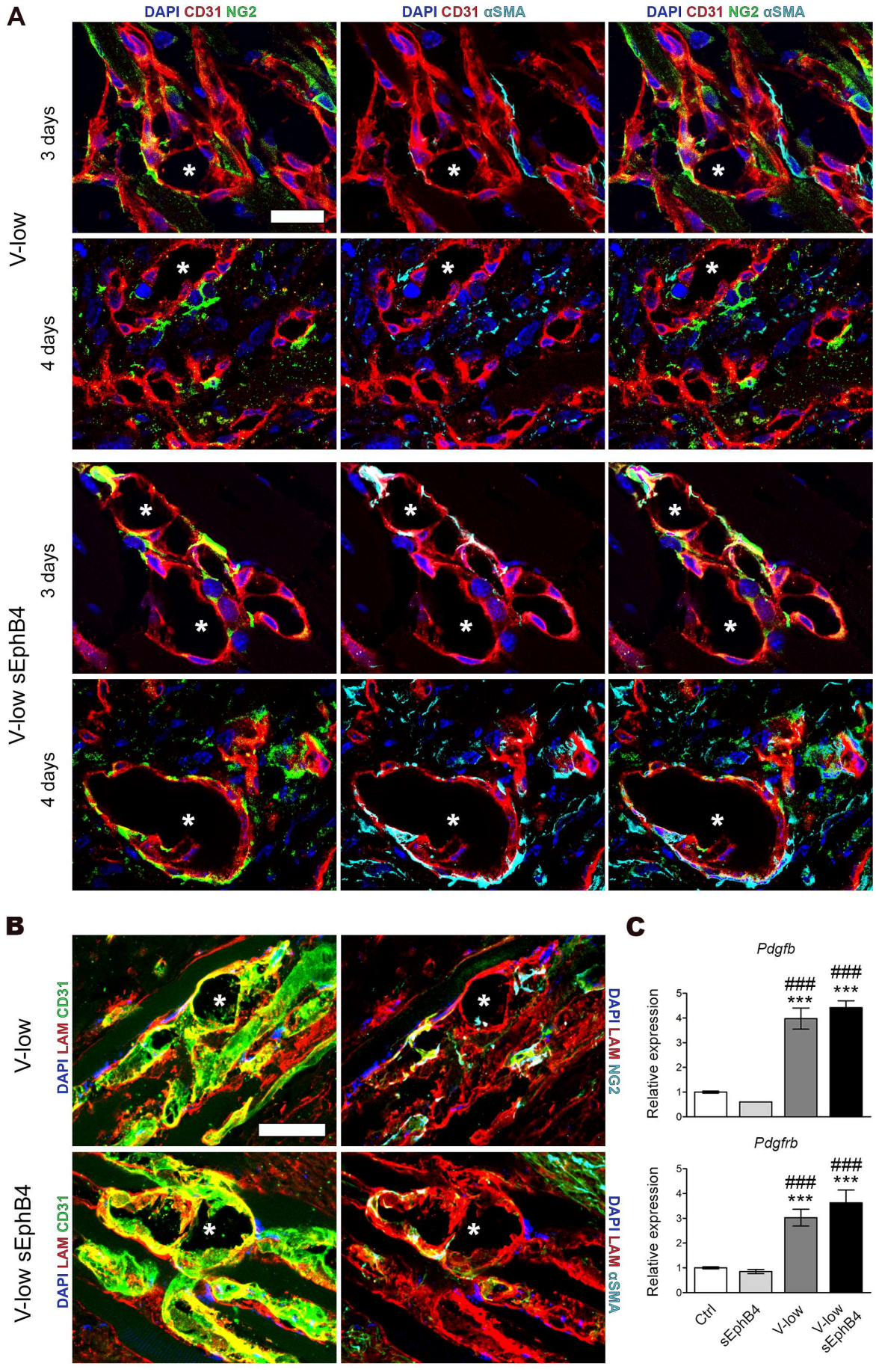
A
DAPI CD31 NG2
DAPI CD31 αSMA
DAPI CD31 NG2 αSMA
V-low
3 days
4 days
V-low sEphB4
3 days
4 days
B
V-low
DAPI LAM CD31
DAPI LAM NG2
V-low sEphB4
DAPI LAM CD31
DAPI LAM αSMA
C
Pdgfb
Relative expression
###
***
Pdgfrb
Relative expression
###
***
Ctrl
sEphB4
V-low
V-low sEphB4

**Figure 5. Inhibition of ephrinB2/EphB4 signaling does not prevent pericyte-recruitment.** Muscles were harvested 3 and 4 days after implantation of V-low or V-low sEphB4 myoblast clones. (**A**) Immunofluorescence staining of endothelium (CD31, red), pericytes (NG2, green), smooth muscle cells (α-SMA, cyan) and nuclei (DAPI, blue). In both conditions initial vascular enlargements were tightly associated with mural cells displaying a pericyte morphology, which however upregulated α-SMA expression in the presence of EphB4 blockade. (**B**) Co-staining for laminin (LAM, red) confirmed the pericyte identity of both α-SMA-positive and –negative mural cells, as both were embedded inside the endothelial basal lamina. * = vascular enlargements; scale bar = 25 μm. (**C**) Gene expression of Pdgfb and Pdgfrb was quantified in skeletal muscles 3 days after myoblast implantation and expressed as fold-change versus control muscles (n=4). ***, ### $p<0.001$ vs Ctrl (*) or vs sEphB4 (#) by 1-way ANOVA with Bonferroni multiple comparisons test, after data normalization by logarithmic transformation.

At 7 days, most of the endothelial cells in the normal capillary networks induced by low VEGF were $Ki67^-$ and became quiescent, as expected, whereas 40% of the endothelium in the aberrant vascular structures generated in the presence of EphB4 blockade were still proliferating (Figure 6A), similarly to those induced by high VEGF alone (Figure 6C). Conversely, EphB4 stimulation by systemic ephrinB2-Fc treatment caused a significant reduction in the proportion of $Ki67^+$ endothelial cells at both 4 and 7 days (Figure 6C), while the frequency of $pHH3^+$ endothelial cells was significantly reduced by about 40% already by 3 days (Figure 6D), reducing it to a similar value as that induced by low VEGF alone (Figure 6B). Furthermore, EphB4 expression in angiogenic vessels *in vivo* was restricted to the endothelium, with no detectable signal on associated pericytes, and was not modified by either VEGF dose or its own stimulation by ephrinB2-Fc or inhibition by sEphB4 (Supplementary Figure 5).

To determine whether EphB4 signaling regulated endothelial proliferation directly or indirectly, we investigated the effects of ephrinB2-Fc treatment on endothelial cell cycle progression *in vitro*. Human dermal microvascular cells (HDMEC), which strongly express EphB4 and are mostly negative for ephrinB2 (Supplementary Figure 6), were stimulated with recombinant VEGF or with the unrelated strong mitogen FGF-2 (35), with or without treatment with recombinant ephrinB2-Fc, and cell cycle analysis was performed by FACS after staining

for Ki67 and pHH3 (Figure 6E). As shown in Figure 6F, in control conditions (no VEGF and 2000 ng/ml of ephrinB2-Fc) about 50% of HDMEC were in G0: VEGF stimulation reduced this percentage to 30%, but treatment with ephrinB2-Fc (50 and 2000 ng/ml) significantly and dose-dependently increased the proportion of non-cycling cells to 40%. Conversely, VEGF stimulation increased the amount of cells undergoing mitosis in the G2-M phase by about 50% (from 0.8% to 1.2%), while ephrinB2-Fc treatment dose-dependently reversed this effect (Figure 6G). Notably, the anti-proliferative effect of ephrinB2-Fc treatment was not restricted to VEGF, as it similarly reduced the mitogenic effects of FGF-2 (Figure 6F-G).

Thus, combined *in vivo* and *in vitro* analyses indicate that EphB4 signaling regulates endothelial proliferation by modulating the mitogenic activity of VEGF.

## EphB4 modulates VEGF signaling output downstream of VEGF-R2 activation

In order to determine the mechanism by which EphB4 modulates VEGF activity, we assessed whether EphB4 stimulation regulated VEGF-R2 internalization, phosphorylation or downstream signaling in HDMEC *in vitro* (36, 37). VEGFR-2 internalization after treatment with VEGF was analyzed by FACS (Fig 7A). VEGF stimulation strongly reduced the staining for surface VEGF-R2 without changing the total amount of VEGF-R2 expressed by the cells. While surface receptor staining could be restored by co-treatment with the VEGF-R2 receptor tyrosine kinase inhibitor Axitinib (22), this was not observed upon co-treatment with 2000 ng/ml of ephrinB2-Fc. Quantification of the fraction of VEGF-R2 internalization (Figure 7B) confirmed that Axitinib could robustly prevent VEGF-induced VEGF-R2 internalization, while ephrinB2-Fc caused a very small, albeit significant, reduction by <5%. Neither Axitinib nor ephrinB2-Fc had any effect in the absence of VEGF stimulation.

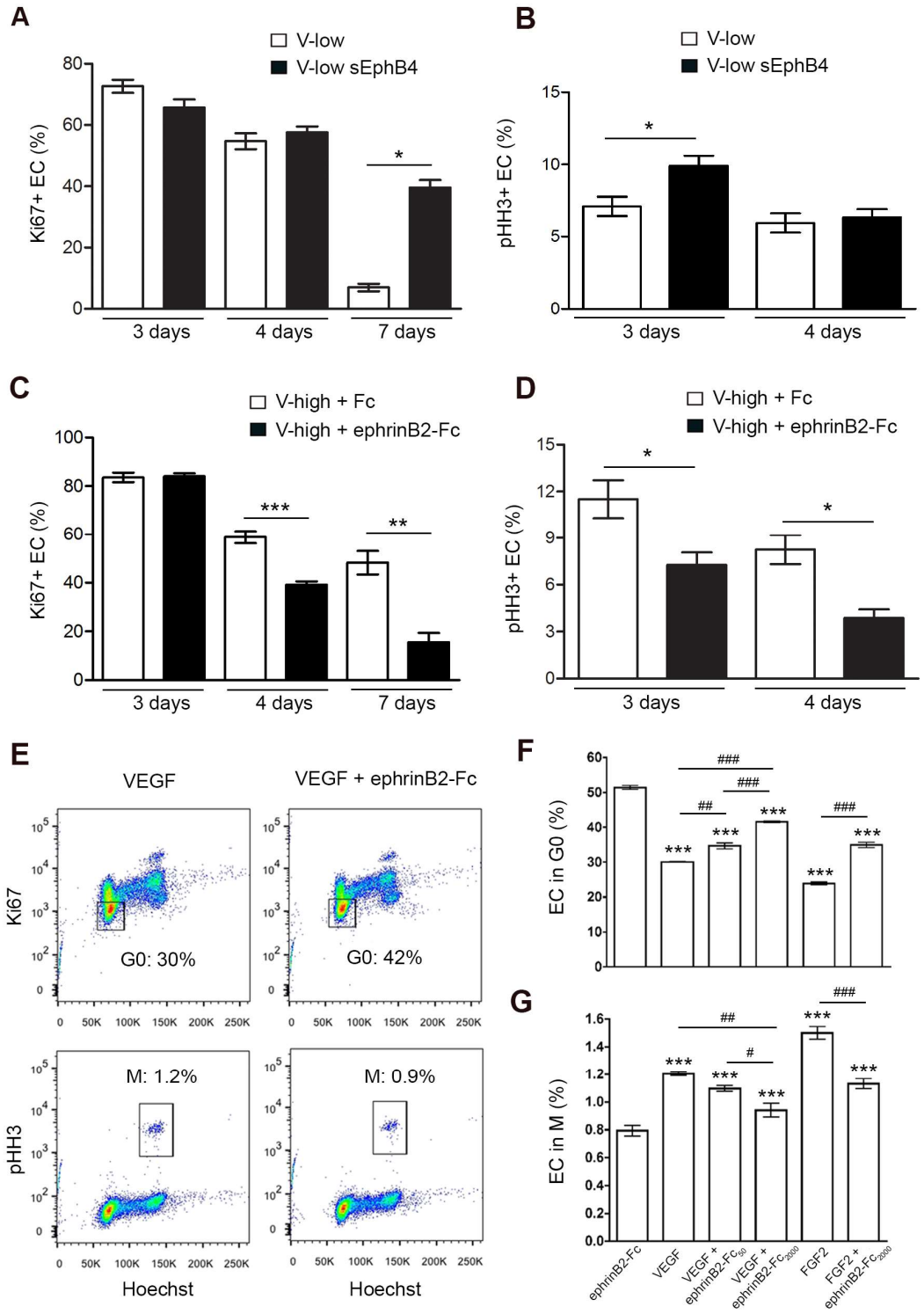


**Figure 6. EphrinB2/EphB4 signaling modulates endothelial proliferation.** (**A-D**) Muscles were harvested 3, 4 and 7 days after implantation of V-low or V-low sEphB4 clones, or V-high cells while treating animals systemically with ephrinB2-Fc or control Fc proteins. Endothelial proliferation was assessed by quantifying the percentage of endothelial cells positive for Ki67, which marks all cycling cells (**A** and **C**), or phosphorylated Histone H3, which marks only cells in the G2/M phase (pHH3, **B** and **D**), by immunofluorescence staining on frozen muscle sections. EphB4 inhibition specifically increased the rate of endothelial proliferation (pHH3+ cells)

and its stimulation by ephrinB2-Fc conversely decreased it. * $p<0.05$, ** $p<0.01$ and *** $p<0.001$ by 1-way ANOVA with Bonferroni multiple comparisons test. (**E-G**) Human dermal microvascular endothelial cells (HDMEC) were treated in vitro with recombinant VEGF or FGF2, while EphB4 was stimulated with ephrinB2-Fc (50 or 2000 ng/ml). Cell cycle analysis was performed by FACS after staining for Ki67 and pHH3 (**E**) and the proportion of cells withdrawn from cycle (G0) or in mitosis (M) were quantified (**F-G**). EphB4 stimulation dose-dependently increased quiescence and decreased mitosis by both mitogens. # $p<0.05$, ## $p<0.01$ and ***, ### $p<0.001$ by 1-way ANOVA with Bonferroni multiple comparisons test (n=3 independent replicates).

To determine whether the minimal reduction in VEGF-R2 internalization by ephrinB2 was functionally relevant, phosphorylation of VEGF-R2 was quantified after staining with a specific antibody for phospho-tyrosine 1175 (pTyr1175), i.e. the key residue by which VEGF-R2 activates the MAPK/ERK pathway and stimulates cell proliferation (38). EphrinB2-Fc treatment did not reduce the increase in pTyr1175 caused by VEGF (Figure 7C), suggesting that EphB4 stimulation did not directly affect VEGF-R2 activation.

The effect of EphB4 activation on VEGF signaling downstream of the receptor was investigated by quantifying the expression of the VEGF-R2 target genes *Esm-1/Endocan* and *Igfbp3*. As shown in Figure 7D, both genes were upregulated by VEGF in HDMEC *in vitro*, as expected. However, ephrinB2-Fc treatment did not affect the expression of *Esm-1/Endocan*, which is regulated by the PI3-kinase/AKT signal transduction pathway (39), but it significantly down-regulated expression of *Igfbp3*, which is instead also regulated by ERK1/2 signaling (40, 41). Therefore, the effects of EphB4 signaling on VEGF-induced ERK1/2 activation were assessed *in vivo* by quantifying the percentage of endothelial cells positive for phosphorylated ERK1/2 (pERK1/2) in the initial vascular enlargements induced 3 and 4 days after implantation of myoblasts expressing low or high VEGF levels and in the presence of EphB4 inhibition or stimulation, respectively, similarly to the experimental set-up described in Figure 4.

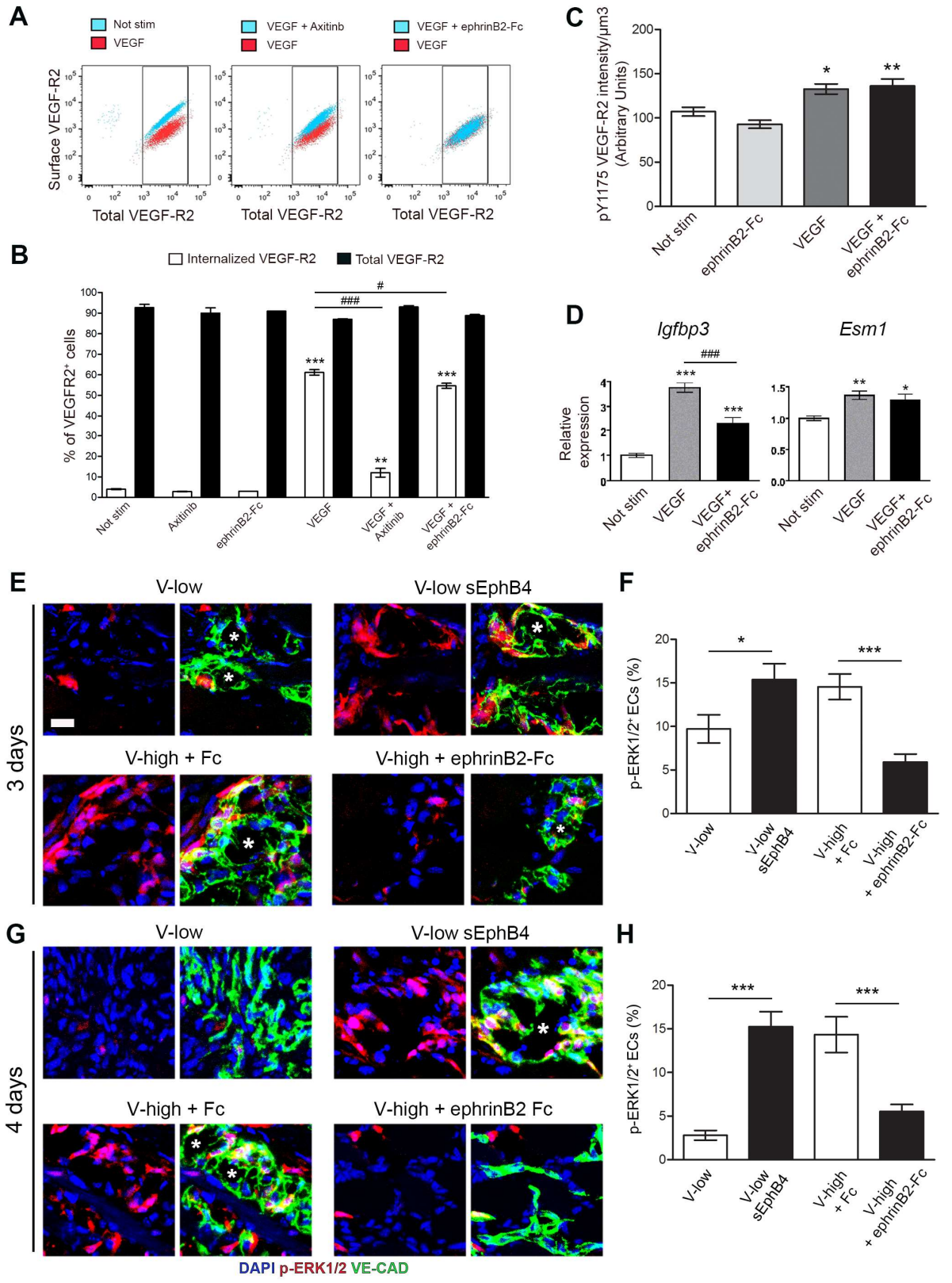


**Figure 7. EphB4 regulates VEGF-induced phosphorylation of endothelial ERK1/2 downstream of VEGF-R2 activation.** (**A-D**) HDMEC were treated *in vitro* with VEGF alone or together with ephrinB2-Fc or the VEGF-R2 small molecule inhibitor Axitinib as a positive control. VEGF-R2 internalization (**A-B**, n=6) and phosphorylation at tyrosine Y1175 (**C**, n=4) were quantified by FACS and immunocytochemistry, respectively.

Expression of VEGF-R2 target genes Igfpb3 and Esm1 was quantified by real-time qRT-PCR **(D**, n=8**).** EphB4 activation by ephrinB2-Fc did not affect either VEGF-R2 internalization or phosphorylation or expression of *Esm1*, which is downstream of PI3K, but reduced that of *Igfpb3*, which is regulated by pERK1/2. (**E**-**H**) Muscles were harvested 3 and 4 days after implantation of V-low or V-low sEphB4 clones, or V-high cells while treating animals systemically with ephrinB2-Fc or control Fc proteins. Frozen sections were immunostained for phosphorylated ERK1/2 (p-ERK1/2) and the endothelial junctional protein VE-Cadherin (VE-CAD) (**E** and **G**) and the percentage of p-ERK1/2-positive endothelial cells was quantified (**F** and **H**, n=4 independent muscles/group). EphB4 inhibition and stimulation respectively increased and decreased ERK1/2 activation downstream of VEGF-R2. Scale bar = 20 μm; *, # $p<0.05$, ** $p<0.01$ and ***, ### $p<0.001$ by 1-way ANOVA with Bonferroni multiple comparisons test. Gene expression data (**D**) were first normalized by logarithmic transformation.

After 3 days, about 10% of endothelial cells in vascular enlargements induced by low VEGF stained positive for pERK1/2, but EphB4 inhibition increased this proportion to about 15%, which was similar to that induced by high VEGF alone. Conversely, EphB4 activation by treatment with ephrinB2-Fc significantly reduced the amount of pERK1/2-positive endothelial cells in structures induced by high VEGF to levels similar to those of low VEGF alone (Figure 7E-F). By 4 days, pERK1/2-positive cells dropped to about 3% with low VEGF alone, but EphB4 inhibition caused this fraction to remain at about 15%, similarly to high VEGF alone, and EphB4 activation in the presence of high VEGF again reduced it significantly to about 5% (Figure 7G-H), in agreement with the day 3 results.

Altogether, these *in vitro* and *in vivo* data show that EphB4 activation by ephrinB2 modulates endothelial proliferation induced by specific VEGF doses without affecting VEGF-R2 activation, but rather by modulating the degree of ERK1/2 activation downstream of the receptor.

## EphB4 stimulation prevents aberrant angiogenesis by uncontrolled adenoviral VEGF gene delivery and reduces muscle necrosis after ischemia

Lastly, we sought to extend our findings, obtained with a controlled myoblast-based gene delivery platform, to a gene delivery system appropriate for clinical translation as a gene therapy approach. Therefore, first we tested whether ephrinB2-Fc treatment could prevent aberrant angiogenesis induced by intramuscular delivery of a VEGF-expressing adenoviral vector (Ad-mVEGF) in immune-deficient SCID mice, to avoid the confounding factor of immune clearance of the viral vector (42). After 2 weeks Ad-mVEGF induced several enlarged and multi-lumenized, smooth muscle-covered aberrant vascular structures, but ephrinB2-Fc treatment prevented their appearance and yielded only normal capillary networks associated with NG2+ pericytes (Figure 8A), with more homogeneous diameters (Figure 8B) and smaller in size (Figure 8C; Ad-mVEGF+Fc=7.4±0.5 μm vs Ad-mVEGF+ephrinB2-Fc=6.1±0.2 μm, $p<0.05$).

To investigate the therapeutic potential of this approach, acute hindlimb ischemia was induced in immune-competent hyperlipidemic mice (24). Intramuscular adenoviral transfer of the human $VEGF_{165}$ gene (Ad-hVEGF) induced capillary growth compared to control vector (Ad-LacZ), but also formation of aberrant, lacunae-like vascular structures (Figure 8D). Concomitant systemic treatment with ephrinB2-Fc prevented the formation of highly enlarged vascular lacunae (Figure 8D) and significantly reduced mean vessel size (Figure 8E; Ad-hVEGF+Fc=5.6±0.2 μm vs Ad-hVEGF+ephrinB2-Fc=5.0±0.2 μm, $p<0.05$), confirming the results in non-ischemic muscle.

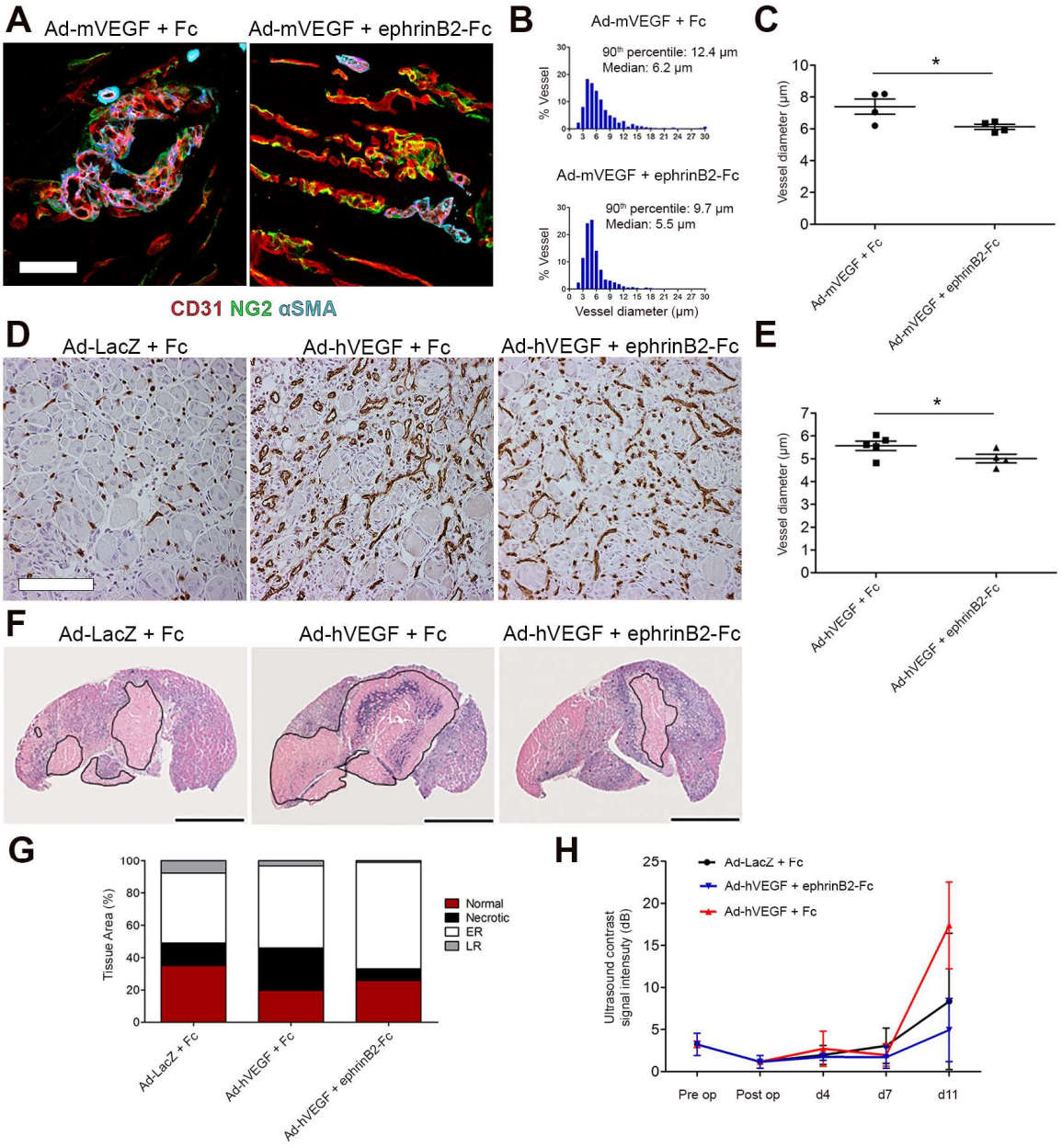


**Figure 8. EphB4 stimulation prevents aberrant angiogenesis by uncontrolled VEGF expression and improves the outcome of adenoviral VEGF delivery in ischemia.** (**A-C**) Immune-deficient SCID mice received intramuscular injections of adenovirus expressing murine $VEGF_{164}$ (Ad-mVEGF) and were treated systemically with ephrinB2-Fc or control Fc proteins. Muscles were harvested 2 weeks later and frozen sections were stained for endothelium (CD31, red), pericytes (NG2, green) and smooth muscle cells (α-SMA, cyan) (**A**). Vessel diameters were quantified (n=4 independent samples/group) and results are shown as size distribution (**B**) and mean of individual measurements in each sample ± SEM (**C**). EphB4 stimulation prevented the appearance of aberrantly enlarged and smooth muscle-covered vascular structures, and reduced the average diameter of induced vessels. (**D-H**) Hindlimb ischemia was induced in immune-competent C57/Bl6 mice. Adenoviral vectors expressing human $VEGF_{165}$ (Ad-hVEGF) or control LacZ (Ad-LacZ) were delivered by intramuscular injection and animals received systemic treatment with ephrinB2-Fc or control Fc proteins. After 11 days muscles were

harvested and immunohistochemical staining for CD31 was performed to assess vessel morphology (**D**) and to quantify vessel diameters (**E**, n=4-5 independent muscles/group), while tissue damage was quantified on H&E-stained sections (**F**, n=4-5 independent muscles/group), distinguishing tissue areas as normal, necrotic, early- and late-regenerating (ER and LR, respectively); (**G**). Blood flow was measured non-invasively by laser Doppler (**H**, n=4-6 animals/group) before and after surgery (Pre op and Post op) and after 4, 7 and 11 days (d4, d7 and d11). EphB4 stimulation prevented the appearance of enlarged vascular lacunae, decreased the size of VEGF-induced vessels, reduced tissue necrosis while increasing regeneration, and normalized blood flow. Scale bars = 50 μm (**A**), 100 μm (**D**) and 2 mm (**F**); * $p<0.05$ by one-tail t-test, after data normalization by logarithmic transformation.

Functionally, although the aberrant vasculature can be highly perfused, it can have deleterious effects on muscle function and recovery from ischemia, e.g. through the formation of arterio-venous shunts that actually reduce effective metabolic exchange in tissue (43). In agreement with the normalization of vascular structure, ephrinB2-Fc treatment also effectively normalized the supra-physiological perfusion increases induced by Ad-hVEGF (Figure 8H) and reduced ischemia-related muscle damage (necrotic area: Ad-hVEGF+Fc=26.2±16.0% vs Ad-hVEGF+ephrinB2-Fc=7.3±3.8%), while increasing tissue regeneration (regenerating area: Ad-hVEGF+Fc=50.9±12.3% vs Ad-hVEGF+ephrinB2-Fc=65.9±11.9%) (Figure 8F-G). Taken together, these results support the therapeutic potential of EphB4 simulation by systemic ephrinB2-Fc treatment in controlling undesired vascular responses of VEGF gene delivery and improving its efficacy.

# Supplementary information

# Supplementary methods

## Retroviral transduction of myoblasts

Primary myoblasts isolated from C57BL/6 mice were infected at high efficiency (44) with retroviruses carrying the cDNA of murine $VEGF_{164}$ linked through an Internal Ribosome Entry Sequence (IRES) to a truncated murine CD8a as a FACS-sortable marker, or only CD8 as controls (16). Early-passage myoblast clones were isolated using a FACS Vantage SE cell sorter (Becton Dickinson, Basel, Switzerland) as described (16), in order to obtain populations in which every cell expressed the same VEGF level. V-low and control cells were further infected with retroviruses expressing LAP, sTie2Fc or sEphB4, or only CD4 as control. Transduced populations were FACS-sorted based on the staining for the CD4 surface marker to eliminate non-infected cells. All myoblast populations were cultured in 5% $CO_2$ on collagen-coated dishes, with a growth medium consisting of 40% F10, 40% low-glucose DMEM, 20% FBS, 1% penicillin/streptomycin and 1% L-Glutamine, supplemented with 2.5 ng/ml basic FGF, as previously described (45).

## CD4 flow cytometric analysis

Expression of the truncated CD4 marker was assessed by staining myoblasts with a FITC- conjugated antibody against rabbit CD4 (clone MCA799F, AbD Serotec, Raleigh, USA), using 0.4 µg of antibody/$10^6$ cells in 200 µl (1:50 dilution) of phosphate-buffered saline (PBS) with 5% BSA for 20 min on ice. Data were acquired using a FACS Calibur flow cytometer (Becton Dickinson) and analyzed using FlowJo software (Tree Star, Ashland, USA). Cell sorting was performed with a BD Influx cell sorter (Becton Dickinson).

## Blocker expression by RT-PCR

Specific expression of the correct blockers in each myoblast population was verified by RT-PCR using primers specific for LAP (FW 5'-GCTGTGGCTACTGGTGCTGA-3' and RV 5'-CCGGGAGCTTTGCAGATGCT-3'), sTie2Fc (FW 5'-GTGGAGTCAGCTTGCTCCTT-3' and RV 5'-TGCACACACAGCTCGTAGTC-3'), and sEphB4 (FW 5'-TTTGGAAGAGACCCTGCTGA-3' and RV 5'-CCGTTCAGGCGGGAAACC-3'). PCR was performed using HiFi PCR Premix (Takara Clonetech, St-Germain-en-Laye, France) with 35 cycles of amplification consisting of denaturation at 98°C for 10 seconds, annealing at 55°C for 15 seconds and extension 72°C for 10 seconds, on a Veriti Thermal Cycler (Applied Biosystems, Basel, Switzerland).

## Blocker functional assays

***LAP***. A TGF-β reporter cell line was produced by transducing HEK293 cells with lentiviral vectors expressing luciferase under the control of a SMAD response element or a control minimal CMV promoter, according to the manufacturer's instructions (pGreenFire™ Transcription Reporters, System Biosciences, Mountain View, USA). Cells were seeded in 96-well plates at 50% confluency and cultured with high-glucose DMEM supplemented with 10% FBS, 1% penicillin/streptomycin, and 1% L-Glutamine. After 12 hours, medium was replaced with conditioned medium from either LAP or control CD4 myoblasts, which was previously incubated on ice for 30 minutes with different amounts of recombinant human TGF-β1 (R&D Systems) and then warmed at 37°C for 15 minutes. After 24 hours, medium was aspirated and cells were lysed on ice in 60 µl of ice-cold lysis buffer for 15 minutes and luciferase activity was measured with the BrightGlo Luciferase Assay System (Promega, Madison, USA), according to manufacturer's instructions. Luminescence from reporter activation was

measured for 1 sec/well on a MicroLumatPlus luminometer (Berthold Technologies, Bad Wildbad, Germany).

***sTie2Fc***. The RAW264.7 macrophage cell line (46) was seeded in 24-well plates at the density of 100,000 cells/well, and cultured with RMPI medium supplemented with 10% FBS, 1% penicillin/streptomycin, and 1% L-Glutamine. For the assay, cells were incubated with conditioned medium from either sTie2Fc or control CD4 myoblasts that was previously kept on ice for 30 minutes with different amounts of recombinant COMP-Ang1 (AdipoGen, Liestal, Switzerland) and then warmed at 37°C for 15 minutes. After 60 minutes, conditioned medium was replaced with fresh RPMI containing 100 ng/ml of LPS and after 24 hours cells were collected for RNA extraction.

***sEphB4***. Human Umbilical Vein Endothelial Cells (HUVEC) were seeded at the density of 500,000 cells/T25 flask and cultured overnight in M199 medium supplemented with 20% FBS, 100 µg/ml Endothelial Cell Growth Supplement (Sigma-Aldrich, St. Louis, USA), 50 U/ml sodium heparin (Sigma-Aldrich) and 1% penicillin/streptomycin. Afterwards, cells were incubated with conditioned medium from either sEphB4 or control CD4 myoblasts that was previously kept on ice for 30 minutes with 2 µg/ml mouse ephrinB2-Fc (R&D Systems) pre-clustered with anti-Fc Ab (27) and then warmed at 37°C for 15 minutes. After 30 minutes, HUVEC were lysed and the amount of phosho-EphB4 was quantified using a human Phosphotyrosine EphB4 ELISA kit (Raybiotech, Norcross, USA) according to manufacturer's instructions.

# Supplementary Figures

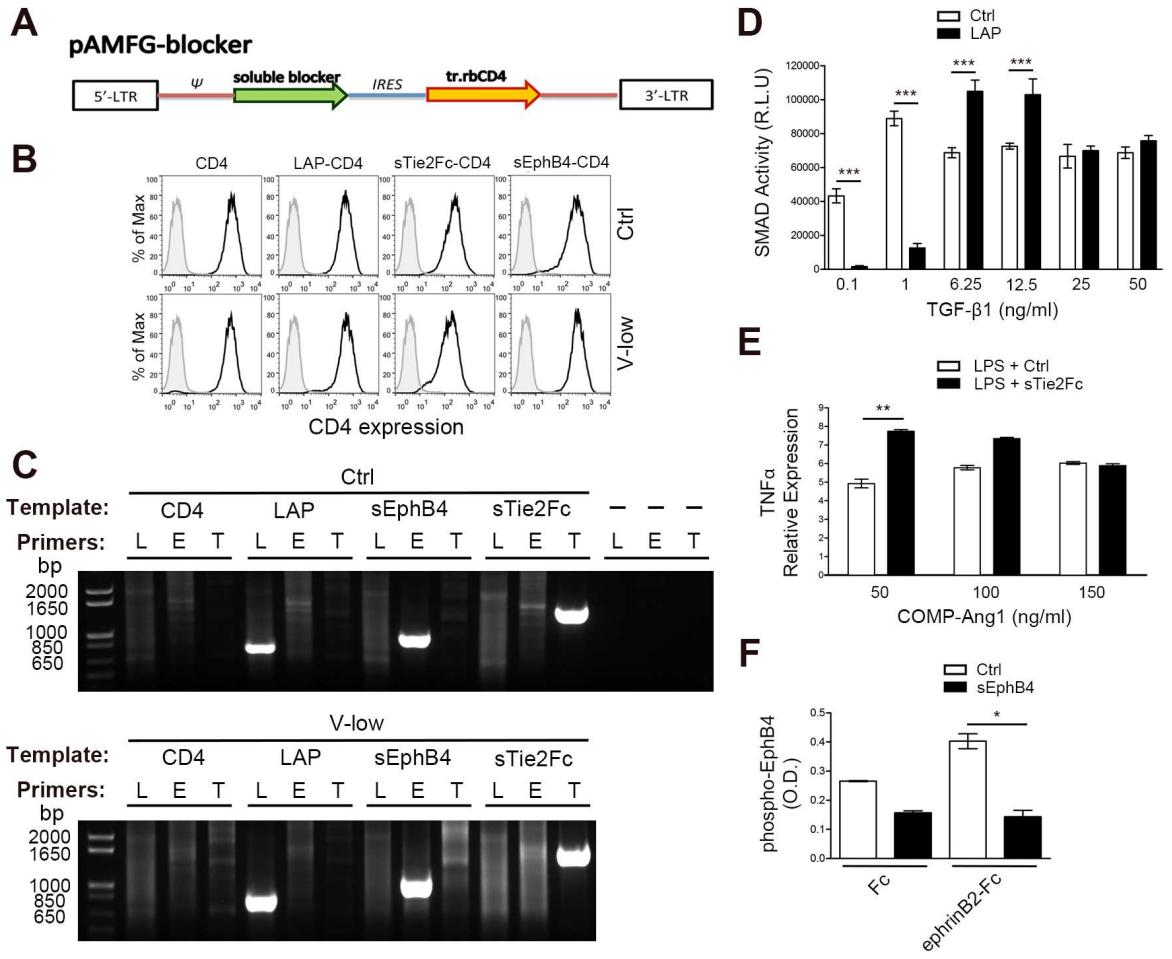


**Supplementary Figure 1. Development and validation of soluble blockers.** (**A**) Retroviral construct carrying a bicistronic cassette coding for one of three signaling blockers (LAP, sEphB4 or sTie2Fc) linked to a truncated version of rabbit CD4 (tr.rbCD4), as a convenient cell surface FACS-sortable marker, through an internal ribosomal entry site sequence (IRES). LTR = retroviral Long Terminal Repeats. (**B**) Blocker-expressing myoblast populations, generated from control cells (Ctrl) or a clone expressing low VEGF (V-low), were FACS-sorted and their purity was determined by analysis of CD4 expression (black curves) vs isotype control (grey curves). (**C**) Expression specificity was determined by RT-PCR on RNA isolated from each population, using primers specific for LAP (L), sEphB4 (E) and sTie2Fc (T), amplifying products of 781, 963 and 1519 bp, respectively. (**D**) Functional activity of the LAP blocker. HEK293N cells were transfected with a TGF-β reporter construct, expressing luciferase under a SMAD-dependent promoter. Conditioned medium from LAP-expressing myoblasts (LAP) inhibited luciferase activity induced by stimulation with 0.1 and 1 ng/ml of TGF-β1 compared to control conditioned medium from CD4 myoblasts (Ctrl). n=3/condition; R.L.U. = Relative Light Units. (**E**) Functional activity of the sTie2Fc blocker. Treatment of RAW264.7 macrophages with LPS causes upregulation of TNFα, which is inhibited by COMP-Ang1. Real-Time qRT-PCR analysis of *Tnfa* gene expression shows that conditioned

medium from sTie2Fc myoblasts (LPS+sTie2Fc) prevented this inhibition by 50 ng/ml COMP-Ang1 compared to control conditioned medium from CD4 myoblasts (LPS+Ctrl). n=6/condition (**F**) Functional activity of the sEphB4 blocker. Human umbilical vein endothelial cells were treated with ephrinB2-Fc or control Fc and phosphorylation of the EphB4 receptor was measured by ELISA. Conditioned medium from sEphB4 myoblasts (sEphB4) inhibited EphB4 phosphorylation compared to control conditioned medium from CD4 myoblasts (Ctrl). n=3/condition; O.D. = Optical Density units.

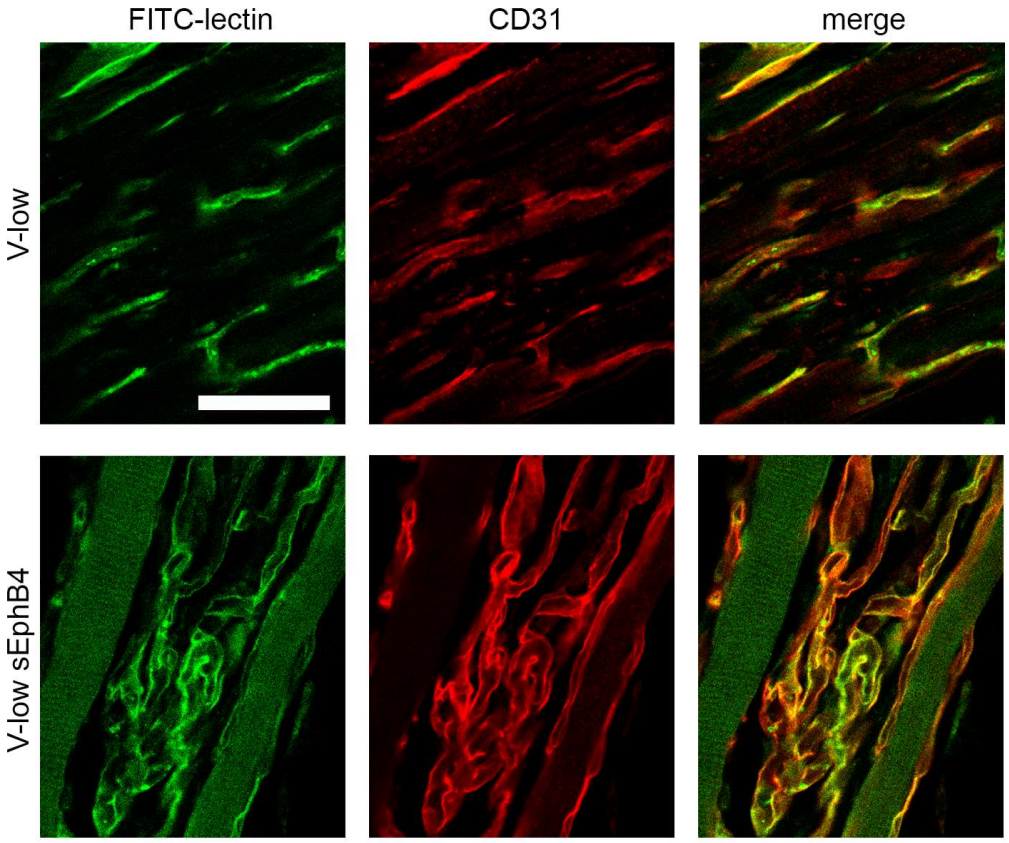


**Supplementary Figure 2. Blockade of ephrinB2/EphB4 signaling does not affect perfusion of VEGF-induced vessels**. Mice received intravenous injections of FITC-lectin 2 weeks after implantation of myoblast clones expressing low VEGF levels alone (V-low) or co-expressing the sEphB4 blocker (V-low sEphB4). Frozen sections of limb muscles were immunostained for CD31 (endothelium, red) and perfused structures were visualized by FITC-lectin co-localization (green). Vascular perfusion was similar in both conditions. Scale bar = 25 μm.

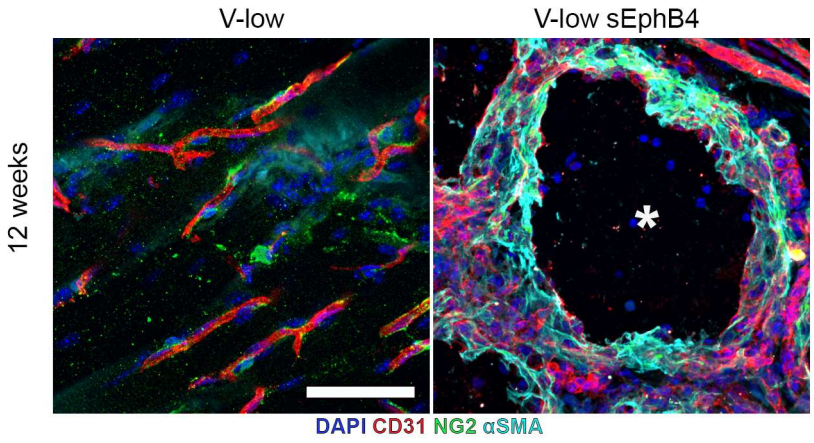


**Supplementary Figure 3. Long-term evolution of aberrant vascular structures induced by low VEGF with ephrinB2/EphB4 blockade**. Immunofluorescence staining of endothelium (CD31, red), pericytes (NG2, green), smooth muscle cells (α-SMA, cyan) and nuclei (DAPI, blue) on frozen sections of limb muscles injected with the V-low clone alone or co-expressing the sEphB4 soluble blocker (V-low sEphB4). Three months after cell implantation aberrant vascular structures induced by ephrinB2/EphB4 signaling blockade were still present and had further enlarged in size, acquiring a thicker smooth muscle coat. Scale bar = 25 µm.

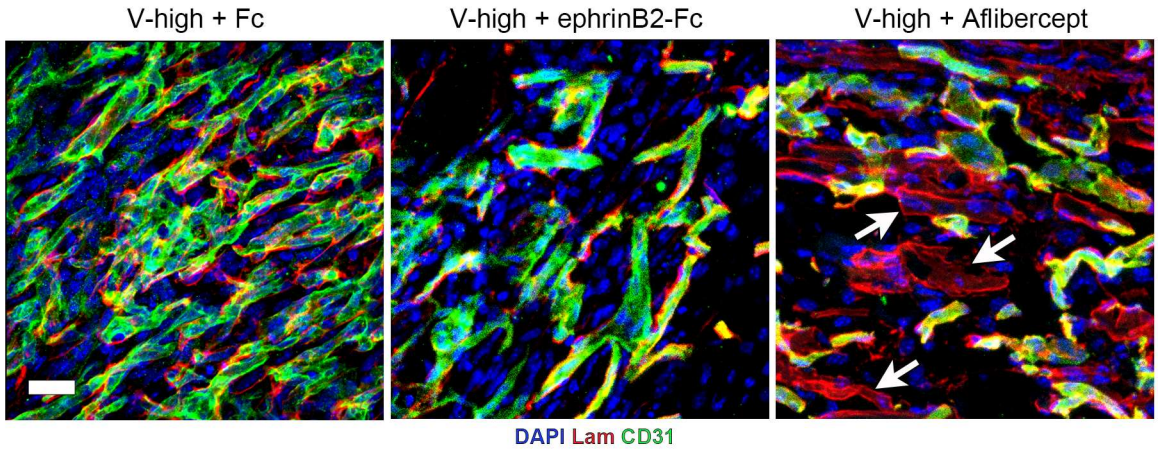


**Supplementary Figure 4. EphB4 stimulation does not cause vessel regression.** Mouse limb muscles were implanted with the V-high myoblast clone, while EphB4 signaling was stimulated by systemic treatment with ephrinB2-Fc or control Fc protein. As a positive control for vessel regression, mice implanted with the V-high clone were treated with the potent VEGF blocker Aflibercept (V-high + Aflibercept). Immunofluorescence staining for endothelium (CD31, green), basal lamina (laminin; lam, red) and nuclei (DAPI, blue) showed that ephrinB2-Fc treatment did not cause any vessel regression, as all basal laminas were associated with endothelial tubes. By contrast, after Aflibercept treatment widespread vessel regression was evident through the detection of empty sleeves of basal lamina (white arrows) devoid of endothelium, remnants of disappeared vessels. Size bar: 25µm.

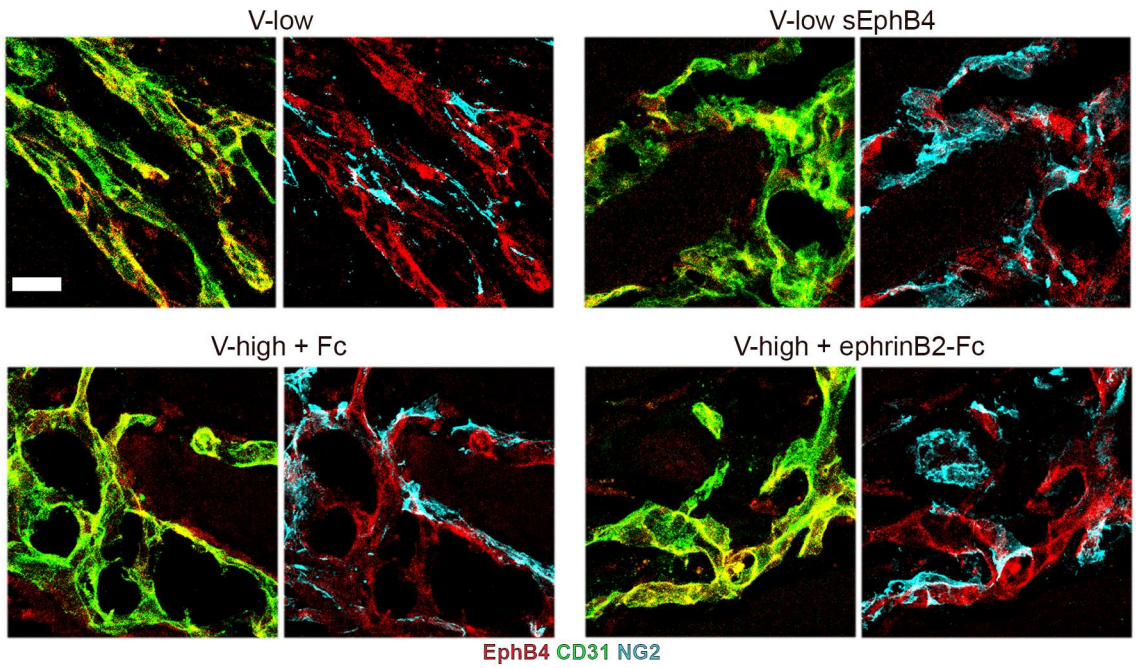


**Supplementary Figure 5. EphB4 is expressed on endothelium of angiogenic microvessels in murine adult skeletal muscle.** Immunofluorescence staining of endothelium (CD31, green), EphB4 (red) and pericytes (NG2, cyan) on frozen sections of limb muscles harvested 4 days after implantation of the V-low clone alone or co-expressing the sEphB4 soluble blocker (V-low sEphB4), or with the V-high clone while EphB4 signaling was stimulated by systemic treatment with ephrinB2-Fc or control Fc protein. EphB4 was strongly expressed by the endothelium of angiogenic micro-vascular structures and not by pericytes. Blockade or activation of EphB4 signaling did not change its expression pattern. Scale bar = 20 µm.

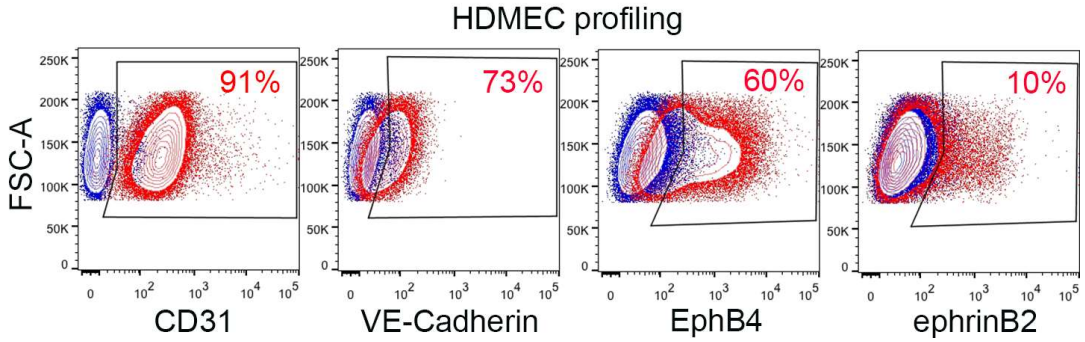


**Supplementary Figure 6. Flow cytometry phenotype of human dermal microvascular endothelial cells (HDMEC).** HDMEC robustly expressed endothelial markers CD31 and VE-Cadherin, as well as EphB4, while ephrinB2 expression was limited to 10% of the cells.

# Discussion

By complementary loss- and gain-of-function approaches we have identified the EphB4 receptor as a key regulator of intussusceptive angiogenesis and a target to control the dose-dependent outcome of VEGF delivery to skeletal muscle for therapeutic purposes. EphB4 activation by systemic treatment with recombinant ephrinB2-Fc protein effectively prevented aberrant vascular growth without interfering with normal angiogenesis, thereby promoting normal microvascular network formation despite high and uncontrolled VEGF doses. Mechanistically, EphB4 activity finely tuned the degree of endothelial proliferation induced by specific VEGF doses without affecting activation of VEGF-R2, but rather converging on its downstream signaling and tuning the phosphorylation of ERK1/2.

While sprouting requires a coordinated interplay between directed migration of tip cells and proliferation of stalk cells behind the tip (47), during intussusceptive angiogenesis pre-existing vessels initially undergo circumferential enlargement that entails exclusively endothelial proliferation without migration (6). The degree of vascular enlargement is proportional to VEGF dose and determines the outcome of subsequent intussusceptive remodeling, as excessive diameters prevent the successful completion of transluminal pillars, leading to failure to split and progressive growth into angioma-like vascular structures (9). Here we identified EphB4 activation as a specific mechanism controlling the outcome of intussusceptive angiogenesis in adult skeletal muscle, by fine-tuning the endothelial proliferation induced by specific doses of VEGF and therefore controlling the degree of circumferential enlargement achieved before transluminal pillar formation and vessel splitting. It is interesting to note how the total amount of proliferating $Ki67^+$ cells 3 days after VEGF delivery was similar with both low and high VEGF doses, in agreement with our previous findings (9), and it was not altered by EphB4 stimulation or inhibition (Figure 6A and 6C). Rather, both VEGF dose and EphB4 activity controlled the proportion of endothelial cells in

the G2-M phase, marked by the phosphorylation of Histone H3 (Figure 6B and 6D), suggesting an effect on the speed of proliferation, i.e. the frequency of transition from G1 to the S-G2-M phase, rather than on the re-entry into the cell cycle from quiescence (G0 to G1 transition) (32, 33).

Pericyte recruitment to nascent vascular structures is crucial for normal morphogenesis, stabilization and function of microvascular networks, through a complex array of signals with endothelial cells (31). Pericyte loss by interference with PDGF-BB/PDGF-Rβ signaling by genetic means during development (48, 49) or blockade during VEGF-induced angiogenesis in adult tissue (12) leads to unabated endothelial proliferation and the growth of aberrantly enlarged vascular structures, which are fragile and cause lethal hemorrhages. Despite the complexity of the pericyte-endothelial molecular crosstalk, here we provide evidence that the ephrinB2-EphB4 pathway is responsible for the pericyte function of regulating the switch between normal and aberrant angiogenesis by VEGF dose. In fact, the effects of EphB4 inhibition or stimulation reported here mimic closely the results obtained in a similar setting by blocking or promoting pericyte recruitment through manipulation of PDGF-BB signaling, respectively (12). Interestingly, the observed lack of effect by TGF-β blockade by LAP over-expression is in agreement with our own recent results, showing that a blocking anti-TGF-β1 antibody did not affect the normal angiogenesis induced by low VEGF, although it significantly impaired endothelial expression of Semaphorin3A and the recruitment of a pro-stabilizing monocyte population (19). These results suggest non-overlapping roles for the two pathways in vascular morphogenesis and stabilization in the setting of intussusceptive angiogenesis.

EphrinB2/EphB4 signaling has well-established functions in arterio-venous differentiation, where ephrinB2 and EphB4 selectively mark the arterial and venous endothelium, respectively (50), and in sprouting angiogenesis. During sprouting, functions of the ephrinB2/EphB4 pathway have been ascribed most clearly to the ephrinB2 partner. In fact,

ephrinB2 was found to localize on the filopodia of tip cells, where it stimulates their motility and sprout formation by increasing endocytosis and signal activity of both VEGF-R2 and -R3 (38, 51), but it does not appear to affect endothelial proliferation during sprouting (38). The role of EphB4, which is absent from the tips and expressed on cells behind the growing front, remains to be elucidated. On the other hand, EphB4 over-expression has been described to suppress sprouting and switch vascular growth to circumferential enlargement, but independently of its kinase activity and rather through stimulation of ephrinB2 reverse signaling (52). In contrast, here we found that EphB4 forward signaling is crucial to regulate intussusceptive angiogenesis, which takes place essentially without migration and rather only through proliferation. In fact, treatment with monomeric sEphB4 not only inhibits activation of endogenous EphB4, but also interferes with ephrinB2 reverse signaling, by preventing interaction and productive multimerization of the two binding partners. While this would be expected to cause reduced VEGF-R2 activation and tip cell migration in the setting of sprouting, we rather observed an increase in the outcome of VEGF signaling specifically on proliferation through ERK1/2 phosphorylation during the process of circumferential enlargement and intussusception, in the absence of tip cells. Conversely, specific activation of EphB4 by treatment with ephrinB2-Fc had the opposite effect, with reduction of ERK1/2 phosphorylation and endothelial proliferation, both *in vitro* and *in vivo*. Taken together, these data suggest a complementary function for ephrinB2 to stimulate VEGF-induced tip cell migration in sprouting and for EphB4 to reduce VEGF-induced ERK1/2 phosphorylation and endothelial proliferation in the absence of tip cells during intussusceptive angiogenesis.

From a therapeutic perspective, it is particularly important that EphB4 stimulation did not completely abolish VEGF-induced endothelial proliferation, but rather only reduced it by about 40%, thereby preventing aberrant angiogenesis without interfering with normal vascular growth. This can be explained considering that VEGF-R2 stimulates endothelial proliferation

through two parallel pathways, one through RAS and the other through PKCβ, which then converge on the RAF-MEK-ERK1/2 cascade (53, 54). The major contributor to ERK1/2 activation by VEGF-R2 *in vivo* has been found to be the PKCβ pathway, through recruitment of PLCγ upon phosphorylation of tyrosine Y1175/1173 (54). However, while mutation of Y1775/1173 both abolished VEGF-induced ERK1/2 activation and caused embryonic lethality (55, 56), global disruption of the *Prkcb* gene, encoding PKCβ, did not cause major vascular phenotypes (57), showing that the control of ERK1/2 activation by VEGF-R2 is redundant downstream of Y1175/1173 phosphorylation. On the other hand, EphB4 directly binds and activates the RAS GTPase Activating Protein RASA1, which negatively regulates RAS activity through its GTPase function (58, 59). Therefore, by inhibiting one branch of a redundant circuit, EphB4 stimulation can achieve modulation of ERK1/2 activation and endothelial proliferation, while sparing sufficient activity to avoid disruption of vascular growth.

Controlling precisely the outcome of VEGF signaling for therapeutic purposes is a significant clinical challenge (60). Recent findings show that delivery of an alternative ligand may activate VEGF-R2 more gently and with less stringent requirements for dose control. For example, VEGF-B binds VEGF-R1 and not VEGF-R2, but it has been found to effectively induce both cardiac angiogenesis and arteriogenesis by displacing R1-bound VEGF-A and making it available for signaling through R2 (61, 62). Since VEGF-R2 is activated only indirectly by endogenously available VEGF-A, even significant VEGF-B overexpression does not cause excessive stimulation of R2 signaling (61). However, the vascular effects of VEGF-B appear restricted to the heart and its delivery does not induce any angiogenesis in skeletal muscle or other tissues (62).

The results reported here show that targeting a separate pathway that converges on downstream signaling provides a new paradigm to modulate VEGF-R2 output. Pharmacologic

targeting of EphB4 can be achieved with systemic treatments offering significant translational potential e.g. in conjunction with VEGF gene therapy.

# References

1. Folkman J. Angiogenesis: an organizing principle for drug discovery? *Nat Rev Drug Discov*. 2007;6(4):273-86.

2. Annex BH. Therapeutic angiogenesis for critical limb ischaemia. *Nat Rev Cardiol*. 2013;10(7):387-96.

3. Giacca M, Zacchigna S. VEGF gene therapy: therapeutic angiogenesis in the clinic and beyond. *Gene Ther*. 2012;19(6):622-9.

4. Yla-Herttuala S, Bridges C, Katz MG, Korpisalo P. Angiogenic gene therapy in cardiovascular diseases: dream or vision? *Eur Heart J*. 2017;38(18):1365-71.

5. Potente M, Gerhardt H, Carmeliet P. Basic and therapeutic aspects of angiogenesis. *Cell*. 2011;146(6):873-87.

6. Gianni-Barrera R, Trani M, Reginato S, Banfi A. To sprout or to split? VEGF, Notch and vascular morphogenesis. *Biochem Soc Trans*. 2011;39(6):1644-8.

7. Carmeliet P, Jain RK. Molecular mechanisms and clinical applications of angiogenesis. *Nature*. 2011;473(7347):298-307.

8. De Spiegelaere W, Casteleyn C, Van den Broeck W, Plendl J, Bahramsoltani M, Simoens P, et al. Intussusceptive angiogenesis: a biologically relevant form of angiogenesis. *J Vasc Res*. 2012;49(5):390-404.

9. Gianni-Barrera R, Trani M, Fontanellaz C, Heberer M, Djonov V, Hlushchuk R, et al. VEGF over-expression in skeletal muscle induces angiogenesis by intussusception rather than sprouting. *Angiogenesis*. 2013;16(1):123-36.

10. Ozawa CR, Banfi A, Glazer NL, Thurston G, Springer ML, Kraft PE, et al. Microenvironmental VEGF concentration, not total dose, determines a threshold between normal and aberrant angiogenesis. *J Clin Invest*. 2004;113(4):516-27.

11. von Degenfeld G, Banfi A, Springer ML, Wagner RA, Jacobi J, Ozawa CR, et al. Microenvironmental VEGF distribution is critical for stable and functional vessel growth in ischemia. *FASEB J*. 2006;20(14):2657-9.

12. Banfi A, von Degenfeld G, Gianni-Barrera R, Reginato S, Merchant MJ, McDonald DM, et al. Therapeutic angiogenesis due to balanced single-vector delivery of VEGF and PDGF-BB. *FASEB J*. 2012;26(6):2486-97.

13. Bottinger EP, Factor VM, Tsang ML, Weatherbee JA, Kopp JB, Qian SW, et al. The recombinant proregion of transforming growth factor beta1 (latency-associated peptide) inhibits active transforming growth factor beta1 in transgenic mice. *Proc Natl Acad Sci U S A*. 1996;93(12):5877-82.

14. Lin P, Polverini P, Dewhirst M, Shan S, Rao PS, Peters K. Inhibition of tumor angiogenesis using a soluble receptor establishes a role for Tie2 in pathologic vascular growth. *J Clin Invest*. 1997;100(8):2072-8.

15. He S, Kumar SR, Zhou P, Krasnoperov V, Ryan SJ, Gill PS, et al. Soluble EphB4 inhibition of PDGF-induced RPE migration in vitro. *Invest Ophthalmol Vis Sci*. 2010;51(1):543-52.

16. Misteli H, Wolff T, Fuglistaler P, Gianni-Barrera R, Gurke L, Heberer M, et al. High-throughput flow cytometry purification of transduced progenitors expressing defined levels of vascular endothelial growth factor induces controlled angiogenesis in vivo. *Stem Cells*. 2010;28(3):611-9.

17. Zisch AH, Schenk U, Schense JC, Sakiyama-Elbert SE, Hubbell JA. Covalently conjugated VEGF--fibrin matrices for endothelialization. *J Control Release*. 2001;72(1-3):101-13.

18. Sacchi V, Mittermayr R, Hartinger J, Martino MM, Lorentz KM, Wolbank S, et al. Long-lasting fibrin matrices ensure stable and functional angiogenesis by highly tunable,

sustained delivery of recombinant VEGF164. *Proc Natl Acad Sci U S A*. 2014;111(19):6952-7.

19. Groppa E, Brkic S, Bovo E, Reginato S, Sacchi V, Di Maggio N, et al. VEGF dose regulates vascular stabilization through Semaphorin3A and the Neuropilin-1+ monocyte/TGF-beta1 paracrine axis. *EMBO Mol Med*. 2015;7(10):1366-84.

20. Kimura M, Kato Y, Sano D, Fujita K, Sakakibara A, Kondo N, et al. Soluble form of ephrinB2 inhibits xenograft growth of squamous cell carcinoma of the head and neck. *Int J Oncol*. 2009;34(2):321-7.

21. Tsaryk R, Peters K, Barth S, Unger RE, Scharnweber D, Kirkpatrick CJ. The role of oxidative stress in pro-inflammatory activation of human endothelial cells on Ti6Al4V alloy. *Biomaterials*. 2013;34(33):8075-85.

22. Hu-Lowe DD, Zou HY, Grazzini ML, Hallin ME, Wickman GR, Amundson K, et al. Nonclinical antiangiogenesis and antitumor activities of axitinib (AG-013736), an oral, potent, and selective inhibitor of vascular endothelial growth factor receptor tyrosine kinases 1, 2, 3. *Clin Cancer Res*. 2008;14(22):7272-83.

23. Hamerlik P, Lathia JD, Rasmussen R, Wu Q, Bartkova J, Lee M, et al. Autocrine VEGF-VEGFR2-Neuropilin-1 signaling promotes glioma stem-like cell viability and tumor growth. *J Exp Med*. 2012;209(3):507-20.

24. Leppanen P, Koota S, Kholova I, Koponen J, Fieber C, Eriksson U, et al. Gene transfers of vascular endothelial growth factor-A, vascular endothelial growth factor-B, vascular endothelial growth factor-C, and vascular endothelial growth factor-D have no effects on atherosclerosis in hypercholesterolemic low-density lipoprotein-receptor/apolipoprotein B48-deficient mice. *Circulation*. 2005;112(9):1347-52.

25. Rissanen TT, Korpisalo P, Karvinen H, Liimatainen T, Laidinen S, Grohn OH, et al. High-resolution ultrasound perfusion imaging of therapeutic angiogenesis. *JACC Cardiovasc Imaging*. 2008;1(1):83-91.

26. Kullander K, Klein R. Mechanisms and functions of Eph and ephrin signalling. *Nat Rev Mol Cell Biol*. 2002;3(7):475-86.

27. Noren NK, Foos G, Hauser CA, Pasquale EB. The EphB4 receptor suppresses breast cancer cell tumorigenicity through an Abl-Crk pathway. *Nat Cell Biol*. 2006;8(8):815-25.

28. Schense JC, Bloch J, Aebischer P, Hubbell JA. Enzymatic incorporation of bioactive peptides into fibrin matrices enhances neurite extension. *Nat Biotechnol*. 2000;18(4):415-9.

29. Schense JC, Hubbell JA. Cross-linking exogenous bifunctional peptides into fibrin gels with factor XIIIa. *Bioconjug Chem*. 1999;10(1):75-81.

30. Baffert F, Le T, Sennino B, Thurston G, Kuo CJ, Hu-Lowe D, et al. Cellular changes in normal blood capillaries undergoing regression after inhibition of VEGF signaling. *Am J Physiol Heart Circ Physiol*. 2006;290(2):H547-59.

31. Armulik A, Genove G, Betsholtz C. Pericytes: developmental, physiological, and pathological perspectives, problems, and promises. *Dev Cell*. 2011;21(2):193-215.

32. Scholzen T, Gerdes J. The Ki-67 protein: from the known and the unknown. *J Cell Physiol*. 2000;182(3):311-22.

33. Crosio C, Fimia GM, Loury R, Kimura M, Okano Y, Zhou H, et al. Mitotic phosphorylation of histone H3: spatio-temporal regulation by mammalian Aurora kinases. *Mol Cell Biol*. 2002;22(3):874-85.

34. Nielsen PS, Riber-Hansen R, Jensen TO, Schmidt H, Steiniche T. Proliferation indices of phosphohistone H3 and Ki67: strong prognostic markers in a consecutive cohort with stage I/II melanoma. *Mod Pathol*. 2013;26(3):404-13.

35. Sahni A, Francis CW. Stimulation of endothelial cell proliferation by FGF-2 in the presence of fibrinogen requires alphavbeta3. *Blood*. 2004;104(12):3635-41.

36. Eichmann A, Simons M. VEGF signaling inside vascular endothelial cells and beyond. *Curr Opin Cell Biol*. 2012;24(2):188-93.

37. Simons M. An inside view: VEGF receptor trafficking and signaling. *Physiology (Bethesda)*. 2012;27(4):213-22.

38. Sawamiphak S, Seidel S, Essmann CL, Wilkinson GA, Pitulescu ME, Acker T, et al. Ephrin-B2 regulates VEGFR2 function in developmental and tumour angiogenesis. *Nature*. 2010;465(7297):487-91.

39. Rennel E, Mellberg S, Dimberg A, Petersson L, Botling J, Ameur A, et al. Endocan is a VEGF-A and PI3K regulated gene with increased expression in human renal cancer. *Exp Cell Res*. 2007;313(7):1285-94.

40. Schweighofer B, Testori J, Sturtzel C, Sattler S, Mayer H, Wagner O, et al. The VEGF-induced transcriptional response comprises gene clusters at the crossroad of angiogenesis and inflammation. *Thromb Haemost*. 2009;102(3):544-54.

41. Sivaprasad U, Fleming J, Verma PS, Hogan KA, Desury G, Cohick WS. Stimulation of insulin-like growth factor (IGF) binding protein-3 synthesis by IGF-I and transforming growth factor-alpha is mediated by both phosphatidylinositol-3 kinase and mitogen-activated protein kinase pathways in mammary epithelial cells. *Endocrinology*. 2004;145(9):4213-21.

42. Dai Y, Schwarz EM, Gu D, Zhang WW, Sarvetnick N, Verma IM. Cellular and humoral immune responses to adenoviral vectors containing factor IX gene: tolerization of factor IX and vector antigens allows for long-term expression. *Proc Natl Acad Sci U S A*. 1995;92(5):1401-5.

43. Zacchigna S, Tasciotti E, Kusmic C, Arsic N, Sorace O, Marini C, et al. In vivo imaging shows abnormal function of vascular endothelial growth factor-induced vasculature. *Hum Gene Ther*. 2007;18(6):515-24.

44. Springer ML, Blau HM. High-efficiency retroviral infection of primary myoblasts. *Somat Cell Mol Genet*. 1997;23(3):203-9.

45. Banfi A, Springer ML, Blau HM. Myoblast-mediated gene transfer for therapeutic angiogenesis. *Methods Enzymol*. 2002;346:145-57.

46. Gu H, Cui M, Bai Y, Chen F, Ma K, Zhou C, et al. Angiopoietin-1/Tie2 signaling pathway inhibits lipopolysaccharide-induced activation of RAW264.7 macrophage cells. *Biochem Biophys Res Commun*. 2010;392(2):178-82.

47. Gerhardt H, Golding M, Fruttiger M, Ruhrberg C, Lundkvist A, Abramsson A, et al. VEGF guides angiogenic sprouting utilizing endothelial tip cell filopodia. *J Cell Biol*. 2003;161(6):1163-77.

48. Hellstrom M, Gerhardt H, Kalen M, Li X, Eriksson U, Wolburg H, et al. Lack of pericytes leads to endothelial hyperplasia and abnormal vascular morphogenesis. *J Cell Biol*. 2001;153(3):543-53.

49. Lindahl P, Johansson BR, Leveen P, Betsholtz C. Pericyte loss and microaneurysm formation in PDGF-B-deficient mice. *Science*. 1997;277(5323):242-5.

50. Wang HU, Chen ZF, Anderson DJ. Molecular distinction and angiogenic interaction between embryonic arteries and veins revealed by ephrin-B2 and its receptor Eph-B4. *Cell*. 1998;93(5):741-53.

51. Wang Y, Nakayama M, Pitulescu ME, Schmidt TS, Bochenek ML, Sakakibara A, et al. Ephrin-B2 controls VEGF-induced angiogenesis and lymphangiogenesis. *Nature*. 2010;465(7297):483-6.

52. Erber R, Eichelsbacher U, Powajbo V, Korn T, Djonov V, Lin J, et al. EphB4 controls blood vascular morphogenesis during postnatal angiogenesis. *EMBO J*. 2006;25(3):628-41.

53. Meadows KN, Bryant P, Pumiglia K. Vascular endothelial growth factor induction of the angiogenic phenotype requires Ras activation. *J Biol Chem*. 2001;276(52):49289-98.

54. Simons M, Gordon E, Claesson-Welsh L. Mechanisms and regulation of endothelial VEGF receptor signalling. *Nat Rev Mol Cell Biol*. 2016;17(10):611-25.

55. Sakurai Y, Ohgimoto K, Kataoka Y, Yoshida N, Shibuya M. Essential role of Flk-1 (VEGF receptor 2) tyrosine residue 1173 in vasculogenesis in mice. *Proc Natl Acad Sci U S A*. 2005;102(4):1076-81.

56. Takahashi T, Yamaguchi S, Chida K, Shibuya M. A single autophosphorylation site on KDR/Flk-1 is essential for VEGF-A-dependent activation of PLC-gamma and DNA synthesis in vascular endothelial cells. *EMBO J*. 2001;20(11):2768-78.

57. Leitges M, Schmedt C, Guinamard R, Davoust J, Schaal S, Stabel S, et al. Immunodeficiency in protein kinase cbeta-deficient mice. *Science*. 1996;273(5276):788-91.

58. Kawasaki J, Aegerter S, Fevurly RD, Mammoto A, Mammoto T, Sahin M, et al. RASA1 functions in EPHB4 signaling pathway to suppress endothelial mTORC1 activity. *J Clin Invest*. 2014;124(6):2774-84.

59. Kim I, Ryu YS, Kwak HJ, Ahn SY, Oh JL, Yancopoulos GD, et al. EphB ligand, ephrinB2, suppresses the VEGF- and angiopoietin 1-induced Ras/mitogen-activated protein kinase pathway in venous endothelial cells. *FASEB J*. 2002;16(9):1126-8.

60. Martino MM, Brkic S, Bovo E, Burger M, Schaefer DJ, Wolff T, et al. Extracellular matrix and growth factor engineering for controlled angiogenesis in regenerative medicine. *Front Bioeng Biotechnol*. 2015;3:45.

61. Kivela R, Bry M, Robciuc MR, Rasanen M, Taavitsainen M, Silvola JM, et al. VEGF-B-induced vascular growth leads to metabolic reprogramming and ischemia resistance in the heart. *EMBO Mol Med*. 2014;6(3):307-21.

62. Lahteenvuo JE, Lahteenvuo MT, Kivela A, Rosenlew C, Falkevall A, Klar J, et al. Vascular endothelial growth factor-B induces myocardium-specific angiogenesis and arteriogenesis via vascular endothelial growth factor receptor-1- and neuropilin receptor-1-dependent mechanisms. *Circulation*. 2009;119(6):845-56.

# IV. The crosstalk between Notch4 and ephrinB2/EphB4 signaling in VEGF-induced angiogenesis

# The crosstalk between Notch4 and ephrinB2/EphB4 signaling in VEGF-induced angiogenesis

Sime Brkic[1,2], Elena Groppa[1,2,3], Andrea Uccelli[1,2], Roberto Gianni-Barrera[1,2] and Andrea Banfi[1,2]

[1]Department of Biomedicine, University Hospital, University of Basel, Basel, Switzerland.
[2]Department of Surgery, University Hospital, Basel, Switzerland.
[3]Current address: The Biomedical Research Centre, The University of British Columbia, Vancouver, Canada.

# Introduction

Therapeutic angiogenesis is a promising strategy for treatment of ischemic diseases like peripheral and coronary artery disease. However, to date gene therapy approaches using VEGF delivery failed to show efficacy in clinical trials, despite the established biological function of the factor as master regulator of vascular growth (1). Angiogenesis is controlled by the concerted actions of different signaling pathways (2). In order to design rational strategies for therapeutic angiogenesis, it is crucial to identify the molecular crosstalk governing the process of both physiological and pathological blood vessel growth. In fact, aberrant vessel growth induced by excessive VEGF stimulus is a significant hurdle for therapeutic benefit, since it can cause the growth of angioma-like vascular tumors. Adenoviruses are robust, clinically established vectors for VEGF gene delivery with many desirable features, such as high transduction rate for efficacy and transient duration of expression for safety (3). However, viral transduction *in vivo* leads to heterogeneous levels of expression in different cells, due to the variable efficiency of infection. This can lead to localized overproduction of VEGF, which remains bound to extracellular matrix in the cellular microenvironment, and these hotspots of excessive VEGF concentration cause aberrant vessel growth. Therefore, it is essential to understand the molecular basis governing the switch between normal and aberrant angiogenesis in order to develop pharmacological targets to prevent angioma growth without interfering with induction of normal microvascular networks. In the previous Chapter we identified ephrinB2/EphB4 signaling as a key molecular pathway responsible for the switch between normal and aberrant angiogenesis by increasing VEGF doses. We demonstrated that EphB4 signaling modulates VEGF-induced endothelial proliferation and therefore the size of initial vascular enlargements, enabling their successful splitting into morphologically normal capillary networks despite high VEGF doses. The molecular mechanism by which EphB4

regulates VEGF signaling does not involve direct regulation of VEGF-R2 activation, but rather modulation of its downstream signaling through pERK1/2.

The Notch4 signaling pathway has also been implicated in the generation of aberrantly enlarged vessels, namely arterio-venous malformations (AVM) (4, 5). Gene polymorphisms in the *Notch4* gene are associated with development of brain arterio-venous malformations and hemorrhagic presentations (6). Notch signaling plays a key role in arterio-venous differentiation during development by inducing an arterial phenotype through expression of the arterial marker ephrinB2 and simultaneous downregulation of the venous marker EphB4 (7, 8). Interestingly, single nucleotide polymorphisms in the *EphB4* gene have also been associated with higher risk of intracranial hemorrhaging presentations in patients with brain arterio-venous malformations (9). While other Notch receptors are expressed in multiple tissue, Notch4 is predominantly restricted to endothelial cells (10). Overactivation of Notch4 in endothelium causes lack of small branched vessels and loss of vessel integrity (11). Using a tetracycline-regulated system, it was shown that mice expressing a constitutively active Notch4 form, develop arterio-venous malformations in the brain that regress once the Notch4 overactivation is abrogated by doxycycline treatment (5, 12-14). It was demonstrated that regression of these AVMs happens by direct restoration of the venous programming and by normalization of blood flow without change in endothelial cell number (5, 13). Furthermore, Murphy et al. demonstrated that expression of EphB4 is markedly reduced during formation of AVM and restored after repression of Notch4 signaling and normalization of vessel morphology. Inhibition of EphB4 signaling by sEphB4 dramatically reduced AVM normalization demonstrating that EphB4 signaling is necessary for this process in this model (5). In a separate project, we have recently investigated the role of Notch4 signaling in the switch between normal and aberrant angiogenesis by increasing VEGF doses. It was found that aberrant angiogenesis, induced by high VEGF doses, was switched to normal capillary growth

in Notch4-deficient mice (Gianni-Barrera, et al, in preparation). On the other hand, in the previous Chapter we demonstrated that EphB4 gain-of-function can similarly normalize aberrant angiogenesis induced by high doses of VEGF. As both Notch4 loss-of-function and EphB4 gain-of-function caused similar effects on VEGF-induced angiogenesis, preventing aberrant vascular growth and enabling microvascular normalization, here we aimed at determining whether ephrinB2/EphB4 signaling may act via Notch4.

In order to investigate whether Notch4 signaling is necessary for this process, we took advantage of a mouse line carrying a mutated *Notch4* allele with a 1.0-kb deletion in the region of exons 21 and 22, coding for a part of the extracellular domain adjacent to the transmembrane domain (B6;129S1-Notch4$^{tm1Grid}$/J; here referred as *Notch4$^{d1}$*) (15). These mice are fertile and viable, with slightly elevated systolic blood pressure after experimental induction of hindlimb ischemia (16), delayed tumor onset and decreased tumor perfusion (17). This mutation leads to production of a truncated Notch4 protein lacking all the transmembrane and intracellular domains (NICD), which is therefore unable to transmit downstream signaling (15). To determine whether EphB4 requires active Notch4 signaling to control the outcome of VEGF dose-dependent angiogenesis, we investigated whether the switch from normal to aberrant angiogenesis caused by EphB4 loss-of-function (sEphB4 co-expression), as described in the previous Chapter, would be prevented in *Notch4$^{d1}$* mice.

# Materials and methods

## *In vivo* myoblast implantation

B6;129S1-Notch4$^{tm1Grid}$/J (referred as Notch4$^{dl}$) carrying a *Notch4* allele with 1.0-kb deletion in the region of exons 21 and 22 (Charles River Laboratories, Sulzfeld, Germany) (15) and control C57BL/6 mice of 8-12 weeks age with equal representation of both genders, were randomly assigned to experimental groups, with a minimum of n=4 mice/group. Monoclonal populations of transduced myoblasts expressing homogeneous levels of VEGF alone or co-expressing sEphB4 were used for all the experiments. Myoblasts expressing CD4 were used as control. Myoblasts were dissociated in trypsin, resuspended in sterile PBS with 0.5% BSA (Sigma-Aldrich Chemie GmbH, Steinheim, Germany) and one or two injections of 10 µl of cell suspension containing $10^6$ cells were injected into the *Tibialis anterior* (TA) or *Gastrocnemius* (GC) lower hindlimb muscles, respectively, using a 30-gauge needle syringe, as previously described (18). All experiments were performed with similar number of samples from both muscle locations and the results were pooled together.

## Histology

Mice were anesthetized with ketamine (100 mg/kg) and xylazine (10 mg/kg) and sacrificed by intravascular perfusion of 1% paraformaldehyde in PBS pH 7.4. TA and GC muscles were harvested, post-fixed in 0.5% paraformaldehyde in PBS for 2 h, cryoprotected in 30% sucrose in PBS overnight at 4°C, embedded in OCT compound (CellPath, Newtown, Powys, UK), frozen in isopentane, and cryosectioned. The areas of engraftment were identified by tracking implanted myoblasts by X-gal staining (20-µm sections) in adjacent serial sections, as described previously (18). For immunofluorescence staining, 10-µm tissue sections were blocked with 5% goat serum and 2% BSA in PBS with 0.3% Triton-X, for 1h at RT and stained

for 1h at RT with the following primary antibodies and dilutions: rat monoclonal anti-mouse CD31 (clone MEC 13.3, BD Biosciences, Basel, Switzerland) at 1:100; mouse monoclonal anti-mouse α-SMA (clone 1A4, MP Biomedicals, Basel, Switzerland) at 1:400; rabbit polyclonal anti-NG2 (Merck Millipore, Darmstadt, Germany) at 1:200; rabbit polyclonal anti-pHH3-Ser28 (Cell Signaling Technology, Danvers, USA) at 1:100 and anti-Notch4 labeled with Alexa647 (clone HMN4-14, Biolegend, USA) at 1:100; rabbit polyclonal anti-Caspase-3-Asp175 (Cell Signaling Technology, Danvers, USA) at 1:150. Fluorescently labeled secondary antibodies (Invitrogen) were used at 1:200.

For pERK1/2 staining, tissue sections were permeabilized with ice-cold methanol for 10 min, and blocked with 5% goat serum and 2% BSA in PBS with 0.3% Triton-X for 1h at RT. Rabbit monoclonal anti-phospho-ERK1/2 antibody (Thr202/Tyr204, clone D13.14.4E, Cell Signaling Technology) was used at dilution of 1:100.

## RNA extraction and quantitative real-time PCR

Freshly harvested *Tibialis anterior* and *Gastrocnemius* muscles were frozen in liquid nitrogen and disrupted using a Qiagen Tissue Lyser (Qiagen, Basel, Switzerland) in 1 ml TRIzol reagent (Invitrogen, Basel, Switzerland) for 100 mg of tissue. Total RNA was isolated according to manufacturer's instructions. Two micrograms of RNA were reverse transcribed into cDNA using the Omniscript Reverse Transcription kit (Qiagen) at 37°C for 60 minutes. Quantitative Real-Time PCR (qRT-PCR) was performed on an ABI 7300 Real-Time PCR system (Applied Biosystems, Basel, Switzerland). Expression of genes of interest was determined using the following TaqMan Gene Expression assays (Applied Biosystems) according to manufacturer's instructions: *Gapdh* (Mm03302249_g1), *Notch4* extracellular domain (Mm00440525_m1), *Notch4* exons 21 and 22 (Mm01134996_g1), *Notch1* (Mm00435249_m1), *Dll1* (Mm01279269_m1), *Dll4* (Mm00444619_m1), *Jag1*

(Mm00496902_m1), *Hes1* (Mm01342805_m1), *Hey2* (Mm00469280_m1), *Egfl7* (Mm00618004_m1), *Rasa1* (Mm00520858_m1), *Klf2* (Mm01244979_g1), *Klf4* (Mm00516104_m1), *ephrinB2* (Mm01215897_m1), *EphB4* (Mm01201157_m1), *Vegfr2* (Mm01222421_m1), *Pdgfrb* (Mm00435546_m1). Reactions were performed in duplicate for each template, averaged and normalized to expression of the *Gapdh* housekeeping gene.

## Vascular analyses

Qualitative analysis of vascular morphology in immunofluorescence was performed on images acquired on an LSM710 3-laser scanning confocal microscope (Carl Zeiss, Feldbach, Switzerland). Images of vascular structures were acquired with 40X objective in at least 5 sections/muscle, cut at 100-150 μm of distance from each other (n = 4 muscles/group).

Vessel diameters were measured on fluorescently immunostained sections as described (18). Briefly, 10 fields/muscle (n = 4 muscles/group) were analyzed, measuring a total of minimum 100 diameters/muscle. Images were overlaid with a square grid, squares were randomly chosen and the diameter of each vessel in the center of selected squares was measured. To avoid selection bias, the shortest diameter in the selected vascular segment was systematically measured.

Vessel length density (VLD) was quantified in fluorescently immunostained cryosections as described (18). Briefly, 5 fields per muscle (n = 4 muscles/group) were analyzed by tracing the total length of vessels in the acquired field and dividing it by the area of the fields. All images for both diameter quantification and vessel length density analysis were acquired with a 20X objective on an Olympus BX63 microscope (Olympus, Volketswil, Switzerland) and analyses were performed with Cell Sens software (Olympus).

The percentage of pHH3+ endothelial cells was quantified for every image based on the total number of endothelial cells and the average value for every experimental group was

calculated. In total, 3000–6000 endothelial cells were analyzed per group. At least 10 areas with a clear angiogenic effect were analyzed per group (n=6 muscles/group).

## Statistical analysis

Data are presented as mean±standard error. The significance of differences was assessed with the GraphPad Prism 6 software (GraphPad Software). The normal distribution of all data sets was tested and, depending on the results, multiple comparisons were performed with the parametric 1-way analysis of variance (ANOVA) followed by the Bonferroni post-hoc test, or with the non-parametric Kruskal-Wallis test followed by Dunn's post-test, while single comparisons were analyzed with the non-parametric Mann-Whitney test or the parametric one-tailed t-test. Gene expression data representing fold-changes versus control, which are asymmetrically distributed, were first normalized by logarithmic transformation and then by t-test with Welch's correction for single comparisons. Vessel diameter values were first normalized by log2-transformation and then analyzed by 1-way ANOVA followed by Bonferroni test for multiple comparisons. $p<0.05$ was considered statistically significant.

## Study approval

Animal studies were performed in accordance with the Swiss Federal guidelines for animal welfare and were approved by the Veterinary Office of the Canton of Basel-Stadt (Basel, Switzerland; Permit 2071).

# Results

## *Notch4$^{d1}$* mice upregulate expression of truncated Notch4 during angiogenesis

*Notch4$^{d1}$* mice carry a deletion of exons 21 and 22 in *Notch4* gene, with an out-of-frame mutation leading to the translation of a truncated Notch4 protein comprising only an incomplete extracellular domain (N4 ECD) (15) (Figure 1A). This was confirmed by qRT-PCR on RNA isolated from unperturbed muscle tissues (Figure 1B), showing that *Notch4$^{d1}$* mice express similar basal levels of N4 ECD as wild-type, whereas the mutated exons are absent. However, during active angiogenesis (4 days after injection of myoblast expressing low levels of VEGF) expression of truncated *Notch4* transcript in *Notch4$^{d1}$* mice appear to increase more than in wild-type mice (Figure 1C). This was confirmed at the protein level, by immunofluorescence staining. Notch4 ECD was detected essentially only in blood vessels stained with CD31 (Figure 1D).

## Differential gene expression in skeletal muscle of *Notch4$^{d1}$* mice

Baseline expression of genes associated with Notch signaling (*Notch1*, *Dll1*, *Dll4*, *Jag1*, *Hes1*, *Hey2* and *Egfl7*), as well as other angiogenic key players, such as the modulator of the MAPK pathway *Rasa1*, the transcription factors *Klf2* and *Klf4*, as well as *ephrinB2*, *EphB4*, *Vegfr2* and *Pdgfrb*, was analyzed in TA and GC skeletal muscles of *Notch4$^{d1}$* and control wild-type mice. Analysis by qRT-PCR showed that Notch-related genes were generally downregulated in *Notch4$^{d1}$* mice as compared to the control, with *Dll4*, *Hey2* and *Egfl7* recaching statistical significance, whereas other angiogenic genes were not differentially expressed in two mouse strains (Figure 2).

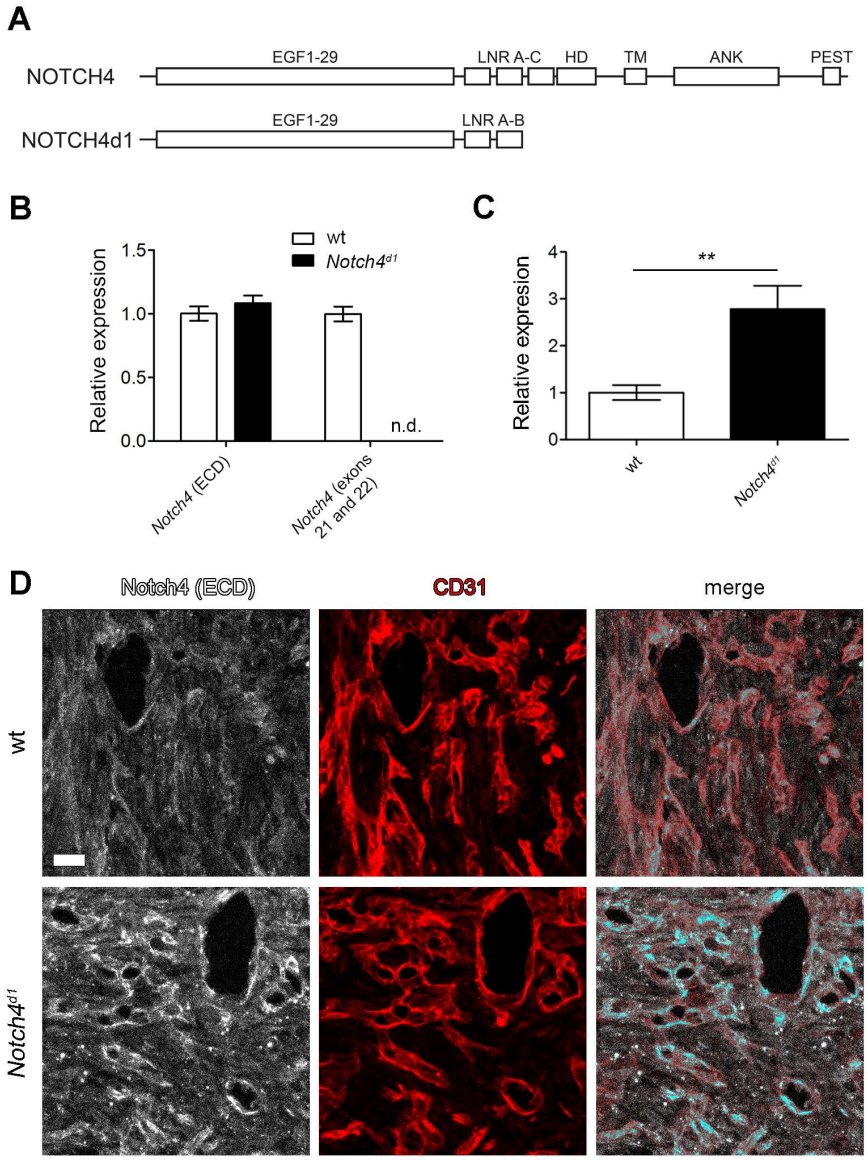


**Figure 1. *Notch4$^{d1}$* mice overexpress truncated extracellular portion of Notch4 protein.** *Notch$^{d1}$* mice carry a mutated *Notch4* allele with a deletion of exons 21 and 22, leading to out-of-frame mutation and production of truncated protein lacking a part of extracellular domain, entire transmembrane (TM) and intracellular domains [Adapted from James, A.C. et al. 2014 (19)] (**A**). Level of *Notch4* transcript was determined on total RNA isolated form TA and GC muscles from wild-type (wt) and *Notch4$^{d1}$* mice by two different probes; one recognizing sequence coding for extracellular domain (ECD) and the other region spanning exons 21 and 22. Presence of truncated *Notch4* transcript containing extracellular portion, but lacking exons 21 and 22, was confirmed in *Notch4$^{d1}$* mice, n=6 muscles/group (**B**). Amount of *Notch4* transcript was also assessed in muscle samples harvested 4 days after injection of myoblasts expressing low levels of VEGF. Analysis showed overexpression of truncated *Notch4* transcript in *Notch4$^{d1}$* mice, as compared to wt mice (n=8 muscles/group), ** $p<0.01$ by t-test, after data normalization by logarithmic transformation. (**C**). Immunofluorescence analysis was performed on the same samples as the one from (B), confirming the overexpression of Notch4 protein in blood vessels (stained with CD31) of *Notch4$^{d1}$* mice. Antibody specific for extracellular domain of Notch4 protein was used, size bar=25µm (**D**).

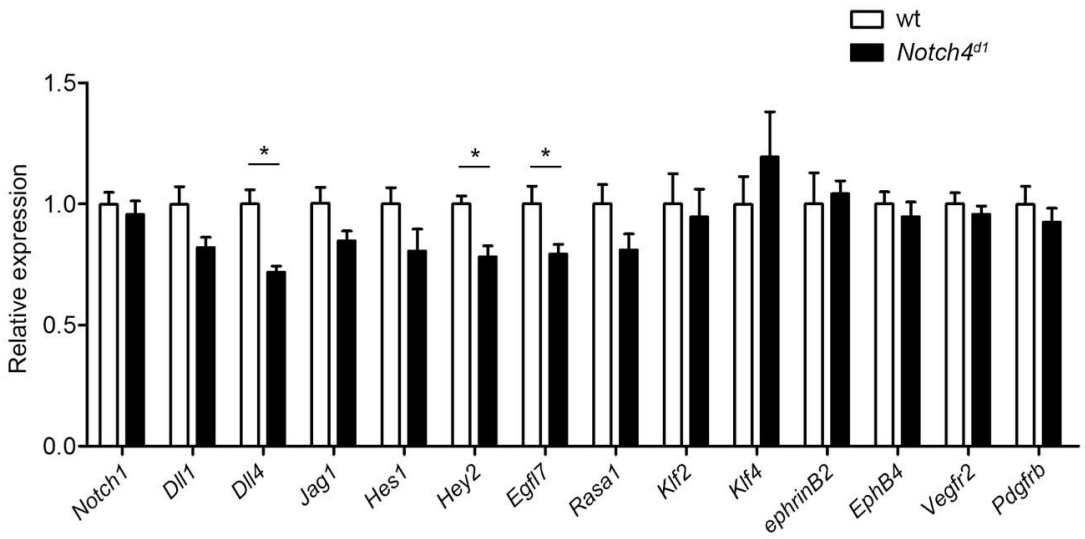


**Figure 2. Differential gene expression in skeletal muscles of wild-type and *Notch4$^{d1}$* mice.** Level of expression of different angiogenesis-related genes was determined on total RNA isolated form TA and GC muscles from wild-type (wt) and *Notch4$^{d1}$* mice, n=6 muscles/group, * $p<0.05$ by t-test, after data normalization by logarithmic transformation.

## Aberrant angiogenesis induced by EphB4 blockade requires Notch4 activity

We injected myoblasts co-expressing low levels of VEGF ($77.6 \pm 0.96$ ng/$10^6$ cells/day) and sEphB4, inhibitor of ephrinB2/EphB4 pathway (V-low sEphB4) in limb muscles of both control C57BL/6 (referred as wild type; wt) and *Notch4$^{d1}$* mice. After two weeks, animals were sacrificed and the muscles were harvested and analyzed histologically. Morphological analysis showed that in wild-type mice, blockade of ephrinB2/EphB4 signaling induced irregularly enlarged aberrant vessels covered with α-smooth muscle actin-positive ($\alpha SMA^+$) mural cells, while in *Notch4$^{d1}$* mice we could observe only morphologically normal capillaries. Some of these were associated with $\alpha SMA^+$ mural cells, which however displayed the typical morphology of pericytes rather than smooth muscle cells (Figure 3A). Vessel diameter analysis showed that blockade of ephrinB2/EphB4 signaling in wt mice induced vessels of larger average diameter, as compared to *Notch4$^{d1}$* mice ($7.4 \pm 0.8$ μm in wt vs $5.0 \pm 0.2$ μm in *Notch4$^{d1}$*, $p<0.01$; Figure 3B). Quantification of vessel diameter distributions on the same samples showed that ephrinB2/EphB4 inhibition in wt mice gave rise to a fraction of

significantly enlarged vessel, with 19% of them being >10 µm, while in *Notch4*$^{d1}$ this was only 4%. The 90$^{th}$ percentile in wt mice was 12.1 µm, while the median was 6.5 µm. In *Notch4*$^{d1}$ mice the 90$^{th}$ percentile was 7.6 µm and the median 4.9 µm (Figure 3C).

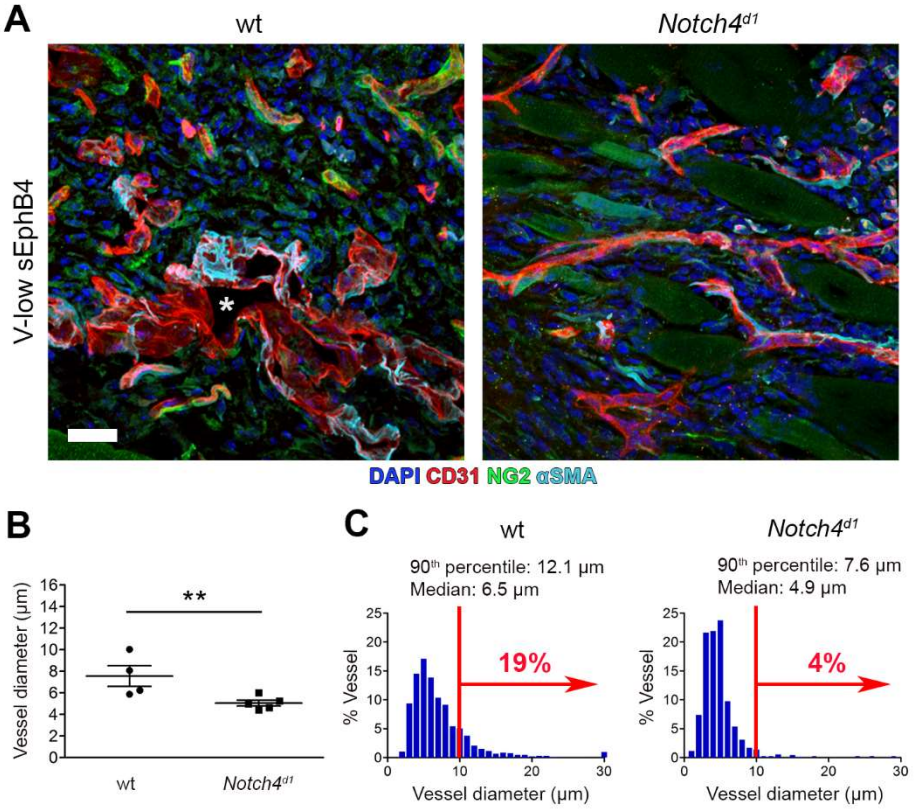


**Figure 3. Aberrant angiogenesis by ephrinB2/EphB4 blockade is prevented in *Notch4*$^{d1}$ mice.** (**A**) Limb muscles of both wild-type (wt) and *Notch4*$^{d1}$ mice were implanted with myoblast clones co-expressing low levels of VEGF and sEphB4, inhibitor of ephrinB2/EphB4 signaling (V-low sEphB4). The muscles were harvested after 14 days and vessel morphology and diameter were analyzed histologically. Morphological analysis was performed by staining for endothelium (CD31, red), pericytes (NG2, green), smooth muscle cells (α-SMA, cyan) and nuclei (DAPI, blue) and it showed that in wt mice, sEphB4 induced aberrant vessels covered with α-SMA coating, while only morphologically normal capillaries were found in *Notch4*$^{d1}$ mice, * = lumen of aberrant structure, size bar=25µm. (**B**) Vessel diameter analysis on the same samples showed that ephrinB2/EphB4 inhibition led to induction of vessels of significantly higher average diameter in *Notch4*$^{d1}$ mice as compared to control mice, n=4-5 muscles/group, ** $p<0.01$ by t-test, after data normalization by logarithmic transformation. (**C**) The diameter distribution analysis showed a decrease of percentage of vessels >10 µm in diameter in *Notch4*$^{d1}$ mice, as compared to wt mice, i.e. from 19% to 4%, respectively.

## Notch4 activity does not control initial vascular enlargements, but is necessary specifically for aberrant remodeling

We have previously found that VEGF-induced angiogenesis in skeletal muscle takes place without sprouting, but rather through the mechanism of intussusception, where pre-existing vessel circumferentially enlarge in response to VEGF and then longitudinally split to form two new vessels (20). We quantified the diameter of initial vascular enlargements 4 days after myoblast implantation and we observed that low and safe VEGF levels (V-low) led to similar size of vascular enlargements irrespectively of Notch4 signaling inactivation (average: 13.9±1.3 μm in wild-type vs. 13.1±2.1 μm in *Notch4*$^{d1}$ mice, 90$^{th}$ percentile: 22.9 μm vs. 23.5 μm, median: 11.5 μm vs. 10.2 μm, respectively; Figure 4A-B, E). As expected, inhibition of ephrinb2/EphB4 signaling by sEphB4 (V-low sEphB4) caused a significant increase in the size of vascular enlargements in wt mice compared to VEGF alone, but again this was not affected by Notch4 signaling (average: 18.5 ± 1.8 μm in wild-type, $p<0.05$ vs V-low, 19.9 ± 0.9 μm in *Notch4*$^{d1}$ mice, $p<0.01$ vs V-low, 90$^{th}$ percentile: 32.5 μm in wt, 36.9 μm in *Notch4*$^{d1}$, median: 14.9 μm in wt, 16.7 μm in *Notch4*$^{d1}$ mice; Figure 4C-E). Seven days after myoblast implantation the process of vessel splitting is normally completed and the appearance of aberrant structures or homogeneous capillary networks can be distinguished. After 7 days, low levels of VEGF induced normal capillaries in both wild-type and *Notch4*$^{d1}$ mice (average: 8.4±0.6 μm in wild-type vs. 7.9±0.4 μm in *Notch4*$^{d1}$ mice, 90$^{th}$ percentile: 14.3 μm vs. 12.1 μm, median: 7.6 μm vs. 7.2 μm, respectively; Figure 4F-G, J). Inhibition of ephrinB2/EphB4 signaling in wild-type mice induced aberrant vessels with irregular shapes and significantly enlarged diameters compared to VEGF alone (average: 14.0±1.6 μm, $p<0.001$, 90$^{th}$ percentile: 24.1 μm, median: 11.0 μm). In contrast, the appearance of aberrant structures was prevented in *Notch4*$^{d1}$ mice despite inhibition of ephrinB2/EphB4 pathway, and only normal capillary networks were detectable, similar to those induced by low VEGF alone (average: 8.5±0.4 μm,

$90^{th}$ percentile: 14.2 µm, median: 7.3 µm). There was a statistical significance between average vessel diameter between the two mouse strains injected with V-low sEphB4 myoblast clone ($p<0.001$). The percentage of vessels of diameter >10 µm in V-low condition in wild-type and *Notch4*$^{d1}$ mice was 25% and 20%, respectively. Inhibition of ephrinB2/EphB4 pathway increased that percentage to 55% in wild-type mice, while in *Notch4*$^{d1}$ mice it was reduced to 27% (Figure 4F-J). As previously shown in Figure 3A, 2 weeks after myoblast implantation, aberrant structures induced by inhibition of ephrinB2/EphB4 continued to grow in control mice, while only normal capillaries were still found in *Notch4*$^{d1}$ mice.

Vessel length density (VLD) was quantified after 7 days to assess the extent of neo-angiogenesis induced by different stimuli. Analysis showed that stimulation with either VEGF alone or parallel inhibition of ephrinB2/EphB4 pathway, induced growth of new blood vessels, as compared to VLD in control condition where myoblast expressed only CD4 marker, but no VEGF. Additionally, VLD was consistently higher in *Notch4*$^{d1}$ mice as compared to wild-type mice in both condition with VEGF stimulation alone or when ephrinB2/EphB4 was also inhibited (Figure 4K). Therefore, the prevention of aberrant vascular growth by Notch4 inactivation was not due to a general inhibition of angiogenesis.

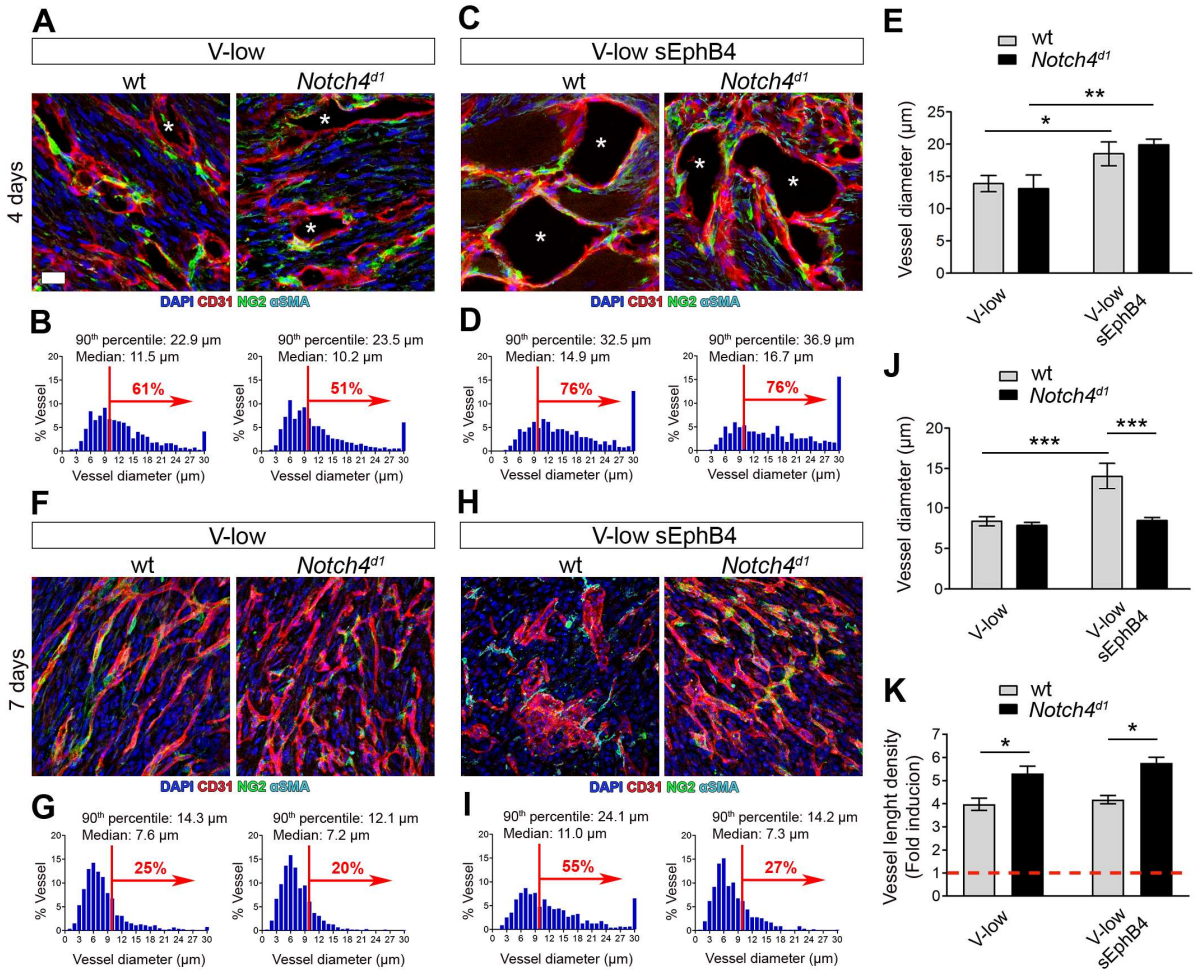


**Figure 4. Notch4 signaling is not controlling initial vascular enlargements, but prevents aberrant angiogenesis by ephrinB2/EphB4 inhibition**. Mouse limb muscles of both wild-type (wt) and *Notch4$^{d1}$* mice were implanted with myoblast clones expressing only low level of VEGF (V-low) or co-expressing sEphB4, blocker of ephrinB2/EphB4 pathway (V-low sEphB4). Immunostaining of frozen sections stained for endothelium (CD31, red), pericytes (NG2, green), smooth muscle cells (α-SMA, cyan) and nuclei (DAPI, blue) and quantification of vessel diameter distribution 4 days after myoblast implantation showed that ephrinB2/EphB4 inhibition increased the size of initial vessel enlargements as compared to VEGF alone, in both wt and *Notch4$^{d1}$* mice, n=4-5 muscles/group, * <0.05, ** p<0.01 by 1-way ANOVA with Bonferroni multiple comparisons test, after data normalization by logarithmic transformation, *=lumen of vascular enlargement, size bar=25 μm (**A-E**). After 7 days, VEGF alone induced normal capillaries in both mouse strains, with similar percentage of vessels of diameter >10 μm (25% and 20% in wt and *Notch4$^{d1}$* mice, respectively) (**F-G**) and similar average vessel diameter (**J**), while inhibition of ephrinB2/EphB4 pathway led to induction of irregular aberrant vessels only in wt, but not in *Notch4$^{d1}$* mice (**H**), with lower percentage of enlarged vessels (**I**) and overall decrease of average vessel diameter (**J**), n=3-4 muscles/group, *** p<0.001 by 1-way ANOVA with Bonferroni multiple comparisons test, after data normalization by logarithmic transformation. Analysis of vessel length density (VLD), performed at 7 days showed higher vessel length density in *Notch4$^{d1}$* mice as compared to wild type mice, both with or without inhibition of ephrinB2/EphB4 pathway. The data is expressed as fold increase in VLD normalized to VLD of

control condition (wt mice injected with myoblasts expressing only CD4; marked with red line). n=4 muscles/group, * $p<0.05$, by Kruskal-Wallis test followed by Dunn's post-test. (**K**).

## Both EphrinB2/EphB4 and Notch4 signaling control endothelial cell proliferation, but not apoptosis

Endothelial cell proliferation has previously been associated with formation of VEGF-induced vascular enlargements, as the initial step of intussusceptive angiogenesis (20). We performed immunofluorescence co-staining using antibodies against endothelial marker CD31 and a proliferation marker, phospho-histone H3 (pHH3), found only in G2-M phase of the cell cycle (21, 22). We asked whether inhibition of ephrinB2/EphB4 signaling requires active Notch4 signaling to stimulate endothelial cell proliferation. Four days after myoblast implantation, VEGF alone caused about 50% less endothelial proliferation in *Notch4*$^{d1}$ mice compared to control animals ($pHH3^+$ endothelial cells = 1.8±0.2% vs. 0.9±0.2%; Figure 5A). As expected, inhibition of ephrinB2/EphB4 led to a 30% increase in endothelial cell proliferation in wild type mice (2.7±0.2%, $p<0.01$). Interestingly, ephrinB2/EphB4 inhibition increased endothelial proliferation by about 50% compared to V-low alone also in *Notch4*$^{d1}$ mice (1.8±0.2%, $p<0.01$). However, Notch4 inactivation still partially inhibited endothelial proliferation caused by ephrinB2/EphB4 inhibition, as this was about 30% lower than in wild-type mice ($p<0.05$; Figure 5A). Representative immunofluorescence images are shown in Figure 5B.

Endothelial cell apoptosis was assessed by the number of cleaved-Caspase-$3^+$ECs and analyzed in muscles collected 7 days after implantation of myoblast expressing only VEGF or co-expressing sEphB4, into *Notch4*$^{d1}$ mice and wild-type mice. No difference in number of apoptotic ECs was observed among different conditions and/or mouse strains (Figure 5C).

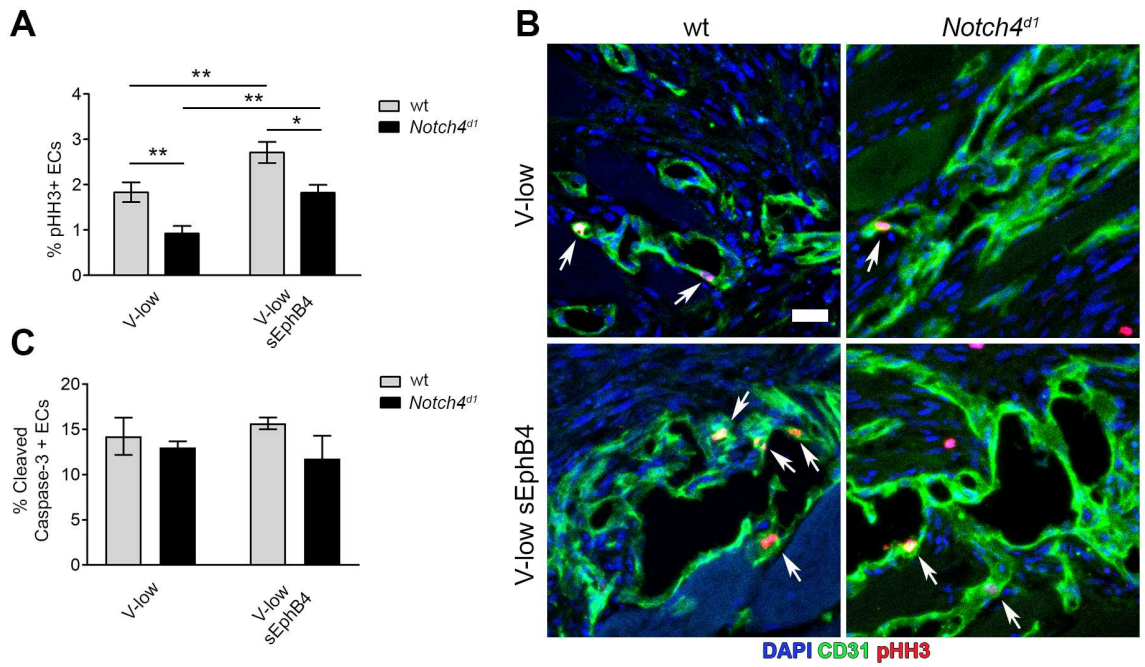


**Figure 5. Both Notch4 and ephrinB2/EphB4 signaling control endothelial cell proliferation, but not apoptosis.** Limb muscles of both wild-type (wt) and *Notch4*$^{d1}$ mice were injected with myoblasts expressing only a low dose of VEGF (V-low) or co-expressing also sEphB4, blocker of ephrinB2/EphB4 pathway (V-low sEphB4). Endothelial cell (EC) proliferation was quantified 4 days after myoblast implantation by immunostaining for endothelium (CD31, green) and proliferation marker phospho-histone H3 (pHH3, red). (**A**) Four days after myoblast implantation, Notch4 inactivation inhibited endothelial proliferation both after delivery of low levels of VEGF alone and with ephrinB2/EphB4 inhibition. However, Notch4 inactivation did not prevent the increase in endothelial proliferation caused by ephrinB2/EphB4 inhibition, as pHH3$^{+}$ ECs were still about 50% more frequent in the V-low sEphB4 condition than in V-low in *Notch4*$^{d1}$ mice; n=6 muscles/group, * $p<0.05$, ** $p<0.01$ by Kruskal-Wallis test followed by Dunn's post-test. (**B**) Representative immunofluorescent images. Phospho-HH3$^{+}$ ECs are marked with white arrows. Size bar=25 µm. (**C**) Apoptotic endothelial cells were analyzed after 7 days by immunofluorescence staining using antibody against cleaved Caspase-3 and CD31. The analysis showed no apparent difference among conditions and/or mouse strains; n=4 muscles/group.

## EphrinB2/EphB4 signaling does not require Notch4 activity to modulate pERK1/2

As shown in the previous Chapter, ephrinB2/EphB4 signaling modulates the MAPK pathway and endothelial proliferation after VEGF stimulation through pERK1/2 (Chapter III, Figure 7E-H). We found that pERK1/2 is controlled without direct modulation of VEGF-R2 activation, i.e. both its internalization and phosphorylation (Chapter III, Figure 7A-C). Here

we investigated whether Notch4 signaling is necessary for this process. The analysis was performed 3 days after myoblast implantation, as VEGF downstream signaling is activated early on during the angiogenic process. Quantification of pERK1/2$^{+}$ endothelial cells (pERK1/2$^{+}$ EC) was performed by immunofluorescence co-staining using antibodies against CD31 and pERK1/2 (Figure 6A). Low levels of VEGF induced pERK1/2 in endothelial cell similarly in both mouse strains. Inhibition of ephrinB2/EphB4 signaling by sEphB4 led to a significant increase in the frequency of pERK1/2$^{+}$ ECs in both wt mice (5.5±0.9% with V-low vs 9.9±1.0% with V-low sEphB4, $p<0.001$) and in *Notch4*$^{d1}$ mice (6.3±0.8% with V-low vs 10.3±1.2% with V-low sEphB4, $p<0.05$), but with no significant differences between wt and *Notch4*$^{d1}$ mice in each condition (Figure 6B), showing that Notch4 inactivation did not affect endothelial ERK1/2 phosphorylation.

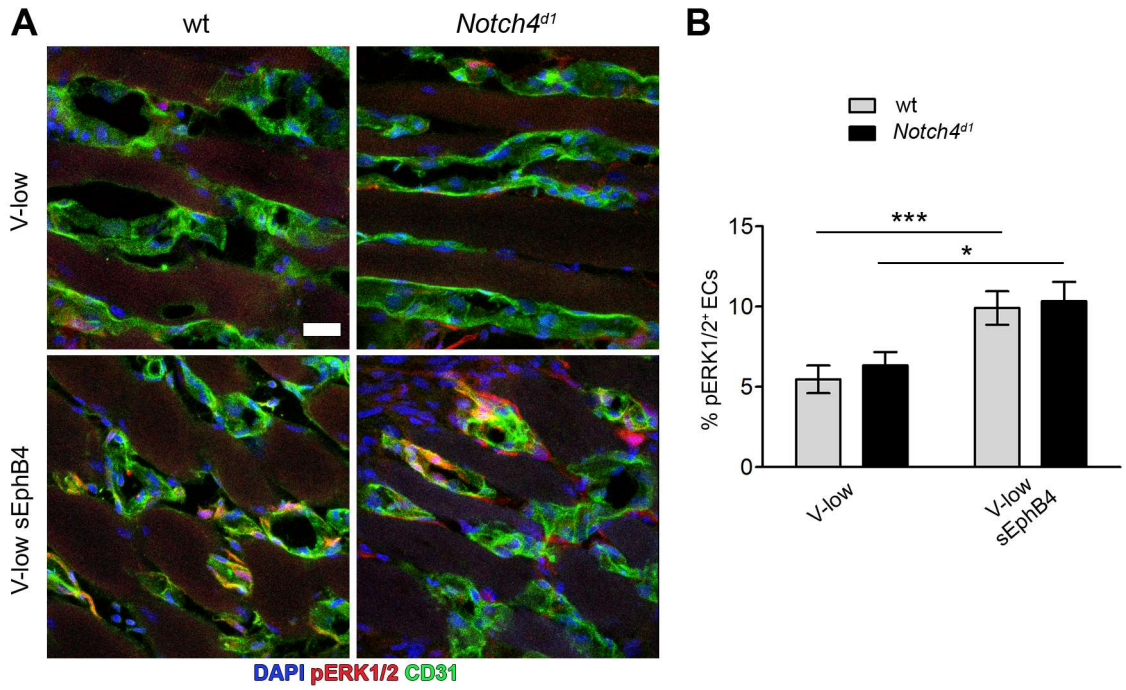


**Figure 6. Notch4 signaling does not regulate endothelial pERK1/2 after VEGF delivery**. Myoblast expressing only VEGF (V-low) or co-expressing sEphB4 (V-low sEphB4) were injected in limb muscle of wild-type (wt) and *Notch4*$^{d1}$ mice. Three days after myoblast implantation, frozen section of injected muscles were immunostained to visualize endothelium (CD31, green) and pERK1/2 (red). The frequency of pERK1/2$^{+}$ endothelial cells was quantified and the analysis showed that sEphB4 could induce significantly higher amount of pERK1/2$^{+}$ECs compared to VEGF alone. However, this effect was similar in both mouse strains (**A-B**); n = 6 muscles/group, * $p<0.05$, *** $p<0.001$ by Kruskal-Wallis test followed by Dunn's post-test. Size bar=25µm

# Discussion

VEGF gene therapy is a promising strategy for treatment of ischemic disease, but aberrant vessel growth, as a consequence of high VEGF dose, is a limitation for achievement of therapeutic benefit (23). Here, we investigated the crosstalk between Notch4 and EphB4 signaling in the switch between normal and aberrant angiogenesis by increasing doses of VEGF and we found that: 1) active Notch4 is required for aberrant angiogenesis induced by EphB4 blockade; 2) Notch4 inactivation reduces, but does not abolish, the increase in endothelial proliferation caused by EphB4 blockade; and 3) while EphB4 blockade stimulates endothelial proliferation by activating ERK1/2 phosphorylation, Notch4 inactivation does not affect this pathway. Taken together, these findings suggest that Notch4 does not control the switch between normal and aberrant vascular growth through EphB4, but rather that both pathways regulate endothelial proliferation in parallel, providing the basis for potential synergistic targeting.

We have previously shown that VEGF delivery to skeletal muscle does not induce angiogenesis by the well-characterized mechanism of sprouting, but rather through an initial step of circumferential vascular enlargement, followed by longitudinal vessel splitting, i.e. intussusception (20). As shown in the previous Chapter of this thesis, inhibition of ephrinB2/EphB4 signaling by sEphB4, caused aberrant vessel growth despite low and safe VEGF levels. This process was characterized by alteration of different cellular and molecular events during early angiogenic response to VEGF (3 and 4 days after myoblast implantation), like increase in the size of initial vascular enlargements and speed of endothelial cell proliferation, as well as increase in pERK1/2 activation. Ultimately, this led to the development of aberrant vessels at later stage (7 and 14 days after myoblast implantation). Here we investigated whether active Notch4 signaling is required for the process of aberrant angiogenesis caused by EphB4 blockade and whether one of the two pathways may control the

other, or they may work in synergy. We made use of the *Notch4*$^{d1}$ mouse model, in which the Notch4 protein is truncated and unable to signal due to a lack of the intracellular and transmembrane domains (15). We have shown that deprivation of Notch4 signaling reduced, but did not abolish, the increase in endothelial cell proliferation caused by EphB4 blockade with sEphB4 and successfully prevented the development of aberrant vascular structures, although it did not affect activation of pERK1/2 that is instead controlled by EphB4 signaling. It is known that Notch signaling acts upstream of ephrinB2 and EphB4, as it can upregulate ephrinB2 and downregulate EphB4, an in that way, promote arterial and suppress venous phenotype (7, 8). However, this function of Notch upstream of ephrinB2/EphB4 does not explain our observations. In fact, a reduction in ephrinB2 caused by a loss of Notch signaling would be expected to rather further reduce EphB4 activity and potentiate the induction of aberrant angiogenesis by EphB4 blockade, rather than preventing it. Further, if Notch4 acted through EphB4 signaling, its loss should decrease the levels of pERK1/2, whereas no such effect was observed. On the other hand, over-activation of Notch4 using a tetracycline-inducible model, causes arterio-venous malformations (AVM) in the brain (5, 12-14). It was also shown that development of AVMs is accompanied by a decrease in EphB4 expression, which is again normalized, after AVMs regress. Furthermore, blockade of ephrinB2/EphB4 signaling by sEphB4 significantly impaired regression of AVMs after termination of Notch4 overactivation (5). These results are in agreement with our previous findings that EphB4 blockade promotes the transition to aberrant vascular growth and here we sought to investigate whether ephrinB2/EphB4 signaling may also act upstream of Notch4. The results showed that, while active Notch4 is required for the induction of aberrant angiogenesis by EphB4 blockade, it does not fully control ephrinB2/EphB4 downstream effects. Rather, the data suggest that both pathways modulate endothelial cell proliferation, but with different non-overlapping mechanisms. While ephrinB2/EphB4 modulates the amount of pERK1/2, a signaling branch

known to regulate VEGF-induced proliferation (24, 25), absence of Notch4 did not affect the amount of VEGF-induced pERK1/2 (Figure 6). Interestingly, it has been shown that overactivation of Notch4 induces vessel enlargement and AVM formation without change in number of endothelial cells (5, 13). Contrary to that, we have observed a decrease in endothelial cell proliferation in *Notch4*$^{d1}$ mice (Figure 5A). It is important to note that VEGF is overexpressed in our model, as compared to the AVM model presented by Murphy et al, and could potentially account for these differences. It was also reported that Notch4 can prevent apoptosis of endothelial cells by both RBPJ-κ-dependent and RBPJ-κ-independent mechanism, and ankyrin repeats in intracellular domain are necessary for anti-apoptotic activity (26), but we did not observe any difference in number of apoptotic cells during active angiogenesis in two different mouse strains (Figure 5C). Given that ephrinB2/EphB4 inhibition can increase endothelial proliferation in *Notch4*$^{d1}$ mice, we can conclude that both Notch4 and ephrinB2/EphB4 signaling can regulate VEGF-induced endothelial proliferation by two independent mechanisms.

It was reported that Notch inhibition enhances intussusceptive angiogenesis by increasing the number of transluminal pillars, leading to higher microvascular density (27). In accordance to that, 7 days after myoblast implantation, we also observed an increase in vessel length density in *Notch4*$^{d1}$ mice as compared to control mice. This increase is noticeable both after stimulation with VEGF alone and together with inhibition of ephrinB2/EphB4 signaling, where normalization of aberrant vessel morphology could also be observed (Figure 4K). This observation suggests that absence of active Notch4 downstream signaling may enhance intussusceptive remodeling of the vessels also in our model, leading to more efficient vessel splitting, although this aspect remains to be investigated by high-resolution morphological analyses and pillar quantification. It is interesting to note that increased efficacy of vessel

splitting may also contribute to the prevention of aberrant angiogenesis, by blocking the process of continued circumferential enlargement.

It was reported that Notch4 can be activated by Notch ligands *in vitro* (28, 29), but others failed to confirm this finding (19, 30). Interestingly, it was shown that Notch4 has a very weak ability to activate downstream signaling, as compared to Notch1 (19). Furthermore, truncated Notch4$^{d1}$ protein, released from expressing endothelium, has the potential to dose-dependently inhibit ligand-induced activation of Notch1 receptor in cultured cells (19). Since the truncated Notch4 protein is overexpressed in the *Notch4$^{d1}$* mice (19), here used for the experiments, it is possible that Notch1 inhibition in *cis* may contribute to the observed reduction in endothelial proliferation. Whether Notch4 inactivation may inhibit endothelial proliferation directly or indirectly through inhibition of Notch1 remains to be investigated.

In conclusion, both ephrinB2/EphB4 and Notch4 signaling control the process of aberrant angiogenesis induced by VEGF, but with distinct mechanism that do not necessarily have same dynamics and could be critical at different stages of the angiogenic process. From a therapeutic perspective, these findings provide a basis to hypothesize that activation of EphB4 and inhibition of Notch4 could have synergistic effects on controlling endothelial proliferation by excessive doses of VEGF and therefore be more efficient in prevention of aberrant angiogenesis compared to targeting each pathway alone.

# References

1. Yla-Herttuala S, Bridges C, Katz MG, Korpisalo P. Angiogenic gene therapy in cardiovascular diseases: dream or vision? *Eur Heart J*. 2017;38(18):1365-71.

2. Potente M, Gerhardt H, Carmeliet P. Basic and therapeutic aspects of angiogenesis. *Cell*. 2011;146(6):873-87.

3. St George JA. Gene therapy progress and prospects: adenoviral vectors. *Gene Ther*. 2003;10(14):1135-41.

4. Kitajewski J. Arteriovenous malformations in five dimensions. *Sci Transl Med*. 2012;4(117):117fs3.

5. Murphy PA, Kim TN, Lu G, Bollen AW, Schaffer CB, Wang RA. Notch4 normalization reduces blood vessel size in arteriovenous malformations. *Sci Transl Med*. 2012;4(117):117ra8.

6. Delev D, Pavlova A, Grote A, Bostrom A, Hollig A, Schramm J, et al. NOTCH4 gene polymorphisms as potential risk factors for brain arteriovenous malformation development and hemorrhagic presentation. *J Neurosurg*. 2017;126(5):1552-9.

7. Lawson ND, Scheer N, Pham VN, Kim CH, Chitnis AB, Campos-Ortega JA, et al. Notch signaling is required for arterial-venous differentiation during embryonic vascular development. *Development*. 2001;128(19):3675-83.

8. Roca C, Adams RH. Regulation of vascular morphogenesis by Notch signaling. *Genes Dev*. 2007;21(20):2511-24.

9. Weinsheimer S, Kim H, Pawlikowska L, Chen Y, Lawton MT, Sidney S, et al. EPHB4 gene polymorphisms and risk of intracranial hemorrhage in patients with brain arteriovenous malformations. *Circ Cardiovasc Genet*. 2009;2(5):476-82.

10. Uyttendaele H, Marazzi G, Wu G, Yan Q, Sassoon D, Kitajewski J. Notch4/int-3, a mammary proto-oncogene, is an endothelial cell-specific mammalian Notch gene. *Development*. 1996;122(7):2251-9.

11. Uyttendaele H, Ho J, Rossant J, Kitajewski J. Vascular patterning defects associated with expression of activated Notch4 in embryonic endothelium. *Proc Natl Acad Sci U S A*. 2001;98(10):5643-8.

12. Carlson TR, Yan Y, Wu X, Lam MT, Tang GL, Beverly LJ, et al. Endothelial expression of constitutively active Notch4 elicits reversible arteriovenous malformations in adult mice. *Proc Natl Acad Sci U S A*. 2005;102(28):9884-9.

13. Murphy PA, Kim TN, Huang L, Nielsen CM, Lawton MT, Adams RH, et al. Constitutively active Notch4 receptor elicits brain arteriovenous malformations through enlargement of capillary-like vessels. *Proc Natl Acad Sci U S A*. 2014;111(50):18007-12.

14. Murphy PA, Lam MT, Wu X, Kim TN, Vartanian SM, Bollen AW, et al. Endothelial Notch4 signaling induces hallmarks of brain arteriovenous malformations in mice. *Proc Natl Acad Sci U S A*. 2008;105(31):10901-6.

15. Krebs LT, Xue Y, Norton CR, Shutter JR, Maguire M, Sundberg JP, et al. Notch signaling is essential for vascular morphogenesis in mice. *Genes Dev*. 2000;14(11):1343-52.

16. Takeshita K, Satoh M, Ii M, Silver M, Limbourg FP, Mukai Y, et al. Critical role of endothelial Notch1 signaling in postnatal angiogenesis. *Circ Res*. 2007;100(1):70-8.

17. Costa MJ, Wu X, Cuervo H, Srinivasan R, Bechis SK, Cheang E, et al. Notch4 is required for tumor onset and perfusion. *Vasc Cell*. 2013;5(1):7.

18. Ozawa CR, Banfi A, Glazer NL, Thurston G, Springer ML, Kraft PE, et al. Microenvironmental VEGF concentration, not total dose, determines a threshold between normal and aberrant angiogenesis. *J Clin Invest*. 2004;113(4):516-27.

19. James AC, Szot JO, Iyer K, Major JA, Pursglove SE, Chapman G, et al. Notch4 reveals a novel mechanism regulating Notch signal transduction. *Biochim Biophys Acta*. 2014;1843(7):1272-84.

20. Gianni-Barrera R, Trani M, Fontanellaz C, Heberer M, Djonov V, Hlushchuk R, et al. VEGF over-expression in skeletal muscle induces angiogenesis by intussusception rather than sprouting. *Angiogenesis*. 2013;16(1):123-36.

21. Crosio C, Fimia GM, Loury R, Kimura M, Okano Y, Zhou H, et al. Mitotic phosphorylation of histone H3: spatio-temporal regulation by mammalian Aurora kinases. *Mol Cell Biol*. 2002;22(3):874-85.

22. Nielsen PS, Riber-Hansen R, Jensen TO, Schmidt H, Steiniche T. Proliferation indices of phosphohistone H3 and Ki67: strong prognostic markers in a consecutive cohort with stage I/II melanoma. *Mod Pathol*. 2013;26(3):404-13.

23. Karvinen H, Pasanen E, Rissanen TT, Korpisalo P, Vahakangas E, Jazwa A, et al. Long-term VEGF-A expression promotes aberrant angiogenesis and fibrosis in skeletal muscle. *Gene Ther*. 2011;18(12):1166-72.

24. Simons M, Gordon E, Claesson-Welsh L. Mechanisms and regulation of endothelial VEGF receptor signalling. *Nat Rev Mol Cell Biol*. 2016;17(10):611-25.

25. Takahashi T, Yamaguchi S, Chida K, Shibuya M. A single autophosphorylation site on KDR/Flk-1 is essential for VEGF-A-dependent activation of PLC-gamma and DNA synthesis in vascular endothelial cells. *EMBO J*. 2001;20(11):2768-78.

26. MacKenzie F, Duriez P, Wong F, Noseda M, Karsan A. Notch4 inhibits endothelial apoptosis via RBP-Jkappa-dependent and -independent pathways. *J Biol Chem*. 2004;279(12):11657-63.

27. Dimova I, Hlushchuk R, Makanya A, Styp-Rekowska B, Ceausu A, Flueckiger S, et al. Inhibition of Notch signaling induces extensive intussusceptive neo-angiogenesis by recruitment of mononuclear cells. *Angiogenesis*. 2013;16(4):921-37.

28. Shawber CJ, Das I, Francisco E, Kitajewski J. Notch signaling in primary endothelial cells. *Ann N Y Acad Sci*. 2003;995:162-70.

29. Shawber CJ, Funahashi Y, Francisco E, Vorontchikhina M, Kitamura Y, Stowell SA, et al. Notch alters VEGF responsiveness in human and murine endothelial cells by direct regulation of VEGFR-3 expression. *J Clin Invest*. 2007;117(11):3369-82.

30. Aste-Amezaga M, Zhang N, Lineberger JE, Arnold BA, Toner TJ, Gu M, et al. Characterization of Notch1 antibodies that inhibit signaling of both normal and mutated Notch1 receptors. *PLoS One*. 2010;5(2):e9094.

# V. Summary and future perspectives

Ischemic diseases are one of the leading causes of death in Western societies. Peripheral artery disease, caused by atherosclerotic occlusions of arteries, has different grades of severity of symptoms, ranging from pain during exercise to limb amputation (1-3). Therapeutic angiogenesis is a promising strategy to induce growth of new blood vessels and restore blood flow in the ischemic tissues by VEGF stimulation (3). Despite the clear biological efficacy of the factor, clinical trials of VEGF gene therapy failed to show patient benefit (2). One of the reasons for disappointing results are low transduction efficiency and insufficient local protein production at safe vector doses (3, 4). Higher VEGF doses, on the other side, lead to induction of aberrant, dysfunctional angioma-like vascular structures (5). Therefore, in order to take advantage of VEGF's therapeutic potential and enable safe delivery of effective doses, we sought to identify molecular targets responsible for normalization of aberrant vascular growth. We found that ephrinB2/EphB4 signaling between pericytes and endothelium controls the switch between normal and aberrant angiogenesis with increasing VEGF doses. We demonstrated that ephrinB2/EphB4 determines the outcome of VEGF-induced angiogenesis by modulating VEGF downstream signaling through pERK1/2, but without directly affecting VEGF-R2 activation, either through its internalization or phosphorylation. This has important therapeutic implications. In fact, by inhibiting one branch of a redundant circuit downstream of VEGF-R2, EphB4 stimulation can achieve modulation of ERK1/2 activation and endothelial proliferation, while sparing sufficient activity to avoid disruption of vascular growth, and therefore ensuring robust normal angiogenesis. We delivered VEGF by three platforms, namely myoblast-based delivery system, fibrin-bound VEGF, and adenoviral delivery. Using all three delivery systems, we showed that aberrant angiogenesis by high VEGF doses can be normalized by systemic treatment with ephrinB2-Fc. Finally, we investigated the therapeutic potential of this approach in a mouse model of limb ischemia and we found that activation of EphB4 signaling together with uncontrolled VEGF delivery by adenoviral vectors yields only

normal and functional vascular growth, decreasing tissue necrosis and increasing tissue regeneration.

As inhibition of Notch4 signaling was found to have a similar effect as stimulation of EphB4, namely preventing aberrant vascular growth by high VEGF doses while enabling only robust normal angiogenesis, we next investigated the crosstalk between the ephrinB2/EphB4 and Notch4 pathways. We found that aberrant angiogenesis induced by inhibition of ephrinB2/EphB4 with low VEGF can be prevented in *Notch4*$^{d1}$ mice, in which the Notch4 protein is mutated and unable to signal (6). Endothelial cell proliferation induced by VEGF stimulation was reduced in these mice compared to controls. Interestingly, upon VEGF stimulation, higher vessel length density was observed in *Notch4*$^{d1}$ mice comparing to control mice. This observation is in line with recent finding that inhibition of Notch signaling during intussusceptive angiogenesis can increase microvascular density (7). The absence of active Notch4 signaling reduced, but did not completely prevent, the increase in endothelial cell proliferation caused by inhibition of the ephrinB2/EphB4 pathway, whereas it had no effect on pERK1/2 activation. These observations suggest that both ephrinB2/EphB4 and Notch4 cooperate in aberrant vessel normalization, but appear to do so via two independent molecular mechanisms. While EphB4 works through the kinase cascade and pERK1/2, the path linking Notch4 to endothelial proliferation remains to be elucidated.

As a future perspective, further development of preclinical proof-of-concept studies of ephrinB2/EphB4 signaling is one of the main objectives. It is known that ephrinB2/EphB4 complexes multimerize upon interaction, and that this is required for maximal activation of downstream signaling (8-10). In order to further develop its therapeutic potential, we are aiming to produce a recombinant ephrinB2-Fc protein that is able to multimerize, creating a stronger activator than the dimers formed by the commercially available IgG-Fc fusion protein. For this, we will exploit a recently published recombinant Fc fragment (11), based on the fusion

of IgG-Fc with an 18-amino acid peptide sequence of the carboxyl-terminus of IgM antibody Fc, responsible for pentamer complexes formation. Two point-mutations in the 18-aa clustering sequence were introduced to achieve that the protein complex assembles as a hexamer, rather than as a pentamer, further improving its activating power. The recombinant IgG-Fc fragment with short peptide elongation can be fused to the ephrinB2 extracellular domain, enabling multimerization of the resulting protein. After *in vitro* characterization of the potency of the novel engineered protein, where it will be compared to the commercially available ephrinB2-IgG-Fc, its ability to normalize aberrant angiogenesis, as well as its stability would be a tested *in vivo* in a mouse model. Next, pre-clinical translation should be carried out in clinically predictive large-animal models of ischemia (rabbit hindlimb or pig heart) by combining a clinically applicable robust vector for gene therapy (adeno-associated or adenovirus) at efficient titers with systemic EphB4 stimulation.

Here, for the first time, we identify specific signaling pathways regulating the outcome of intussusceptive angiogenesis, namely ephrinB2/EphB4 and Notch4, as their previously known functions related to sprouting angiogenesis (12) or arterio-venous malformation development (13, 14), respectively. Further downstream effectors of these pathway need to be identified, possibly by transcriptomic analysis of FACS-sorted endothelial cells isolated after inhibition/activation of ephrinB2/EphB4 or inhibition of Notch4 pathway. This could be complemented by (phospho-)proteomic analysis in order to systematically investigate the downstream molecular network and its interaction with VEGF and other signaling pathways.

It would be also interesting to investigate the effect of ephrinB2/EphB4 signaling modulation on pericyte biology. We have observed that inhibition of ephrinB2/EphB4 pathway changes pericyte characteristics during the early phase of angiogenesis, as they become double positive for NG2 and αSMA, and activation of the pathway, on the other side, recruits pericytes. It will be important to investigate how their gene expression profile and proliferation change

upon modulation of this pathway. Generally, very little is known about downstream mechanism of action of ephrin/Eph pathway. These signaling molecules have been connected with other pathologies, like cancer and neurodegeneration, so this could also open possibilities for treatment of these conditions (10).

Taking advantage of the unique model provided by the monoclonal populations expressing specific doses of VEGF in skeletal muscle, the kinetics of EphB4 and Notch4 actions and the underlying cellular mechanisms should be rigorously investigated by *in vivo* imaging of early morphological changes during angiogenesis by two-photon microscopy. These experiments would be performed in the ear muscle of Tie2-GFP mice that have spontaneously fluorescent endothelium, as this muscle is superficial and accessible to imaging without surgical procedures. This would help us understand how ephrinB2/EphB4 modulates the growth of initial vascular enlargements, and how Notch4 signaling influences vessel remodeling at later stages of angiogenesis.

Finally, activating EphB4 by ephrinB2-Fc recombinant protein in Notch4-deficient mice would answer the question whether the double targeting is more efficient in normalization of aberrant angiogenesis by high VEGF, as compared to modulation of only EphB4 or Notch4 pathways alone. In case double therapy would be proven more efficient, one could increase the dose of VEGF in order to identify the upper limit of the putative therapeutic window to normalize aberrant vessel growth. Ultimately, this would set the stage to design rational therapeutic approaches that could overcome current limitations of VEGF gene delivery and lead to a clinical benefit.

# References

1. Dragneva G, Korpisalo P, Yla-Herttuala S. Promoting blood vessel growth in ischemic diseases: challenges in translating preclinical potential into clinical success. *Dis Model Mech*. 2013;6(2):312-22.

2. Gorenoi V, Brehm MU, Koch A, Hagen A. Growth factors for angiogenesis in peripheral arterial disease. *Cochrane Database Syst Rev*. 2017;6:CD011741.

3. Yla-Herttuala S, Baker AH. Cardiovascular Gene Therapy: Past, Present, and Future. *Mol Ther*. 2017;25(5):1095-106.

4. Yla-Herttuala S, Bridges C, Katz MG, Korpisalo P. Angiogenic gene therapy in cardiovascular diseases: dream or vision? *Eur Heart J*. 2017;38(18):1365-71.

5. Karvinen H, Pasanen E, Rissanen TT, Korpisalo P, Vahakangas E, Jazwa A, et al. Long-term VEGF-A expression promotes aberrant angiogenesis and fibrosis in skeletal muscle. *Gene Ther*. 2011;18(12):1166-72.

6. Krebs LT, Xue Y, Norton CR, Shutter JR, Maguire M, Sundberg JP, et al. Notch signaling is essential for vascular morphogenesis in mice. *Genes Dev*. 2000;14(11):1343-52.

7. Dimova I, Hlushchuk R, Makanya A, Styp-Rekowska B, Ceausu A, Flueckiger S, et al. Inhibition of Notch signaling induces extensive intussusceptive neo-angiogenesis by recruitment of mononuclear cells. *Angiogenesis*. 2013;16(4):921-37.

8. Davis S, Gale NW, Aldrich TH, Maisonpierre PC, Lhotak V, Pawson T, et al. Ligands for EPH-related receptor tyrosine kinases that require membrane attachment or clustering for activity. *Science*. 1994;266(5186):816-9.

9. Egea J, Nissen UV, Dufour A, Sahin M, Greer P, Kullander K, et al. Regulation of EphA 4 kinase activity is required for a subset of axon guidance decisions suggesting a key role for receptor clustering in Eph function. *Neuron*. 2005;47(4):515-28.

10. Kania A, Klein R. Mechanisms of ephrin-Eph signalling in development, physiology and disease. *Nat Rev Mol Cell Biol*. 2016;17(4):240-56.

11. Mekhaiel DN, Czajkowsky DM, Andersen JT, Shi J, El-Faham M, Doenhoff M, et al. Polymeric human Fc-fusion proteins with modified effector functions. *Sci Rep*. 2011;1:124.

12. Pitulescu ME, Adams RH. Eph/ephrin molecules--a hub for signaling and endocytosis. *Genes Dev*. 2010;24(22):2480-92.

13. Carlson TR, Yan Y, Wu X, Lam MT, Tang GL, Beverly LJ, et al. Endothelial expression of constitutively active Notch4 elicits reversible arteriovenous malformations in adult mice. *Proc Natl Acad Sci U S A*. 2005;102(28):9884-9.

14. Kitajewski J. Arteriovenous malformations in five dimensions. *Sci Transl Med*. 2012;4(117):117fs3.

# VI. Acknowledgements

I would like to thank my supervisor PD Dr. Andrea Banfi for giving me the opportunity to do a PhD in his lab.

I thank my Committee Members for being always so constructive and helpful during our PaC meetings.

One special thank goes to Emma, my dear friend and colleague who was always my biggest support. She was always there whenever I needed her help in or outside the lab.

I thank Elena for all her help and support and to all my colleagues at the Department of Biomedicine for all the scientific discussions and helpful advices and for all the fun nights out.

I thank to all the people from AngioMatTrain network for all the wonderful meetings and all the amazing time we had together.

I thank my beloved family and all my friends for being always so supportive and for encouraging me throughout my PhD and life journey.

I have met so many wonderful people in Basel and I would like to thank them all for never feeling alone.